Studying BDNF signalling using neurons derived from human embryonic stem cells

Spyridon Merkouris

A thesis submitted to Cardiff University in accordance with the requirements for the degree of Doctor of Philosophy in the discipline of Neuroscience

School of Biosciences, Cardiff University

June 2020

DECLARATION

This work has not been submitted in substance for any other degree or award at this or any other university or place of learning, nor is being submitted concurrently in candidature for any degree or other award.

Signed …… (candidate) Date ……

STATEMENT 1

This thesis is being submitted in partial fulfillment of the requirements for the degree of ……(insert MCh, MD, MPhil, PhD etc, as appropriate)

Signed …… (candidate) Date ……

STATEMENT 2

This thesis is the result of my own independent work/investigation, except where otherwise stated.

Other sources are acknowledged by explicit references. The views expressed are my own.

Signed …… (candidate) Date ……

STATEMENT 4: PREVIOUSLY APPROVED BAR ON ACCESS

I hereby give consent for my thesis, if accepted, to be available online in the University's Open Access repository and for inter-library loans **after expiry of a bar on access previously approved by the Academic Standards & Quality Committee.**

Signed …… (candidate) Date ……

“The energy of mind is the essence of life”

Aristotle’s Metaphysics 12.1072b25

“ἡ γὰρ νοῦ ἐνέργεια ζωή”

ACKNOWLEDGEMENTS

First and foremost, I would like to thank my supervisor, Yves Barde, for giving me the opportunity to work in his lab and providing his continuous guidance and advice throughout my PhD. His endless ideas and passion for science encouraged me when experiments did not work as expected. Thank you for your support and the exciting discussions during the last four years. Special thanks go to my co-supervisor Meng Li, who's experience on human stem cells greatly facilitated my project. Meng and Claudia Tamburini introduced me to the techniques of human stem cell culture and for possibility to use equipment. Claudia was always there for scientific discussions, and the exchange of ideas made me more productive. I would like to extend my gratitude to Nick Allen whose experience on differentiating human stem cells offered me a very useful system to work with. I also wish to thank the whole Barde lab, but specific thanks go to Pedro Chacon Fernandez who always gave help when I needed it and for his advices; Hayley Dingsdale for giving me valuable feedback on this thesis; Xinsheng Nan for always being willing to share his great experimental expertise. Katharina, Laura, Sven, Jess and Natalia: thank you for the many enjoyable moments that we spent together, for the support and for the productive discussions. Thanks to all the members of the 3rd floor of the BIOSI 3 for creating an ideal working environment.

Last, but not least I want to thank my friends and family for their reassurance and inspiration. I would like to thank in particular my parents for their love, continuous support and for always believing in me. Thank you, mam and dad, for everything that you have done for me. Special thanks also go to my sister Katerina for always being there when I needed her. I would also like to thank my good friend Giannis Kessidis for our long and stimulating discussions.

ABSTRACT

As a result of a large number of *in vitro* as well as *in vivo* experiments with rodents, brain-derived neurotrophic factor (BDNF) and its tyrosine kinase receptor TrkB are now widely appreciated to play major roles in brain function. There is also a growing appreciation that decreased BDNF signalling may be a significant component in a wide range of brain dysfunction in humans based on the discovery of mutations and polymorphisms in the corresponding genes. Yet still very little is known about BDNF expression and TrkB activation in human neurons or the human brain. In order to begin to address these questions, human embryonic stem cells (hESCs) have been used to generate large numbers of neurons suitable for biochemical experiments. In the work reported in the following chapters, two different protocols have been used to grow and differentiate hESCS. In the first, excitatory neurons were generated exhibiting detectable levels of BDNF albeit at low levels and after well over 2 months of culture. Detailed biochemical analyses that could significantly advance the field within a manageable time frame were also hampered by uncontrolled cell division still occurring in excitatory neurons even after extended culture periods. The use of a second, recently published differentiation protocol led to the significantly faster, more reproducible generation of large numbers of TrkB- expressing, mostly inhibitory neurons. A key feature of this robust differentiation protocol was the high proportion of BDNF-responsive cells allowing BDNF-induced phosphorylation to be studied with regard to time course and dose response. This system also allowed comparisons to be made between BDNF, the related factor neurotrophin-4 (NT4) and newly generated TrkB-activating antibodies. These TrkB-activating ligands were compared by extracting RNA from neurons treated for different time periods. One of the TrkB-activating antibody (designated #85) turned out to activate human TrkB at concentrations close to those of the natural ligands and with a strikingly similar pattern of induced mRNA transcripts, especially at early time points. The main conclusion of this work is that a test system based on the generation of BDNF-responsive neurons can be used to develop new reagents able to meaningfully activate TrkB. This work has been published in Merkouris et al 2018 in PNAS (https://www.pnas.org/content/115/30/E7023.long)

ABBREVIATIONS

7,8-DHF	7,8-Dihydroxyflavone
Aβ	Amyloid Beta
ACAN	Aggrecan
ACKR3	Atypical Chemokine Receptor 3
AD	Alzheimer's Disease
ADF	Advanced DMEM F12
Akt	*see* PKB
AMPK	5' Adenosine Monophosphate-Activated Protein Kinase
AP-1	Activator Protein 1
Arc	Activity-Regulated Cytoskeleton-Associated Protein
ATF3	Activating Transcription Factor 3
BAD	Bcl-2-associated Death Promotor
Bcl-2	B-cell Lymphoma 2
BDNF	Brain-Derived Neurotrophic Factor
BDNF-AS	BDNF Antisense
bFGF	Basic Fibroblast Growth Factor
BMP	Bone Morphogenetic protein
BP	Base Pairs
BSA	Bovine Serum Albumin
BTG2	B-Cell Translocation Gene 2
CamKII	Calcium/Calmodulin-Dependent Protein Kinase II
cAMP	Cyclic Adenosine Monophosphate

CaREs	Calcium-Response Elements
CaRF	Calcium-Responsive Transcription Factor
Cdk	Cyclin-Dependent Kinase
cDNA	Complementary DNA
CNS	Central Nervous System
CR	Calretinin
CRE	cAMP Response Element
CREB	cAMP response element-binding protein
CSRNP1	Cysteine and Serine Rich Nuclear Protein 1
Ct	Cycle Threshold
CTIP2	Chicken Ovalbumin Upstream Promotor Transcription Factor-Interacting Protein 2
CUX1	Cut Like Homeobox 1
CYR61	Cysteine Rich Angiogenic Inducer 61
DAPI	4',6-diamidino-2 phenylindole
DARPP-32	Dopamine- and cAMP-regulated neuronal phosphoprotein
DIV	Days *in vitro*
DMAQ-B1	Demethylasterriquinone B-1
DMEM	Dulbecco's Modified Eagle Medium
DMSO	Dimethyl Sulfoxide
DNA	Deoxyribonucleic Acid
dNTP	Deoxynucleotide Triphosphates
DTT	Dithiothreitol
DUSP1	Dual Specificity Phosphatase 1
EC50	Half Maximal Effective Concentration
EDTA	Ethylenediaminetetraacetic Acid
EGF	Epidermal Growth Factor

EGR	Early Growth Reponse
ERK	Extracellular-Signal-Regulated Kinase
ESC	Embryonic Stem Cell
ETV5	ETS Variant 5
FAM	6-carboxyfluorescein
FAM83G	Family With Sequence Similarity 83 Member G
FCS	Foetal Calf Serum
FGF	Fibroblast Growth Factor
FOXP	Forkhead Box Protein P
FPKM	Fragments Per Kilobase Million
FRET	Fluorescence Resonance Energy Transfer
GABA	Gamma-Aminobutyric Acid
GAD	Glutamate decarboxylase
GEM	Guanosine-5'-Triphosphate (GTP) Binding Protein Overexpressed in Skeletal Muscle
GFAP	Glial Fibrillary Acidic Protein
GFR	Growth Factor-Reduced
GO	Gene Ontology
GPR	G Protein-Coupled Receptor
GSK3	Glycogen Synthase Kinase-3
GSX2	Genetic-Screened Homeobox 2
HAP1	Huntingtin Associated Protein 1
HD	Huntington's Disease
HESCs	Human Embryonic Stem Cells
HIV	Human Immunodeficiency Virus
HRP	Horseradish peroxidase
HT	High Throughput

Ig	Immunoglobulin
IPA	Ingenuity Pathway Analysis
iPSCs	Induced Pluripotent Stem Cells
JAK	Janus Kinase
kDa	Kilodalton
KLF	Kruppel-like Factor
LDS	Lithium Dodecyl Sulphate
LGE	Lateral Ganglionic Eminence
LIF	Leukaemia Inhibitor Factor
LOXHD1	Lipoxygenase Homology Domains 1
LRRTM1	Leucine Rich Repeat Transmembrane Neuronal 1
LTM	Long-Term Memory
LTP	Long-Term Potentiation
MAPK	Mitogen-activated Protein Kinase
MECP2	Methyl Cpg Binding Protein 2
MES	2-(N-Morpholino) Ethanesulfonic Acid
MGB	Minor Groove Binder
MMP1	Matrix Metalloproteinase-1
mRNA	Messenger RNA
MSN	Medium Spiny Neurons
NAT	Natural antisense transcript
NF-κB	Nuclear Factor Kappa B
NGF	Nerve Growth Factor
NPAS4	Neuronal PAS Domain-Containing Protein 4
NR4A	Nuclear Receptor Subfamily 4 Group A
NT3	Neurotrophin-3

NT4	Neurotrophin-4
NTR	Neurotrophin Receptor
Oct-4	Octamer-Binding Transcription Factor 4
OLIG2	Oligodendrocyte transcription factor 2
PALD1	Phosphatase Domain Containing, Paladin 1
PAX6	Paired Box Protein 6
PC	Principal Component
PCA	Principal Components Analysis
PBS	Phosphate Buffered Saline
PBS-T	Phosphate Buffered Saline, 0.1 % Triton X-100
PCR	Polymerase Chain Reaction
PD	Parkinson's Disease
PDYN	Prodynorphin
PFA	Paraformaldehyde
PI3K	Phosphoinositide 3-kinase
PKB	Protein kinase B (*also Akt*)
PLCγ1	Phospholipase Cγ1
PMA	Purmorphamine
PMCH	Pro-Melanin Concentrating Hormone
PNS	Peripheral Nervous System
PTB	Phosphotyrosine Binding
PSD95	Postsynaptic Density Protein 95
qPCR	Quantitative PCR
RIN	RNA Integrity Number
RIPA	Radioimmunoprecipitation Assay
RNA	Ribonucleic Acid

ROCK	Rho-associated Protein Kinase
RPM	Revolutions Per Minute
rRNA	Ribosomal RNA
RT-PCR	Reverse Transcription Polymerase Chain Reaction
RTK	Receptor Tyrosine Kinase
SDS	Sodium Dodecyl Sulphate
SH2	Src Homology 2
shRNA	Small Hairpin RNA
siRNA	short interfering RNA
SNP	Single-Nucleotide Polymorphism
SOX2	Sex determining region Y (SRY)-Box 2
SPOC1	Survival Time Associated PHD Finger Protein in Ovarian Cancer 1
SPOCD1	SPOC Domain Containing 1
SPRY4	Sprouty RTK Signaling Antagonist 4
STAT	Signal Transducer and Activator of Transcription
STC1	Stanniocalcin 1
SSEA	Stage-Specific Embryonic Antigen
SYNPO	Synaptopodin
SYTL5	Synaptotagmin Like 5
TACR1	Tachykinin Receptor 1
TBR1	T-box, brain, 1
TBS-T	Tris-Buffer Saline, 0.1 % Tween 20
TFIIS	Transcription Elongation Factor
TGFβ	Transforming Growth Factor Beta
TH	Tyrosine Hydroxylase
TNFRSF	Tumour Necrosis Factor Receptor Superfamily

Trk	Tropomysin Receptor Kinase
TRPC	Transient Receptor Potential Cation Channel
TSHR	Thyroid Stimulating Hormone Receptor
TTX	Tetrodotoxin
TuJ1	Neuron-Specific Class III Beta-Tubulin
TWEAK	TNF-related weak inducer of apoptosis
VGF	VGF Nerve Growth Factor Inducible
VGLUT	Vesicular Glutamate Transporter
WAGR	Wilms tumour, Aniridia, Genitourinary Anomalies and Mental Retardation

TABLE OF CONTENTS

LIST OF FIGURES

Figure 5.28: Interactive MD plot generated with the Glimma package of Bioconductor displaying all genes that are differentially expressed between cultures treated with NT4 for 2 (N2) and 12 hours (N12)

Figure 5.29: Heat map of hierarchical cluster analysis with GO annotation for the top 1000 differentially expressed genes with absolute fold change >2 and $p < 0.01$

Figure 5.30: Venn diagrams illustrating the number of genes that are upregulated in the 3 treatment conditions (BDNF, AB85 and NT4) and 4 time points (30 min, 2 hours, 12 hours and 24 hours) in comparison to the untreated (control) cultures. The genes presented in this illustration are selected based on fold change > 1.5

Figure 5.31: Venn diagrams illustrating the number of genes that are downregulated in the 3 treatment conditions (BDNF, AB85 and NT4) and 4 time points (30 min, 2 hours, 12 hours and 24 hours) in comparison to the untreated (control) cultures. The genes presented in this illustration are selected based on fold change < -1.5

Figure 5.32: Venn diagrams illustrating the number of genes that are upregulated in the 3 treatment conditions (BDNF, AB85 and NT4) and 4 time points (30 min, 2 hours, 12 hours and 24 hours) in comparison to the untreated (control) cultures. The genes presented in this illustration are selected based on fold change >2

Figure 5.33: Venn diagrams illustrating the number of genes that are downregulated in the 3 treatment conditions (BDNF, AB85 and NT4) and 4 time points (30 min, 2 hours, 12 hours and 24 hours) in comparison to the untreated (control) cultures. The genes presented in this illustration are selected based on fold change < -2

Figure 5.34: Venn diagrams illustrating the number of genes that are upregulated in the 3 treatment conditions (BDNF, AB85 and NT4) and 4 time points (30 min, 2 hours, 12 hours and 24 hours) in comparison to the untreated (control) cultures. The genes presented in this illustration are selected based on fold change > 4

Figure 5.35: Venn diagrams illustrating the number of genes that are downregulated in the 3 treatment conditions (BDNF, AB85 and NT4) and 4 time points (30 min, 2 hours, 12 hours and 24 hours) in comparison to the untreated (control) cultures. The genes presented in this illustration are selected based on fold change < -4

Figure 5.36: Venn diagrams illustrating the number of genes that are upregulated in the 3 treatment conditions (BDNF, AB85 and NT4) and 4 time points (30 min, 2 hours, 12 hours and 24 hours) in comparison to the untreated (control) cultures. The genes presented in this illustration are selected based on fold change > 10

Figure 5.37: Venn diagrams illustrating the number of genes that are downregulated in the 3 treatment conditions (BDNF, AB85 and NT4) and 4 time points (30 min, 2 hours, 12 hours and 24

hours) in comparison to the untreated (control) cultures. The genes presented in this illustration are selected based on fold change < -10

Figure 5.38: Figure 5.38 Venn diagrams illustrating the number of genes that are upregulated in the 3 treatment conditions (BDNF, AB85 and NT4) and 4 time points (30 min, 2 hours, 12 hours and 24 hours) upon comparison of the three TrkB ligands with each other. The genes presented in this illustration are selected based on adjusted p value < 0.01 and fold change > 1.5 (A.), fold change > 2 (B.), fold change > 4 (C.)

Figure 5.39: Venn diagrams illustrating the number of genes that are downregulated in the 3 treatment conditions (BDNF, AB85 and NT4) and 4 time points (30 min, 2 hours, 12 hours and 24 hours) upon comparison of the three TrkB ligands with each other. The genes presented in this illustration are selected based on adjusted p value < 0.01 and fold change > 1.5 (A.), fold change > 2 (B.), fold change > 4 (C.).

Figure 5.40: Expression fold changes relative to the control of 7 genes obtained with RNA SEQ and RT PCR

LIST OF TABLES

Table 5.13: Table with gene names and description preferentially upregulated by NT4 at time point 12 hours with adjusted p value <0.01 and fold change > 4.

Table 5.14: Table with genes preferentially upregulated by both BDNF and NT4 compared to AB85 at time point 12 hours with adjusted p value <0.01 and fold change > 2.

Table 5.15: Table with gene names preferentially downregulated by AB85 at time point 12 hours with adjusted p value <0.01 and fold change > 2.

Table 5.16: Table with G0 analysis for the 252 genes preferentially downregulated by NT4 at time point 12 hours compared to BDNF and AB85 with adjusted p value <0.01 and fold change > 2.

Table 5.17: Table with genes downregulated and preferentially downregulated by NT4 at time point 12 hours with adjusted p value <0.01 and fold change > 4.

Table 5.18: Table with the names of genes preferentially downregulated by NT4 at time point 12 hours with adjusted p value <0.01 and fold change > 4.

Table 5.19: Table with G0 analysis for the 93 genes preferentially downregulated by AB85 at time point 24 hours compared to BDNF and NT4 with adjusted p value <0.01 and fold change > 2.

Table 5.20: Table with genes upregulated by both BDNF and NT4 compared to AB85 at time point 24 hours with adjusted p value <0.01 and fold change > 4.

CHAPTER 1: INTRODUCTION

1.1 Nerve growth factor and its discovery

The early discovery of nerve growth factor (NGF) by Rita Levi-Montalcini was a major milestone in the history of biology as it was the first growth factor to have been identified (Levi-Montalcini, 1987). In addition, the rapid exploitation of this discovery allowed the early demonstration that a defined molecular entity is critical for the development of specific populations of neurons (Cohen, 1960). The origin of this discovery can be traced to manipulations of developing chick embryos consisting in particular in the early extirpation of limb or wing buds followed by observation of the developing spinal cord and dorsal root ganglia (Bueker, 1948). Initial experiments by Marian Lilian Shorey (1909, not in Pubmed), later repeated by Viktor Hamburger (1934) had suggested that peripheral tissues can somehow regulate the number of developing neurons, including in particular spinal cord motoneurons destined to innervated the limbs. In the absence of limb or wing buds, the observation was that fewer motoneurons survived in the ventral spinal cord on the side of the embryos that had been operated (Hamburger,1934 not in pubmed). Elmer D. Bueker, a PhD student working with Hamburger tested then the possibility that any cell mass could substitute for the missing limb and support the survival of neurons (Bueker, 1948). Amongst three tumour cell lines tested, sarcoma 180 cells not only survived but also led to an increase in the size of dorsal root ganglia and to sensory nerves invading the tumour tissue (Bueker, 1948). By contrast, these sarcoma cells failed to rescue motoneurons. Following the publication of these observations, Rita Levi-Montalcini joined the laboratory of Viktor Hamburger at Washington University (St Louis, Missouri) to clarify the interpretation of the limb ablation experiments on motoneuron development. Indeed, using the chick she had performed similar limb ablation experiments in Turin with Giuseppe Levi and whilst she obtained similar results, i.e., a loss of motoneurons following limb ablation, she favoured the interpretation that it may be a loss of synaptic contacts as opposed to a limb-derived factor favouring the division of motoneurons that could best account for the loss of motoneurons (Levi and Levi-Montalcini, 1942). During her stay in St. Louis, Levi-Montalcini became aware of Bueker's findings and

decided to replicate them, also using a second sarcoma, line 37. An important initial result of the collaboration between Levi-Montalcini and Hamburger was also a well-documented observation on the phenomenon of naturally occurring cell death in dorsal root ganglia, as well as its attenuation by the removal of the corresponding limb-bud (Hamburger and Levi-Montalcini, 1949). When Levi-Montalcini repeated the tumour transplantation work initiated by Bueker, she noted a dramatic increase in the size of sympathetic and sensory ganglia, as well as in the number of their axons (Levi-Montalcini and Hamburger, 1951). As some of the hyper-innervated territories were distant from the tumour, the important new conclusion was also reached that the tumour cells may secrete a “diffusible agent” (Cohen et al., 1954)(Levi-Montalcini and Hamburger 1953). The next crucial step was the design and use of an *in vitro* assay using explanted dorsal root ganglia grown in a plasma clot (Levi-Montalcini et al., 1954). Exposing this explant to tumour extracts led to massive axonal outgrowth (designated as “halo”), which then became the assay used by Stanley Cohen to purify what later became known as nerve growth factor NGF (Levi-Montalcini and Hamburger, 1951, Cohen et al., 1954, Levi-Montalcini, 1952). NGF was ultimately purified from the adult male mouse submandibular gland that turned out to contain large amounts of NGF (Cohen, 1960). The combined efforts of Levi-Montalcini and Cohen not only resulted in the characterization of NGF but also in the demonstration of its biological relevance following the administration of antibodies blocking its biological activity to new-born mice (Cohen, 1960, Levi-Montalcini and Booker, 1960). These discoveries were awarded with the Nobel Prize in 1986 "for their discoveries of growth factors".

1.2 BDNF

1.2.1 BDNF: a member of the neurotrophin family

The characterization of NGF was facilitated by the identification of the adult male mouse submandibular gland as a uniquely rich source of NGF, as well as of epidermal growth factor (EGF (Cohen, 1964). There is still no satisfactory explanation for such an enrichment in this particular organ in the mouse. The list of growth factors beyond NGF and EGF grew slowly given the considerable technical difficulties in characterising growth factors and cytokines typically present in minute amounts in tissue. Whilst BDNF turns out to be the most widely expressed neurotrophin in the adult central nervous system (CNS), the initial study reporting on its characterization indicated that 2 µg could be purified from 3 kg of pig brain, thus suggesting that it is a protein of very low abundance (Barde et al., 1982). Indeed, it turned out to be challenging to obtain reliable sequence information as the last step of the procedure involved a two-dimensional gel electrophoresis and an exceedingly high purification factor (Barde et al., 1982); Barde, personal communication). Reliable sequence information could eventually be obtained following significant modifications of the initial procedure and could be used to amplify the corresponding BDNF nucleotide sequences from a pig genomic DNA template (Hofer and Barde, 1988, Leibrock et al., 1989). When expressed in COS cells this cDNA directed the secretion of biological activity allowing the survival of a population of sensory neurons complementary to those supported by NGF (Leibrock et al., 1989). Whilst BDNF does not support the survival of sympathetic neurons, it does act on placode-derived sensory neurons not supported by NGF. Sequence analysis revealed that NGF and BDNF are structurally related (Leibrock et al 1989) and the use of short, highly conserved sequences between BDNF and NGF allowed the generation of primers amplifying not only NGF and BDNF sequences, but also of neurotrophin-3 (Hohn et al., 1990, Jones and Reichardt, 1990, Maisonpierre et al., 1990, Rosenthal et al., 1990) and neurotrophin-4 (NT4) (Berkemeier et al., 1991, Hallbook et al., 1991, Ip et al., 1992).These 4 secreted factors, namely NGF, BDNF, NT3 and NT4 form the neurotrophin family. They all bind to the same receptor, the neurotrophin receptor p75, a member of the tumor necrosis factor receptor family, as well as to one of three tyrosine kinase

receptors of the tropomyosin-related kinase (or Trk) family causing dimerization and auto-phosphorylation of their tyrosine residues (Barbacid, 1995, Kaplan et al., 1991).

1.2.2 BDNF: Gene organisation and transcription

The organization of the BDNF gene is quite complex, more so than the 3 other neurotrophins genes (West et al., 2014). It contains multiple 5' noncoding exons and one protein-coding exon. The human BDNF gene spans about 70 kb of chromosome 11p14.1 and contains 11 exons that are spliced into 17 splicing variants. Eight exons are conserved between humans, mice and rats and as many as nine promoters have been identified (West et al., 2014).

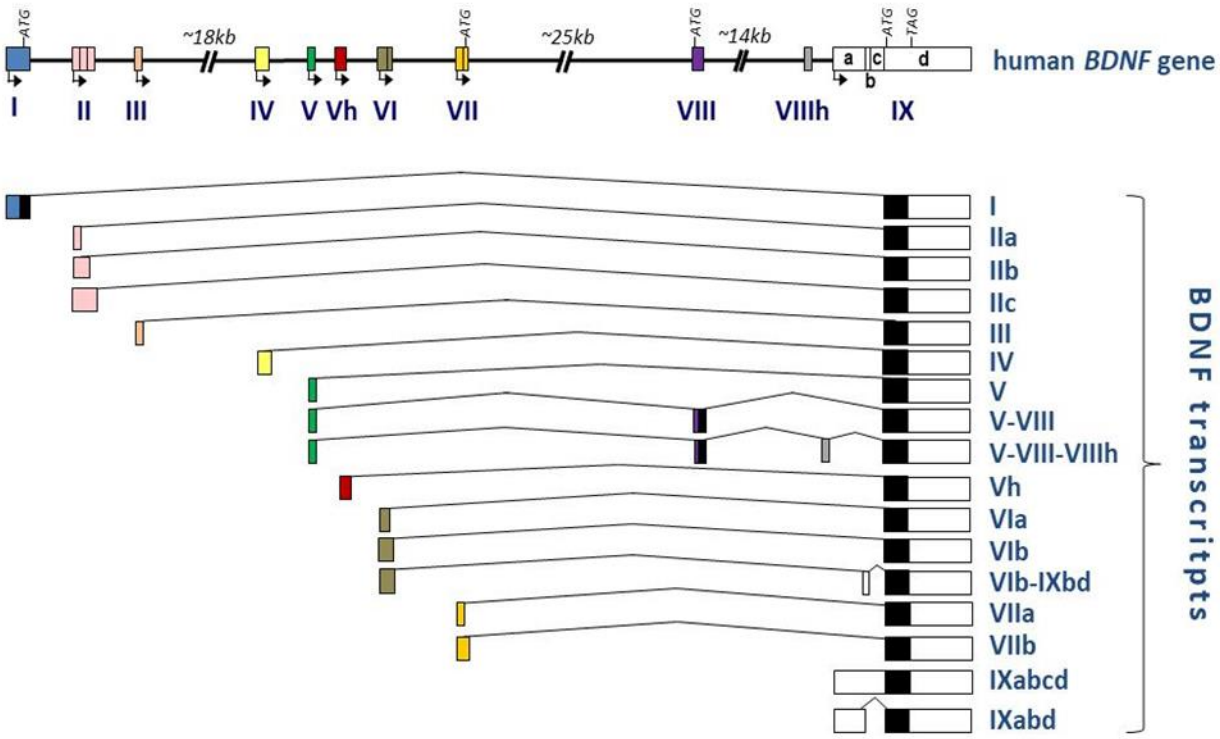

Figure 1.1 *Human BDNF gene contains 11 exons, but only exon IX is coding for* BDNF *protein (top). These exons are spliced into 17 splicing variants (bottom). The exons are shown as boxes and introns as lines. Filed boxes correspond to the translated regions of the exons and open boxes correspond to the untranslated regions of the exons. Exon numbers are shown are shown in Roman numerals. BDNF exon IV is divided into regions a,b,c,d. The figure is adapted from Pruunsild et al., 2007.*

Whilst the functional relevance of these numerous promoters is not yet fully understood, the expression of BDNF in a range of different cells and tissues suggests that gene expression is likely to be regulated by different mechanisms. The most studied promoters are I and IV which are known to be particularly responsive to neuronal activity. This involves mechanisms able to sense the levels of intracellular calcium and regulate CREB activity (West et al., 2014). Thus, for example in the mouse, promoter IV contains different calcium-response elements (caREs) inside the proximal Bdnf promoter, as well as cAMP Response Element (CRE) where CaRF and CREB bind and initiate transcription. At least eight different transcription factors have been demonstrated to bind to CaREs in Bdnf promoter IV including the activity-inducible transcription factor NPAS4, an immediate-early gene with minimum expression in the absence of membrane depolarization. Following calcium influx, NPAS4 levels increase rapidly and robustly (Lin et al., 2008).

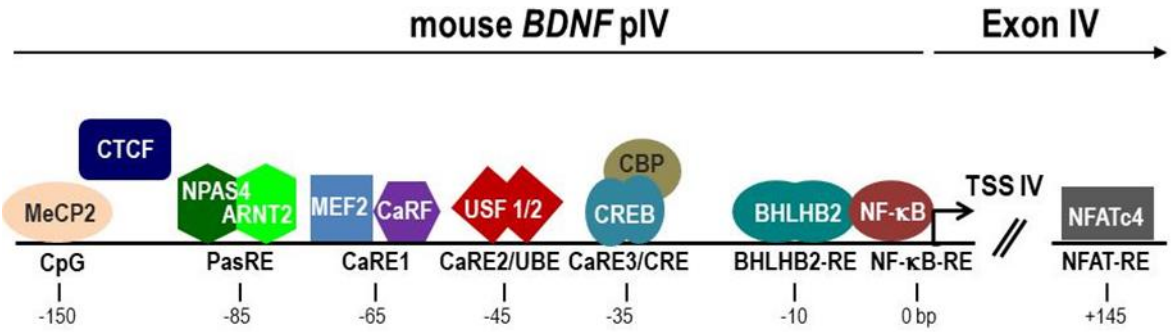

Figure 1.2 *Promoter IV of BDNF is regulated by neuronal activity and more than eight different transcription factors bind to its calcium-reponse elements. The Transcription Factors (TFs) that are known to regulate activity-dependent Bdnf exon IV transcription are methyl-CpG binding protein (MeCP2), CCCTC-binding factor (CTCF), Neuronal PAS Domain Protein 4, Aryl Hydrocarbon Receptor Nuclear Translocator 2 (ARNT2), Myocyte Enhancer Factor 2A (MEF2), Calcium Responsive Transcription Factor (CaRF), Upstream Transcription Factor 1&2 (USF1/2), CAMP Responsive Element Binding Protein 1 (CREB) and CREB Binding Protein (CBP), Basic Helix-Loop-Helix Family Member E40 (BHLHE40), nuclear factor kappa-light-chain-enhancer of activated B cells (NF-kB), Nuclear Factor Of Activated T Cells 4 (NFATc4). The TFs that bind to cis-regulatory DNA elements in the promoters are presented above the line that represents DNA, and the cis-elements are shown below the factors. CTCF which is known to contribute to regulation, but its exact binding site is uknown, therefore it is presented above the promoter. Transcription start site 4 (TSSs) is indicated with an arrow. Distance in base pairs (bp) relative to TSS IV is presented below the line*

Intriguingly, a human natural antisense transcript (NAT) transcribed from the opposite strand has been identified by RT-PCR in 22 different adult human tissues including the brain, kidney, spinal cord and testes (Pruunsild et al., 2007). The gene encoding the antisense transcript spans over 191 kb and consists of 10 exons. The transcription seems to be directed by a single promoter. A total of sixteen splice variants have been described with one exon common to all. No open reading frames have been identified in any of them. Its 225 nucleotides are 100% complementary to all splice variants of BDNF mRNA. As BDNF NATs are expressed in the human brain, it is conceivable that BDNF NATS may form RNA-RNA complexes *in vivo* with BDNF sense mRNAs. One study indicates that such NATs may also exist in the mouse (Modarresi et al., 2012). Despite differences in the structure of antisense mRNAs between two species the 225-bp overlapping region show 90% homology whereby the antisense levels were reported to be present at 10- to 100-fold lower levels compared to the Bdnf sense transcripts, with the exception of testes, kidney and heart. Moreover, knockdown of BDNF NATS with short interfering RNA (siRNA) molecules in HEK293T cells have been found to increase BDNF levels *in vitro*. As a further validation of a regulatory role of BDNF-AS mRNA for the sense mRNA, mouse neuroblastoma N2a cells have been treated with single-stranded DNA oligonucleotides (antagoNAT) to inhibit the activity of the antisense transcript, resulting in an increase of the *Bdnf* mRNA levels (Modarresi et al., 2012). However, the physiological relevance of the antisense transcript is still unclear, as are the mechanisms potentially regulating the activity of the antisense promoter.

1.2.3 Roles of BDNF in the development of the nervous system

A physiological role for BDNF during development was first suggested by *in vivo* experiments consisting of the addition of purified BDNF to developing quail embryos (Hofer and Barde, 1988). These experiments revealed that normally occurring cell death could be reduced in (neural crest-derived) dorsal root ganglia as well as in (placode-derived) nodose ganglia (Hofer and Barde, 1988). The *in vivo* requirement for BDNF for the survival of specific populations of sensory neurons was later demonstrated using mice lacking functional BDNF expression (Ernfors et al., 1994, Jones et al., 1994). This mutation is not compatible with long-term survival of the animals with most of them dying during the first few weeks after birth. Later experiments suggested that the absence of BDNF in non-neuronal tissues is likely to explain the loss of sensory neurons associated with blood pressure regulation, the development of balance and feeding. Indeed, the conditional deletion of BDNF specifically from the nervous system is compatible with long-term survival of the animals (Rauskolb et al., 2010). With regard to peripheral sensory ganglia, a detailed analysis of BDNF conditional knockout mice suggested that the movement and balance abnormalities could be explained by a severe loss (up to 90%) of neurons in the vestibular ganglia, whilst the number of neurons remained unchanged in the cochlear ganglia. In the trigeminal ganglia, up to 40% of the neurons were lost, in agreement with earlier *in vitro* experiments indicating that placode-derived neurons are BDNF-responsive, whilst the neural crest-derived neurons respond to and need NGF for survival (Davies and Lindsay, 1985). In the nodose-petrosal complex the sensory ganglia are involved in the regulation of respiration, heart rate and blood pressure, and the number of surviving neurons was reduced by 68% (Conover et al., 1995), with most remaining neurons responding to NT-4 . The early death of animals carrying germline deletion of both *Bdnf* alleles precluded for some time meaningful analyses of the role of BDNF in the brain. This was particularly problematic as BDNF levels, whilst still very low in the adult CNS (see above) increase by about 10-fold in rodents during the first three post-natal weeks. A role for BDNF in the adult mouse brain became evident following the use of floxed alleles of *Bdnf* selectively excised by the Cre recombinase driven by the α-calcium/ calmodulin-dependent protein kinase II (CamKII) promoter, which drives expression in postmitotic neurons (Minichiello et al., 1999) leading to elimination of *Bdnf* mRNA expression after the second postnatal week from hypothalamus, hippocampus and cortex (Rios et al., 2001). Consequently,

this animal model can be used to study BDNF depletion in the adult brain. Another animal model was designed using the Emx1 promoter expressed as early as E10.5 in the developing cerebral cortex (Chan et al., 2006, Chan et al., 2008, Baquet et al., 2004).The selective elimination of BDNF from the cortex led to a significant reduction of the size of the striatum and single cell analysis of the medium spiny neurons (MSN) revealed smaller cell somas, fewer branches on dendrites as well as reductions in spine numbers (Baquet et al., 2004) . Analyses of these animals after 12 months revealed a 35% decrease in the number of striatal neurons, suggesting that long term deprivation of BDNF may affect the survival of these inhibitory neurons. Neuronal shrinkage and dendritic retraction were also observed in the visual cortex of these animals (Gorski et al., 2003). The work with these animals suffering from BDNF deprivation in the striatum also fits well with previous work indicating that the striatum receives its BDNF supply from the cerebral cortex by anterograde transport (Altar et al., 1997). Indeed, there is minimal expression of the *Bdnf* gene in the striatum and experiments interrupting the supply from the cortex by surgery had indicated that the BDNF levels in the striatum are massively reduced upon surgery (Altar et al., 1997). Using Cre-mediated excision of floxed *Bdnf* alleles and the Tau promoter that is active in all neurons, later allowed the demonstration that BDNF is not essential for the survival of most CNS neurons up to 2 months after birth (Rauskolb et al., 2010). Detailed investigations in the hippocampus in particular revealed that the morphology of the pyramidal cells is barely affected, whilst the phenotype of striatal neurons caused by the interruption of the cortical supply of BDNF could be replicated (Rauskolb et al., 2010; see above). It thus appears that the GABAergic, medium spiny neurons that comprise the vast majority of the striatum require BDNF for their postnatal dendritic growth and that this requirement is ensured by a BDNF supply from sources external to the striatum, principally the cerebral cortex.

1.2.4 BDNF and synaptic plasticity

The availability of mice lacking normal levels of BDNF expression in the brain made it also possible to explore its role in synaptic transmission in the hippocampus. The lack of only one allele of *Bdnf* led to severe reduction in the ability of high frequency stimulation of the Schaffer collaterals to cause long-term potentiation of synaptic transmission in CA1 neurons (Korte et al., 1995). Conversely, the addition of recombinant BDNF to hippocampal slice cultures potentiates synaptic transmission

(Kang and Schuman, 1995) and can restore LTP in slice cultures from BDNF-deprived animals (Patterson et al., 1996, Figurov et al., 1996). Furthermore, acute inhibition of BDNF activity in adult hippocampus using BDNF scavenger TrkB-IgG reduced LTP (Figurov et al., 1996).

LTP is widely viewed as a useful cellular model for long-term memory (LTM), and in line with results indicating that decreased levels of BDNF compromise LTP, impaired memory performance could be observed in mice lacking one allele of *Bdnf*, that were tested in the Morris water maze (Linnarsson et al., 1997) as well as in contextual fear conditioning (Liu et al., 2004). In addition, transgenic mice over-expressing truncated TrkB in neurons display impaired long-term spatial memory (Saarelainen et al., 2000), whereas over-expression of full length TrKB lead to enhanced learning and memory as assessed by water maze, contextual fear conditioning, and conditioned taste aversion tests (Koponen et al., 2004).

1.2.5 The Val66Met BDNF polymorphism

Following the identification of a single-nucleotide polymorphism (SNP) in the human BDNF gene, tests of episodic memory were performed on homozygote carriers of this polymorphism that leads to the substitution of valine (V) by methionine (M) at the residue 66 (Val66Met) in the pro-domain of BDNF. In this study, it was shown that the Val66Met carriers had impaired episodic memory (Egan et al., 2003). The results of these studies later confirmed in a different cohort (Cathomas et al., 2010) generated considerable interest even if the biochemical consequences of this amino acid replacement in human pro-BDNF remain unclear. Reduced BDNF secretion and/or altered interactions between BDNF and its pro-peptide have been suggested to explain the functional consequences of this Val/Met polymorphism, but the results remain open to criticism given that most have been obtained using overexpression paradigms (Egan et al., 2003, Chiaruttini et al., 2009). Interestingly, a mouse model has been generated in an attempt to mimic this polymorphism, but while memory was not affected in these animals, they showed increased anxiety (Chen et al., 2006). Also, the Met BDNF pro-peptide has been shown to cause growth cone collapse (Anastasia et al., 2013)

In sum, the discovery of the Val/Met polymorphism represents an important development and the link with memory is of great interest, not least because of the

role of BDNF in LTP. However, the absence of reliable data regarding the biochemical impact of the Val/Met substitution and the fact that the mouse model does not seem to replicate the phenotype observed in humans are a source of concern, not least because the incidence of the Val/Met polymorphism varies considerably when different ethnic groups are compared. A study involving 58 different groups and 68 SNPs spanning the BDNF genomic region indicated that the frequency of the Val/Met polymorphism varies between 0% and 72% across the 58 global populations (Petryshen et al., 2010). These results suggest a positive selection of an entire genomic region during the course of evolution and caution is needed in order to establish a direct causality between the single Val/Met polymorphism and memory performance.

1.2.6 BDNF and the regulation of body weight

Energy balance and body weight are tightly controlled by interactions between the brain and peripheral tissues and their dysregulation can lead to obesity or cachexia. The first suggestion for BDNF involvement in the control of feeding behaviour came from rodent studies demonstrating that the intra-ventricular delivery of BDNF can reduce weight gain (Lapchak and Hefti, 1992). *Bdnf*$^{+/-}$ *mice* were shown in later studies to be hyperphagic and obese, suggesting that BDNF is involved in the regulation of food intake (Lyons et al., 1999, Kernie et al., 2000). In line with this, mice expressing 25% of the normal levels of TrkB exhibit excessive feeding (Xu et al., 2003). A more recent study indicated that low levels of BDNF correlate with decreased function of the α2δ-1 calcium channel subunit that is also a thrombospondin receptor in the hypothalamus, a structure known to be critical for the regulation of food intake and body weight regulation. Thus, inhibiting alpha2/delta-1 in wild-type animals causes significant increase in food intake and weight gain whilst conversely, correcting the alpha 2/delta-1 deficiency reduces overeating and weight gain (Cordeira et al., 2014). Genetic studies in humans strongly support the role of BDNF/TrkB signalling in energy balance regulation. Severe hyperphagia and obesity have been reported in young patients carrying a de novo missense (Y722C) mutation in the TrkB gene that perturbs MAP kinase activation (Yeo et al., 2004). Moreover, a more recent study of WAGR syndrome (Wilms tumour, Aniridia, Genitourinary anomalies, and mental Retardation) which is caused by the loss of one functional BDNF allele, found decreased adaptive behaviour and cognitive function (Han et al., 2013). WAGR syndrome is caused by

11p13 deletions of varying size near the BDNF locus and can be used as a model for studying human BDNF haploinsufficiency. Interestingly 100% of WAGR patients that are BDNF haploinsufficient are obese by 10 years of age whilst only 1 in 5 patients become obese when BDNF gene is not affected by the deletion (Han et al., 2008).

1.2.7 BDNF and neurodegeneration

Given its role during development and in the adult rodent brain, numerous studies have attempted to correlate the levels of BDNF with various conditions, including Huntington's, Alzheimer's and Parkinson's (HD, AD and PD) diseases. Whilst most of the measurements of BDNF levels have been determined from human serum samples, results are very difficult to interpret not least because of technical problems. Indeed, there are difficulties in measuring BDNF levels accurately in human serum with commercially available immunoassays. Whilst it has been known for several years that human platelets store high levels of BDNF (Yamamoto and Gurney, 1990), it has been recently argued that the accumulation of BDNF in platelets is unlikely to reflect brain levels and that the platelet progenitors, bone marrow megakaryocytes are a more likely source (Chacon-Fernandez et al., 2016). Indeed, these cells express the BDNF gene at significant levels, which is not the case in the mouse. This correlates with the absence of detectable levels of BDNF in mouse blood, including platelets (Chacon-Fernandez et al., 2016). Given the demonstration that BDNF does not cross the blood-brain barrier (Pardridge et al., 1994), correlations between BDNF levels in the brain and neurodegenerative diseases can only be established post-mortem. Early reports that the levels of *BDNF* mRNA are decreased in several brain areas in the brain of AD patients (Phillips et al., 1991) were recently confirmed in the prefrontal cortex (Buchman et al., 2016). Likewise decreased levels of *BDNF* mRNA have been reported in the substantia nigra of PD patients (Howells et al., 2000). In HD the plausibility of an involvement of BDNF is mostly supported by work in the mouse as well as cell culture experiments. Huntingtin is a ubiquitous protein of unknown function that is elongated by polyglutamine repeats in HD. The severity of the condition has been correlated with the length of these repeats and the mutant protein is thought to have a toxic effect on striatal neurons (Andrew et al., 1993, Li et al., 2000) . Whilst it is conceivable that the death of the striatal neurons may be due to the loss of some unknown beneficial activity of the wild-type protein or alternatively that these neurons are particularly sensitive to the mutant forms of huntingtin, an involvement of BDNF is

also possible and has been closely examined in rodent and cellular models. As noted (see above), an anterograde supply of BDNF from cortical neurons seems to be necessary for the post-natal development of striatal neurons (Baquet et al., 2004). Additionally, the transcription of BDNF has been reported to be negatively affected by mutant forms of huntingtin (Zuccato et al., 2001). In addition, post-mortem studies on the brains of HD patients indicate that BDNF levels in the striatum are reduced, but are unaffected in the cortex (Ferrer et al., 2000, Gauthier et al., 2004). It has also been proposed that mutant forms of huntingtin interfere with the anterograde transport of BDNF-containing vesicles (Gauthier et al., 2004).

1.2.8 Increasing BDNF levels

The studies summarised in the above have generated considerable interest in the possibility of increasing the levels of BDNF in order to improve neurological conditions. This notion is also supported by a considerable body of work indicating that physical exercise may retard cognitive decline during ageing and in patients at risk for AD (Ahlskog et al., 2011, Lautenschlager et al., 2008). Work in rodents has firmly established that brain levels of BDNF increase as a function of activity (Berchtold et al., 2010). Whilst in humans, the levels of BDNF also increase in serum after physical exercise (Ferris et al., 2007), although the reasons for this increase are still not understood. Because the increase in serum BDNF levels can often be observed after short periods of time following exercise, they may indicate changes in platelet reactivity and the possible impact of increased platelet-derived BDNF on brain function remains a matter of speculation. As BDNF exerts its function through binding to TrkB receptor it is important to ensure that TrkB expression is not significantly altered in patients. BDNF cannot be administered peripherally as previous studies have indicated that much of what is injected does not diffuse away significantly from the site of injection and what does reach the blood circulation is rapidly eliminated by filtration through the kidney with no relevant quantities reaching the brain (Pardridge et al., 1994). BDNF has also been administered intrathecally in the context of a clinical trial that examined the potential benefits of BDNF infusion in patients with amyotrophic lateral sclerosis (Ochs et al., 2000). However, the premature termination of the trial made it difficult to draw definitive conclusions as to the potential benefits of this therapy, which also appears unlikely to be applicable on a large scale. Alternative strategies such as delivery using lentivirus and other vectors are also being considered but so far have

not reached a stage where they can be evaluated (Nagahara and Tuszynski, 2011). Whether or not BDNF levels can be increased by increasing neuronal activity has also been considered. Whilst initial attempts using excitatory neurotransmitter mimics such as ampakines looked promising (Simmons et al., 2009) it remained unclear if positive effects could be clearly dissociated from excitotoxicity. More recently, the sphingosine analogues Fingolimod, a mild immunosuppressant used extensively in the context of multiple sclerosis has been shown to increase brain BDNF levels in mice (Deogracias et al., 2012) and to also improve the behaviour of mice lacking Mecp2 (Deogracias et al., 2012), a gene mutated in most cases of Rett syndrome (Amir et al., 1999).

1.3 NEUROTROPHIN RECEPTORS

1.3.1 Introduction

The 4 mammalian neurotrophins are known to interact with 4 receptors, namely p75NTR, TrkA, TrkB and TrkC (Bothwell, 1991). All 4 neurotrophins bind and activate p75NTR both as pro-neurotrophins and as mature neurotrophins. Interestingly, pro-neurotrophins have been reported to bind to p75NTR with a substantially higher affinity than mature neurotrophins and to efficiently cause cell death (Lee et al., 2001). Mature NGF preferentially binds to TrkA, NT3 to TrkC, but also activates significantly TrkA and TrkB whilst BDNF and NT4 both bind to TrkB with similar affinities (Barbacid, 1995) (Figure 1.1). What is now known as p75NTR was the first neurotrophin receptor to have been discovered and was initially named the NGF receptor. Indeed, NGF was the only known neurotrophin to have been characterized at the time and it was used to identify its first receptor by expression cloning using human and rat libraries (Johnson et al., 1986, Radeke et al., 1987). This “NGF receptor” was also the founding member of what turned out to be the large tumor necrosis factor receptor family (Armitage, 1994). Following the characterization of BDNF, binding studies indicated that BDNF also binds to the then NGF receptor (Rodriguez-Tebar et al., 1990), later renamed p75NTR, or TNFSR16. The Trk receptors were discovered later whereby a milestone was the discovery and characterization of an oncogene associated with human colon carcinoma and the realization that it was a fusion protein consisting of tropomyosine fused with the kinase domain of what later became known as TrkA (Martin-Zanca et al., 1986, Martin-Zanca et al., 1989). The specific expression of TrkA in neurons known to respond to NGF (revealed by in situ hybridization) was rapidly

followed by the demonstration that NGF activates its kinase domain. TrkB and TrkC were discovered based on their sequence homology to TrkA and as BDNF, NT3 and NT4 had been identified in the meantime, their respective ability to bind and activate their respective receptors could be rapidly confirmed (Kaplan et al., 1991, Klein et al., 1991b, Hempstead et al., 1991, Klein et al., 1991a, Soppet et al., 1991, Squinto et al., 1991, Berkemeier et al., 1991, Lamballe et al., 1991, Klein et al., 1992, Ip et al., 1992). Like all TNFRS, p75NTR is devoid of enzymatic activity and needs to interact with cytoplasmic proteins to transduce messages following ligand binding (Volonte et al., 1993, Susen et al., 1999). This has greatly complicated the definition of the exact role played by this receptor in the nervous system whereby a consensus has emerged that p75NTR often mediates effects that counteracts those of Trk activation, in some cases even cell death, like other TNFRS members (Dechant and Barde, 2002). The Trk family of tyrosine kinase receptors are single-pass transmembrane proteins composed of a heavily glycosylated extracellular domain containing three leucine-rich repeats, two cysteine repeats and two immunoglobulin-like C2 motifs, a transmembrane domain and a kinase domain. The tyrosine kinase domain faces the cytoplasm and is highly related between the 3 Trk receptors and shares many structural features with other tyrosine kinase receptors, such as the insulin receptor (Geetha et al., 2013). The interaction of Trk with their corresponding ligands is mediated through the second Ig domain (Ultsch et al., 1999, Wiesmann et al., 1999).

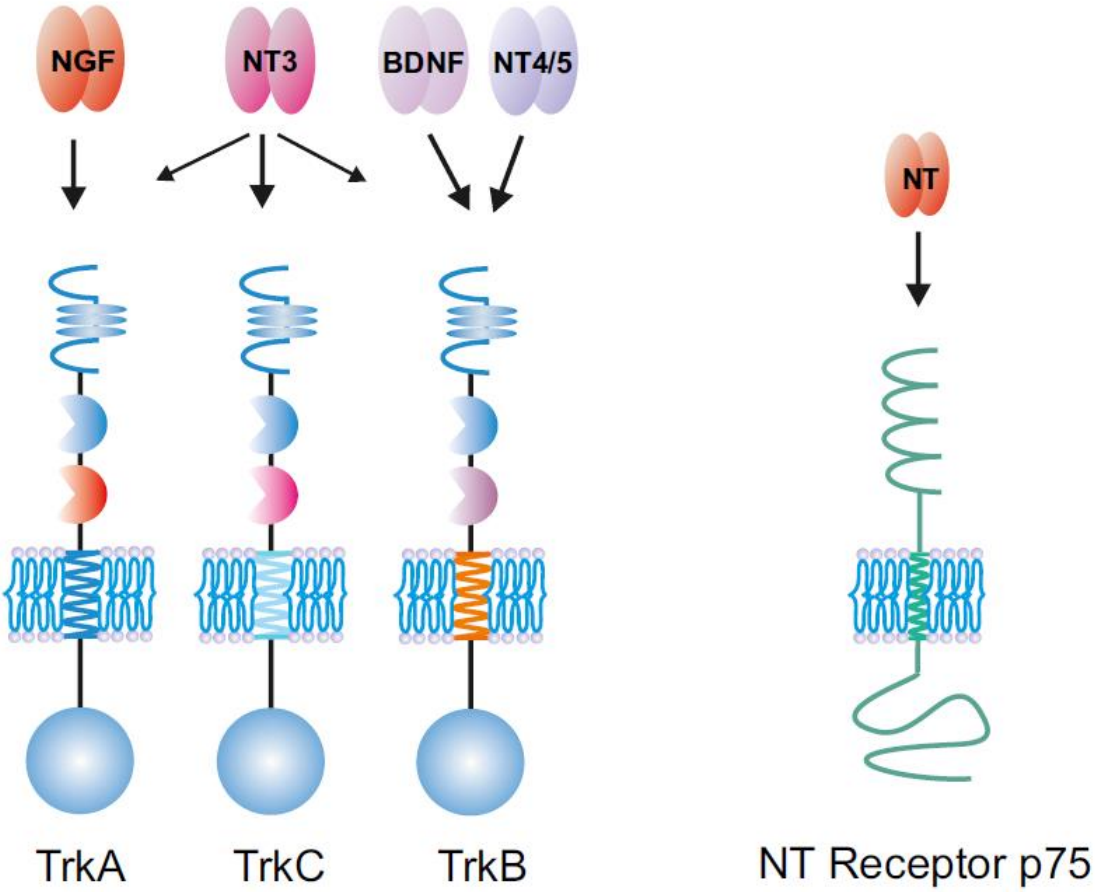

Figure 1.3 *All neurotrophins activate p75 receptor, while mature neutrophins bind and activate Trk receptors as indicated in the scheme.*

1.3.2 Relevance of neurotrophin receptors *in vivo*

Like has been the case with neurotrophins, gene targeting experiments have been informative in delineating the role of the 4 neurotrophin receptors *in vivo*. Most of the trophic effects of the neurotrophins are mediated by the activation of one of the Trk receptors and detailed analyses of mouse mutants lacking each of the Trk receptors essentially confirmed what could be expected given the results of *in vitro* binding specificities (Klein et al., 1993, Klein et al., 1994, Smeyne et al., 1994). However, detailed analyses indicated that mutant mice lacking NT3 lose more neurons than those lacking TrkC both in sensory and in sympathetic ganglia (Liebl et al., 1997). One possible explanation for this observation could be that early in the development, when p75NTR levels are low, NT3 signals not only through TrkC but also through TrkA and TrkB. Indeed, TrkA expressing trigeminal neurons are lost by E13.5 and TrkB expressing trigeminal neurons are lost by E11.5, when NT-3 knockout embryos had been exposed to antisera specific for TrkA and TrkB respectively (Huang et al., 1999). A further explanation could be found in the discovery that TrkC acts as a dependence receptor, i.e. a receptor causing death in the absence of its cognate ligand (Tauszig-Delamasure et al., 2007). Intriguingly, a recent study extended these findings to TrkA, eventually explaining why TrkA-expressing neurons require NGF during development as it is the expression of the NGF receptor that makes them dependent on NGF for survival (Nikoletopoulou et al., 2010). Re-analysis of the corresponding mouse mutants confirmed that the death of sympathetic and sensory neurons lacking TrkA is delayed compared to wild-type animals. With regard to p75NTR, like is the case with most TNFR members, the elimination of the gene does not cause the death of the animals but does lead to changes in the innervation of target fields by sensory and sympathetic neurons (Lee et al., 1992). Additionally, *in vitro* experiments indicated that the lack of p75NTR increases the concentrations of neurotrophin needed for survival (Lee et al., 1994), in line with binding experiments indicating that the expression of p75NTR together with TrkA increases the binding affinity of NGF (Hempstead et al., 1991).

1.3.3 BDNF and TrkB signalling

The BDNF/NT4 receptor TrkB is widely expressed throughout the CNS and the PNS. TrkB isoforms with different extracellular domains can be generated through differential mRNA splicing, with some of these splice variants modulating the binding

characteristics of ligands to TrkB. In particular, a short insert in the juxta-membrane region of TrkB facilitates its activation by NT3 and NT4, whereas the absence of this insert increases the specificity for BDNF (Strohmaier et al., 1996). Additionally, two alternatively spliced truncated receptors designated TrkB-T1 and TrkB-T2 with extracellular and transmembrane domains identical to full length TrkB lack the entire kinase domain. The function of these two splice variants that are highly expressed by glial cells in particular is not entirely clear though it has been proposed that they may further limit the diffusion of BDNF from its sites of secretion (Biffo et al., 1995). Conversely, when use as soluble, i.e., non-membrane bound reagents they facilitate the diffusion of BDNF (Croll et al., 1998). Like all neurotrophins, the BDNF homodimers cause TrkB activation by dimerization (Barbacid, 1995). Upon ligand binding the intracellular tyrosine kinase domains are activated and the close proximity brought about by dimerization causes tyrosine residues to be phosphorylated. Tyrosine phosphorylation generates binding sites for adaptor proteins such as Src homology 2 (SH2) domain- and phosphotyrosine binding (PTB) domain-containing proteins. These proteins initiate signalling cascades including the activation of protein kinases including mitogen-activated protein kinases (MAPKs), phosphoinositide 3-kinase (PI3K) and phospholipase Cγ1 (PlCγ1) (Patapoutian and Reichardt, 2001, Reichardt, 2006). The MAPK signalling pathway has been shown to enhance cell survival by mechanisms including phosphorylation and inhibition of the pro-apoptotic proteins such as BAD (Bonni et al., 1999) , as well as by increased expression of pro-survival genes in a CREB-dependent manner. For example, the pro-survival gene BCL-2 is a target of CREB in cerebellar granule neurons (Finkbeiner, 2000). The PI3K pathway has also been suggested to exert a prominent pro-survival role upon activation (Atwal et al., 2000). The downstream effector of PI3K activation is Akt (also designated PKB), a serine/threonine kinase (Franke et al., 1997) and the PI3K/Akt pathway is necessary for neurotrophin-dependent survival in CNS neurons (Brunet et al., 2001). The PLCγ pathway activation caused by phospho-TrkB also activates the transient receptor potential cation channels (TRPC) (Li et al., 1999, Amaral and Pozzo-Miller, 2007) . The resulting increase in intracellular calcium levels subsequently positively regulates BDNF expression through a positive feed-back loop (Shieh et al., 1998) as BDNF is synthesized and released in an activity-dependent manner (Hartmann et al., 2001). As noted, (see above) the significance of TrkB during development has been demonstrated *in Trkb*$^{-/-}$ mice which turned out to have a similar

phenotype to *Bdnf*$^{-/-}$ mice. Both mutants die in the first days or few weeks after birth as a result of neuronal losses affecting primarily the peripheral nervous system (see above). The loss of motor neurons that was initially reported in TrkB null- mutant mice (Klein et al., 1993) could not be replicated in subsequent studies, not even in mice mutants lacking both BDNF and NT4 (Liu et al., 1995). Up until now, it is unclear what are the factors that may support the survival of spinal cord motoneurons during normal development. Whilst a number of studies have indicated that the survival of motoneurons is dramatically improved following the addition of BDNF to either cultured spinal cord motoneurons or after axotomy *in vivo* (Sendtner et al., 1992), it is also known that such manipulations also dramatically increase the levels of expression of "death receptors" such as p75NTR (Ernfors et al., 1989). Although the expression of TrkB ensures the survival of the neurons despite the expression of p75NTR, expression of p75NTR after injury has been suggested to delay motor axonal regeneration (Boyd and Gordon, 2001).

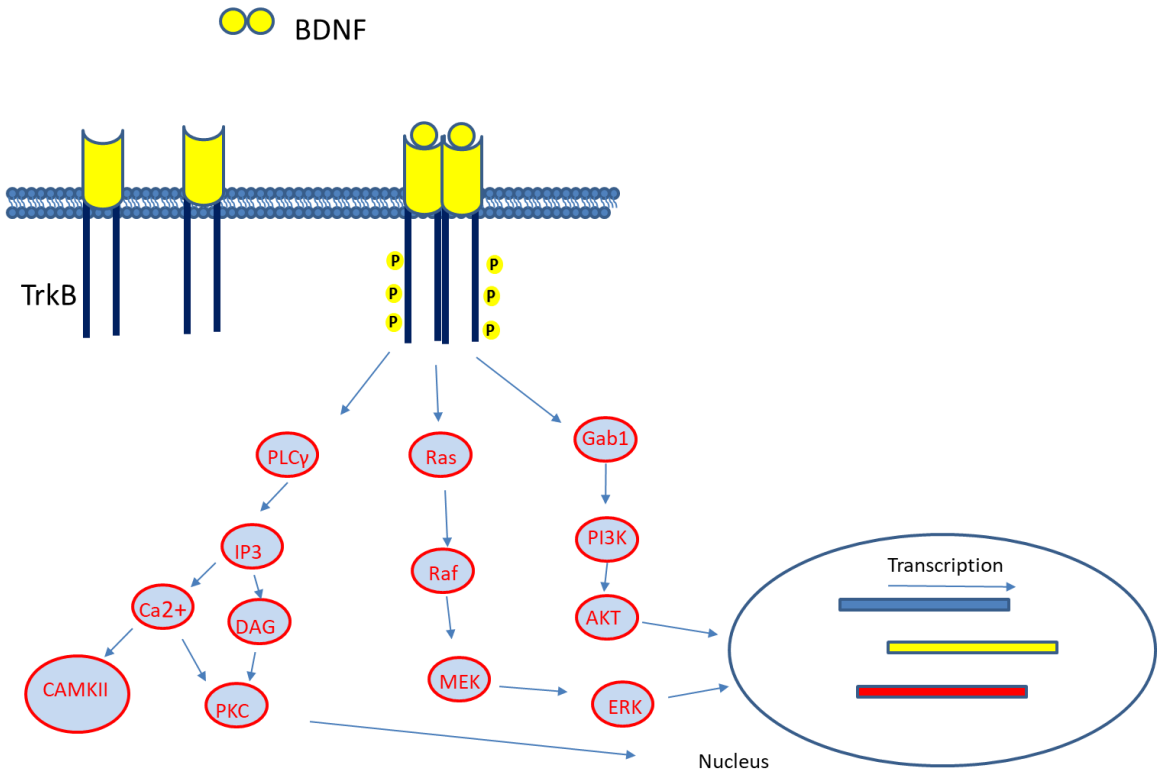

Figure 1.4 *BDNF-TrkB signalling cascade is initiated upon binding of BDNF to TrkB and subsequent dimerization of the receptor. Subsequently the phosphorylation of specific tyrosine residues mediates the downstream signalling by creating docking sites for the effector proteins that initiate the activation of downstream instracellular pathways PLCγ, ERK and PI3K. The three pathways lead to increase of the transcription factor CREB that enhances transcription of several genes.*

1.3.4 TrkB as a drug target

Given the role of BDNF/TrkB signalling in dysfunction of the nervous system (see 1.2.7 for examples), the development of TrkB agonists is receiving considerable attention. This included the identification of small molecules activating TrkB using *in vitro* reporter assays. DMAQ-B1 was amongst the first to be identified by screening a library for activators of the insulin receptor (Zhang et al., 1999) and has been reported to activate TrkA, TrkB and TrkC (Wilkie et al., 2001). More recently, 7,8-DHF has identified as a compound protecting against staurosporine-induced apoptosis in a murine brain-derived cell line overexpressing TrkB (Jang et al., 2010). The compound was shown to bind to the extracellular domain of TrkB, and reported to induce phosphorylation of the receptor in rat primary cortical neuron cultures. In addition, a compound, LM22A-4, was identified by in silico screening of a small molecule library based on detailed structural analysis of BDNF and of specific sequences thought to interact with TrkB (Massa et al., 2010). It was then shown to activate TrkB and downstream components in mouse hippocampal neuron culture. Also, *in vivo* administration of this compound in mouse models of Rett syndrome and Huntigton's disease were reported to improve motor and respiratory functions (Schmid et al., 2012, Simmons et al., 2013). However, a more recent analysis of the efficacy of DAMQ-B1, 7,8-DHF and LM22A-4 on cultured rat cortical neurons and human cell lines expressing TrkB showed that none of them were effective TrkB agonists (Boltaev et al., 2017). In addition to small molecules, a number of antibodies have been reported to activate TrkB (Bai et al., 2010, Cazorla et al., 2011) and one main objective of this Thesis work was to characterize a novel TrkB antibody developed at the Scripps Institute in a collaboration between the laboratories of Richard Lerner and Zebra Biologics, a recently founded biotechnology company. Using a near-neighbour antibody screening strategy, new TrkB activating antibodies have been selected amongst a $>10^9$-member combinatorial library. One of them designated #85 was characterized in this work and compared to the natural TrkB ligands BDNF and NT4.

1.4 Embryonic stem cells as a research tool

1.4.1 Mouse pluripotent stem cells

Embryonic stem cells (ESCs) were isolated from the inner cell mass of blastocysts at the pre-implantation stage of mouse embryos (Evans and Kaufman, 1981). This cluster of 10-20 unspecialized cells have been characterized as being in a “ground state” or of naive pluripotency. Crucially they can be cultured *in vitro* initially in the presence of leukaemia inhibitor factor (LIF) (Niwa et al., 1998) . Furthermore, inhibition of the differentiation inducing signalling from mitogen-activated protein kinase and inhibition of the glycogen synthase kinase 3 is all that is required to isolate and maintain mouse ESCs in a ground state (Ying et al., 2008). A further demonstration of the pluripotent nature of the cultured ESCs was the possibility to generate mouse chimeras and progeny from such mice, by contributing to all somatic lineages as well as to the germline (Bradley et al., 1984, Evans et al., 1985).

1.4.2 Human pluripotent stem cells (hESCs)

As in the case with the mouse, human embryonic stem cells (hESCs) are also derived from the inner cell mass of embryos and are characterised by their apparent ability to self-renew while maintaining a significant degree of multipotency when exposed to extrinsic signals (Thomson et al., 1998). However, given the impossibility to generate a whole organism from hESCs there has been a great deal of work as well as controversies to better define the exact nature of cultured hESCs (De Los Angeles et al., 2012, Davidson et al., 2015, Rossant, 2015). From the outset it became clear that there must be significant differences with mESCS if only because of the inability of LIF to promote their survival and self-renewal (Daheron et al., 2004). More generally the culture conditions needed to maintain and propagate hESCS are very different from those established for mESCs (Lin and Talbot, 2011). Currently there seems to be a consensus to consider the hESCs cultured under the protocols used by most researchers as not really naïve but “primed” stem cells, possibly unable to differentiate into all somatic and germ cell lineages (Nichols and Smith, 2009) . Ongoing work is aiming at further refining the culture conditions so as to obtain truly naïve stem cells able to generate any cell type, either as cells derived from very early human embryos or else reprogrammed from somatic cells (Guo et al., 2016, Wang et al., 2018c) . A new concept has recently emerged suggesting that there may be an intermediate state

between the naïve and primed state designated the “formative” state, possibly preparing for the orderly and coordinated naïve state during the early phase of human development, which is clearly significantly longer than is the case in the mouse (Smith, 2017).

The better understanding and characterisation of pluripotency in mESCs including in particular the detailed molecular characterisation of pluripotent cells laid the foundation for the next significant development in stem cell biology with the discovery by Takahashi and Yamanaka that the combination of 4 factors expressed in mESCs allowed the reprogramming of mouse and soon after of human somatic cells. Specifically, the expression of OCT3/4, SOX2, KLF4 and c-Myc (Takahashi and Yamanaka, 2006, Takahashi et al., 2007) was sufficient to reprogram fibroblasts back to the pluripotent state. In the mouse, it was possible to demonstrate that the reprogramming of fibroblasts and other cells was so profound that animals could be generated from these induced pluripotent stem cells (iPSCs) (Boland et al., 2012). Work with human somatic cells also generate the same type of question as with embryonic stem cells, namely the generation of primed as opposed to naïve ES cells. However, recent work suggests that the primed cells can be taken back to a more primitive state, with characteristics similar to cells derived from the inner cell mass of primates by procedures involving, for example, the inhibition of histone deacetylation (Guo et al., 2017).

1.4.3 Neuronal differentiation of hESC

While the exact nature of hESCs continues to be a matter of debate, these cells offer nonetheless a unique way to recapitulate and study aspects of human embryonic development that would otherwise remain inaccessible. In particular, a number of different cell types can be generated *in vitro* allowing unprecedented opportunities to define their biochemical and molecular biological characteristics, as well as their response to extracellular signals such as growth factors or components of the extracellular matrix (Vidarsson et al., 2010, Akiyama et al., 2018, Espuny-Camacho et al., 2013). Using co-culture systems, cell-cell interactions can now also be studied using human cells and determine the degree to which such interactions may differ from what was determined with rodent systems (Lam et al., 2017). This is particularly relevant in the context of drug development, as well as towards a better understanding of conditions affecting human health, especially those where single genes have been

identified as being causally related to disease conditions. In this context, the possibility of generating patient-specific iPSCs is likely to change our understanding of the pathways leading to diseases of the nervous system in particular (Tamburini and Li, 2017).

Amongst other exciting developments, it also appears likely that the possibility to generate organoids form cultured iPSCs may revolutionize our understanding of early steps of organ formation. Whilst it is still not entirely clear whether the development of large organs such as the brain can meaningfully be followed in the absence of a functional vascular system, successes with smaller structures such as the eye in particular are impressive and may open new possibilities to access complex processes such as morphogenetic movements as well as multilayer formation (Nakano et al., 2012). The impact of genes acting early during development of such structures is likely to be much better understood using this type of approach.

The work at the core of this PhD thesis benefits from recent developments allowing the generation of unlimited quantities of human neurons. It also illustrates both the current problems as well as the successes that can be achieved using recent protocols allowing the generation of human neurons from hESC. As detailed in the subsequent chapters it still remains challenging to reproducibly generate monolayers of human neurons of sufficient quality for detailed molecular, quantitative analyses.

Whilst a large number of protocols leading to the generation of human neurons from hESCs have been published (Espuny-Camacho et al., 2013, Arber et al., 2015), just like has been previously the case with mESCs (Bibel et al., 2004, Wu et al., 2012), only few are robust enough to be used on a routine basis. In addition to reproducibility, the main problems are cellular heterogeneity and the difficulties of generating monolayer cultures allowing meaningfully biochemical analyses following cell lysis. In most cases, the proportion of cells responding to the addition of a particular agent –a central aspect of the work presented here- has been exceedingly difficult to analyse. Following many years of experimentation largely based on a better understanding of neural induction in model systems such as Xenopus Laevis, many protocols including those used here rely on inhibition of the mesoderm pathway, following early suggestions that neural induction involves inhibition of extracellular signals (Sasai et al., 1994, Smith and Harland, 1992) . In particular, inhibition of TGFβ signalling as well

as of its downstream targets SMAD have been repeatedly shown to promote early commitment of multipotent hESCs towards the neural lineage (Chambers et al., 2009).

Work with amphibian embryos in particular (Munoz-Sanjuan and Brivanlou, 2002) has indicated that layer specification may rely on downstream effectors of the TGFβ superfamily, including SMADs. The SMADs are thought to block the BMP pathway inducing mesoderm fates. Dual SMAD inhibition of hESCs was shown to generate neural-tube structures like rosettes and neurons. A significant proportion of the neurons generated by this type of protocol display some of the characteristics of excitatory neurons populating the dorsal telencephalon. By contrast, exposure of the cultures to sonic hedgehog leads to the generation of neuronal populations resembling those found in the ventral part of the brain, the ganglionic eminence (Aubry et al., 2008). Altering both the concentration and the timing of treatment with growth factors and pathway inhibitors lead to populations resembling those found in various brain regions including the hypothalamus or cortical interneurons, in addition to striatal interneurons (Danjo et al., 2011, Germain et al., 2013, Ma et al., 2012). Furthermore, the additional use of anterior and posterior regional patterning factors including fibroblast growth factor 8 and 15 (FGF8 and FGF15) and activin can lead to different subtypes of neurons (Lim et al., 2015, Kim et al., 2014, Arber et al., 2015).

As detailed in the following Chapters, a triple SMAD inhibition protocol modified from the Vanderhaeghen group (Espuny-Camacho et al., 2013) was initially used to generate excitatory, BDNF-expressing neurons. Subsequently, a dual SMAD inhibition protocol, relying on the instructive role of Activin A, was used to generate TrkB-expressing inhibitory neurons.

1.5 Aims and Hypothesis

As decades of basic research using animal models have established that BDNF and TrkB signaling play essential roles in the nervous system, there is increasing interest in understanding the biochemistry of BDNF in human neurons and in developing reagents activating the BDNF signaling pathways in the human brain. The generation of neurons from embryonic stem cells begins to make such goals achievable whereby the emphasis of the work detailed in the subsequent chapters is on novel TrkB activating antibodies that became available during the course of this PhD Thesis. The goal of combatting neurodegeneration using antibodies begins to be a realistic option

given the extensive use of antibodies in various conditions such as cancer (Scott et al., 2012), wet macular degeneration (Volz and Pauly, 2015), multiple sclerosis (Gajofatto and Turatti, 2018) and Alzheimer's disease (AD) (Sevigny et al., 2016). Even if targeting the amyloid precursor peptide or Aβ with antibodies turned out not be successful thus far, the principle of using of antibody to treat conditions affecting the function of the nervous system and to target antigen expressed by neurons has already been tested in humans. The work detailed in the following chapters is divided into four sections:

1) Generation of excitatory neurons from human embryonic stem cells to study the regulation of BDNF expresison
2) Generation of TrkB-expressing inhibitory neurons from human embryonic stem cells to study TrkB activation by novel agonists
3) Comparison of TrkB activation by natural and engineered ligands
4) Detailed comparison of gene expression using RNAseq following TrkB activation by BDNF, NT4 and a novel TrkB-activating antibody

CHAPTER 2: METHODS

2.1 Cell culture

All cell cultures were maintained at 37 °C and 5 % CO2 in a Heracell™ 150i incubator (ThermoFisher Scientific). Cell work was performed under a laminar flow hood (MAXISAFE 2020, ThermoFisher Scientific) under sterile conditions. Cells were grown on plastic multi-well plates (ThermoFisher Scientific) or glass coverslips (VWR).

2.1.1 hESC culture

All experiments described in this Thesis were carried out using the H9 human embryonic stem cell (hESC) line or the H7 hESC line (WiCell). Multi-well plates were coated with hESC qualified Matrigel (Corning) diluted in Dulbecco's Modified Eagle Medium (DMEM)/F-12 (ThermoFisher Scientific) according to manufacturer's instructions, for 1 hour at 37 °C. H7 cells were maintained in mTSER1 media, and H9 were maintained in mTSER1 supplemented with 10 ng/ml of basic fibroblast growth factor (bFGF). Media was changed daily and stem cells were passaged when they reached approximately 80 % confluency, as described below. Media was aspirated and cells were washed once with D-Phosphate Buffered Saline (D-PBS; Gibco) and 0.02 % ethylenediaminetetraacetic acid (EDTA; Sigma) was added and cells were incubated at 37 °C for 2 minutes. Subsequently EDTA was aspirated and 3 ml of mTSER1 was added. Cells were then manually dissociated into small clusters with the use of a 5 ml serological pipette. The resulting cell suspension was then centrifuged at 1150 rpm for 3 minutes (5810 R centrifuge, Eppendorf) and the supernatant was removed. The pellet was re-suspended in fresh media and cells were seeded at a 1:3 ratio.

2.1.2 hESC freezing and thawing

Cryogenic vials with frozen hESCs were maintained in liquid nitrogen tanks for future experiments. Cells were passaged as previously described (hESC culture) and re-suspended in 1 ml mTSER1 medium containing 10 % dimethyl sulfoxide (DMSO). Cell suspension from one well of a 6-well plate was transferred into a cryogenic vial and kept inside a Mr. Frosty™ Freezing Container (Nalgene, ThermoFisher Scientific) in order to slow down the rate of freezing upon storing at -80 °C. Frozen cells were maintained at -80 °C overnight and transferred to liquid nitrogen the next day. Cell thawing was performed by placing the frozen cryogenic vials directly at 37 °C. Upon thawing, the cell suspension was added to 3 ml of pre-warmed mTSER1 and centrifuged at 1150 rpm for 3 minutes. The cell pellet was re-suspended in 3 ml of fresh mTSER1 and plated into a single well

2.2 Neuronal differentiation

2.2.1 Cortical excitatory neurons

This protocol is based on a publication by Espuny Camacho and colleagues (Espuny-Camacho et al., 2013) and subsequently modified by Li and colleagues (personal communication). H7 and H9 hESCs were plated onto Matrigel (VWR) and maintained in mTSER1 (Stem Cell Technologies). H7 and H9 hESC were passaged and plated onto Matrigel-growth factor-reduced (VWR) 2 days prior to differentiation. Cells were maintained for the first 6 days of differentiation in N2B27 media (2 parts DMEM-F12 to 1-part Neurobasal supplemented with 1:100 N2 and 1:200 B27; Life Technologies) with triple smad inhibition: Stemolecule LDN-193189 (Stemgent, cat no 04-0074) at final concentration of 100 nM, SB431542 (Tocris, cat no 1614) at a final concentration of 10 μM and Dorsomorphin (Tocris cat no 3093), at a final concentration of 200 nM. From days 6-12 progenitors were maintained in N2B27 media with dual smad inhibition, LDN and Dorsomorphin. After day 12 the cells were maintained in plain N2B27 media. At day 12 the first passage was performed the cells were washed with D-PBS and then treated with 0.02% EDTA for 2 minutes at 37 °C. Subsequently EDTA was removed and progenitors detached from the plate with gentle mechanical dissociation. Progenitors were collected into a 15 ml conical tube (Sarstedt) and centrifuged for 3 minutes at 1150 rpm. Then cells were plated in fibronectin-coated wells (15 μg/ml). Cells from 2 wells of a 6-well plate were plated to 3 wells of a new 6-well plate. At day 20 the second passage was performed with the use of EDTA and

mechanical dissociation. In this case the dissociation step was harsher in order to acquire all the progenitors attached to the plate. The splitting ratio in this passage was 1:5, although other ratios had been successfully tested. Neurons can be observed about 3 to 4 days after the second passage and they can be maintained up to 110 days in culture (Figure 2.1) Due to the extended proliferation time observed with this protocol it is possible to freeze the progenitors at different time points. Progenitors had been frozen successfully in three time-points day 16, day 30, day 50 (data not shown). In order to freeze the progenitors, media was removed and cells were washed once with D-PBS. 1 ml of 0.02 % EDTA was then added and cells were incubated at 37 °C for 2 minutes. Subsequently EDTA was removed and 1 ml of freezing media (90 % N2B27, 10 % DMSO) was added to the well. Harsh mechanical dissociation was performed with the use of 5 ml serological pipettes. Subsequently the cells were transferred into cryovials and were left at -80 °C overnight inside a Mr. Frosty™ Freezing Container. Vials were transferred to liquid nitrogen the following day.

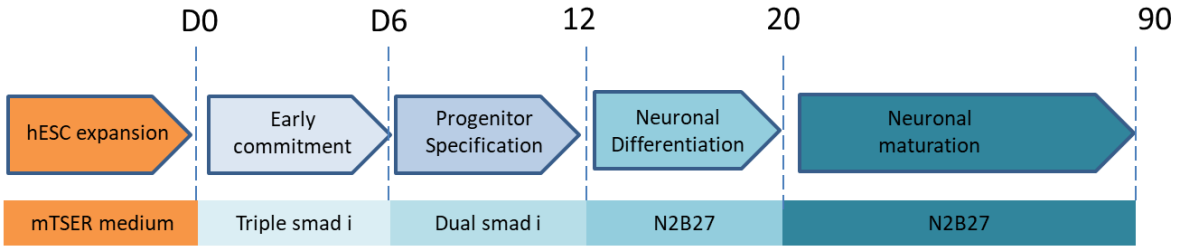

Figure 2.1: Summary of the differentiation protocol used for the generation of hESCs-derived neurons using triple Smad inhibition. At day -2, H7 & H9 hESCs are plated on Matrigel, and passaged after 2 days onto growth factor-reduced Matrigel (Matrigel GFR). Triple Smad (LDN, Dorsomorphin and SB431542) starts at day 0. At day 6, SB431542 is removed from the media. Progenitors need to be passaged at day 12 and day 20 to ensure appropriate differentiation. Subsequently the neurons can be maintained *in vitro* for more than 3 months.

2.2.2 LGE neurons

This protocol supports the differentiation of human induced pluripotent stem cells (IPSC) and human embryonic stem cells (hESC) into neurons that express markers of the lateral ganglionic eminence (LGE) (Telezhkin et al., 2016). H9 hESC stem cells were maintained in mTSER1 medium with Matrigel used as a substrate. Four different media were used upon differentiation (Figure 2.2). SLI medium, which was used for the first 8 days, includes ADF (ADF-Base medium) (Advanced DMEM/F12 98%, Macs Brew supplement without Retinoic Acid, Glutamax 1%, Penicillin/Streptomycin 5000 units/5000 µg), 1.5 µM IWR1 (Tocris) dual smad inhibition (10µM SB431542 (Abcam) and 1 µM LDN193189 (Reinnervate). These two molecules are necessary for blocking the mesoderm pathway and induction of neuronal differentiation (Chambers et al., 2009). Furthermore, the use of IWR1, an inhibitor of Wnt signalling, was used in order to block premature differentiation of forebrain progenitors into cortical neurons. Indeed, Wnt3a has been described to be involved in this procedure (Munji et al., 2011). LIA medium was used from day 16 to day 23 and was composed of ADF media, Macs Brew supplement without Retinoic Acid (Miltenyi Biotec), 200 nM LDN193189 (Reinnervate), 1.5 µM IWR1 (Tocris) and 20 ng/mL Activin A (Peprotech). Activin A seems to orchestrate the differentiation of human pluripotent stem cells into neurons with the characteristics of striatal projection neurons, including expression of striatal transcription factors CTIP2, GSX2, FOXP2 and the post-mitotic marker DARPP32+, in addition to the expected electrophysiological properties (Arber et al., 2015). SynaptoJuice A is used from day 16 to day 23 and was composed of ADF, Macs Brew supplement with RA (20%), 20 µM PD0332991 (Tocris), 100 µM DAPT (Tocris), 30 µM CHIR 99021 (Tocris), 100 µM Forskolin (Tocris), 3 mM GABA (Tocris) and 2 mM Ascorbic Acid (Sigma). SynaptoJuice B was used from day 23 to day 37 and it is composed of ADF, Macs Brew supplement with RA (20%), Neurobasal A-Base medium (Neurobasal A medium 98%, Glutamax 1%, Penicillin/Streptomycin (5000 Units/ 5000 µg), 20 µM PD0332991 (Tocris), 30 µM CHIR 99021 (Tocris) and 2 mM ascorbic acid Sigma). PD0332991 is a Cdk 4/6 inhibitor (Finn et al., 2009), DAPT is an inhibitor of γ-secretase (Dovey et al., 2001), Forskolin is an activator of adenylyl cyclase that induces neuronal differentiation (Kim et al., 2005)(Kim et al 2005), CHIR99021 is a GSK-3 inhibitor (Ring et al., 2003) and ascorbic acid (Yan et al., 2001) improves the yield of dopamine neurons *in vitro*.

On day 0, mTSER was removed from the wells and cells were washed twice with 2 ml of PBS, pH 7.4 (containing Ca2+ & Mg2+). Subsequently, prewarmed (37 °C) SLI medium was added to the cultures. Media was replaced every day until day 7. On day 7, Matrigel plates for the passage at day 8 were prepared. Matrigel matrix (growth factor-reduced) was diluted in DMEM F/12 according to manufacturer's instructions. Subsequently 1 ml of diluted Matrigel was used to coat each well of a 6 well plate, or 350 µl in each well of a 24 well plate, containing a coverslip. On day 8, the cultures were incubated for 1 hour at 37 °C with 10 µM of the ROCK/RHO pathway inhibitor Y-27632 (Abcam) in order to block apoptosis. Subsequently the media was aspirated and cells were washed two times with D-PBS. 1 ml of pre-warmed Accutase (StemCell Technologies) was then added and plates were incubated at 37 °C for 5 minutes. In the next step, 2 ml of ADF media was added and cells were detached with the use of a 1 ml pipette. The cell suspension was centrifuged at 740 rpm for 3 minutes and the cell pellet was re-suspended in 3 ml of SLI differentiation medium containing 10 µM Y-27632. The splitting ratio was 1:2 and full media changes with LIA differentiation medium were performed daily until day 16. The second passage was then performed with the same method. Cell number was quantified with the NucleoCounter (Chemometec) and 2 million cells were plated per well of a 6-well plate or 350.000 per well of a 24-well plate, containing coverslips.

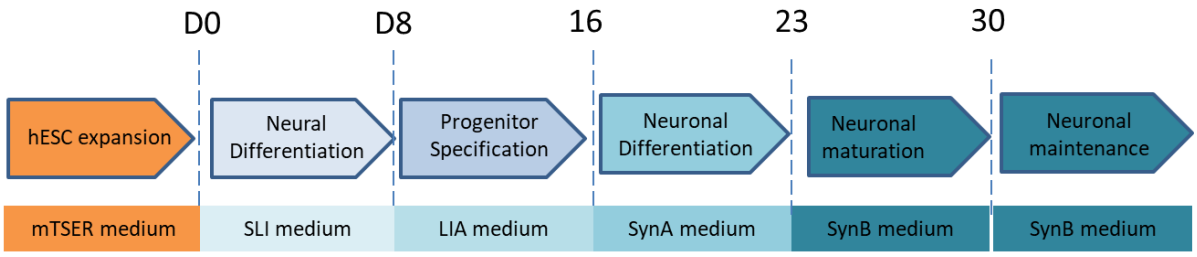

Figure 2.2: Summary of the differentiation protocol used for the generation of hESCs-derived neurons using dual inhibition, Activin A and cell cycle inhibitors. At day 0, dual media was replaced with SLI media containing dual smad inhibition and Wnt inhibitors. At day 8 progenitors were passaged and media was replaced to LIA medium containing Activin A. Progenitors needed to be passaged again at day 16 and the media was replaced with Synaptojuice A. After day 23, media was replaced with Synaptojuice B. Subsequently the neurons could be maintained *in vitro* for more than 2 months.

Media	Component	Component Function
SLI media	ADF-Base medium (98%)	Base medium
	MACS Neurobrew-21 without RA (2%)	supplement
	IWR1 (1.5 µM)	Inhibit Wnt signalling, blocks premature differentiation of forebrain progenitors into cortical neurons.
	LDN193189 (1.0 µM)	Blocking mesoderm pathway, induction of neuronal differentiation
	SB431542 (10 µM)	Blocking mesoderm pathway, induction of neuronal differentiation
LIA Media	ADF-Base medium (98%)	Base medium
	MACS Neurobrew-21 without RA (2%)	supplement
	Activin A (20 ng/mL)	Promote differentiation into neurons with characteristics of striatal projection neurons
	IWR1 (1.5 µM)	Inhibit Wnt signalling, blocks premature differentiation of forebrain progenitors into cortical neurons.
	LDN-193189 (200 nM)	SMAD Inhibition
SynaptoJuice A	ADF-Base medium (76%)	Base medium
	MACS NeuroBrew-21 with RA (20%)	Supplement
	CHIR 99021 (30 µM)	GSK-3 inhibitor
	DAPT (100 µM)	Inhibitor of γ-secretase
	Forskolin (100 µM)	Activator of adenylyl cyclase that induces neuronal differentiation
	PD0332991 (20 µM)	Cdk 4/6 inhibitor
	GABA (3 mM)	neurotransmitter

	Ascorbic Acid (2 mM)	Improves yield of neuronal cells
SynaptoJuice B	ADF-Base medium (39%)	Base medium
	Neurobasal-base medium (39%)	Base medium
	MACS NeuroBrew-21 with RA (20%)	Supplement
	CHIR 99021 (30 µM)	GSK-3 inhibitor
	PD0332991 (20 µM)	Cdk 4/6 inhibitor
	Ascorbic Acid (2 mM)	Improves yield of neuronal cells

Table 2.1 Composition of the media used for the LGE protocol.

2.3 Western blot

2.3.1 Lysis

2.3.1.1 Standard procedure (cortical differentiation protocol)

Neurons were plated in 12-well plates or 35 mm dishes and were cultured for various time points from 20 DIV to 80 DIV. Upon lysis the media was removed before adding 200 µl of RIPA lysis buffer which contained 50 mM Tris-HCl, pH 7.4, 150 mM NaCl, 1 mM EDTA, 1% Triton X-100, and 0.2 % Sodium deoxycholate, supplemented with protease and phosphatase inhibitor cocktail mix (Sigma) containing 1:100 dilution of Protease inhibitors, 1:100 dilution of Phosphatase inhibitors, 100 mM 1-10 Phenantroline, 100 mM 6-aminohexanoic acid, 10 mg/ml aprotinin and 0.1 % sodium dodecyl sulphate (SDS). With the use of a cell scraper, neurons were detached from the wells, collected into a 1.5 ml Eppendorf tube, and incubated on ice for 30 minutes. Subsequently insoluble debris was removed from the samples by centrifugation of the samples for 5 minutes at 14,000 rpm at 4 °C. Supernatants were then kept at -80 °C until further analysis.

2.3.1.2 Procedure for phosphorylation experiments (LGE differentiation protocol)

Neurons were plated in 12-well plates and were culture for various time points from 37 to 60 DIV. Before lysis the cells were washed with PBS and Sodium Orthovanadate NaO4V (2mM), and subsequently treated with 300 µl of 0.05 % Trypsin (ThermoFisher Scientific) and NaO4V for 3 minutes. Following this 800 µl foetal calf serum (FCS) (BioSera)-containing medium and NaO4V was added. Cells were then detached from the dish by pipetting and the cell suspension was transferred to 1.5 ml Eppendorf tubes. All the following steps were performed on ice. Cells were centrifuged for 5 minutes at 14,000 rpm at 4 °C. Then the supernatant was removed and cells were washed with 700 µl PBS and NaO4V (2mM). Protein was extracted with 100 µl of RIPA lysis buffer containing 50 mM Tris-HCl, pH 7.4, 150 mM NaCl, 1 mM EDTA, 1% Triton X-100, 0.2 % sodium deoxycholate and 0.1 % SDS, supplemented with protease and phosphatase inhibitor cocktail mix (Sigma-Aldrich) at 1:100 dilution, 100 mM 1-10 Phenantroline, 100 mM 6-aminohexanoic acid, 10 mg/ml aprotinin and 2 mM of sodium orthovanadate.

2.3.2 Western blotting

Lysates were combined with ¼ of the total sample volume of 1x lithium dodecyl sulphate (106 mM Tris HCL, 141 mM Tris base, 2% LDS, 10% glycerol, 0.51 mM EDTA, 0.22 mM G250 Coomasie Blue, 0.175 m Phenol Red; Ph 8.5) sample loading buffer and 50 mM DTT and then boiled at 70 °C for 10 minutes. Equal volumes of lysate were loaded on a NuPAGETM NovexTM 4-12 % Bis-Tris gel (ThermoFisher Scientific) and run at 120 V for 90 minutes in 2-(N-morpholino) ethanesulfonic acid (MES) running buffer (50 mM MES, 125 mM Tris base, 0.1 % SDS, 1 mM EDTA, pH 7.3). The protein gel, the nitrocellulose membrane and the blotting papers were immersed in transfer buffer (25 mM Bicine, 25 mM Bis-Tris, 1 mM EDTA, 20% methanol). The gel and the membrane were placed between two blotting papers, and transferred inside the semi-dry Bio-Rad Trans-Blot unit. Protein gels were transferred to nitrocellulose membranes using the semi-dry technique, by applying 17 V for 90 minutes. After transfer the membrane was blocked in blocking solution for 1 hour. The blocking solution used consisted of 3 % Amersham ECL Prime blocking reagent (GE Healthcare) and 3 % BSA (Sigma) in TBS-T (24.7 mM Tris base, 137 mM NaCl, 2.6 mM KCl, 0.1 % Tween-20, pH 7.5). The primary antibodies were diluted in blocking solution as described above. The concentrations of the primary antibodies used are provided in Table 1. The membranes probed with all primary antibodies, except synaptophysin, were incubated at 4 °C overnight. The membranes probed with synaptophysin were probed for 1 hour at room temperature. After incubation with the primary antibody, the membrane was washed three times for 20 minutes with TBS-T and subsequently incubated with the secondary antibody for 1 hour at room temperature. The secondary antibodies were donkey anti-Mouse HRP-conjugated and donkey anti-Rabbit HPR-conjugated (Table 2). The membrane was subsequently washed three times for 20 minutes each with TBS-T. The signal of the membrane was developed using the membrane LumiGLO Reserve Chemiluminescent Substrate Kit (KPL) and visualisation was achieved using the Image Lab software and the Universal Hood III camera system (Bio-Rad). The camera can detect the chemiluminescent signal, whilst the software controls for saturation. Exposure times for each membrane were adjusted in order to avoid saturation. Analysis of the acquired images was performed as explained below (Densitometry analysis). As an additional measure to control for equal loading, the membrane was stained with the Pierce Reversible Protein Stain Kit (ThermoFisher Scientific). With this method one can detect all the proteins present and ensure equal loading. Briefly, the membrane was washed 3 times

for 5 minutes with TBS-T, before incubation for 5 minutes at room temperature with 1 ml of Pierce solution. Then, the membrane was washed three times for 5 minutes with water and pictures were taken with GenoSmart2 (VWR).

2.3.3 Densitometry analysis

Western blot data from experiments with phosho-TrkB and TrkB were quantified by the ImageJ software (https://imagej.nih.gov/ij/). A square was drawn manually around each band ensuring that the entire band was inside the square. Subsequently one peak was generated per band and the area below the peak was measured using ImageJ tools. The values from pTrkB or TrkB western blots were divided with the corresponding values of synaptophysin and internal normalisation was performed.

Antibody	Type	Dilution	Species	Provider
anti-BDNF	mAb	1 to 2.000	mouse	Icosagen 3C11
anti-synaptophysin	mAb	1 to 10.000	mouse	Sigma cat no S5768
anti-pTrkB (Tyr706/7	mAb	1 to 2.000	rabbit	Cell signaling (4621S)
anti-TrkB	mAb	1 to 10.000	rabbit	Abcam 134155
anti-PTrkB (Tyr516)	pAb	1 to 1000	rabbit	Cell Signaling (9141)

Table 2.2: Primary antibodies used in western blotting

Antibody	Dilution	Species	Provider
anti-mouse HRP	1:7500 0.13 µg/ml	goat	Promega cat.no. W4021
anti-rabbit HRP	1:7500 0.13 µg/ml	goat	Promega cat.no. W4011

Table 2.3: Secondary antibodies used in western blotting

2.4 Real Time PCR

2.4.1 Principle

In real-time PCR or quantitative-PCR (qPCR), the rate of amplification of the target DNA is measured by using fluorescent detection methods. The fluorescence accumulation is directly proportional to DNA quantity and correlates with the amount of DNA product present after each cycle. The exponential phase of the PCR reaction is used for quantification, and quantitative analysis is based on the cycle number at which fluorescence levels exceed a threshold level (Ct value). Ct value is determined by the point at which the accumulation of fluorescent PCR products becomes exponential.

The fluorescence detection method used here includes Taqman probes, or double dye probes. The probe has a fluorescent dye (FAM) attached to the 5' end and a quencher dye (TAMRA) on the 3' end. When the probe is still intact the energy is transferred from the FAM to the TAMRA dye through fluorescence resonance energy transfer (FRET). In the annealing step of the PCR, the sequence-specific probe binds to the DNA template and Taq polymerase extends the primer sequence. It will then dislocate the 5' end of the probe, which will be degraded by the 5'-3' exonuclease activity of the Taq polymerase. When the reporter dye is separated from the quencher dye, FRET cannot be induced, and fluorescence will be emitted (Bustin, 2000).

2.4.2 Real time PCR and conventional PCR.

Total RNA was extracted from human neurons using the RNeasy Mini kit (Qiagen,). Cultures were washed with D-PBS and lysed with 350 µl of RLT RNA lysis buffer containing 1 % β-mercaptoethanol (Sigma). Lysates were either frozen at -80 °C or processed with the RNeasy Mini Kit according to the manufacturer's instructions, followed with a DNase treatment for 15 minutes at room temperature. RNA was

quantified with a BioSpectrometer (Eppendorf) which also quantifies the 260/280 nm absorbance ratio. This ratio is expected to be in the range of 1.8 to 2.0 in order to exclude protein contamination. Subsequently 1200 ng of total RNA was reverse transcribed using the SuperscriptIII reverse transcriptase (ThermoFisher Scientific). In the first step, 1 mM of dNTP MIX (Promega) and 0.5 µg of random hexamer primers (Promega) were mixed with the RNA and diluted with RNAse-free H2O to a final volume of 13 µl. Subsequently the mixture was heated at 65 °C for 5 minutes, while the master mix for the second step of cDNA synthesis was prepared. The master mix was composed of 4 µl 5x First-Strand Buffer (ThermoFisher Scientific), 1 µl (0.1 M DTT), 1 µl 40 U/µl RNAsin Ribonuclease Inhibitor (Promega) and 1 µl 200 U/µl Superscript III reverse transcriptase. Then, 7 µl of master mix was added per tube containing the RNA-dNTP-Random Primer mix and was incubated at 50 °C for 2 hours. Eventually the reaction was inactivated by heating the mixture to 70 °C for 15 minutes. The complementary DNA (cDNA) was used directly for qPCR analysis or stored at -80 °C.

A master mix was also used for qPCR, containing per reaction, 12.5 µl of Taqman polymerase (TaqMan™ Universal PCR Master Mix, ThermoFisher Scientific), 1.25 µl of 20 X MasterMix (ThermoFischer Scientific) containing forward, reverse primer and probe sets, and made up to 23 µl with RNAse-free H20. Each TaqMan Gene Expression Assay tube contained: forward and reverse primers at a concentration of 900 nM, and one 6-FAM™ dye-labeled TaqMan® MGB probe at a concentration of 5 µM. The master-mix was distributed into the wells of a 96-well plate (23 µl per well; ThermoFisher Scientific) and 2 µl of cDNA (60 ng) from each sample was added to triplicate wells. The StepOne plus software was used to run the Fast qPCR programme: 40 cycles consisted of 1 second at 95oC and 30 seconds at 72oC.

qPCR was performed on the StepOne plus PCR system (Applied Biosystem, Weterstadt, Germany), using TaqMan probes and primers as presented in Table 2.4.

Conventional PCR for the different *Bdnf* transcripts was performed using primers and annealing programme as described previously (Pruunsild et al., 2007).

name of gene	catalogue number (ThermoFisher Scientific)
VGF	Hs00705044_s1
SYNPO	Hs00702468_s1
PALD1	Hs01012869_m1
NPAS4	Hs00698866_m1
EGR2	Hs00166165_m1
EGR1	Hs00152928_m1
EGR3	Hs00231780_m1
Eukaryotic 18S rRNA	Hs03003631_g1

Table 2.4: Genes tested in Real Time PCR (Taqman gene expression assays, ThermoFisher Scientific).

2.5 RNA seq

2.5.1 Bioinformatics

RNA-sequencing was performed at the Genome Hub of Cardiff University by Angela Marchbanck. At least 500 ng of RNA was sent for RNA sequencing and the RNA integrity number (RIN) was above 9 as measured with Agilent Bioanalyser 2100 (Agilent Technologies, Inc). The TruSeq® Stranded mRNA Sample Preparation Guide and the high-throughput (HT) kit from Illumina was used according to the manufacturer's instructions. RNA-sequencing was performed on an Illumina HiSeq 2500 sequencing system at a sequencing depth of 50 million 50 nucleotide single-pair end reads using the Truseq stranded mRNA guidelines (HT protocol). The transformation of the raw data to .txt files with the list of dysregulated genes was performed by Dr Robert Andrews and Dr Katherine Tansey.

Briefly, RNAseq single-end fastq files were trimmed using trimmomatic (version 0.35) (Bolger et al., 2014) with default parameters. Trimmed fastq files were mapped to human assembly GRCh38 using STAR (version 2.5.1) (Dobin et al., 2013) and GRCh38 version 87 GTF. Transcript counts were produced with FeatureCounts (version 1.4.6) (Liao et al., 2014). Data were normalised using the Bioconductor package, DESeq2 (release 3.6) (Love et al., 2014) in R (version 3.4.1) (https://www.R-project.org/) to obtain gene expression values as FPKM (Fragments per Kilobase Million). Differential expression analysis was undertaken in DESeq2.

2.5.2 Data analysis

The Ingenuity Pathway Analysis program (IPA version, Ingenuity Systems Inc., www.ingenuity.com) was used to extract information about the significantly altered canonical functions associated with the genes that were up/down regulated upon addition of the TrkB ligands.

Hierachical clustered heatmap was generated with R software (https://www.r-project.org) and GO enrichment analysis was performed with the help of Dr.Jia Xie from Scripps Institute using G0 enrichment analysis software provided by Bioconductor (https://bioconductor.org). Genes with a fold change ≥2 and p adjusted <0.05 were run for GO terms involved in neuronal processes.

2.6 Immunocytochemistry

Stem cells (hESC H9) were cultured and differentiated as described above, onto glass coverslips (VWR). These coverslips were treated chemically to create a rough surface that enhances the attachment of the neurons. Initially the coverslips were pre-treated with pure nitric acid overnight and then washed with ultrapure water. Then the water was removed and the coverslips were washed again with ultrapure water until pH 7 was achieved and before washing for 1 hour with 100 % ethanol. Subsequently the coverslips were dried on a filter paper and autoclaved. Prior to seeding of the cells, the surface of the coverslips was coated with poly-L-lysine and laminin (Sigma) (cortical protocol) or poly-L-lysine and Matrigel growth factor-reduced (LGE protocol). Substrates were prepared as described previously (neuronal differentiation section). For the cortical protocol, various seeding concentrations were tested ranging from 150.000 to 500.000 cells per 13 mm coverslip, while for the LGE protocol 300.000 cells per 10 mm coverslip were used for all the experiments described in the results section. Neurons or progenitors cultured *in vitro* for different time points were washed once with PBS and subsequently fixed with 4 % formaldehyde (PFA) for 30 minutes. Cells were then washed again with PBS, before they were permeabilized for 15 minutes with 0.5 % Triton X-100 (Sigma) in PBS. Then cells were washed again 3 times for 5 minutes with PBS-T (PBS and 0.1 % Triton X-100) before blocking for 1 hour with PBS-T and 10 % donkey serum (Sigma Aldrich) (donkey serum was used to maintain the same specificity as the secondary antibody used). Samples were then incubated with primary antibody (Table 4) for 1 hour diluted in PBS-T and 10 % Donkey serum and washed 3 times for 5 minutes each time with PBS-T. The next step was incubation with secondary antibody (Table 5) in PBS-T and 10 % Donkey serum for 1 hour. Then cells were washed with PBS-T 3 times for 5 minutes. Nuclei were stained with DAPI (4’6- diamidino-2-phenylindole dihydrochloride; cat.no D9542, Sigma) 1:10.000 in PBS, for 5 minutes and subsequently washed again with distilled water for a further 5 minutes. Finally, samples were washed with distilled H20 and coverslips were mounted with Dako mounting medium (Dako North America, USA). All procedures mentioned above were carried out at room temperature.

Pictures were obtained with a Nikon microscope and data analysed with ImageJ software.

Antibody	Type	Dilution	Species	Provider
anti-cFOS	pAb	1 to 500	rabbit	Santa Cruz sc-52
anti-GAD65/67	pAb	1 to 1000	rabbit	Abcam 11070
anti-β-III tubulin	mAb	1 to 1000	mouse	Abcam 78078
anti-Cux1	mAb	1 to 500	mouse	Abcam 54583
anti-Trb1	mAb	1 to 500	rabbit	Abcam 183032
anti-Ctip2	mAb	1 to 500	rat	Abcam 18465
anti-Foxp1	pAb	1 to 200	rabbit	Abcam 16645
anti-Foxp2	pAb	1 to 250	rabbit	Abcam 16046

Table 2.5: Primary antibodies used in Immunocytochemistry

Antibody	Dilution	Species	Provider
anti-mouse Alexa 488	1:1000 2µg/ml	donkey	Abcam 150109
anti-rabbit Alexa 488	1:1000 2µg/ml	donkey	Abcam 150073
anti-rat Alexa 488	1:1000 2µg/ml	donkey	Abcam 150153
anti-rabbit Alexa 555	1:1000 2µg/ml	donkey	Abcam 150074
anti-mouse Alexa 555	1:1000 2µg/ml	donkey	Abcam 150106

Table 2.6: Secondary antibodies used in Immunocytochemistry

Chapter 3: The use of human excitatory neurons to study the of BDNF regulation

3.1 Introduction

Even though the levels of BDNF are very low in the brain, BDNF is the most abundant and widely distributed neurotrophin in the central nervous system (Ernfors et al., 1990, Hofer et al., 1990). The gene is primarily expressed in excitatory neurons in an activity-dependent fashion and is known to play critical roles in development and diseases (refer to 1.2.2, 1.2.3 and 1.2.7 of Introduction). However virtually nothing is known about the mechanisms regulating BDNF expression in human neurons, hence the attempt in the following study to investigate basic aspects of BDNF biochemistry and molecular biology using neurons derived from human embryonic stem cells.

3.2 Results

3.2.1 Generating excitatory neurons from human embryonic stem cells

The hESC lines H7 and H9 were used in all experiments described below. Both of them are XX (Allegrucci and Young, 2007) and display similar morphologies. However, under the tissue culture conditions used, the rate of cell division was found to be significantly different: the doubling time was 24 h for H7 and 48 h for H9.

In the first part of this work, a modified version of previously published protocols was used with the aim of generating a significant proportion of BDNF-expressing, glutamatergic neurons as opposed to GABA-ergic neurons (known to express the gene at very low levels, see also below) (Chambers et al., 2009, Espuny-Camacho et al., 2013)

In these experiments, H7 and H9 embryonic stem cells were cultured on a Matrigel substrate and in mTSER medium (see Fig. 2.1 for a summary of the procedure). It was found that progenitors undergo an extended period of proliferation and it did not become clear when proliferation would actually stop. Numerous Nestin positive progenitors were observed after 16 days *in vitro* (DIV) and the transcription factor Pax6 could be observed at 20 DIV (data not shown). The expression of these two markers is an important indication of the appropriate differentiation of the progenitors, as Pax6 is confined *in vivo* to forebrain progenitors (Georgala et al., 2011) and Nestin is an intermediate filament protein which is expressed in dividing cells during the early stages of development in the CNS, in PNS and in other tissues. Elongated cells with long filaments were observed about 3 days after the second passage and 23 days in culture (Figure 3.1). After 80 DIV 3D structures composed of progenitors and neurons are visible in all cultures. At this stage and by using higher magnification mature neurons with thick soma and process could be observed. A major difficulty encountered with this protocol is that the generation of neuronal progenitors is intermingled with the generation of post-mitotic neurons, resulting in the formation of 3D structures that made immunofluorescence analysis and quantification difficult. Passaging the culture for a third time partially overcame this obstacle. Indeed, the cultures were dissociated and replated to multiple wells 3 weeks after the second passage, at day 42. The post mitotic neurons would not have survived this procedure, however the numerous progenitor cells already proliferated at day 50, 8 days after the last passage. At these stage single neurons can be seen throughout the plate, and they start to migrate together in what later would become big clusters (Fig 3.2 C. and D.). Interestingly cultures of the same age (day 50) that have not been passaged for a 3rd time are much denser, while clusters of progenitors and neurons can already be observed (Figure 3.2 A. and B.) Through phase contrast microscopy of these cultures, it was observed that proliferation of progenitor cells continued in parallel with the differentiation of other populations to neurons, leading to mixed cultures containing both neurons and progenitors that keep dividing. In the case of cultures that have been passaged only for 2 times 3D clusters occupy most of the dish after 70 days in culture, and neurons can only be seen in few openings (Figure 3.3 A. and B.). Although cultures that have been passaged for three times are somewhat less dense and neurons can be seen in more openings, 3D clusters still occupy the largest part of the dish (Figure 3.3 C. and D.).

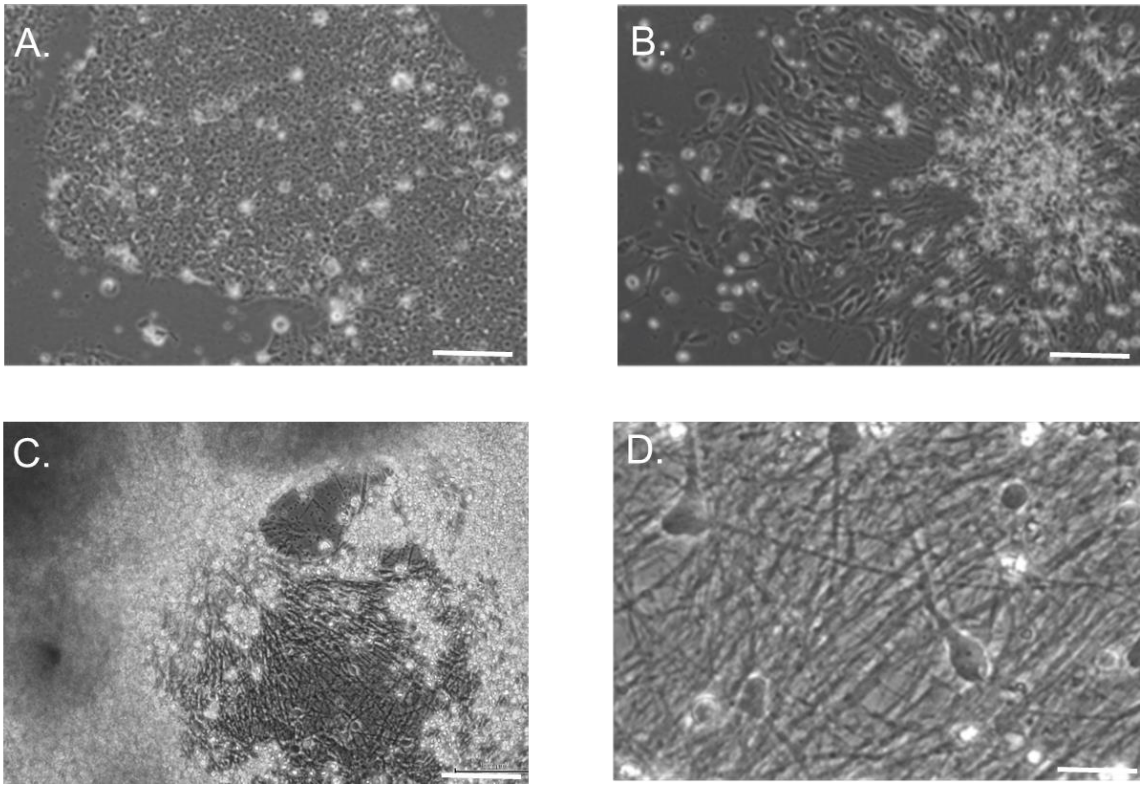

Figure 3.1: ***Phase contrast microscopy of culture of human embryonic stem cells and neurons***. *A) H7 embryonic stem cells, B) day 23 progenitors, 3 days after the second passage, C) and D) day 80 neurons, 60 days after the second passage. Scale bars are 100 µm except in D) where it is 20 µm*

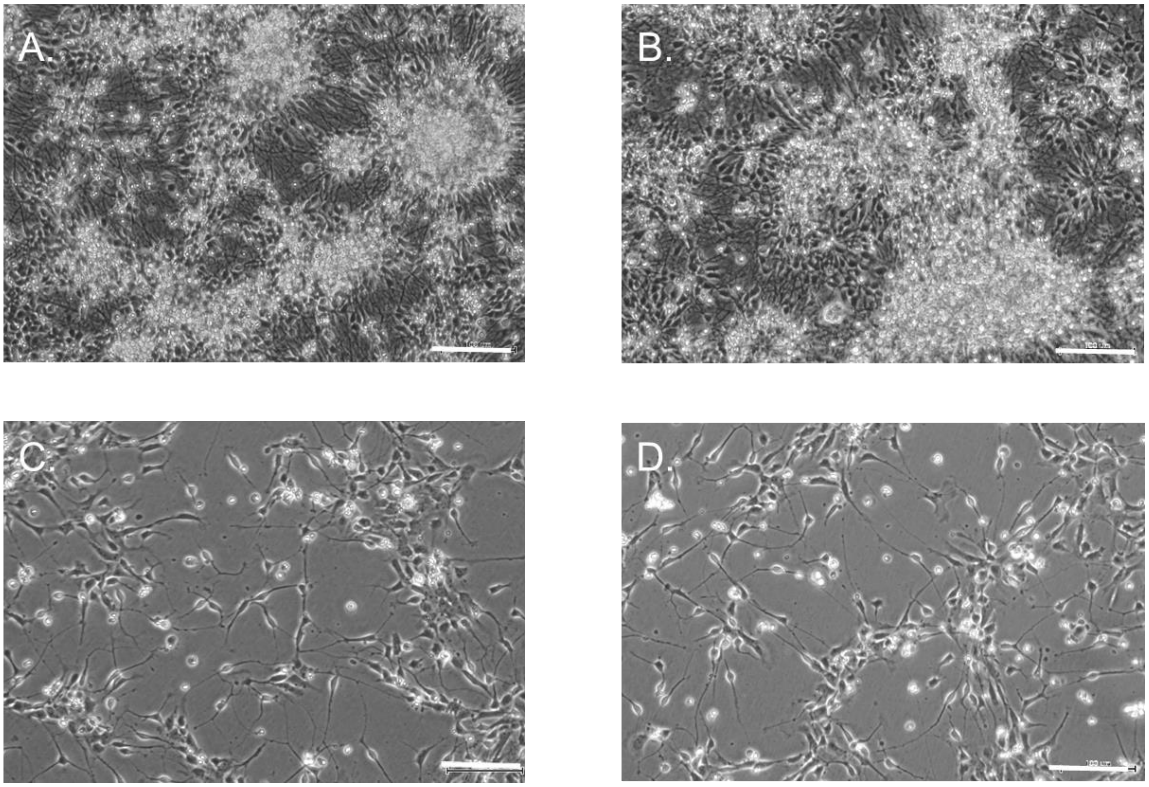

Figure 3.2: Phase contrast microscopy of cultures of day 50 neurons derived from human embryonic stem cells. *A. and B. cultures passaged two times, at day 12 and day 20. Large clumps consisted of progenitor cells and neurons can be seen throughout the dish. C. and D. cultures passaged for three times a day 12, day 20 and day 42. Single neurons can be seen throughout the dish 8 days after the last passage. Scale bars are 100 µm.*

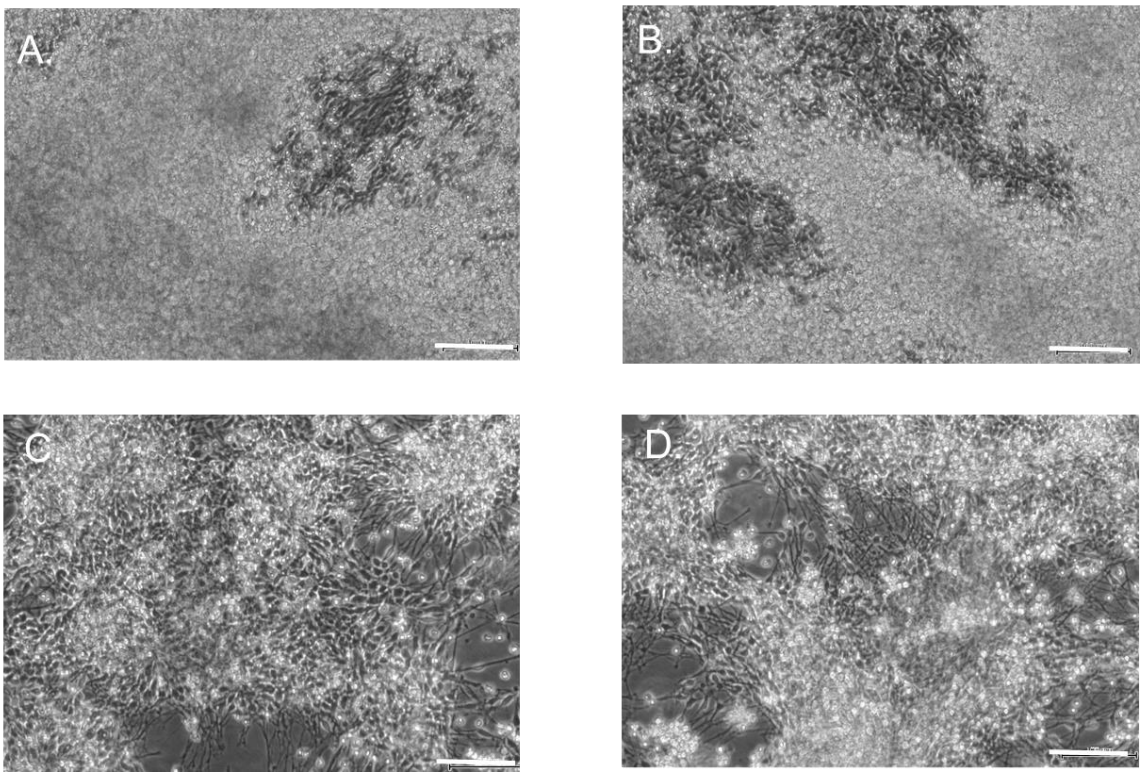

Figure 3.3: Phase contrast microscopy of cultures of day 70 neurons derived from human embryonic stem cells. *A and B cultures passaged for 2 times at day 12 and day 20. Large clumps occupy most of the dish, whereas neurons can be seen in few openings. C and D cultures passaged for 3 times at day 12, day 20 and day 50. 20 days after the last passage many clumps appear through the dish, albeit less than in A. and B. Scale bars are 100 µm.*

In order to determine the identity of the neurons and of their progenitors, the cells were fixed and stained at different time-points. The nature of the cultures that were largely composed by clusters of cells that grow into 3D structures prohibit quantification of these populations. Additionally, it was particularly difficult to acquire sufficient number of pictures of decent quality, since cells grow in different layers. Therefore, it was only possible to assess the expression of different transcription factors/markers in fixed cultures in a non-quantitative manner. Many of these neurons expressed Tbr1, a transcription factor mostly expressed by neurons residing in deep pyramidal layer VI during human development (Saito et al., 2011) . Tbr1 could be detected in 25 DIV neurons (Figure 3.4 A) and its expression was still maintained after 68 DIV (Figure 3.4. B). Ctip2, another transcription factor mainly expressed by neurons of deep pyramidal layer V during human development (Saito et al., 2011) was moderately expressed at 25 DIV (Figure 3.4 C) and markedly upregulated after 68 DIV (Figure 3.4 D). Cux1, a transcription factor expressed by neurons of upper pyramidal layers II-IV (Saito et al., 2011) is moderately expressed at 34 DIV and significantly upregulated after 77 DIV (Figure 3.4 F). Taken together, these results suggest that the hESC-derived neurons acquire some characteristics of cortical identity in a time-dependent manner. These observations replicate what has been previously described (Espuny-Camacho et al., 2013).

A.

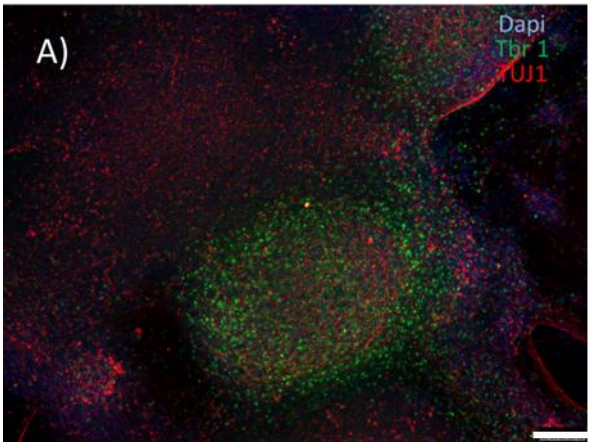
A)
Dapi
Tbr 1
TUJ1

B.

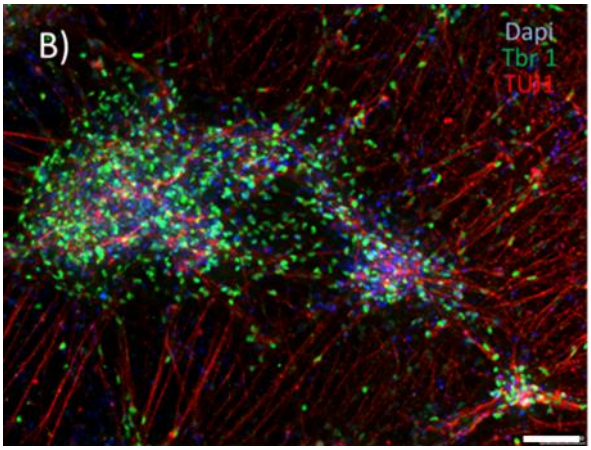
B)
Dapi
Tbr 1
TUJ1

C.

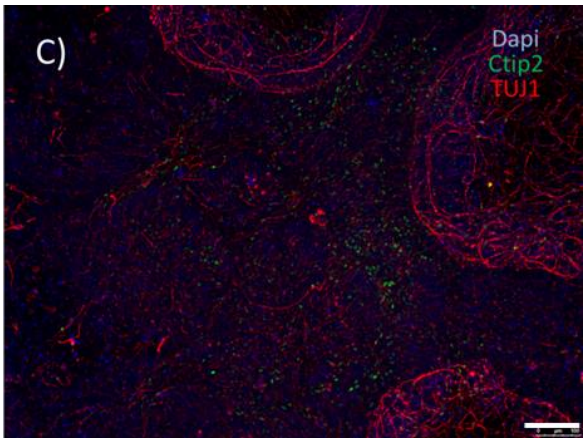
C)
Dapi
Ctip2
TUJ1

D.

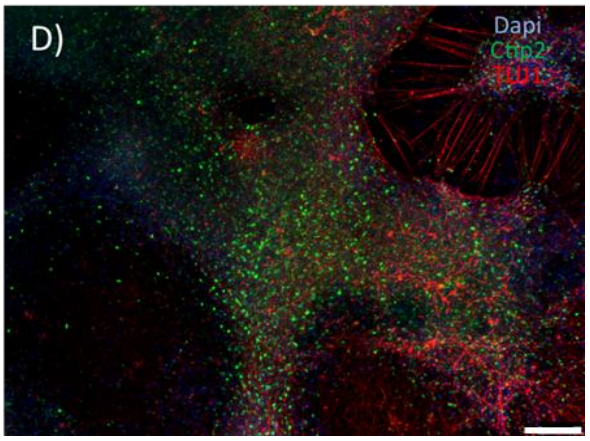
D)
Dapi
Ctip2
TUJ1

E.

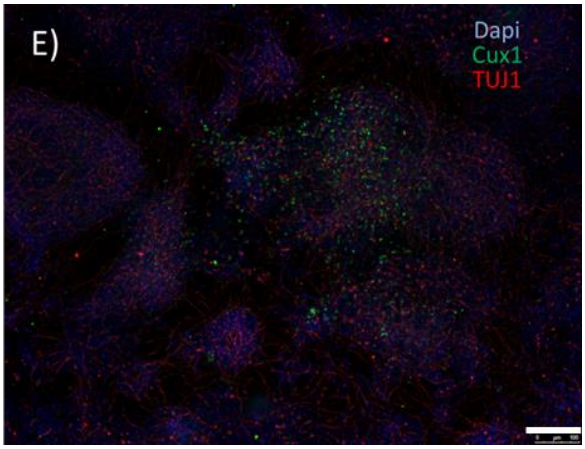
E)
Dapi
Cux1
TUJ1

F.

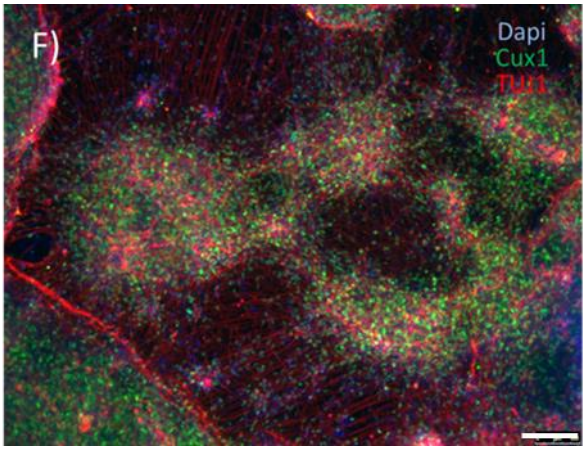
F)
Dapi
Cux1
TUJ1

Figure 3.4: Neurons derived from hESCs express the transcription factors Tbr1, Ctip2, and Cux1. *A) & B) Immunofluorescence analysis for Tbr1 (layer VI) and β-III tubulin on DIV 25 neurons and DIV 68. C) & D) Immunofluorescence analysis for Ctip2 (layer V) and β-III tubulin on DIV 25 and DIV 68 neurons. E) & F) Immunofluorescence analysis for Cux1 (layer III) and Tuj1 on DIV 34 and DIV77. Dapi is used to stain the nuclei. Scale bar is 100 µm in all pictures except B) where it is 50 µm*

3.2.2 *BDNF* mRNA expression in neurons derived from H7 human embryonic stem cells

The expression of the BDNF gene was tested at 33 and 82 DIV. RNA was extracted as detailed in Materials & Methods. Subsequently cDNA was generated by reverse transcription and the levels of coding transcripts were determined by reverse transcription-polymerase chain reaction (RT-QPCR). In these experiments 18s ribosomal RNA was used as a normalisation gene (internal control). 18S rRNA has been identified as a reliable normalization gene for RT-PCR that remains unaltered even upon viral treatment, when compared to other commonly used housekeeping genes (Kuchipudi et al., 2012). The expression levels of 18S RNA have been tested at various stages of differentiation and found to be similar. Additionally, the limited amount of mRNA that was extracted from each well, in addition to the necessity for technical triplicates limited the internal control to one gene instead of two or more. The Taqman primers and probe were designed to amplify the coding exon IX. *BDNF* mRNA could be detected already at day 33 and was significantly upregulated (more than 10-fold, Mann-Whitney test, $p<0.05$, $n=4$) following an additional 50 days of culture (Figure 3.5 A). This increase is not unexpected and may reflect the presence of an increasing proportion of more mature neurons after almost 3 months *in vitro*. To test whether the increase in *BDNF* mRNA levels may be due to increased synaptic activity, the cultures were treated with 25 mM KCl to depolarise cell membranes, thereby presumably also increasing synaptic transmission. Surprisingly, even after 2 months of culture *BDNF* mRNA levels remain unchanged by treatment with 25 mM KCL (Mann-Whitney test, $p>0.05$, compared to the corresponding control, $n=7$). In line with this, exposing the cells to 1µM of the sodium channel blocker tetrodotoxin (TTX) failed to change the levels of *BDNF mRNA* Mann-Whitney test, $p>0.05$, compared to the corresponding control, $n=7$. (Figure 3.5 B) It thus appears that until 60 days, the levels of *BDNF* mRNA are not regulated by neuronal activity or by membrane depolarisation. This raises questions as to the identity of the cells expressing the BDNF gene in these cultures (see Discussion).

By contrast, neurons that had been cultured for 82 days when treated with 25mM KCl or 1µM TTX did change the levels of *Bdnf* mRNA. Thus, the addition of KCl led to an approximate 2-fold increase (Unpaired t-test $p<0.001$, compared to the corresponding control, $n=7$), whereas the addition of TTX led to a decrease by about 10-fold

(Unpaired t-test $p<0.001$, compared to the corresponding control, n=6) (Figure 3.6 A) and B).

A.

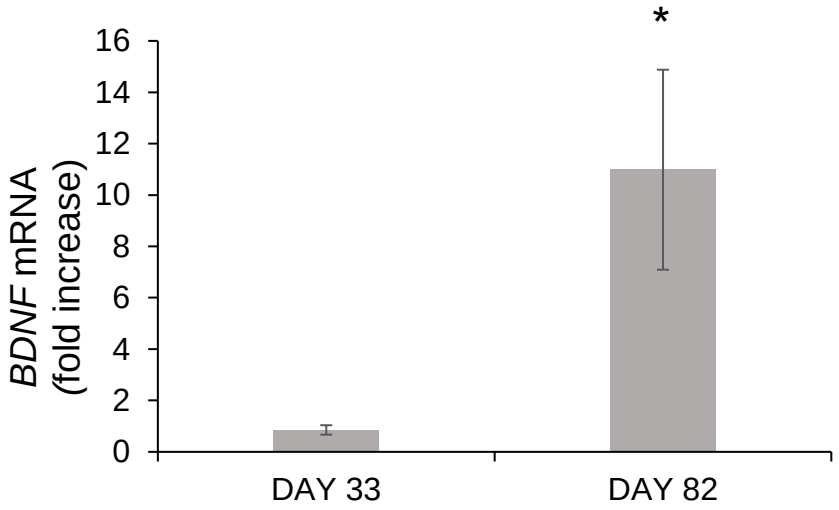
*
16
14
12
10
8
6
4
2
0
BDNF mRNA (fold increase)
DAY 33
DAY 82

B.

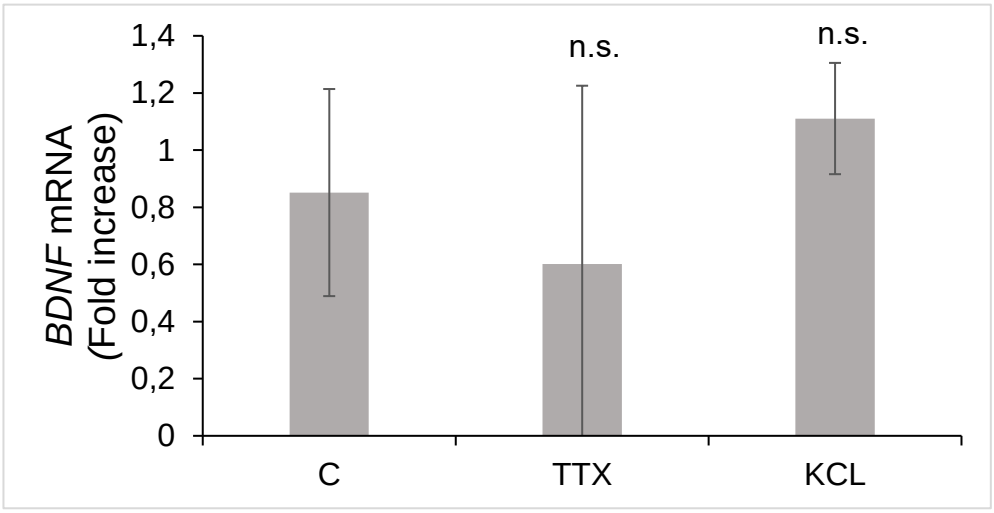
n.s.
n.s.
1,4
1,2
1
0,8
0,6
0,4
0,2
0
BDNF mRNA (Fold increase)
C
TTX
KCL

Figure 3.5*:* **Real-time PCR analysis of *BDNF* mRNA levels in cDNA extracted from human neurons.** *A) BDNF mRNA is already detected at DIV33 and significantly upregulated at DIV82* (*Mann-Whitney test, *p<0.05, n=4). B) BDNF mRNA is not regulated upon treatment with 1 μM TTX or 25 mM KCL treatment for 24 hours at DIV 60* (*Mann-Whitney test, p>0.05, n=7. Data represent mean +/- standard deviation.*

A.

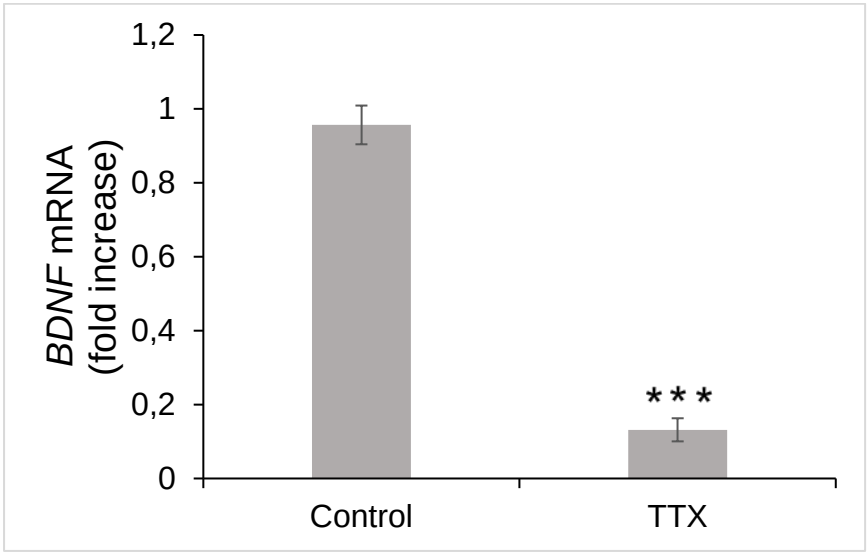

B.

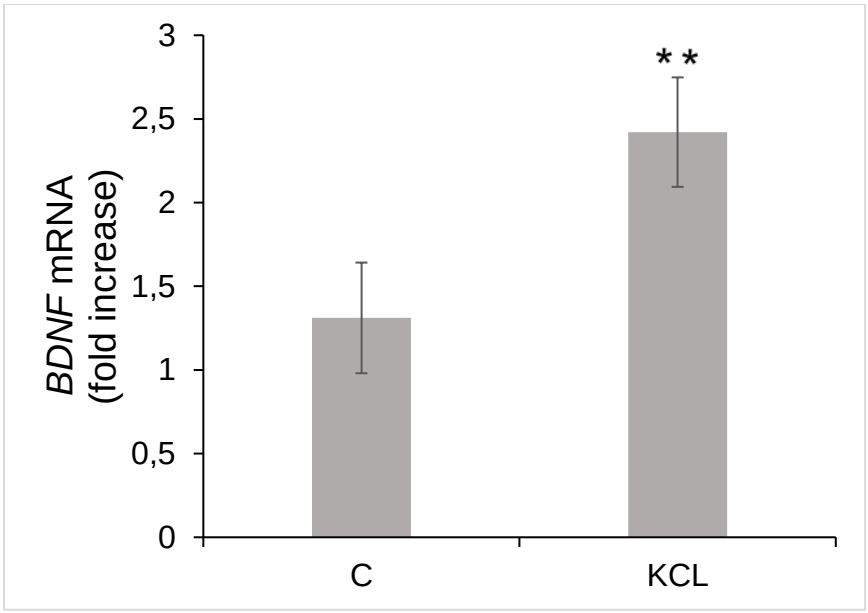

***Figure 3.6**: **Real-time PCR analysis of BDNF mRNA levels in cDNA extracted from DIV 80 human neurons.** A) BDNF mRNA is significantly downregulated upon treatment with 1µM TTX for 24 hours (unpaired t-test, ***p<0.001, n=6). B) BDNF mRNA is upregulated about 2-fold upon treatment with 25 mM KCL for 24 hours (unpaired t-test, **p<0.01, n=7). Data represent mean +/- standard deviation.*

Subsequently, conventional reverse transcription PCR (RT-PCR) experiments with RNA extracted from 58 DIV neurons were performed, in order to explore which *BDNF* transcripts may be expressed by hESCs-derived neurons. It turned out that most of the transcripts expressed in human post-mortem cortex (Pruunsild et al., 2007) could also be detected in cultured human neurons, including exon I and IV, the primary transcripts regulated by neuronal activity in rodent neurons (Figure 3.7).The most striking difference between neurons derived from hESCs and post-mortem cortex is the absence of exon III in the former. This difference might be attributed to a lack of mature neurons or a particular cell type that could express this particular transcript.

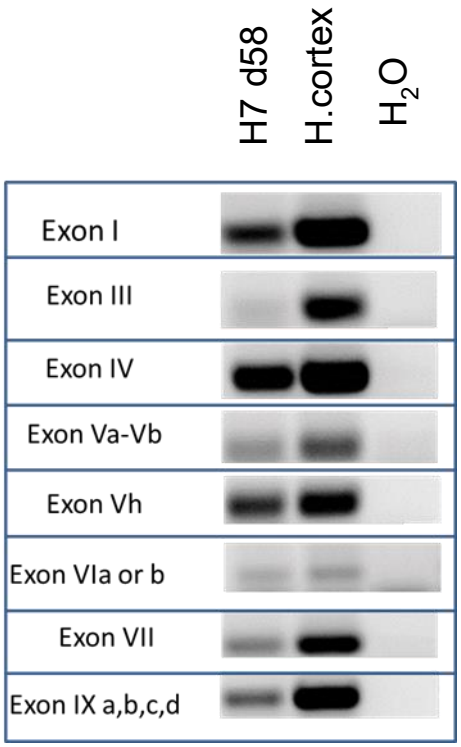

Figure 3.7: Amplification products generated from cDNA derived from DIV 58 H7 neurons*. Most BDNF transcripts found in samples of human cortex (normal human brain, total RNA from cerebral cortex, pooled from 4 males Asians, ages 26-41), can also be detected on neurons derived from hESCs. H_2O was used as a control, as H2O was added to the PCR mix in the absence of cDNA, ensuring the absence of genomic contamination of the reagents.*

3.2.3 *BDNF-AS* mRNA expression in neurons derived from H7 embryonic stem cells

A major objective of this work was to investigate the expression of the *BDNF-AS* mRNA. Using RNA extracted from hESC-derived neurons, *BDNF-AS* mRNA could be detected at the same time points as the *BDNF* sense mRNA, namely 33 DIV and 82 DIV (Figure 3.8 A), although no statistical difference between the expression levels at these stages was found (Unpaired t-test $p>0.05$, $n=4$). However, the levels of *BDNF-AS* mRNA turned out to be 10 to 15-fold lower than the levels of *BDNF* mRNA. Also, and for reasons that remained unclear, the standard deviation turned out to be particularly large. Similarly, to what is the case for *Bdnf* mRNA, *BDNF-AS* mRNA levels are not regulated by neuronal activity or by membrane depolarisation at day 60 (Unpaired t-test $p>0.05$, compared to the corresponding control, $n=9$) (Figure 3.8 B). Interestingly, treatment of day 80 DIV neurons with 25 mM KCl for 24 hours resulted in a reduction of *BDNF-AS* mRNA by about 50% (Mann-Whitney test, $p<0.001$, compared to the corresponding control, $n=7$) (Figure 3.9 A). However, the addition of 1 µM TTX treatment failed to consistently increase the levels of *BDNF-AS* (Unpaired t-test $p>0.05$, compared to the corresponding control, $n=6$) (Figure 3.9 B).

A.

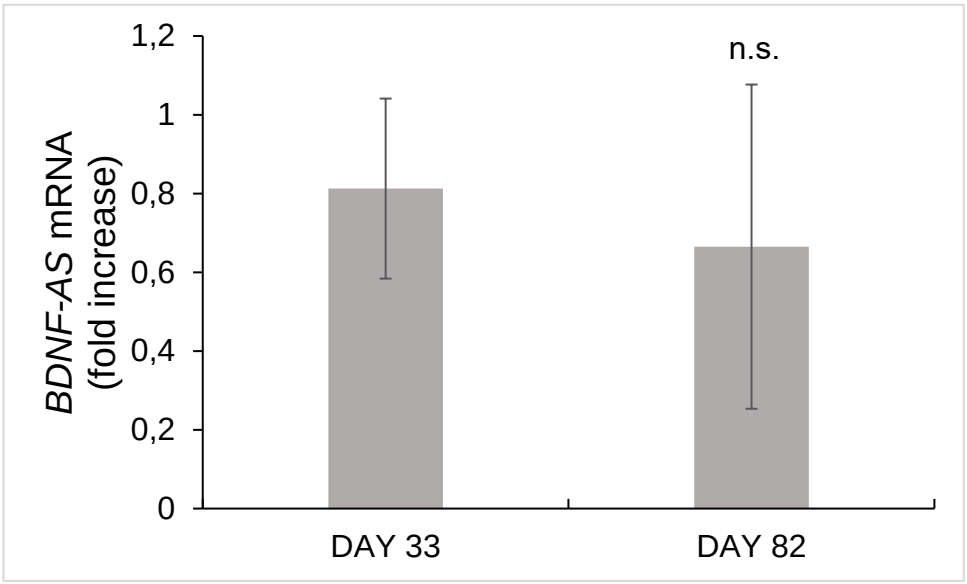
1,2
1
0,8
0,6
0,4
0,2
0
BDNF-AS mRNA (fold increase)
n.s.
DAY 33
DAY 82

B.

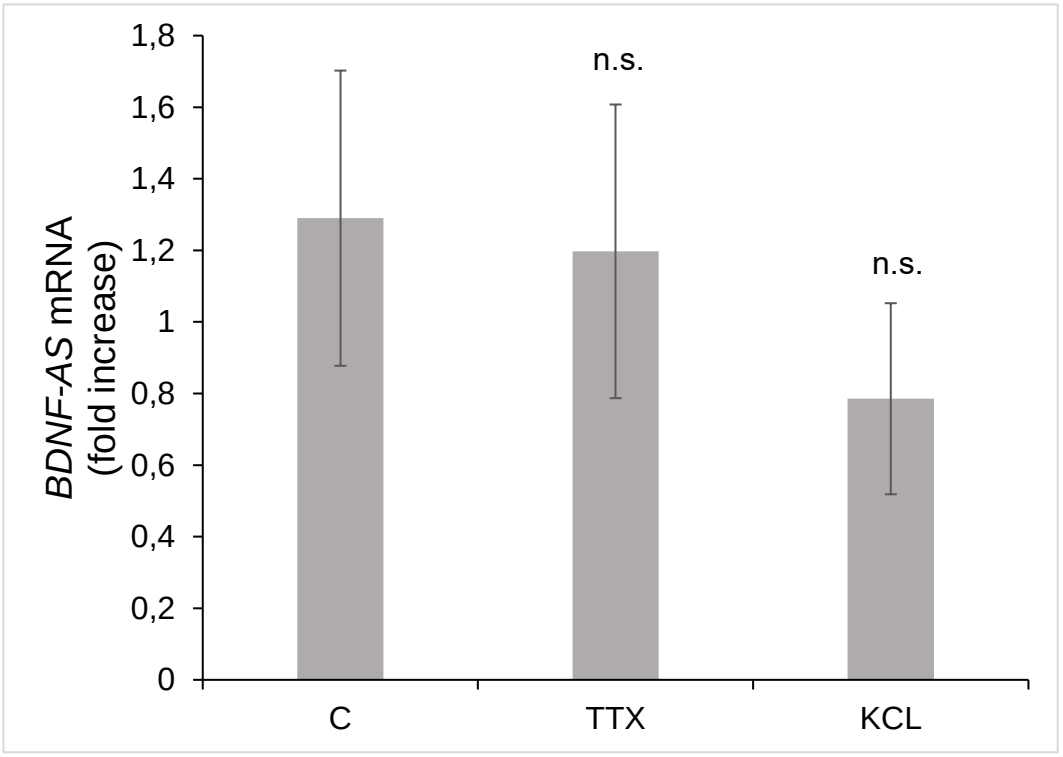
1,8
1,6
1,4
1,2
1
0,8
0,6
0,4
0,2
0
BDNF-AS mRNA (fold increase)
n.s.
n.s.
C
TTX
KCL

Figure 3.8: **Real-time PCR analysis of *BDN-AS* mRNA levels in cDNA extracted from human neurons.** *A) BDNF-AS mRNA is already detected at DIV33 and no significant difference of the expression levels can be detected at DIV82 (Unpaired t-test p>0.05, compared to the corresponding control, n=4). B) BDNF-AS mRNA is not regulated upon treatment with 1 μM TTX or 25 mM KCL treatment for 24 hours at DIV 60* (*Unpaired t-test p>0.05, compared to the corresponding control, n=9). Data represent mean +/- standard deviation.*

A.

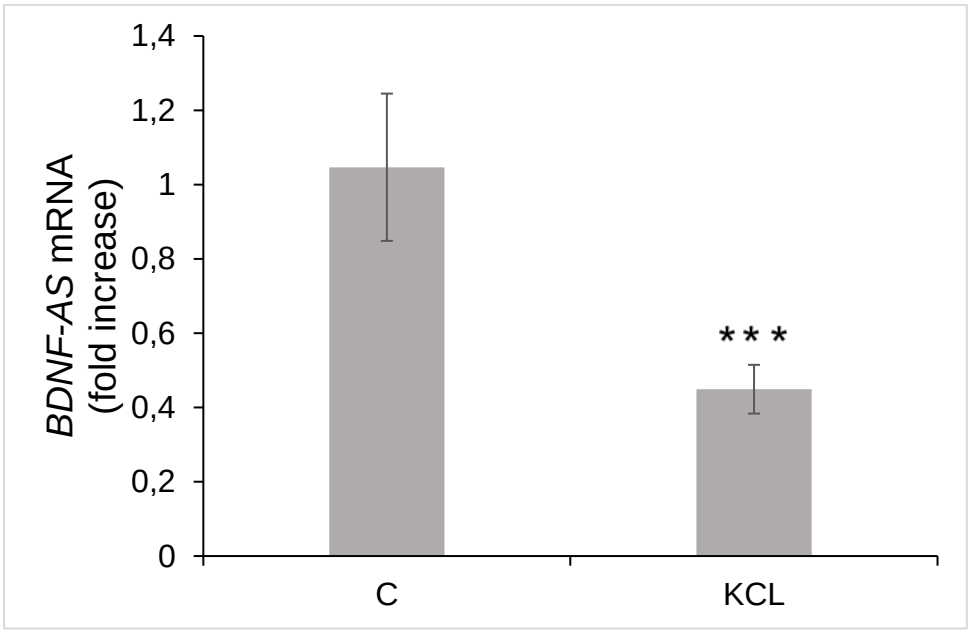

B.

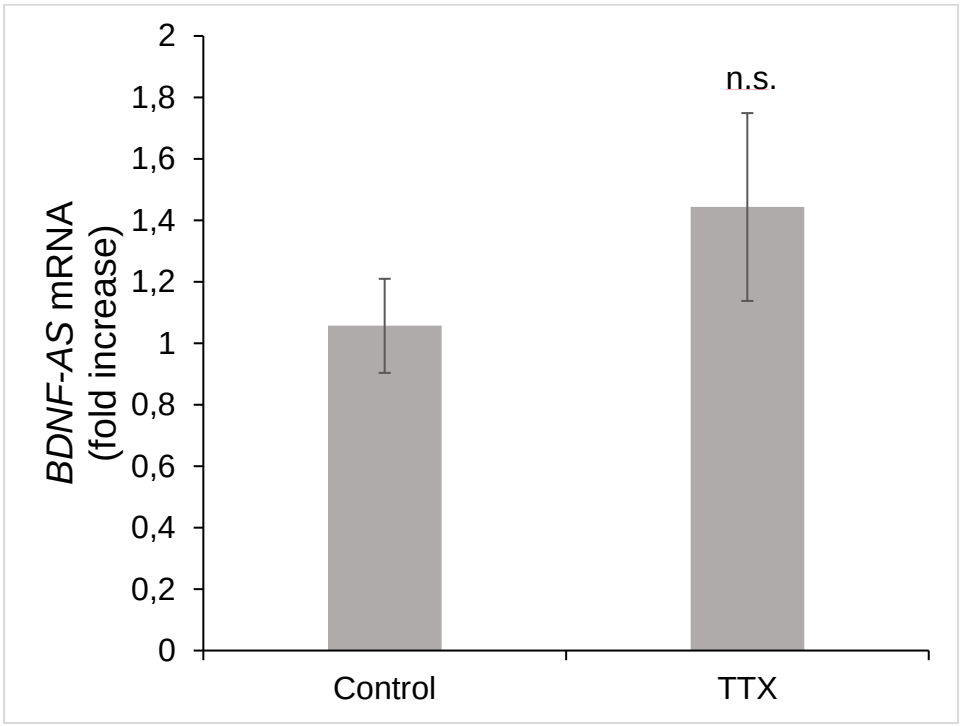

***Figure 3.9**: **Real-time PCR analysis of BDNF-AS mRNA levels in cDNA extracted from DIV 80 human neurons.** A) BDNF-AS mRNA levels are significantly downregulated upon treatment with 25 mM KCL for 24 hours (Mann-Whitney test, ***p<0.001, compared to the corresponding control, n=7) B) BDNF-AS mRNA levels do not change significantly upon treatment with 1 μM TTX for 24 hours (Unpaired t-test p>0.05, compared to the corresponding control, n=6) (Figure 3.9 B). Data represent mean +/- standard deviation.*

The question was then asked whether BDNF protein could also be detected in neurons derived from hESCs. After 23 days of differentiation very low, but detectable levels of BDNF could be revealed by Western blot analysis. These low levels remained the same at 40 DIV, but increased after 50 and 60 and 80 DIV (Fig. 3.10 A and B). Interestingly an additional band was occasionally observed in DIV 80 neurons, at the expected size of pro-BDNF (slightly above 30 kDa). It is not clear why this band was not observed in earlier time points or in other samples from DIV80, but it could be attributed to different levels of the enzymes that are responsible for the processing of mature BDNF, which is most likely proprotein convertase convertase 7 (Wetsel et al., 2013).

In an attempt to ensure that the band detected by the antibody was specific, extracts from cells presumed not to express the protein at significant levels were used, including (undifferentiated) H7 and H9 hESCs and SHSY5Y neuroblastoma cells, either treated or not treated with retinoic acid to differentiate them (Figure 3.10 B). Levels of BDNF did not seem to change upon treatment with TTX or KCL for 24 hours in DIV80 neurons, while the protein levels varied between duplicate/triplicate wells (Figure 3.11 A). This observation could be attributed to the presence of 3D cell clumps that could not be dissolved completely.

As a marker of neuronal differentiation, synaptophysin antibodies were used. Significant levels of this presynaptic markers were observed after 2 months of differentiation, but not after 33 days, suggesting that the cultures require long periods of time to significantly mature (Figure 3.11 B). Whilst no further increase of the synaptophysin levels was observed by 70 DIV, the levels decreased after 80 DIV, possibly caused by enhanced death of neurons after prolonged culture periods. The notion that synaptophysin and therefore synaptic maturation is achieved at later time-points of the differentiation further highlights the necessity of culturing neurons derived from human embryonic stem cells for extended periods of time to begin to be able to study the biochemistry and molecular biology of BDNF. Beyond the very long periods of time needed to reach detectable levels of BDNF protein, the observation that the levels of synaptophysin begin to decrease at later time points raised questions about the suitability of the cell culture system used, and indeed about the feasibility of successfully achieving the goals that were set out for this part of the project.

A.

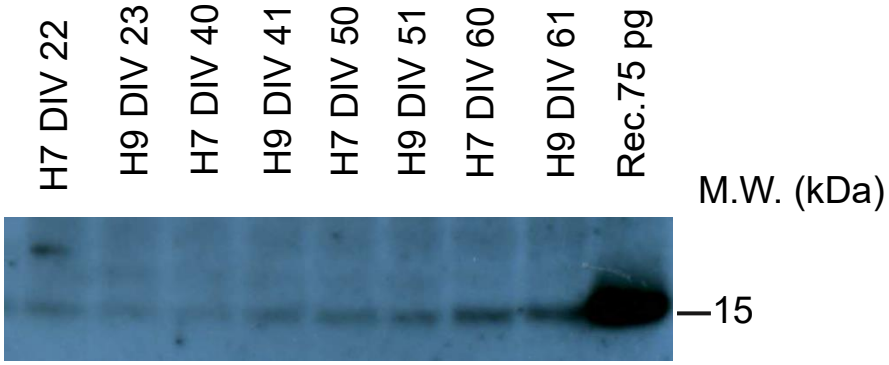

B.

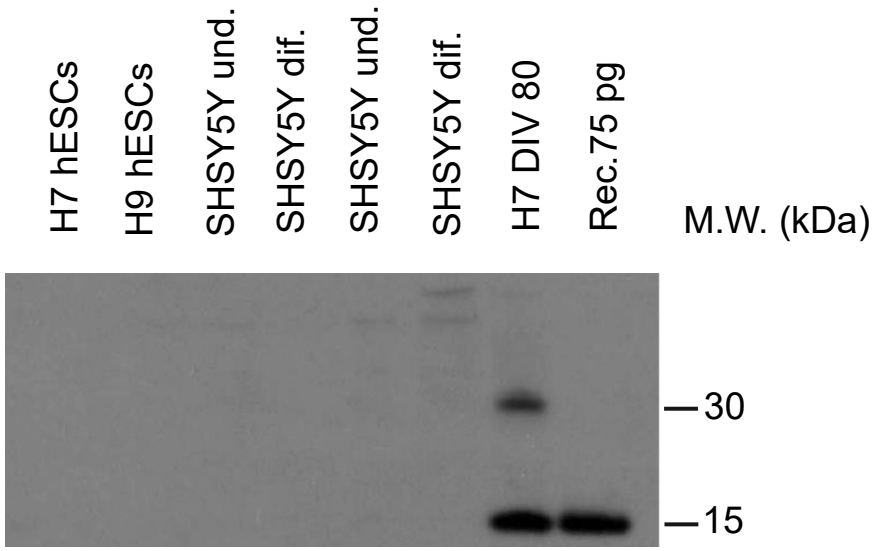

Figure 3.10: ***Western blot analysis for BDNF using protein extracted from H7 and H9 neurons****. Panel A). Lysates (60 µg) prepared from neurons grown for the indicated length of time were separated by SDS gel electrophoresis. Following transfer, the blot was incubated with the BDNF antibody 3C11 (Icosagen) Panel B) Lysates (60 µg) prepared from the cells indicated were separated by SDS gel electrophoresis as in A) and the blot was incubated with* the *BDNF antibody 3C11 (Icosagen). Recombinant BDNF (75 pg) was used as a control of the molecular size of the band corresponding to BDNF.*

A.

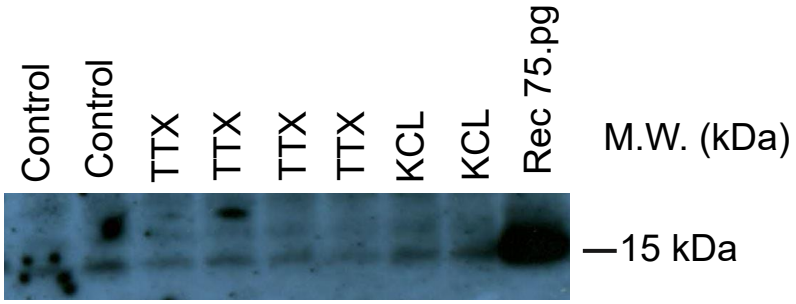

B.

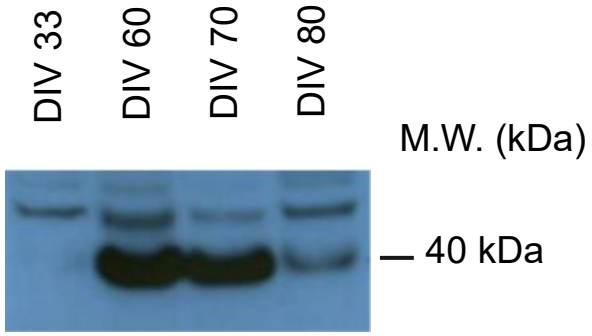

Figure 3.11: Western blot analysis for BDNF and synaptophysin using protein extracted from H7 neurons*. Panel A) Lysates (60 µg) prepared from DIV 80 neurons treated for 24 hours with either 1µM TTX or 25 mM KCL, were separated by SDS gel electrophoresis. Following transfer, the blot was incubated with the BDNF antibody 3C11 (Icosagen). Panel B) Lysates (60 µg) prepared from neurons grown for the indicated length of time were separated by SDS gel electrophoresis as in A) and the blot was incubated with the synaptophysin antibody (Sigma). Recombinant BDNF (75 pg) was used as a control of the molecular size of the band corresponding to BDNF.*

3.3 Discussion

Despite the implication of BDNF in numerous diseases, its mode of action and especially the regulation of its expression in the human brain is still poorly understood. Here human neurons differentiated from ESCs *in vitro* were shown to express *BDNF* mRNA, which is significantly upregulated after 80 DIV. Interestingly *BDNF* mRNA did not change in response to treatment with TTX or KCL before 80 DIV. These results are in line with data from other studies, where multiple action potentials start to be generated after 50 days of *in vitro* differentiation of human ESCs to neurons (Shi et al., 2012). These results suggest that newly generated neurons may not be used to study neuronal activity- dependent mechanisms such as BDNF transcription, and mature neurons need to be obtained by culturing the neurons for long time periods. Yet the levels of protein expression remained very low at 80 DIV and did not increase upon treatment with KCL, as it would have been expected. Thus, although *BDNF* gene was expressed in the cultures described above, its regulation cannot be meaningfully modelled using this system.

Another significant difficulty that occurred in this study was the presence of 3D cell clumps, that were composed of a mixture of dividing progenitors and post-mitotic neurons. As a result of the constant cell division even at late stages of the differentiation a pure neuronal population could not be obtained, and the variability between triplicate wells in each differentiation was high. The identification of particular cell types based on the transcriptional factors that were expressed by the cultures was proven not to be possible. Not only a monolayer was not achievable, but the presence of 3D cell clumps made quantification of the proportion of cells expressing each transcription factor not feasible. Especially after DIV50, neurons could only be observed at the few open spaces between the clumps, thus decent representative pictures could not be obtained. Overall, the uncontrolled differentiation of the progenitors resulted in the inability to control cell numbers and identity between and within differentiations excluding any meaningful quantitative analysis such as single cell RNA-seq. Modifications of the protocol discussed above were deployed in order to overcome the presence of the clumps. Initially a wide range of plating concentrations were tested in an effort to achieve a monolayer of neurons. More specifically plating densities close to the default ones at the second passage did not

have an impact on the cultures, while lower (1:2 to 1:5 of the default) densities only shifted 4-5 days the formation of the thick clumps, while much lower densities (1:7 to 1:10 of the default) led to cultures with very few neurons that expressed undetectable amounts of BDNF. Another approach included 1 or 2 additional passages of the cultures in an effort to further dilute them and enhance differentiation (section 3.2.1 and figures 3.2 and 3.3). Although monolayers of neurons were initially generated, a few days after the passage clumps appeared and eventually occupied most of the plate. Interestingly *BDNF* expression levels were about the same as when the cultures have only been passaged for 2 times (data not shown). Freezing and thawing of the progenitors was an alternative approach that was tested. Since the presence of progenitors was evident until late stages of differentiation it was hypothesized that they will be able to survive the freezing procedure, which will serve as a means of selecting only the progenitor populations, leading therefore to a more homogeneous culture. However monolayer of neurons were only maintained for the first week after the thawing and subsequently clumps were generated due to the ongoing proliferation, resulting in similar data as mentioned above. It was then tested whether embedding the progenitors in thick Matrigel gels would enhance differentiation. These trials were also proven to be unsuccessful as very low concentrations were needed in order to avoid the generation of the clumps, while due to the presence of the extracellular matrix from which Matrigel is composed, the extraction of proteins from the samples was challenging. The last attempt focused on blocking cell division using an anti-cancer drug Floxuridine (5-FDU). Cultures were treated with 5 μg/ml of 5-FDU every 3 days for a period of 6 days, but while cell division stopped the cultures faced widespread cell death and 3-4 days after the end of treatment very few alive cells could be observed. A single dosage or lower doses of the drug had no visible effect. Overall, despite the various approaches that were deployed the derivation of monolayer of neurons had not been possible.

Whilst it was interesting to detect the presence of the *BDNF-AS* mRNA and its apparent downregulation by increased KCL levels, the decision was made not to pursue these investigations further, in particular studies aiming at investigating the role of the *BDNF* antisense transcript. While it is tempting to speculate that the depolarization-induced downregulation of the levels of antisense transcripts, together with the increase of the levels of sense transcripts could contribute to further enhance

the levels of BDNF protein, causality could only be established by manipulating the genome of the hESCs to eliminate the promoter driving the expression of the *BDNF* antisense mRNA. Not only is this promoter not described in sufficient details at this time but in addition, the extended time periods needed to observe detectable levels of BDNF protein and the heterogeneous character of the cultures indicate that the objectives may not have been reached within a useful timeframe. Future studies would characterise the promoter of *BDNF-AS* using bioinformatics analysis and luciferase reporters and subsequently use an improved protocol to study the interaction of BDNF mRNA with *BDNF-AS* and its effect on the levels of BDNF protein.

In order to be able to study the regulation of BDNF and BDNF-AS transcripts and BDNF protein using human neurons derived from human embryonic stem cells a novel protocol would be needed. The two key characteristics of this protocol would be the fast and robust generation of monolayers of neurons that will express sufficient amounts of BDNF. Under the standard procedure for the generation of excitatory cortical neurons that was widely used in several publications, neuralisation was achieved through the inhibition of BMP and TGF-β signalling, neurons are produced slowly and begin to mature after many weeks *in vitro*. A recent publication combined expression of neutralizing transcription factor NGN2 with inhibition of SMAD and WNT to generate neurons of the upper layers that present neuronal activity after 42 DIV (Nehme et al., 2018). Under this protocol populations of progenitor cells were also present, therefore they used the expression of the CAMK2A::GFP reporter gene as a marker for the more differentiated cells. The use of this novel protocol might be useful for the study of *BDNF* gene regulation in a human *in vitro* model.

Chapter 4: Comparing TrkB activation following the addition of BDNF, NT4 and #85

4.1 Introduction

BDNF as well as NT4 (to which it is even more related than to NGF and NT3) exert their trophic function through the activation of a tyrosine kinase receptor TrkB (see Introduction and (Klein et al., 1993). Upon binging of a neurotrophin dimer at two TrkB receptor molecules, the intracellular part of the receptor is autophosphorylated in several tyrosine residues, that serve as docking sites for proteins like Shc, PLC-γ that activate the downstream signalling pathways that enhance survival, neurogenesis, and synaptogenesis (Binder and Scharfman, 2004). TrkB is highly expressed in the CNS and BDNF-TrkB signalling has been linked to neurodegenerative diseases in studies using animal models, for example, TrkB has been implicated in Parkinson's disease. A study that used a *TrkB* hypomorphic mice mutant showed that the significantly reduced TrkB expression delays the onset of the disease until 12 months of age (Baydyuk et al., 2011). Additionally, genetic data strongly support the relevance of this signalling system in humans. Humans that carry a SNP in the human BDNF gene (Val66Met) have been reproducibly identified with impaired episodic memory (Egan et al., 2003, Cathomas et al., 2010). *BDNF* mRNA levels are decreased in the substancia nigra of PD patients (Howells et al., 2000) and BDNF levels are decreased in the striatum of HD patients (Ferrer et al., 2000). Furthermore, the loss of one BDNF allele in WAGR syndrome has been associated with severe cognitive impairment (Han et al., 2013). Defects in TrkB also lead to early-onset obesity, hyperphagia and severe developmental delay in humans (Yeo et al., 2004, Gray et al., 2007, Han et al., 2008, Sonoyama et al., 2020). More specifically a de novo missense mutation of *NTRK2* was detected in an 8-year-old patient with severe obesity and developmental syndrome. As he had normal karyotype, normal proinsulin levels and did not have mutations in the genes of leptin, leptin receptor, POMC and MC4R, the mutation in the gene encoding for TrkB was suggested as the cause for these symptoms (Yeo et al., 2004). Additionally, a very recent study identified in humans one BDNF variant and 10 TrkB variants that were linked with severe obesity, spectrum of learning difficulties, impaired short-term memory and hyperactivity (Sonoyama et al., 2020). For the reasons

mentioned above, BDNF is widely considered as a therapeutic target. However, BDNF is not favoured for infusion, as the half-life of the protein in serum is very short (Poduslo and Curran, 1996) and it is rapidly eliminated by filtration though the kidney with no significant quantities reaching the brain (Pardridge et al., 1994).

Several alternative strategies have been used to increase BDNF/NT4/TrkB signalling, for example the use of drugs penetrating the blood-brain barrier and increasing *Bdnf* transcription such as the sphingosine-1 phosphate analogue Fingolimod (Deogracias et al., 2012) or else directly activating TrkB (Wilkie et al., 2001). As an alternative to small chemical entities activating TrkB, monoclonal antibodies that activate TrkB have also been developed (Bai et al., 2010, Cazorla et al., 2011). Most of this research so far has been performed in rodents. Therefore, the next objective of the Thesis was to study BDNF-TrkB signalling using human neurons. Human embryonic stem cells were differentiated to neurons using a previously described protocol that generates mainly GABAergic neurons (Telezhkin et al., 2016). Under this differentiation protocol neurons that express TrkB receptor are produced and BDNF, NT4, and a novel TrkB agonistic antibody #85 were tested based on their ability to phosphorylate TrkB.

4.2 Generating inhibitory neurons from human embryonic stem cells

Following this differentiation protocol (detailed in Chapter 2), it was observed that hESC undergo a much shorter proliferation period of only 16 days at which time many rosettes were already formed. These rosettes represent typical clusters of neural progenitors. At day 16 progenitors were dissociated and re-plated, to be kept in culture for a period of two weeks. Young neurons can be observed already the next day after the dissociation. Based on phase contrast microscopy, at day 30 all cultures consist of a neuronal monolayer, with remarkably few cells of a non-neuronal morphology. Although relatively high cell densities had to be used for biochemical experiments, single neurons can nonetheless be observed under the microscope (Figure 4.1 A and 4.1 B). Day 16 progenitors were dissociated and plated into coverslips as detailed in materials and methods. At day 30 neurons were fixed and immunohistochemistry experiments were performed as described in Materials & Methods. The cell population generated by day 30 consisted primarily of neurons as demonstrated by β-III tubulin staining (Figure 4.1 D) and most of these neurons expressed GAD65/67, which is expressed by GABAergic neurons (Figure 4.1 C). Indeed, about 75% of neurons were

positive for GAD65/67 cells (Figure 4.2). More than 90% of the cells express β-III tubulin and no signal was detected for Olig2 which is considered as an oligodendrocyte marker or GFAP which is used as an astrocyte marker (data not shown). Vglut, a vesicular transporter expressed by glutamatergic neurons was also not detected (data not shown).

A.

B.

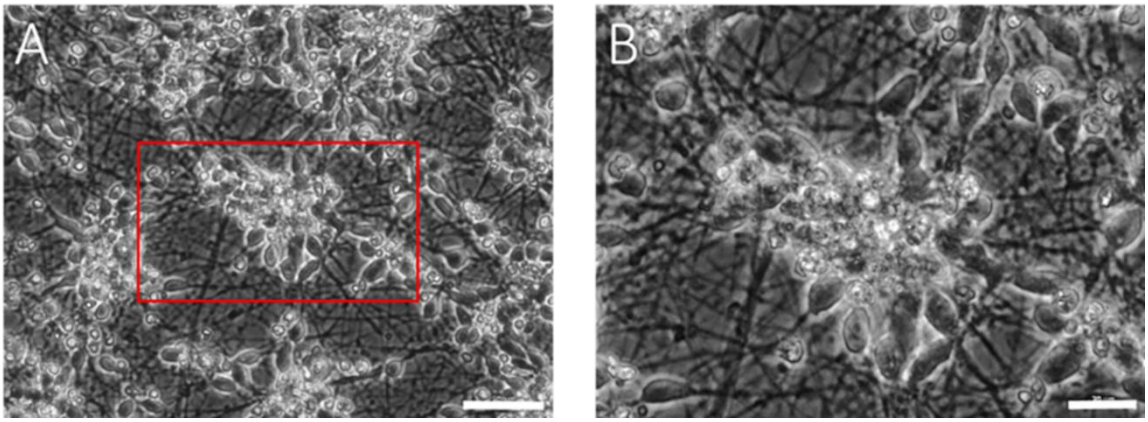

C.

D.

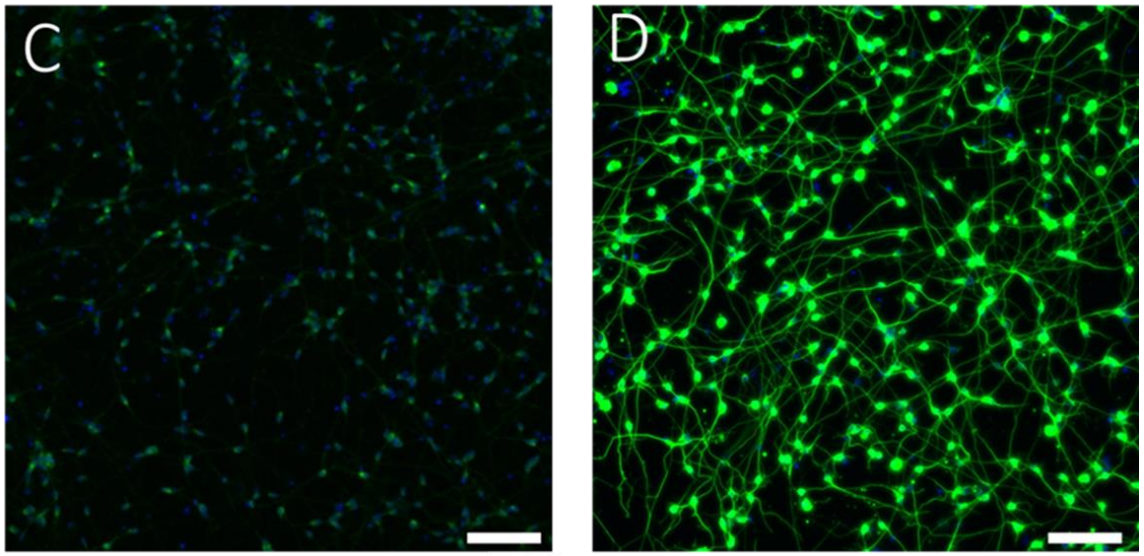

Figure 4.1 H9 hESCs differentiated as a monolayer of neurons, 30 DIV. *A representative image of day 30 neurons is shown in A and the area inside the red box is shown in B. Scale bar is 100μm in A and 20 μm in B. C) and D) Immunocytochemistry experiment with day 30 neurons for GAD65/67 and β-III tubulin respectively. Dapi is used to stain the nuclei. Scale bar is 100 μm.*

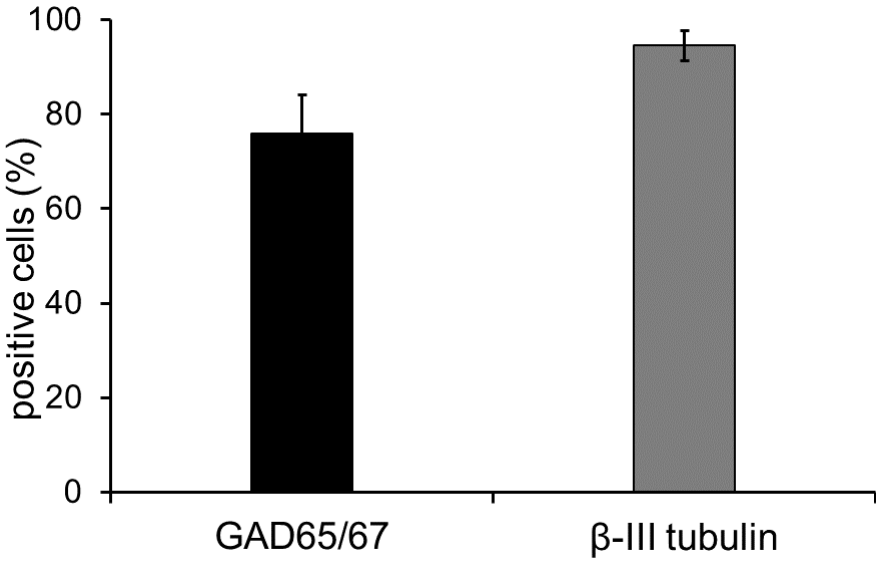

Figure 4.2 Immunocytochemistry quantification analysis of 4.1 C) and D) *Number of total cells was equal to the number of DAPI positive cells. Three independent differentiations were analyzed. Data represent mean +/- standard deviation.*

Immunocytochemistry experiments also included various transcription factors expressed by CNS neurons. Transcription factors characteristic of neurons with cortical identity such as CTIP2 and Cux1 were found not expressed at all (data not shown), whereas transcription factor Tbr1 is mildly expressed, in accordance to a study that established the role Activin A in the generation of striatal projection neurons from human ESCs (Arber et al., 2015). Foxp1 and Foxp2 that are present in neurons of the lateral ganglion eminence (Tamura et al., 2004, Takahashi et al., 2003) were detected (Figure 4.3 A, B and C). Quantification of the immunocytochemistry results was possible due to the absence of 3D structures that were developed in the protocol discussed in Chapter 2. However, co-localization data were not obtained as the antibodies for the markers mentioned above were generated using antibodies belonging to same species (rabbit) and the major focus of the study was a comparison of the efficacy of BDNF, NT4 and the TrkB activating antibodies in including TrkB activation as it will be discussed in the next two chapters. In future studies double-labeling experiments would be necessary to fully characterize the cultures and determine whether some neurons are more responsive to BDNF than others. The necessary comparisons would include Foxp1 with Foxp2, Foxp1 with GAD65/67, Foxp2 with GAD65/67, Tbr1/GAD65/67, Foxp1/Tbr1 and Foxp2/Tbr1. For this purpose, antibodies of different species could be used, or alternatively the primary antibodies could be coupled directly with different fluorophores.

Immunofluorescence experiment quantification of 2 independent experiments was performed using 5 images per marker and differentiation and roughly 300 cells per image. Foxp1 is expressed by approximately 50% of the neurons, Tbr1 by 24% and Foxp2 by 32% (Figure 4.4)

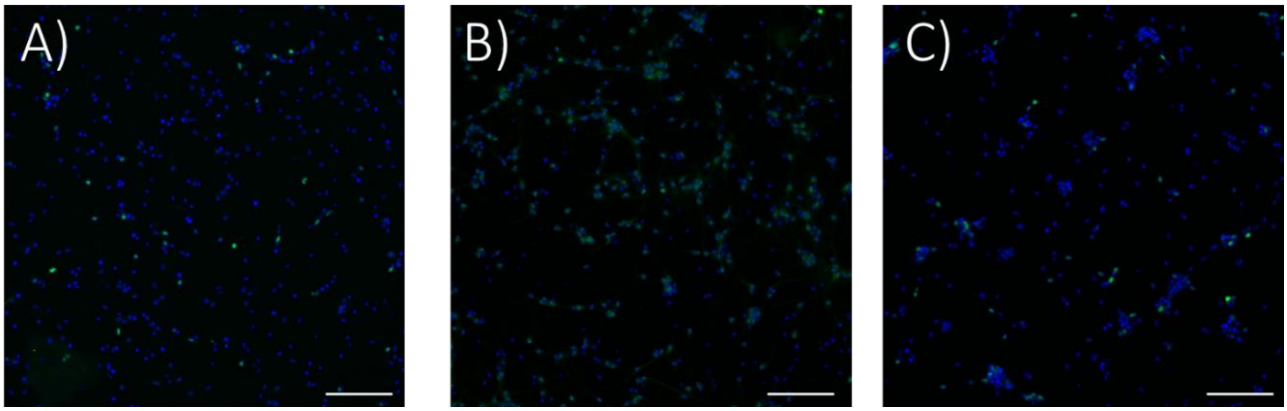

.

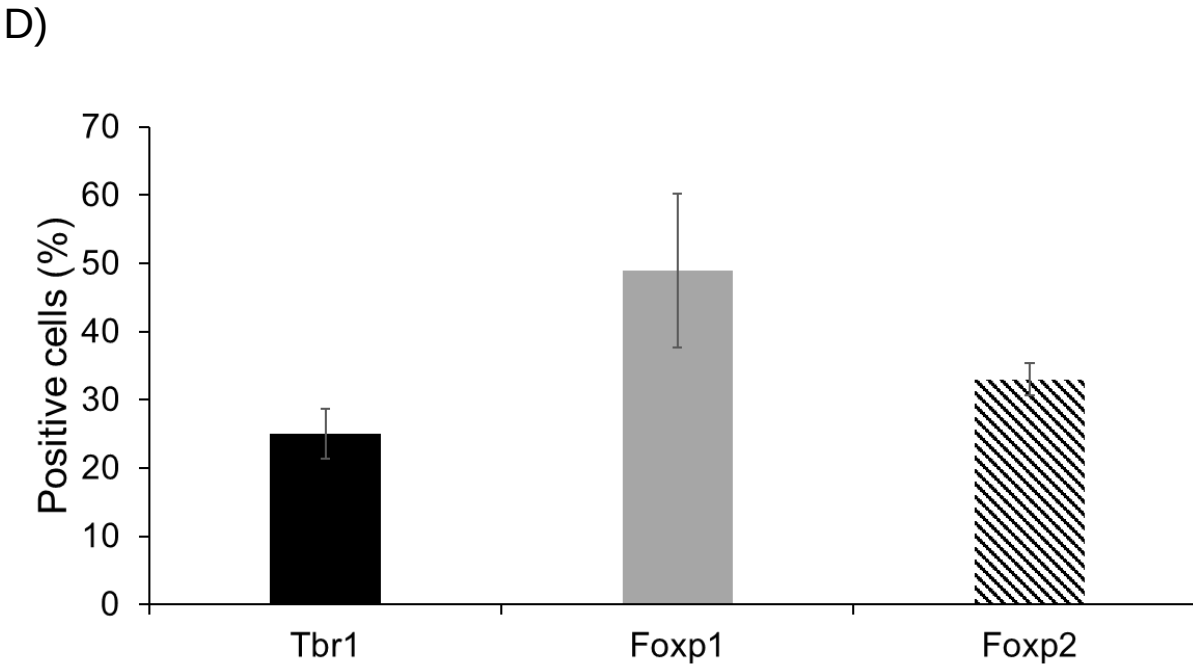

Figure 4.3 H9 hESCs differentiated as a monolayer at 30 DIV. Immunocytochemistry using A) Tbr1 (green), B) Foxp1 (green) and C) Foxp2 (green). Blue is DAPI. Scale bar is 100 µm D) Immunocytochemistry quantification of Tbr1, Foxp1 and Foxp2 positive neurons in figure 4.3. The number of total cells was equal to the number of DAPI positive cells. Cells were counted manually using ImageJ software. Two independent differentiations were analyzed. Data represent mean +/- standard deviation.

4.3 BDNF, NT4 and a novel TrkB agonist phosphorylate TrkB in a time- and dose-dependent manner

Given the growing interest in TrkB-mediated signalling, especially in the context of conditions affecting the function of the human brain, strategies have been developed to activate TrkB using antibodies directed against this receptor. Through a collaboration with Zebra Biologics and the group of Richard Lerner at the Scripps Institute, we tested 4 TrkB-activating antibodies on neurons derived from the protocol discussed above, to determine how their activity compared to natural TrkB ligands, BDNF and NT4. These TrkB-activating antibodies have been generated using the near neighbor library assay (Xie et al., 2013) which screens a phage library containing about 1.0 x 10^9 members. The first step of this protocol involved the generation of a TrkB reporter cell line by infecting a CHO cell line with a lentiviral vector encoding the full-length human *NTRK2* gene under the EF1a promoter and with a lentiviral vector encoding the β-lactamase protein regulated by an NFAT response element. Upon binding to TrkB receptor the downstream signaling would be activated leading to the activation of the NFAT response element and therefore the expression of the gene Beta lactamase. The readout of this system is based on Förster resonance energy transfer or fluorescence energy transfer (FRET) and it relies on the FRET-based substrate termed CCF2-AM (or the alternative substrate CCF4-AM). CCF2-AM is composed of a Hydroxycoumarin donor conjugated to a Fluorescein acceptor via a β-lactam ring. In the absence of β-lactamase, excitation at 409 nm results to Förster resonance energy transfer (FRET) between the fluorescent donor and acceptor molecules, leading to emission at 520 nm. Upon expression of β-lactamase, the β-lactam ring is cleaved by β-lactamase, the two molecules are separated, FRET is disrupted and a fluorescence shift from 520 nm to 447 nm is produced. The specificity of this system was validated by flow cytometry, in which the reporter line was shown to bind BDNF, but not NGF. The TrkB reporter line also bound NT3 and NT4 that also bind TrkB receptor. In the second step of the agonist antibody selection a large (10^{10}) combinatorial scFv antibody library was expressed in phage. The binding antibodies that were identified (10^6) were cloned into a lentiviral vector and each unique scFv sequence was encoded together with a transmembrane domain and an Ig Fc domain. Thus, when expressed in individual cells each scFv protein is tethered to the

extracellular side of the plasma membrane as an Fc-dimer. Subsequently a single plate (1-2 x 10^7 cells) of the CHO-NFAT TrkB reporter cell line was infected with the virus, turning each cell into an independent autocrine assay point. When an scFV fragment binds and therefore activate the TrkB receptor a fluorescent signal is generated as explained above, and the cells can be selected by FACS. Using this method about 50 clones were selected for further analysis (Merkouris et al., 2018)

The 4 four most potent different monoclonal antibodies were compared to BDNF using phosphorylation of TrkB as a readout. H9 derived neurons were differentiated and maintained *in vitro* for a period of 7 weeks before treatment. Before testing the phosphorylation levels induced by BDNF or TrkB agonists, the cultures were tested for expression of BDNF in the absence of any stimuli, in order to determine whether there is any background expression of BDNF. BDNF was added in one culture in order to ensure that the protein is truly not detected in the system, and is not for example stuck in the Matrigel substrate. GDNF (Glial cell line-derived neurotrophic factor) was also tested in one culture to examine whether it could promote the expression of BDNF. It was found that BDNF protein is not present in this system (Figure 4.4.) Some wells were differentiated in the absence of activin A, in an effort to explore its necessity in the generation of TrkB positive neurons. Activin A has been shown to direct the differention of human ESCs towards neurons with characteristics of striatal projection neurons (Arber et al., 2015). BDNF was tested at 0.895 nM and 1.79 nM, while the four TrkB agonists were tested at 450 nM. All wells were treated for 15 minutes before lysis. Cell lysates were processed as described in Materials & Methods and equal amounts of proteins were loaded to NuPAGE gradient gel for western blot analysis. Subsequently the membrane was incubated with PhosphoTrkB antibody (Tyr706/707). The untreated samples did not show any signal, while in the samples treated with BDNF a single band above 110 kDA was detected (figure 4.5 A.). The intensity of the signal is higher in the neurons that were generated in the presence of Activin A, and therefore Activin A was used in all the subsequent experiments. Additionally, treatment with 1.79 nM of BDNF gives a stronger signal of pTrKB than treatment with 0.895 nM. Initially two of the four TrKB activating antibodies, designated #30 and #85 seem to activate TrkB to a similar level to BDNF at a concentration of 450 nM while treatment with antibodies #44 and #27 at the same concentration led to a weak signal of TrkB phosphorylation (Figure 4.5A). The next step was to treat

neurons that were cultured for 42 DIV with different concentrations of #30 and #85. Based on preliminary data with mouse ES cell-derived neurons and rat primary cultures (data not shown), four different concentrations had been selected: 45 nM, 90 nM, 225 nM and 450 nM. Antibody #85 was shown to saturate the P-TrkB response already at 45 nM, while #30 potency was increased until 450 nM, indicating that antibody #85 was more efficient than antibody #30. (Figure 4.5 B). Therefore #85 was selected for a detailed comparison with BDNF and NT4.

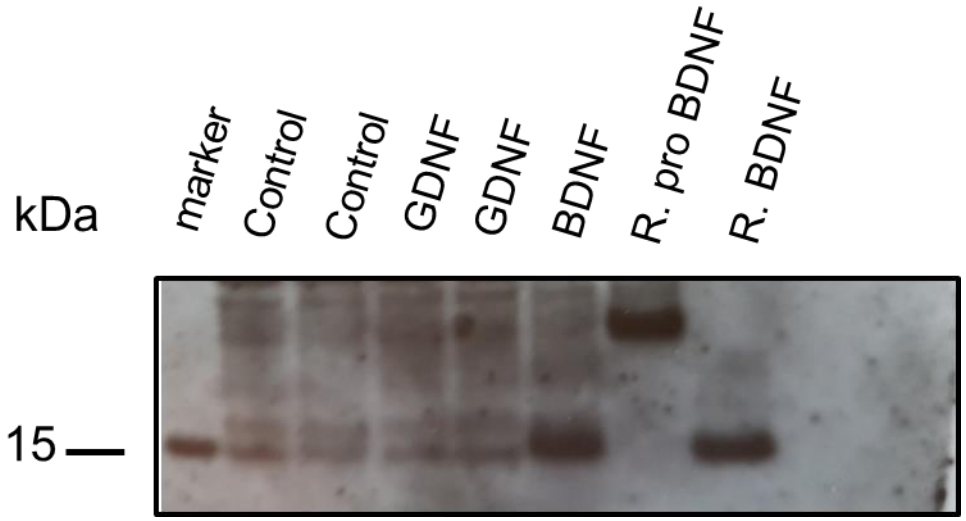

Figure 4.4 Western blot analysis of BDNF on protein extracted from H9 neurons at 37 DIV that had been treated with 0.358 nM of GDNF, 0.358 nM of BDNF and controls. Recombinant pro BDNF used is 4 pM and recombinant BDNF is 2 pM. *Lysates (30 µg) prepared from neurons treated for 24 hours with either BDNF or GDNF were separated by SDS gel electrophoresis. Following transfer, the blot was incubated with the BDNF antibody 3C11 (Icosagen). Recombinant BDNF was used as a control of the molecular size of the band corresponding to BDNF.*

A.

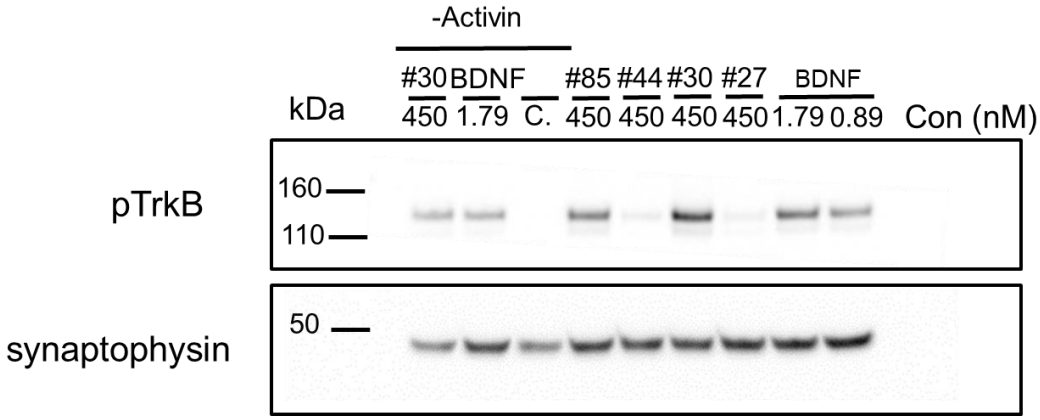

B.

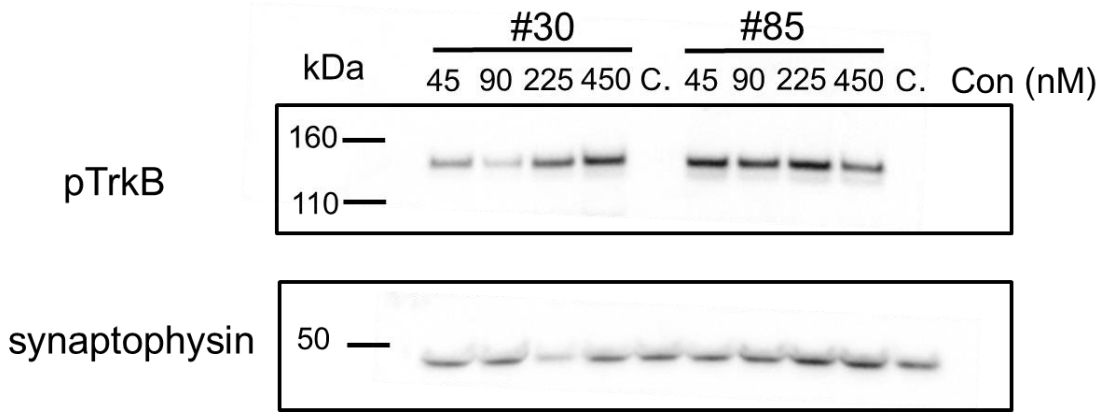

Figure 4.5 Western blot analysis of TrkB phosphorylation on protein extracted from H9 neurons at 42 DIV that had been treated with BDNF or TrkB-activating antibodies.

A) Comparison of 0.895 nM and 1.79 nm of BDNF with four different TrkB activating antibodies at 450 nM. B) Comparison of different concentrations of the TrkB activating antibodies #30 and #85. Lysates (30 µg) prepared from the cells indicated were separated by SDS gel electrophoresis and the blots were incubated with the PhosphoTrkB *antibody (Tyr706/707) (Cell Signaling). The blots were reprobed for a synaptophysin antibody in order to normalize for protein levels.*

Phosphorylation is known to be a reversible and relatively unstable protein post-translational modification (Fischer, 2010). Thus, the ability of the three TrkB ligands to phosphorylate TrkB receptor was tested over a period of 24 hours. Based on experiments where neurons were treated with different concentrations of BDNF, NT4 and #85, concentrations that are well above saturation were selected for a time-point experiment: BDNF at 1.79 nM, #85 at 45 nM and NT4 at 2.88 nM. The data were normalized to synaptophysin protein levels, which was used as a control. Furthermore, the densitometry values were transformed to 100% values. In all experiments the value of treatment with 30 minutes for BDNF was set as 100% while the other concentrations were calculated accordingly by the following type (value of x treatment/ value of 30 minutes BDNF * 100). These transformations were necessary in order to make the data comparable, as the raw densitometry values did vary between experiments due to exogenous factors and not caused by treatment, as will be discussed in the Discussion section. TrkB receptor is N-glycosylated in 10 sites in the extracellular domain and its molecular weight is 145 kDa (Haniu et al.,2005). The upper band corresponds to this molecular weight, and in many western blots for pTrkB a lower band at 110 kDa was observed. This lower band most likely corresponds to non-glycosylated (unprocessed) TrkB (Perez et al.,2019), and it was included in the area measured in densitometry analysis.

It was found that upon treatment of the neuronal cultures with either of BDNF, NT4 and #85 for 30 minutes the levels of TrkB phosphorylation are similar, while untreated samples have undetectable levels of pTrkB (Figure 4.6 A) and B). After 2 hours of treatment the level of TrkB phosphorylation is somewhat decreased, whereas it is significantly decreased after 12 hours and further decreased after 24 hours of treatment (Figure 4.6 A). When cultures were treated for 48 or 72 hours with BDNF, NT4 and #85 no signal was detected (data not shown). Figure 4.6 B illustrates the results of 4 independent differentiations, two of them performed in triplicates and one in duplicates. No pTrkB signal was detected in any of the experiments where no TrkB agonists were added. All values were normalized to synaptophysin levels and all conditions were normalized to the samples that were treated with BDNF for 30 minutes, the value of which was set as 100%. The signal was highest after treatment of the culture for 30 minutes. There was a tendency for the signal to be reduced after

2 hours, while it was dramatically reduced when neurons were treated for 12 and 24 hours.

There is a significant difference between the 4 time-points for the cultures treated with **BDNF** with **p<0.00001** (Kruskal-Willis test). Especially significant differences are located in 30min vs 2h (**p<0.0001**), 30min vs 12h (**p<0.0001**), 30min vs 24h (**p<0.0001**), 2h vs 12h (**p<0.0001**) and 2h vs 24h (**p<0.0001**) (Mann-Whitney test). In the case of 12h vs 24 h there is no significant difference detected (p=0.191).

There is a significant difference between the 4 time-points for the cultures treated with **#85** with p<0.0001 (Kruskal-Willis test). Especially significant differences are located in 30min vs 2h (**p=0.019**), 30min vs 12h (**p<0.0001**), 30min vs 24h **(p<0.0001**), 2h vs 12h (**p=0.001**), 2h vs 24h (**p<0.0001**), and 12h vs 24h (**p=0.007**) (Mann-Whitney test).

There is a significant difference between 3 time-points for the cultures treated with **NT4** with **p=0.013** (Kruskal-Willis test). Especially significant differences are located in 2h vs 12h **(p=0.004**), 2h vs 24h (**p=0.004**) and 12h vs 24h (**p=0.016**) (Mann-Whitney test). In the case of 30 min vs 2 h (0.278), 30 min vs 12 h (0.143) and 30 min vs 24 h (0.056) there is no significant difference detected. Cultures have been treated with NT4 for 30 minutes in only 2 out of 4 differentiations, which can explain why statistical significance is not achieved. Finally, comparisons between time-points for the 3 different substances do not present significant differences (Mann-Whitney test): BDNF with 30 min vs #85 with 30 min: no significant differences p=0.146, BDNF with 30 min vs NT4 with 30 min: no significant differences p=0.998, 85 with 30 min vs NT4 with 30 min: no significant differences p=0.998, BDNF with 2 h vs #85 with 2 h: no significant differences p=0.399, BDNF with 2 h vs NT4 with 2 h: no significant differences p=0.311, #85 with 2h vs NT4 with 2 h: no significant differences p=0.362, BDNF with 12 h vs #85 with 12 h: no significant differences p=0.287, BDNF with 12 h vs NT4 with 12 h: no significant differences p=0.064, #85 with 12 h vs NT4 with 12 h: no significant differences p=0.262 ,BDNF with 24 h vs #85 with 24 h: no significant differences p=0.221, BDNF with 24 h vs NT4 with 24 h: no significant differences p=0.416, , #85 with 24 h vs NT4 with 24 h: no significant differences p=0.111.

Overall and while TrkB phosphorylation with BDNF, #85 and NT4 is reduced after 30 minutes, there is no statistically significant difference between the three TrkB ligands in any time-point. The particularly high variability of standard error of the mean (s.e.m)

between differentiations could be attributed to the variability between different western blots. Indeed, triplicate or duplicate samples from four differentiations were run using 9 different gels and subsequent blots. It is likely that small but significant differences in the efficiency of transfer in particular may explain the variability between experiments.

A.

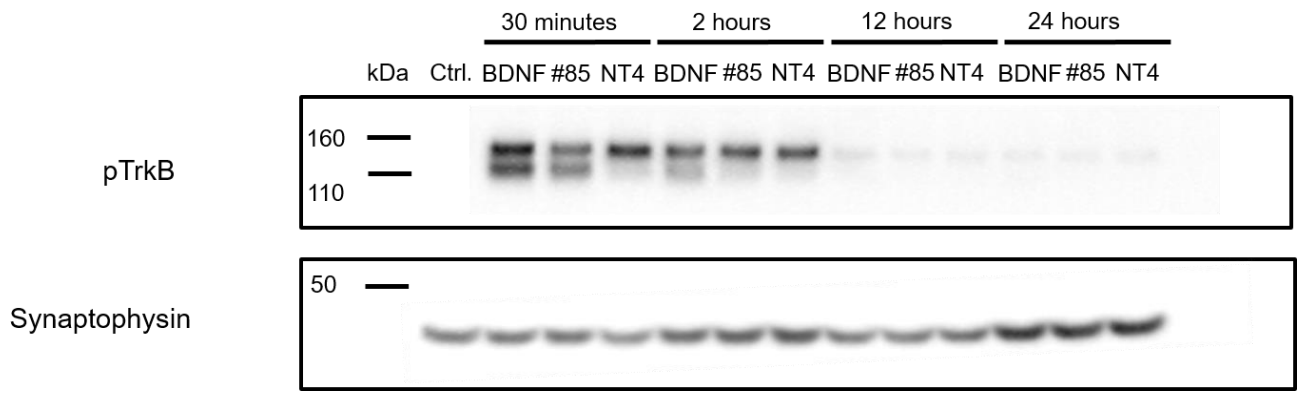

B.

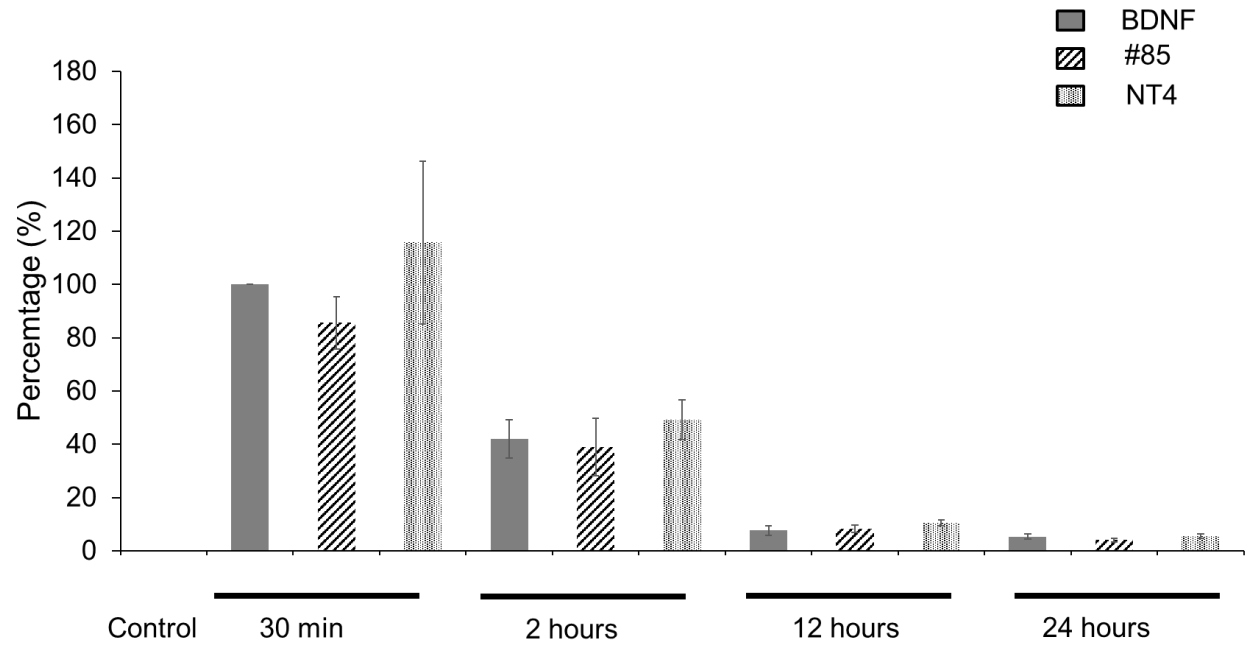

Figure 4.6 Western blot analysis of pTrkB levels using lysates prepared from H9 neurons, 30 DIV treated for different time-points with BDNF, #85 or NT4. *A) Representative immunoblot of the time course of TrkB phosphorylation. Cultures were treated with BDNF at 1.79 nM, #85 at 45 nM and NT4 at 2.88 nM for 30 minutes, 2 hours, 12 hours and 24 hours. Cell lysates were subjected to Western blot analysis for phosphor-TrkB or synaptophysin (used as loading control) B) Densitometric values quantified from the blots of 4 independent differentiations experiments. Data represent mean +/- standard error of the mean.*

In the 3 out of 4 independent experiments described above the expression of non-phosphorylated TrkB was also tested (Figure 4.7). TrkB signal appears to be somewhat increased in 30 minutes and 2 hours timepoints, when compared to the control cultures, and subsequently decrease at 12- and 24-hours' time-points (Figure 4.7 A). However, there is no significant difference between control samples and samples treated with one of the three substances for any time-point. In more detail there is no significant differences detected between control samples and samples treated with BDNF for 30 minutes (p=0.559), control vs #85 for 30 minutes (p=0.639), control vs NT4 for 30 minutes (0.286), control vs BDNF for 2 hours (p=0.639), control vs #85 for 2 hours (p=0.755), control vs NT4 for 2 hours (0.730), control vs BDNF for 12 hours (p=0.202), control vs #85 for 12 hours (p=0.149), control vs NT4 for 12 hours (0.905), control vs BDNF for 24 hours (p=0.106), control vs #85 for 24 hours (p=0.134), control vs NT4 for 24 hours (0.452) (Mann-Whitney test).

There is no significant difference between the 4 time-points for the cultures treated with **BDNF** with p=0.096 (Kruskal-Willis test). Especially significant differences are located 30min vs 12h (**p=0.017**). There is no significant difference for 30min vs 2h (p=0.690), 30min vs 24h (p=0.180), 2h vs 12h (p=0.165), 2h vs 24h (p=0.073) (Mann-Whitney test) and 12h vs 24 h (p=0.402).

There is a significant difference between the 4 time-points for the cultures treated with **#85** with **p=0.046** (Kruskal-Willis test). Especially significant differences are located in 30min vs 12h (**p=0.038**), 30min vs 24h (**p=0.038**). There is no significant difference for 30min vs 2h (p=0.710), 2h vs 12h (p=0.053),2h vs 24h (p=0.128), and 12h vs 24h (p=0.451) (Mann-Whitney test).

There is no significant difference between 3 time-points for the cultures treated with **NT4** with p=0.258 (Kruskal-Willis test). There is no significant difference for 30 min vs 2 h (p=0.998), 30 min vs 12 h (p=0.2) and 30 min vs 24 h (p=0.2) ,2h vs 12h (p=0.343), 2h vs 24h (p=0.2) and 12h vs 24h (p=0.886) (Mann-Whitney test).

Finally, comparisons between time-points for the 3 different substances do not present significant differences (Mann-Whitney test): BDNF with 30 min vs #85 with 30 min: no significant differences p=0.180, BDNF with 30 min vs NT4 with 30 min: no significant

differences p=0.073, 85 with 30 min vs NT4 with 30 min: no significant differences p=0.788, BDNF with 2 h vs #85 with 2 h: no significant differences p=0.998, BDNF with 2 h vs NT4 with 2 h: no significant differences p=0.527, #85 with 2h vs NT4 with 2 h: no significant differences p=0.648, BDNF with 12 h vs #85 with 12 h: no significant differences p=0.998, BDNF with 12 h vs NT4 with 12 h: no significant differences p=0.109, #85 with 12 h vs NT4 with 12 h: no significant differences p=0.230 ,BDNF with 24 h vs #85 with 24 h: no significant differences p=0.402, BDNF with 24 h vs NT4 with 24 h: no significant differences p=0.115, , #85 with 24 h vs NT4 with 24 h: no significant differences p=0.230. In conclusion there is no significant difference between the three ligands in any time-point.

A.

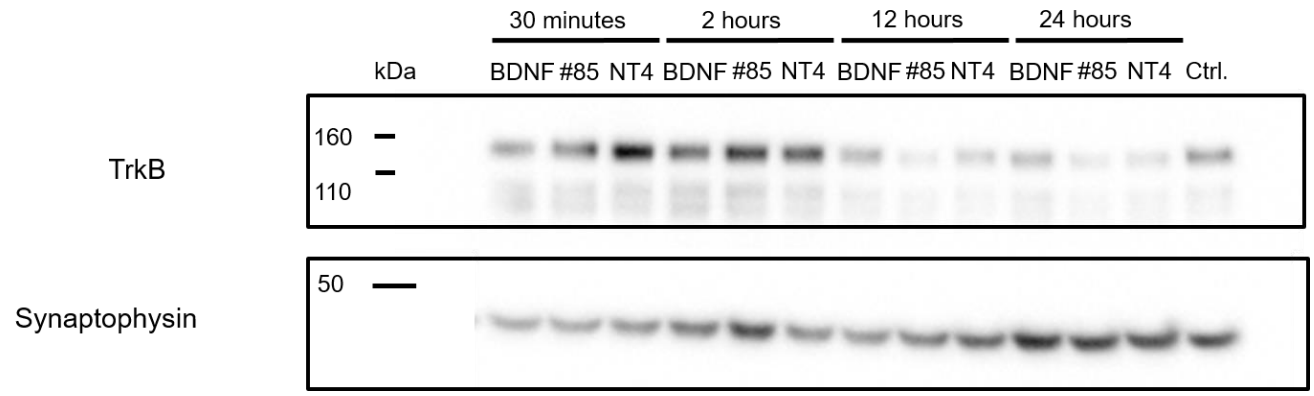

B.

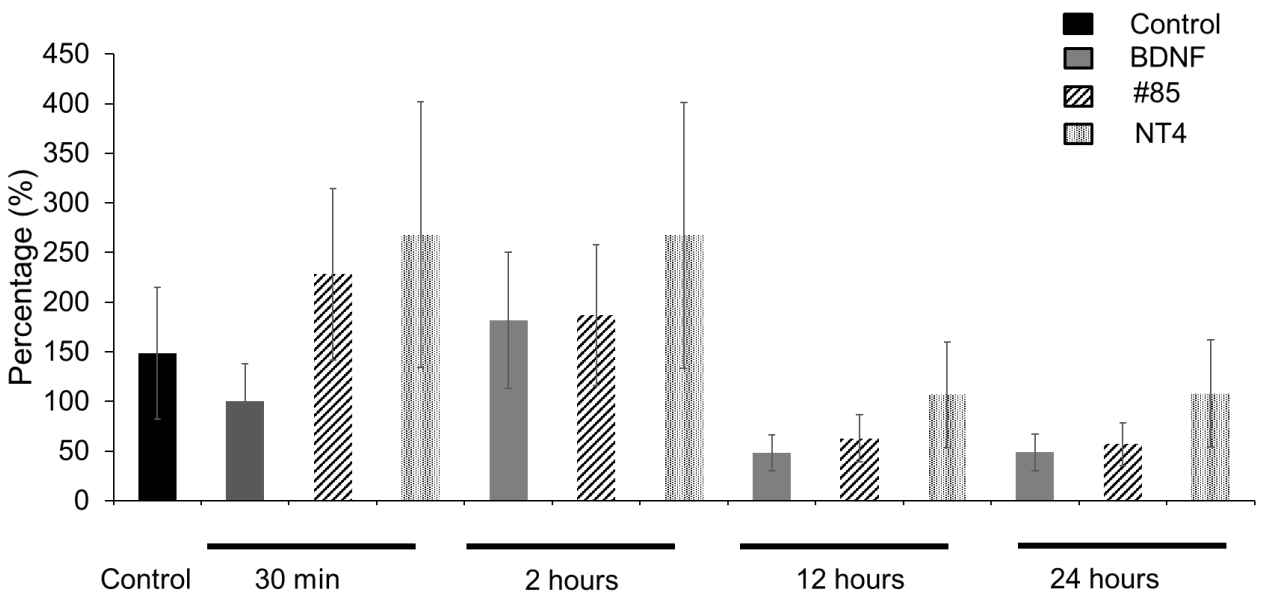

Figure 4.7 Western blot analysis of TrkB levels using lysates prepared from H9 neurons, 30 DIV, treated for different time-points with BDNF, #85 or NT4. *A) Representative immunoblot of the time course of TrkB expression. Cultures were treated with BDNF at 1.79 nM, #85 at 45 nM and NT4 at 2.88 nM for 30 minutes, 2 hours, 12 hours and 24 hours. Cell lysates were subjected to Western blot analysis for TrkB or synaptophysin (used as loading control) B) Densitometric values quantified from the blots of 3 independent differentiations experiments. Data represent mean +/- standard error of the mean.*

In order to investigate any potential correlation between phosphorylated pTrkB levels and total TrkB levels the ratio of pTrkB/TrkB for the experiments mentioned above was calculated (Figure 4.8)

There is no significant difference between the 4 time-points for the cultures treated with BDNF with p=0.093 (Kruskal-Willis test). Especially there are no significant differences for BDNF 30min vs 2h (p=0.106). 30min vs 12h (p=0.073), 30min vs 24h (p=0.146), 2h vs 12h (p=0.234), 2h vs 24h (p=0.318) and 12h vs 24 h (p=0.418) (Mann-Whitney test).

There is no significant difference between the 4 time-points for the cultures treated with #85 with p=0.490 (Kruskal-Willis test). Especially there are no significant for 30min vs 2h (p=0.805), 30min vs 12 (p=0.228), for 30min vs 24 h (p=0.259), 2h vs 12h (p=0.620) ,2h vs 24h (p=0.259), and 12h vs 24h (p=0.456) (Mann-Whitney test).

There is no significant difference between 3 time-points for the cultures treated with NT4 with p=0.702 (Kruskal-Willis test). There is no significant difference for 30 min vs 2 h (p=0.998), 30 min vs 12 h (p=0.143) and 30 min vs 24 h (p=0.486) ,2h vs 12h (p=0.2), and 12h vs 24h (p=0.486) (Mann-Whitney test). There is significant difference located in 2h vs 24h (p=0.029)

Finally, comparisons between time-points for the 3 different substances do not present significant differences (Mann-Whitney test): BDNF with 30 min vs #85 with 30 min: no significant differences p=0.146, BDNF with 30 min vs NT4 with 30 min: no significant differences p=0.194, #85 with 30 min vs NT4 with 30 min: no significant differences p=0.315, BDNF with 2 h vs #85 with 2 h: no significant differences p=0.710, BDNF with 2 h vs NT4 with 2 h: no significant differences p=0.115, #85 with 2h vs NT4 with 2 h: no significant differences p=0.264, BDNF with 12 h vs #85 with 12 h: no significant differences p=0.267, BDNF with 12 h vs NT4 with 12 h: no significant differences p=0.305, #85 with 12 h vs NT4 with 12 h: no significant differences p=0.414 ,BDNF with 24 h vs #85 with 24 h: no significant differences p=0.402, BDNF with 24 h vs NT4 with 24 h: no significant differences p=0.158, , #85 with 24 h vs NT4 with 24 h: no significant differences p=0.324. In conclusion there is no significant difference between the three ligands in any time-point.

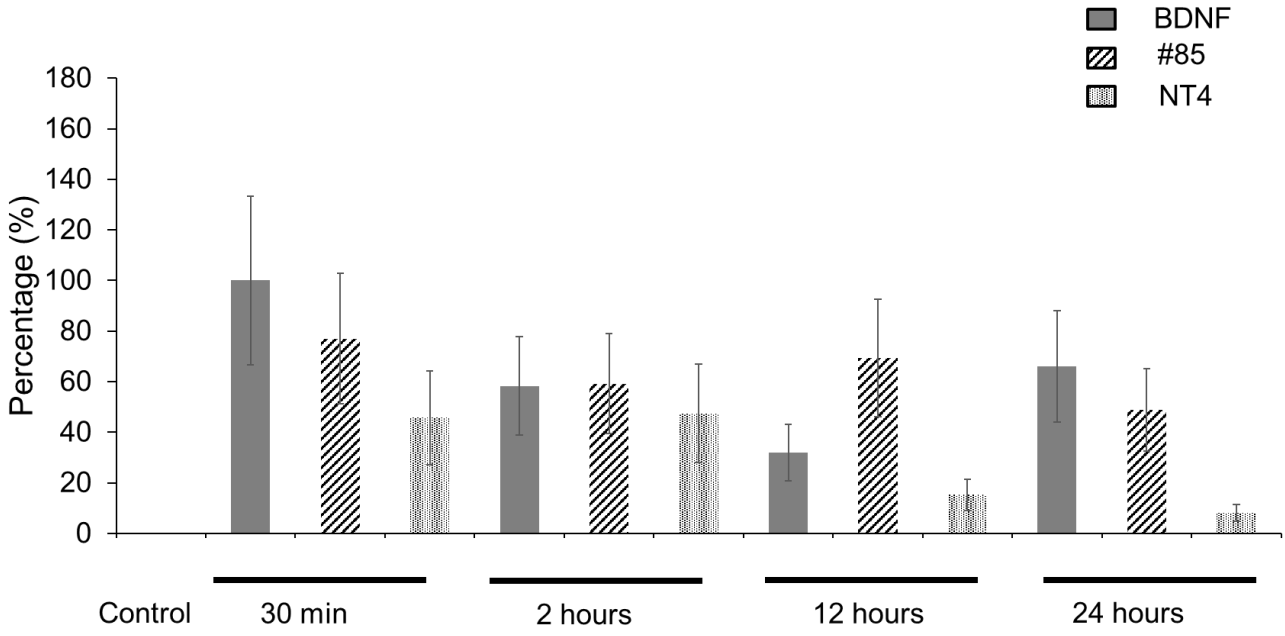

Figure 4.8 Quantification of the ratio pTrkB/TrkB described in figures 4.6 and 4.7*. Densitometric values quantified from the blots of 3 independent differentiations experiments. Data represent mean +/- standard error of the mean.*

In order to determine the relative potency of each ligand, cultures were treated with various concentrations of BDNF, NT4 and #85 for 30 minutes. A wide range of concentrations was used in order to try and determine the EC50, which is the concentration of ligand that achieves half maximal activation of TrkB. The concentrations tested are presented in Figure 4.10. The data were normalised to synaptophysin protein levels, which was used as a control. Furthermore, the densitometry values were transformed to 100% values. In all experiments 1.79 nM of BDNF was set as 100% while the other concentrations were calculated accordingly by the following type (value of x concentration/ value of 1.79 nM BDNF * 100). Interestingly, the lowest concentration tested for BDNF, which was 0.0358 nM did not significantly induce phosphorylation of TrkB, although saturation was reached between 0.179 nM and 1.79 nM. Higher concentrations up to 35.8 nM did not lead to further increase of the signal. The relatively narrow gap between zero and full response may suggest that the dimerization of TrkB receptor caused by the BDNF dimer may be close to an all or none phenomenon. This may also be a consequence of the relative homogeneity of the cultures in terms of TrkB expression and their degree of maturation. Similarly, the antibody #85 did not significantly activate TrkB at 0.045 nM whilst full activation is reached between 0.45 nM and 45 nM. As is the case with BDNF, higher concentrations do not seem to induce further phosphorylation of the receptor. Interestingly, compared to BDNF, higher concentrations of NT4, were required to achieve significant TrkB activation. Saturation of TrkB phosphorylation was achieved between 0.76 and 2.89 nM (Figure 4.9 A). Figure 4.9 B illustrates the results of 4 different experiments and like with the time course experiments (see above), variability of the standard error of the mean (s.e.m) was quite high in all concentrations tested.

Comparison between the values of the percentages under the 3 different substances using the concentrations mentioned above, led to the following results:

There is a significant difference between the 5 concentrations tested for **BDNF** with **p=0.012** (Kruskal-Willis test). Especially significant differences are located in 0.0358 nM vs 0.179 nM (**p=0.001**), 0.0358 nM vs 0.895 nM (**p=0.000291**), 0.0358 nM vs 1.79 nM (**p=0.000013**), 0.0358 nM vs 35.8 nM (**p=0.000031**), 0.895 nM vs 1.79 nM

(**p=0.049**) and 1.79 nM vs 35.8 nM (**p=0.001**). There are no significant differences located in 0.179 nM vs 0.895 nM (p=0.075), 0.179 nM vs 1.79 nM (p=0.115), 0.179 nM vs 35.8 nM (p=0.076), and 0.895 nM vs 35.8 nM (p=0.239).

There is a significant difference between the 5 concentrations tested for **#85** with **p<0.0001** (Kruskal-Willis test). Especially significant differences are located in 0.045 nM vs 0.225 nM (**p=0.017**), 0.045 nM vs 0.45 nM (**p=0.011**), 0.045 nM vs 9 nM (**p=0.0000001**), 0.045 nM vs 45 nM (**p=0.000001**), 0.225 nM vs 0.45 nM (**p=0.030**), 0.225 nM vs 9 nM (**p=0.000009**), 0.225 nM vs 45 nM (**p=0.000001**). There are no significant differences located in 0.45 nM vs 9 nM (p=0.116), 0.45 nM vs 45 nM (0.063), 9 nM vs 45 nM (p=0.085) (Mann-Whitney test).

There is a significant difference between the 3 concentrations for **NT4** with **p=0.004** (Kruskal-Willis test). Especially significant differences are located in 0.76 nM vs 2.89 nM (**p=0.004**), 0.76 nM vs 14.42 nM (**p=0.004**). There is no significant difference located in 2.89 nM vs 14.42 nM (p=0.949) (Mann-Whitney test).

Finally, comparisons between concentrations for the 3 different substances give us the following results (Mann-Whitney test):: 0.0358 nM of BDNF vs # 0.045 nM of #85 no significant differences p=0.157,), **0.179 nM of BDNF vs 0.225 nM of #85**: significant differences **p=0.001,** 0.895 nM of BDNF vs 0.45 nM of # 85**:** no significant differences p=0.058, 35.8 nM of BDNF vs 45 nM of #85: no significant differences with p=0.423), **0.895 nM of BDNF vs 0.76 nM of NT4**: significant difference with **p=0.001**, 1.79 nM of BDNF vs 2.89 nM of NT4: no significant difference with p=0.117, 35.8 nM of BDNF vs 14.42 nM of NT4 : no significant difference with p=0.123, **0.45 nM of #85 vs 0.76 nM of NT4** : significant differences with **p=0.008**, 45 nM of #85 vs 14.42 nM of NT4: no significant differences with p=0.418. Overall, when similar concentrations of BDNF and #85 are compared there are no significant differences observed, when the concentrations tested are located at the threshold of the activation of TrkB ligand. However, BDNF induced 4-fold higher phosphorylation of TrkB than #85 in intermediate concentrations (0.179 and 0.895 nM BDNF compared to 0.225 and 0.45 nM #85, while there is no difference in the maximum concentrations tested, indicating that #85 can reach the same plateau in TrkB phosphorylation as BDNF. Additionally, similar intermediate concentrations of BDNF and #85 induces 26- fold and 11-fold

higher levels of TrkB phosphorylation when compared to 0.76 nM NT4. NT4 can also reach the same plateau in TrkB phosphorylation with BDNF and #85.

The concentrations tested here do not provide sufficient detail to accurately determine the half maximal potency or the saturation of each ligand. Based on the graph in figure 4.6 B the EC50 of BDNF is achieved between 0.0358 and 0.179 nM and the EC50 of #85 between 0.045 and 0.45 nM. In order to get a precise value more closely spaced concentrations between the estimates for the EC50 values would be required.

A.

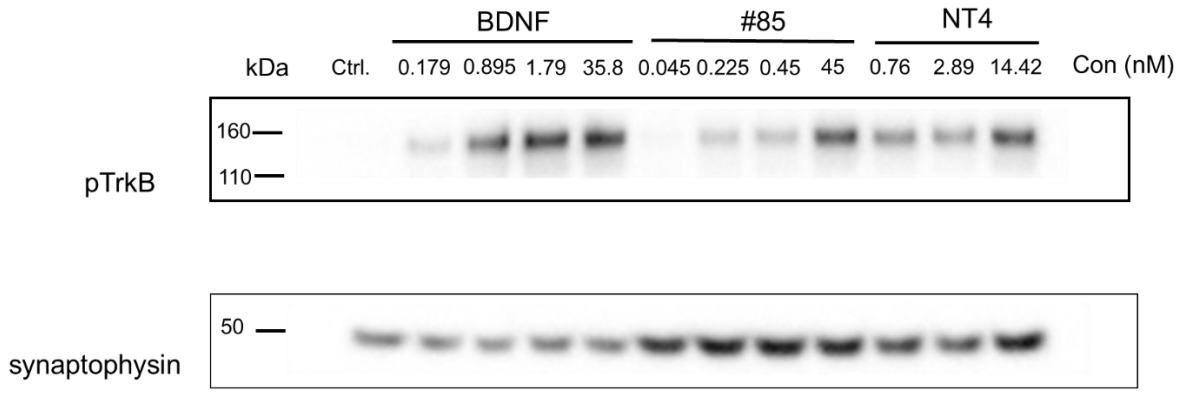

B.

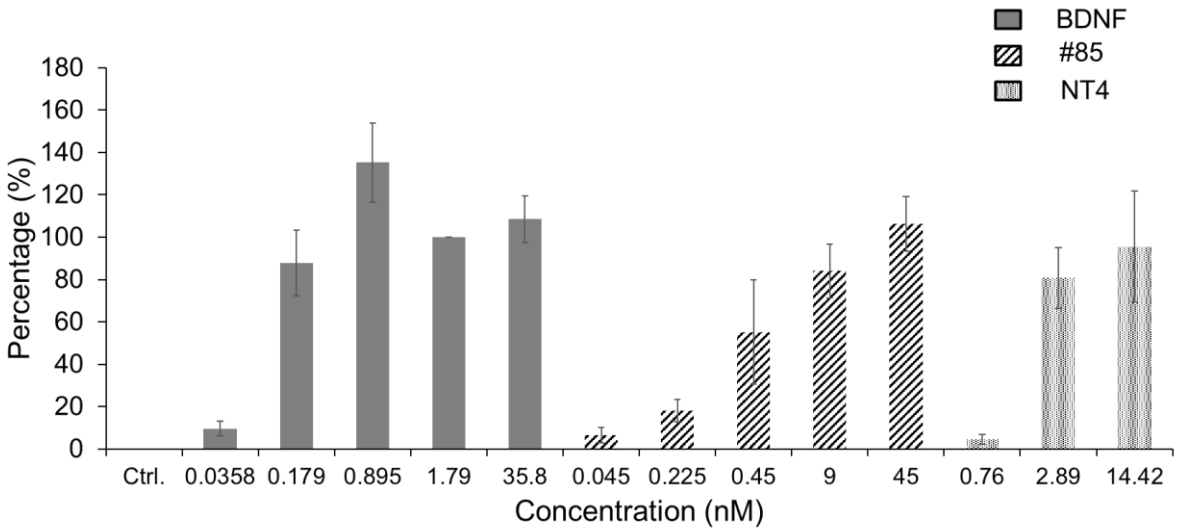

Figure 4.9 Western blot analysis of pTrkB levels using lysates prepared from H9 neurons, 30 DIV treated with various concentrations of BDNF, #85 or NT4 *A) Representative immunoblot of the different TrkB activating ligand concentrations tested. Cell lysates were subjected to Western blot analysis for phosphorylated TrkB or synaptophysin (used as loading control) B) Densitometric values quantified from the blots of 6 independent differentiations experiments. Data represent mean +/- standard error of the mean.*

	N(number of wells)	number of differentiations
BDNF 0.0358 nM	7	3
BDNF 0.179 nM	11	5
BDNF 0.895 nM	7	3
BDNF 1.79 nM	13	6
BDNF 35.8 nM	11	5
#85 0.045 nM	11	5
#85 0.225 nM	11	5
#85 0.45 nM	3	2
#85 9 nM	12	5
#85 45 nM	11	5
NT4 0.76 nM	7	3
NT4 2.89 nM	7	3
NT4 14.42 nM	7	3

Figure 4.10 Number of samples and hESC differentiation used to provide the data in figure 4.9 B for each ligand and ligand concentration used.

The next question was to determine the percentage of neurons responding to the addition of TrkB ligands as this was key to appreciate the suitability of the culture system used to meaningfully perform complex experiments such as RNA-seq. To this end 30 DIV neurons were plated on coverslips and treated with BDNF and #85 for 12 hours and subsequently fixed (Figure 4.11). Immunocytochemistry experiment used cFOS as an indication of TrkB activation, since this is a known transcriptional target of BDNF and a widely recognised marker of neuronal activity (Cohen et al., 2011, Bullitt, 1990). Importantly the activation of #85 by cFOS was only tested in one differentiation, therefore no firm conclusions can be established, whereas the activation of BDNF by cFOS was tested in two differentiations.

Immunofluorescence experiment quantification of each independent experiment was performed using 5 images per marker and differentiation and roughly 300 cells per image. These experiments revealed that 75% of the neurons treated with BDNF expressed clearly detectable levels of cFOS in the nucleus (Figure 4.12). For reasons that are unclear (but see below) the signal intensity was lower following treatments of the culture with #85 (Figure 4.11).

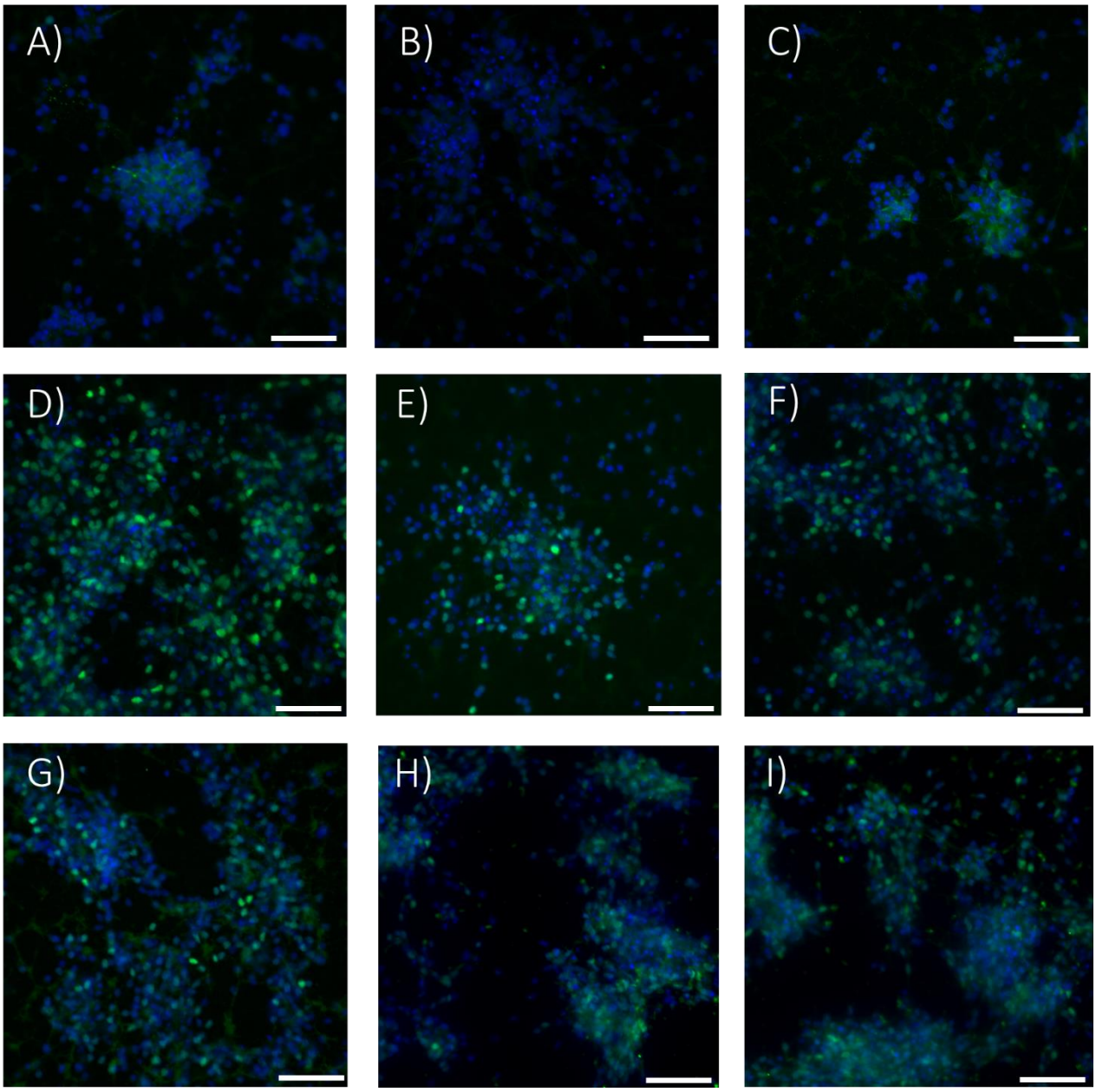

Figure 4.11 Immunocytochemistry analysis on day 30 H9 neurons. *Green is cFOS and blue is DAPI. A-C) untreated culture, D-F) treatment with BDNF for 12 hours and G-I) treatment with #85 for 12 hours. Scale bar is 50 µm.*

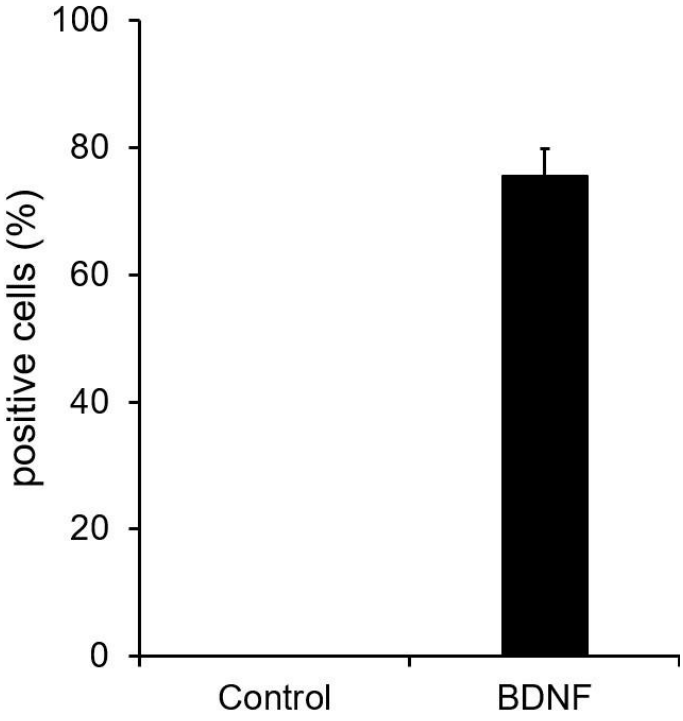

Figure 4.12 Immunocytochemistry quantification of cFOS positive neurons in figure 4.11*. The number of total cells was equal to the number of DAPI positive cells. Cells were counted manually using ImageJ software. Two independent differentiations were analyzed. Data represent mean +/- standard deviation.*

4.4 Discussion

In this chapter it was shown that neurons differentiated from human embryonic stem cells as described before (Telezhkin et al., 2016) express TrkB but not BDNF (see Figure 4.4). In the human brain apart from the full-length receptor (TrkB-FL), two C-terminal truncated receptors TrkB-T1 and TrkB-Sch are expressed, which lack the tyrosine kinase domain (Klein et al., 1990, Stoilov et al., 2002). The antibody that was used to detect TrkB was generated by immunizing rabbits with a synthetic peptide within Human TrkB aa 100-200 (internal sequence). Therefore, it can recognize the three main TrkB isoforms that are known to be expressed in the human brain. The band with the stronger signal detected approximately at 150 kDa corresponds to the full-length isoform, whereas two bands detected at 100 kDa and approximately 90 kDa are also detected and correspond presumably at the TrkB-T-Sch and TrkB-T1 protein isoforms respectively. A more recent study relying on *in silico* analysis has identified novel alternative transcripts and 36 potential protein isoforms, which are generated by alternative splicing in the exons encoding the extracellular and intracellular domain. This study also identified 5 exon containing transcripts which create the N-terminally truncated TrkB proteins that lack 156 N-terminal amino acids residues including the signal sequence. These isoforms most likely cannot be transported to the cell membrane (Luberg et al., 2010). Since many TrkB protein isoforms have similar sizes, western blot analysis is not the optimal method for a detailed investigation of their expression. Real Time PCR analysis of the different TrkB mRNA transcripts would verify the presence of the TrkB isoforms expressed in neurons derived from hESCs. Most of the neurons generated with the protocol discussed above, are GABAergic as they express GAD65/67 and they also express some of the markers found in the Lateral Ganglionic Eminence (LGE). BDNF and NT4 have been shown to activate TrkB receptor by phosphorylation in a dose-dependent and time-dependent manner. The same *in vitro* system was used to test the potential of four novel TrkB activating antibody generated by Zebra Biologics and Richard Lerner group in Scripps. One of these antibodies, designated #85 was found to be comparable to BDNF in its ability to activate and phosphorylate TrkB, and was therefore selected for further testing. TrkB activating antibody #85 was demonstrated to activate TrkB receptor in a dose-dependent and time-dependent manner that was similar to the two neurotrophins. Interestingly TrkB levels were found to be decreased upon treatment for 12 hours with

BDNF and #85, but not with NT4. Down-regulation of TrkB upon prolonged treatment with BDNF has been observed in other studies using neuronal cell lines and it was largely prevented by addition of proteasome inhibitors (Sommerfeld et al., 2000), whereas a recent study reported that treatment of cultured cortical neurons with BDNF and NT4 resulted in differential endocytic sorting of TrkB receptors, as NT4 resulted in reduced TrkB ubiquitination at endosomal pH. As a result, NT4 sustained the downstream signalling pathways for longer time period (Proenca et al., 2016). The use of surface biotinylation experiments and fluorescent microscopy using the *in vitro* system discussed in this chapter could compare the kinetics of TrkB internalization upon treatment with BDNF, NT4 and antibody #85. The investigation of ubiquitination of TrkB upon treatment with the three ligands could potentially reveal differences that may be particularly relevant in the context of future *in vivo* therapies.

The TrkB receptor has 3 phosphorylation sites; Tyr515 provides a docking site for Shc and initiates the Ras/Raf/MAPK signalling cascade (Obermeier et al., 1993), Tyr 706 is located in the activation loop and initiates the TrkB auto- phosphorylation (Cunningham et al., 1997) and Tyr816 is involved in the PLC –γ1 pathway (Kaplan and Miller, 2000). For the pTrkB experiments discussed in these chapters the antibody that was used recognized the Tyr706/707 residues and this monoclonal antibody was produced by immunizing rabbits with a synthetic phosphopeptide corresponding to residues surround Tyr674/675 of human TrkA. The phosphorylation sites are conserved between TrkA and TrkB and Tyr674/675 of TrkA corresponds to Tyr706/707 of the human TrkB sequence (Huang and Reichardt, 2003). In one preliminary experiment an antibody that recognized Tyr515 residue of TrkB was also tested and BDNF and #85 were found to behave in a similar manner as with the antibody recognizing residues Tyr706/707 (data not shown). This monoclonal antibody was produced by immunizing rabbits with a synthetic phosphopeptide corresponding to residues corresponding to residue Tyr490 and the analogous residue Tyr515 in TrkB (Huang and Reichardt, 2003). It would be informative to compare the phosphorylation levels of Tyr515 and Tyr818 residues of TrkB upon treatment with BDNF, NT4 and antibody #85 in different time-points and compare these results with the available data for Tyr706/707.

Although TrkB agonist antibody #85 had the same potency in terms of TrkB phosphorylation, the Emax could not be accurately determined from the available data,

as there is no significant difference between some of the concentrations tested. It was found that full activation of #85 was reached between 0.45 nM and 45 nM, whereas full activation of BDNF was reached between 0.179 nM and 1.79 nM. Similarly, the EC50 values for the neurotrophins and #85 could not be accurately determined from the available data, as more closely spaced concentrations would be needed. Based on the experiments discussed above EC50 of BDNF is achieved between 0.0358 and 0.179 nM and the EC50 of #85 between 0.045 and 0.45 nM. In order to accurately determine these values future studies would need to include additional concentrations located between the range of the concentrations described above. For the reasons discussed in the results it is also possible that western blot analysis is not the optimal technique in order to analyse the EC50 values.

Importantly in this study it was shown that most of the neurons are responsive to treatment with BDNF as measured by the early response gene cFOS, which is a downstream target of BDNF and a well-studied marker for neuronal activity. In one differentiation experiment the antibody #85 was also tested for cFOS activation and many neurons were found to be positive for cFOS expression. However, the signal intensity was lower than that of BDNF and in many areas the signal appeared to be diffused over the area of the cytoplasm. Additional immunocytochemistry experiments that will test cFOS staining upon treatment with BDNF, NT4 and #85 would be an additional readout to compare the efficacy of the three TrkB ligands. Double staining with GAD65/67 and the LGE markers would identify the subtypes of neurons that are particularly responsive. The extensive characterisation of the cultures using immunocytochemistry would address the question about the reproducibility of the system in terms of TrkB activation. Although the GABAeric identity of these neurons was firmly established, it remains elusive whether the percentage of neurons that respond to cFOS are comparable between BDNF, NT4 and #85. It is possible that significant variability in the expression of LGE markers, TrkB and cFOS between differentiations could generate big fluctuation in the pTrkB data. The protein levels of pTrkB, TrkB and synaptophysin have been found to vary between triplicates and differentiations. These fluctuations could mask small differences of 20-30%. A first step to examine the reproducibility of differentiations for TrkB and synaptophysin would be RT-PCR. Subsequently samples from different experiments need to be tested side by side in the same gel. Additionally, running these samples in multiple

gels would exclude the possibility of variability occurring during the western blot procedure.

A modified ELISA approach, the highly sensitive amplified luminescent proximity homogeneous assay LISA (Alphalisa) format, could be used in order to study the TrkB phosphorylation levels with enhanced accuracy. The principle of this assay relies on the generation of signal when donor and acceptor beads are brought into close proximity. The Alpha donor bead is coated with streptavidin which captures the biotinylated anti-pTrkB antibody. The acceptor bead is coated with pTrkB specific antibody. When TrkB is phosphorylated, the two coated beads are brought into proximity through binding to tyrosine 706 (Tyr 706) of TrkB. After excitation by laser at 680 nm, the singlet oxygen released by alpha donor bead travels to the nearby acceptor bead where it causes acceptor bead to emit fluorescence at 615 nm. The increase of AlphaLISA signal is proportional to the concentrations of pTrkB (Traub et al., 2017). The same technique was successfully used for measuring phosphorylation of ERK, AKT and CREB. In the Alphalisa format 384-well microplates are used offering the possibility to use less biological material to investigate multiple concentrations in one experimental set.

In order to further demonstrate that the TrkB agonist antibody #85 and NT4 are comparable to BDNF, the canonical downstream signalling needs to be tested in future studies. The downstream signalling cascades that are activated upon binding of BDNF to TrkB are critical for neuronal survival, morphogenesis and plasticity. The various intracellular signalling pathways include the mitogen-activated protein kinase/ extracellular signal-regulated protein kinase (MAPK/ERK), phospholipase Cγ (PLCγ) and phosphoinositide 3-kinase (PI3K). It has already been shown in the recent publication associated with this Thesis that the agonist-induced levels of PLCγ, AKT and ERK phosphorylation by #85 are almost identical to those of BDNF across two time-points when CHO-NFAT TrkB reporter was treated for 5 minutes and 30 minutes. In the same study antibody #85 was found to bind at, or very near, the BDNF agonist site on TrkB receptor. More specifically treatment of HEK293-CRE-TrkB cell line with 4- and 12-fold molar excess of BDNF led to reduced binding of #85 to TrkB by 80% and 89% respectively (Merkouris et al., 2018). The validation of these results using as a model system the differentiation system described in this chapter would further support the notion that antibody #85 is a full agonist of TrkB.

Additional experiments would include dissection of the kinetics and the sensitivity of downstream TrkB signalling pathways after stimulation with BDNF, NT4 and #85. Using as a readout the Alphalisa format mentioned above different stimulation schemes could be used to analyse how the three TrkB ligands regulate the phosphorylation of TrkB, ERK, AKT and CREB kinetically. In the first scenario, the restimulation efficacy is measured by applying each agonist for a short pulse period, then the cultures are washed off and a second short pulse follows after few minutes. In the second scenario, the single-pulse stimulation each agonist is administered for a short pulse period, then washed off with no new addition of the agonists. The phosphorylation levels are measured at different time-points. In the third scenario, the continuous stimulation each agonist is administered for the whole time of the experiment, and different time-points can be tested, for example 2 hours, 12 hours, 24 hours.

Therefore, and due to the results presented above, antibody #85 is now considered as an interesting candidate for further validation in *in vivo* models of Huntigton's disease. This is due to the well-established role of BDNF in this neurodegenerative disease. Indeed, BDNF has been demonstrated to enhance survival in striatal neurons that die in HD (Bemelmans et al., 1999), therefore suggesting that reduced trophic support by the neurotrophin could contribute to the disease onset and progression. In line with this suggestion reduced BDNF levels have been reported in the cerebral cortex and striatum of people with HD (Zuccato et al., 2001). Additionally, BDNF withdrawal affects the viability of differentiated HD iPSC cultures in a CAG repeat-dependent manner. The longer the repeat number, the greater was the effect of BDNF withdrawal, whereas non-disease cell line with normal number of repeats was not affected (Consortium, 2012). Future studies could test whether #85 and NT4 are able to rescue differentiated HD iPSC cultures to the same extend as BDNF.

.

Chapter 5: Global transcriptome analyses (RNA-seq) following exposure of hESC-derived neurons to BDNF, #85 and NT4

5.1 Introduction

As described previously in Chapter 4 the addition of BDNF, NT4 and the antibody #85 to inhibitory neurons differentiated from hESC triggers TrkB phosphorylation in a time- and dose- dependent fashion. TrkB activation is known to lead to transcriptional changes (Zheng et al., 2009, Groth and Mermelstein, 2003, Maynard et al., 2018) and one recent study has reported on some of the changes following BDNF addition as well as an activating antibody (Traub et al., 2017) (see Discussion). No data are yet available on changes following the addition of NT4. Using culture conditions allowing a large proportion of cultured neurons to respond to TrkB activation by c-Fos expression in the nucleus (see preceding Chapter), RNA sequencing (RNA-seq) was used to characterize and compare the transcriptome changes following exposure of human neurons to BDNF, NT4 and #85.

5.2 Experimental setup of RNA seq

Day 30 neurons derived from H9 hESCs were treated with 1.79 nM of BDNF, 2.89 nM of NT4 and 45 nM of #85. The time points selected were 30 minutes, 2 hours, 12 hours and 24 hours. Three wells (triplicates) were treated per each condition and in each time point three wells were untreated (controls) (Table 5.1). In total 48 wells from the same differentiation were used in this experiment. In order to minimise transcription differences attributed to time rather than treatment, the wells were treated as explained in figure 5.1. Briefly, in the time point designated as T=0 3 wells were treated with BDNF, 3 wells were treated with NT4 and 3 wells with antibody #85 and subsequently lysed after 24 hours. In time point designated as T=6 hours 9 wells were treated for 12 hours, and in T=20 hours 9 wells were treated for 2 hours. Finally, in T=29.5 hours 9 wells were treated for 30 minutes. Under this configuration 36 of the samples were lysed within 6 hours of each other and the remaining 12 samples were lysed 6 hours later. After treatment with TrkB ligands neurons were lysed and RNA was extracted as detailed in Materials & Method. Subsequently RNA quality was accessed by loading

small amount of RNA in a polyacrylamide gel and measuring the RIN value, the ratio of 28s to 18 s ribosomal subunit (Figure 5.2). The recommended threshold for RNA seq analysis was 7, and all of the samples had a RIN value higher than 9.

Timepoint	BDNF (50 ng/ml)	NT4 (100 ng/ml)	#85 (5 µg/ml)
30 minutes	triplicate	triplicate	triplicate
2 hours	triplicate	triplicate	triplicate
12 hours	triplicate	triplicate	triplicate
24 hours	triplicate	triplicate	triplicate

Table 5.1 indicating the time points and conditions used in the RNA seq experiment. *Each condition was analysed in triplicates*

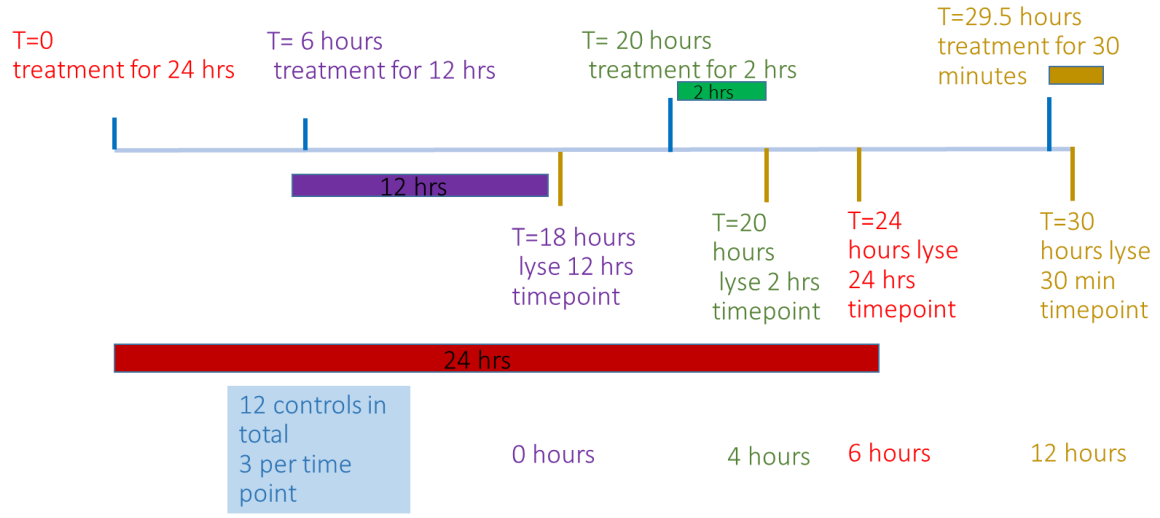

Figure 5.1: Scheme describing the experimental setup of the RNA seq experiment. *12 wells were treated and lysed at each time point, 9 were treated and 3 remained untreated (controls)*

A.

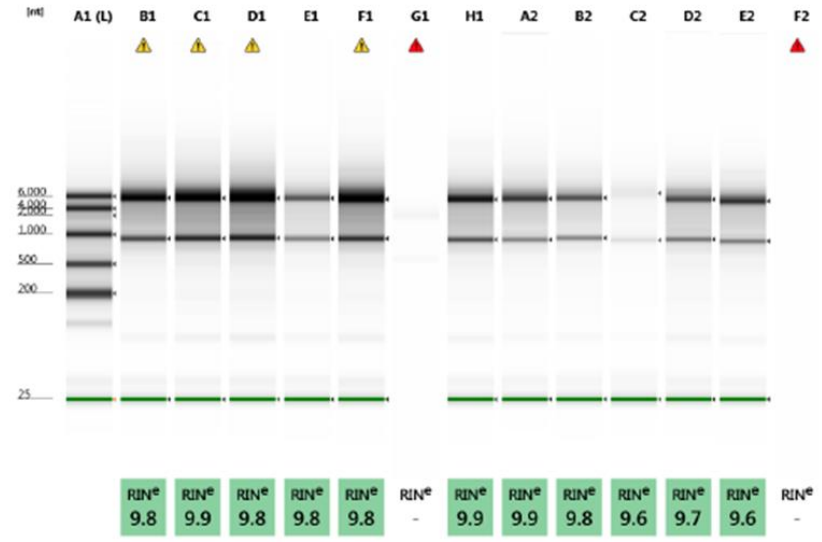

Default image (Contrast 100%), Image is Scaled to view larger Molecular Weight range

B.

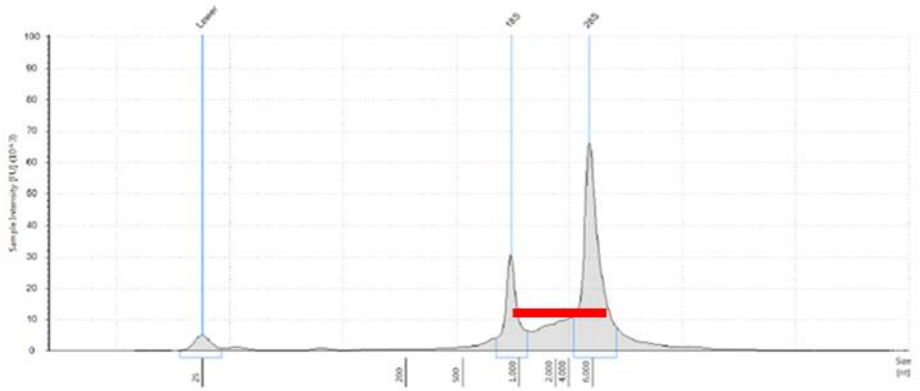

Sample Table

Well	RINe	28S/18S (Area)	Conc. [ng/µl]	Sample Description	Alert	Observations
B1	9.8	2.9	583	85 1	⚠	RNA concentration outside recommended range for RINe

Figure 5.2: Quality control of RNA samples. *A) All 48 samples were run in acrylamide gels, and 11 of the samples are presented here. The RNA marker was loaded in the first lane from the left. B) The bands separated in the acrylamide gels were automatically measured by Agilent Software. A representative RNA sample is shown here. The RIN value was calculated by diving the 28s ribosomal subunit to 18 s ribosomal subunit (red line).*

5.3 RAW DATA HANDLING AND ANALYSIS

5.3.1 R ANALYSIS OF THE DATA

The RNA-seq raw data obtained here were more than 120 GB and in order to efficiently analyse them, edgeR and limma packages from the Bioconductor project were used. Bioconductor is an R-based open-source software development project widely used in genomics (Anders et al., 2013, Huber et al., 2015). R and Bioconductor could be installed from the below links:

(https://www.R-project.org) (https://www.bioconductor.org)

The analysis also included Glimma package that generated interactive graphics, allowing a detailed exploration of the data at both sample and gene-level, which was not possible with the use of static R plots. The starting material was counts for the genes expressed in the different samples. In this chapter, the RNA-sequencing data in the form of gene-level counts were imported in R, organized, filtered and normalised using edgeR package, then the limma package with its voom method used linear modelling and empirical Bayes moderation to assess differential expression. The use of Glimma package offers interactive exploration of the results, making possible the examination of each sample and gene in a simple manner.

5.3.2 DATA PRE-PROCESSING

5.3.2.1TRANSFORMATION FROM THE RAW-SCALE

Raw counts are usually not used in differential expression analyses, as differences in the library size during sequencing between samples will results in difference in the number of counts. Therefore, raw counts are usually transformed into a scale that takes into account the differences in the library sizes. Here raw counts were converted to CPM (counts per million) and log-CPM values (log_2-counts per million) using the cpm function in edgeR. In this function log- transformations use a prior count of 0.25 to circumvent the calculation of the log of zero.

5.3.2.2 Removing lowly expressed genes

Since the data will include genes that are not expressed, or expressed at a very low level a logical step is to filter them out as they do not offer any biologically meaningful information. Upon examination of log-CPM it became apparent that a significant fraction of the genes within all samples are not expressed or are minimally expressed (Figure 5.3 A). A nominal value of 1 (equivalent to log-CPM value of 0) has been used, thus if a gene in any sample was considered as expressed when it was over this threshold, otherwise it was unexpressed. Genes expressed in at least one sample (three triplicates) were maintained for downstream analysis. Using this standard, the number of genes was reduced to approximately one third of the number that existed initially, 20.184 genes from 58051 (Figure 5.3 B). The distributions of log-CPM values were similar throughout all samples tested, with the exception of sample A4 (one of the triplicates treated with AB85 for 2 hours), as will be discussed later.

A.

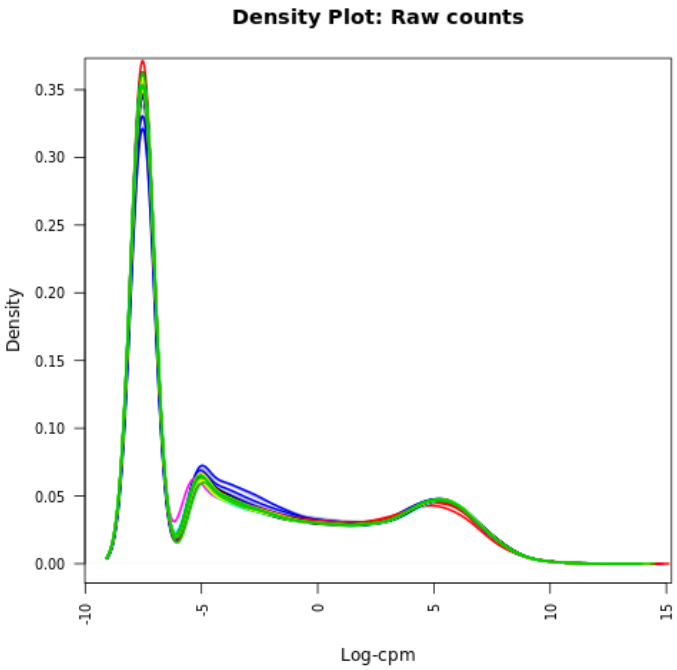

B.

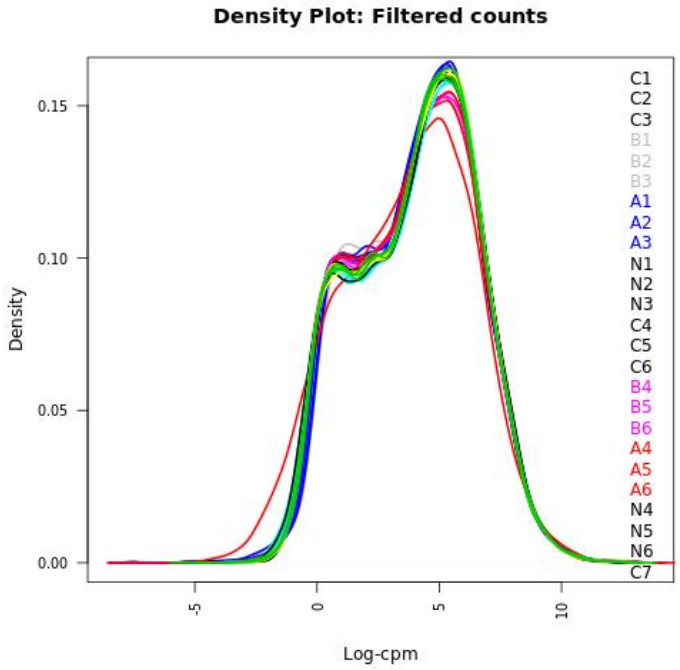

Figure 5.3. *A) The density of log-CPM values for raw pre-filtered data and B) post-filtered data are shown for each sample. C stands for control samples, A for samples treated with AB85, B for samples treated with BDNF and N for samples treated with NT4. Samples labelled with 1-3 correspond to the triplicates of time-point 30 minutes, samples labelled with 4-6 correspond to the triplicates of time-point 2 hours, samples labelled with 7-9 correspond to the triplicates of time-point 12 hours and samples labelled with 10-12 correspond to the triplicates of time-point 24 hours.*

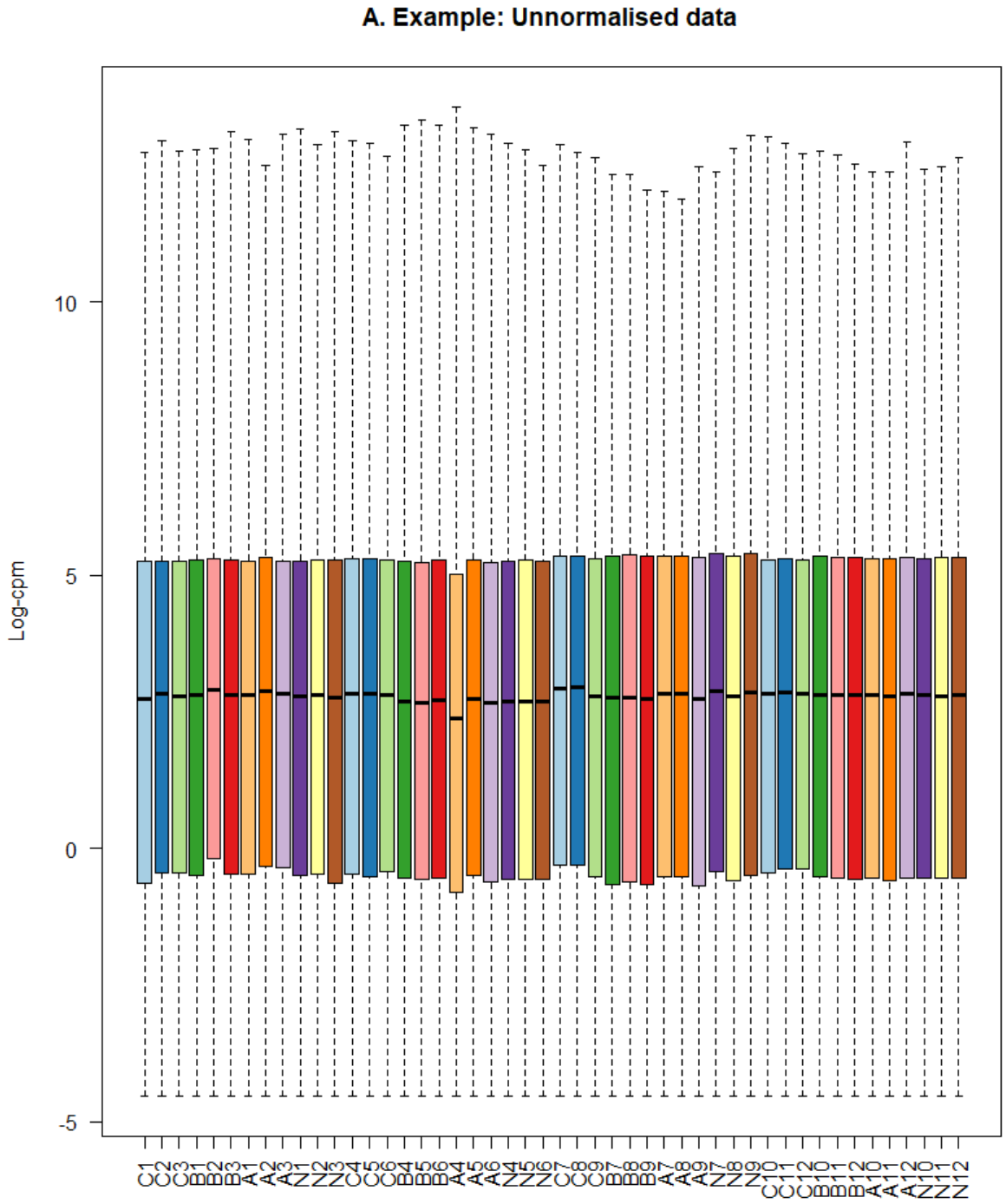

Figure 5.4.: *Boxplots of log-CPM values showing expression distributions for unnormalized data for each sample. C stands for control samples, A for samples treated with AB85, B for samples treated with BDNF and N for samples treated with NT4. Samples labelled with 1-3 correspond to the triplicates of time-point 30 minutes, samples labelled with 4-6 correspond to the triplicates of time-point 2 hours, samples labelled with 7-9 correspond to the triplicates of time-point 12 hours and samples labelled with 10-12 correspond to the triplicates of time-point 24 hours.*

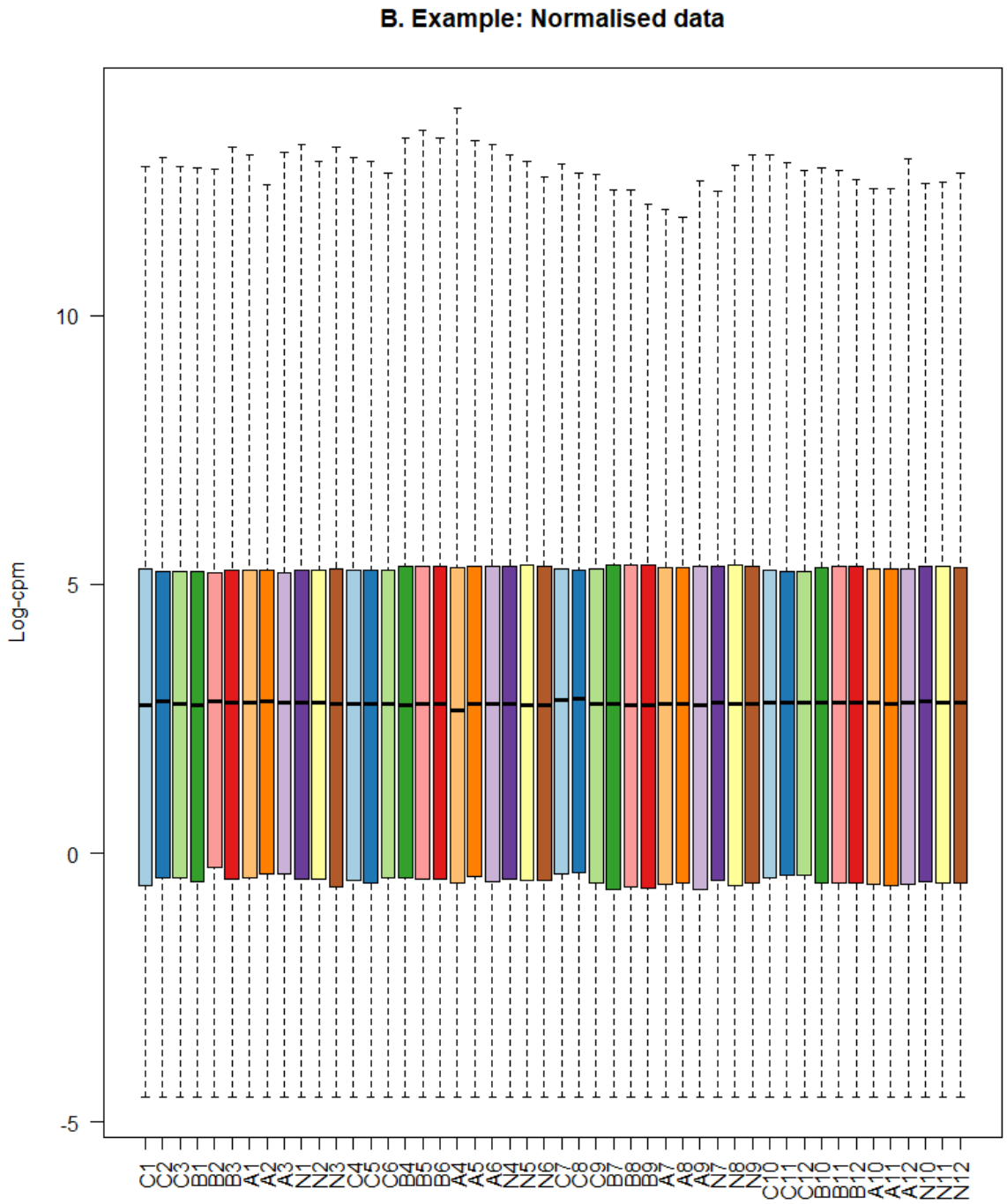

Figure 5.5: *Boxplots of log-CPM values showing expression distributions for normalized data for each sample. C stands for control samples, A for samples treated with AB85, B for samples treated with BDNF and N for samples treated with NT4. Samples labelled with 1-3 correspond to the triplicates of time-point 30 minutes, samples labelled with 4-6 correspond to the triplicates of time-point 2 hours, samples labelled with 7-9 correspond to the triplicates of time-point 12 hours and samples labeled with 10-12 correspond to the triplicates of time-point 24 hours.*

5.3.2.3 Normalising gene expression distributions

It is possible that during the sample preparation or the sequencing process, non-biological factors could influence the gene expression levels of individual samples. For example, one batch of the experiment could be sequenced more deeply than samples processed in another. Thus, normalisation is used in order to ensure that the expression distributions of all samples are similar to each other. In this chapter the normalisation method of trimmed mean of M-values (TMM) was used through the calcNormFactors function in edgeR. As expected from the data mentioned above the library sizes were similar for all samples before normalisation, with the exception of sample A4, one of the triplicate cultures treated with AB85 for 2 hours (Figure 5.4). The data after normalisation are presented in figure 5.5.

5.3.2.4 Unsupervised clustering of samples

The multidimensional scaling (MDS) plot is a useful preliminary plot for gene expression analyses, that displays similarities and dissimilarities between samples in an unsupervised manner. Thus, it is possible to examine the magnitude of differential expression before the downstream analysis. In the ideal scenario the samples would cluster according to the treatment condition and the technical triplicates would localise very close to each other. The MDS plot was made using the plotMDS function of the limma package. The first dimension corresponds to the leading-fold-change that explains most of the variation in the data, while subsequent dimensions have a smaller impact and they are orthogonal to the preceding dimension. In this experiment dimension 1 and 2 were used in the MDS plot and samples cluster well within experimental condition (Figure 5.6). Control samples from the 4 time-points cluster very close together, and in a small distance the treated samples from time-point 30 minutes are located in another cluster. On the bottom right part of the plot there is a cluster with the samples treated for 2 hours with the three TrkB ligands. The sample A4 as expected is located further apart from its triplicates and the other samples. On the top right part of the plot there are the samples treated for 12 and 24 hours. It is clear that samples treated with BDNF and NT4 for 12 hours are located closer to each other than to samples treated with AB85. Interestingly at time-point 24 hours the samples treated with BDNF and NT4 cluster together, while the samples treated with

AB85 are located further apart. Additionally, the samples treated with BDNF for 12 hours are located very close to the cluster of the samples treated for 24 hours. It needs to be emphasized that the biological triplicates, except sample A4 cluster well together. The largest transcriptional differences between control samples and samples treated for 2, 12 and 24 hours are observed over dimension 1, while the largest transcriptional differences between control samples and samples treated for 30 minutes are observed over dimension 2. The subsequent dimensions 3 to 8 account for only a small amount of the transcription variation and were not further examined (Figure 5.7).

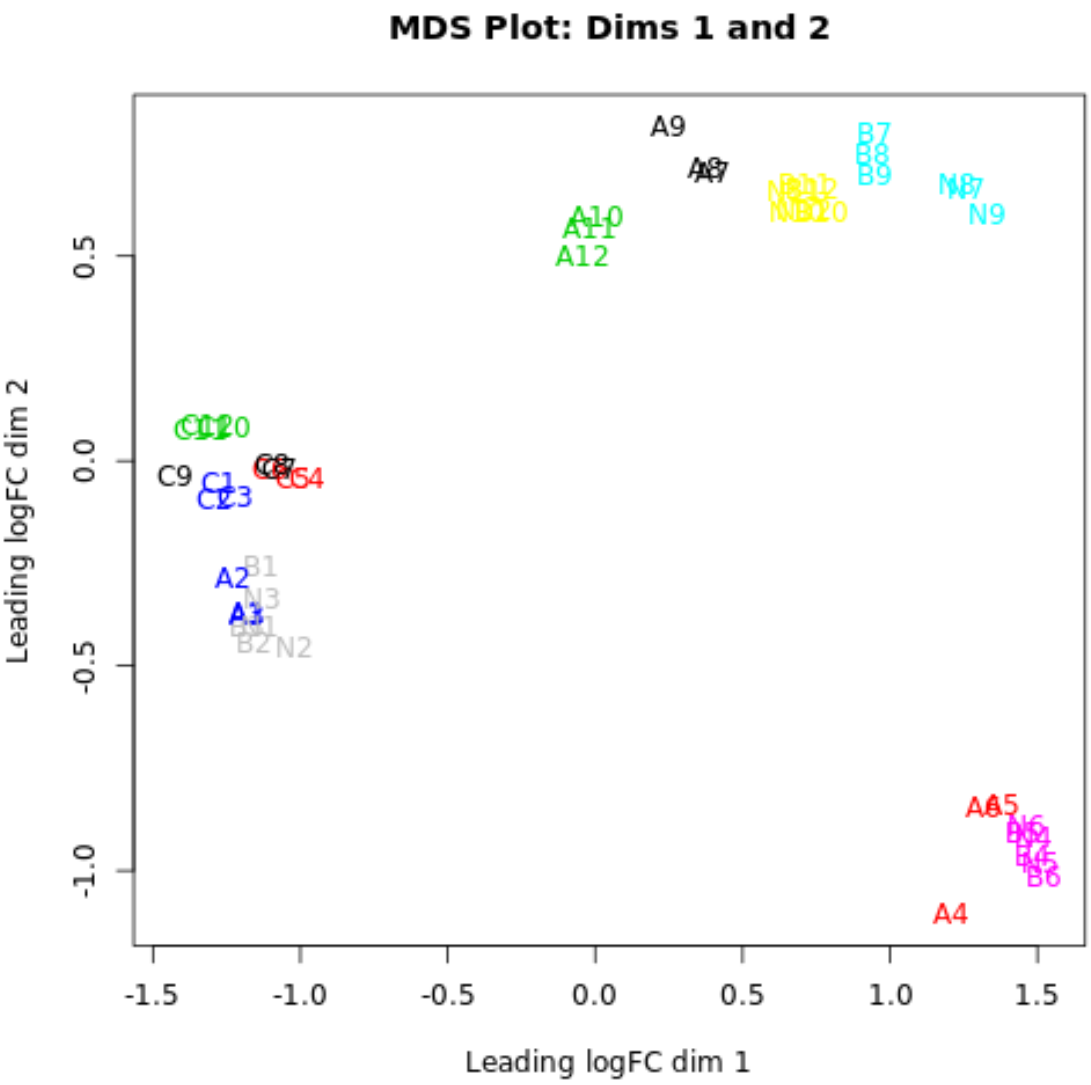

Figure 5.6: *MDS plots of loc-CPM values over dimensions 1 and 2 with samples coloured and labeled by group (treatment and time point). The samples are labeled as follows: C (control), A (#85), B (BDNF) and N (NT4). Numbers 1-3 correspond to time point 30 minutes, numbers 4-6 correspond to time point 2 hours, numbers 7-9 correspond to time point 12 hours and numbers 10-12 correspond to time point 24 hours. Distances on the plot correspond to the leading fold-change, which is the average (root-mean-square) log_2-fold change for the 500 genes most divergent between each pair of samples.*

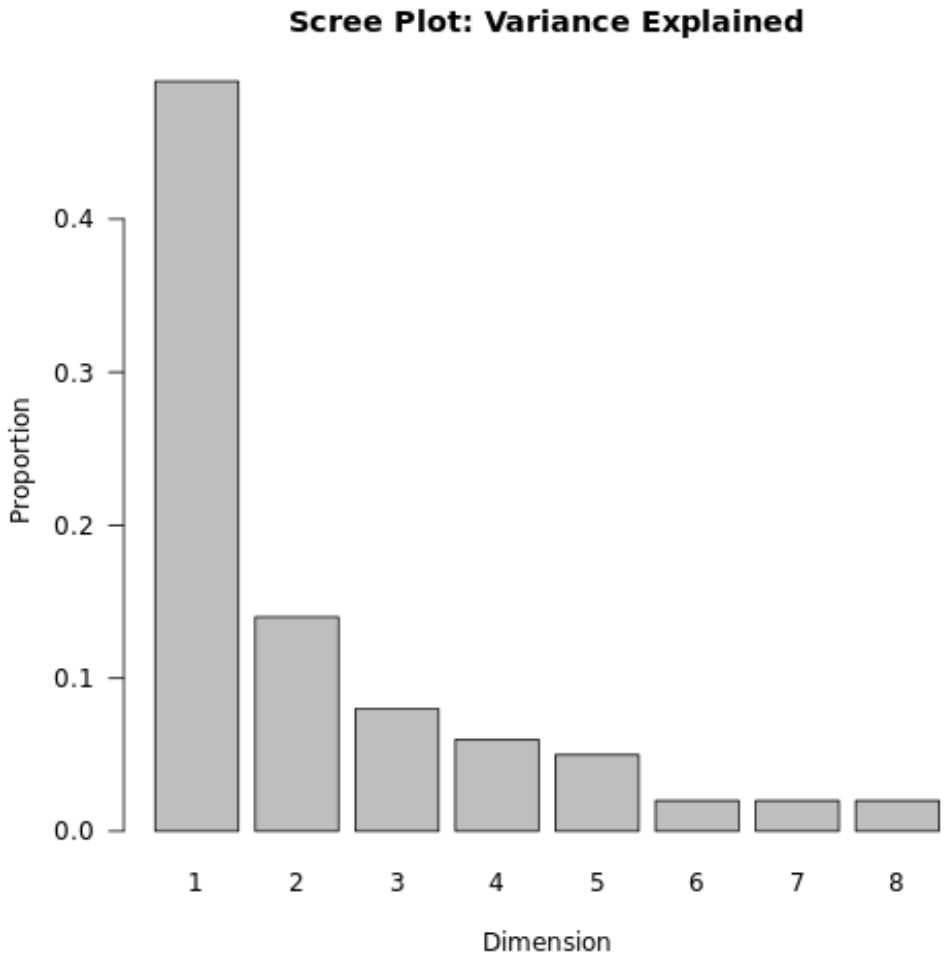

Figure 5.7: *The scree plot visualizes which dimensions account for which fraction of total variance in the data. The dimensions are listed by decreasing order of contribution to the total variance.*

5.4 RNA SEQ DATA ANALYSIS

5.4.1 Principal Components Analysis (PCA)

RNA seq analysis was performed as explained in Materials & Methods and raw data were converted to FPKM (Fragments Per Kilobase Million) values and log2-fold values with the help of Bioinformaticians Dr. Robert Andrews and Dr. Katherine Tansey (College of Biomedical & Life Sciences - Cardiff University). The first step of the bioinformatics analysis included clustering of the 48 samples based on whole transcriptome changes. The genomatix software was used to create linear combinations of the data and the first two components (PC1) and (PC2) described the largest variability. Principal Component Analysis (PCA) converts a high-dimensional dataset (where the number of dimensions equals the number of samples) into two or three dimensions. It can also transform a large set of variables (the counts for each individual transcript detected in each smaller) to a smaller set of orthogonal principal components. The first principal component (PC1) specifies the direction with the largest variability in gene expression, the second component (PC2) captures the direction with the second largest variation in gene expression and so on. PCA combines the read count from all genes multiplied with their influence on the Principal Component variation to get a single value. For example, PC1 score= (read count*influence) +… for all genes. The genes with the largest variation between different conditions will have the most influence on the principal components, i.e., genes that are highly expressed in some conditions and not expressed in others will have a lot of variation and influence on the PCs. The expression of the 4.703 genes that are differentially expressed with adjusted p value < 0.01 in 48 different samples and 16 conditions were included in the analysis. Each dot in the graph represents the expression profile of one out of 48 samples. Different time points are presented with different colours (under Time) and different treatment conditions are presented with different symbols (Figure 5.8).

Principal-component analysis (PCA) separated controls and treated samples by principal component 1 (PC1) and further separated different treatment conditions by principal component 2 (PC2). This analysis revealed that all treated samples for 30 minutes clustered together (blue circle) together with the corresponding controls,

indicating that there are no significant transcriptome changes at this early time point. Interestingly all the untreated samples clustered together indicating that within a short time period of 12 hours the transcription of neurons remained essentially unchanged. The samples treated with BDNF, NT4 or #85 for 2 hours were also tightly clustered together, with the exception of one triplicate treated with AB85 for 2 hours (A4 sample mentioned earlier), indicating that the three TrkB ligands affected transcription to the same extent and direction at this time point. The sample A4 was considered an outlier and excluded from further analysis. At 12 hours the samples treated with BDNF or NT4 clearly clustered together, whereas samples treated with #85 (for 12 hours as indicated) clustered together with samples treated with BDNF or NT4 for 24 hours. Finally, the triplicates treated with #85 for 24 hours cluster together but were located far away from the samples treated with BDNF and NT4 for the same length of time. With the exception of one sample treated with #85 for 2 hours, all other 47 samples clustered together, based on treatment and time point and were used for downstream bioinformatics analysis.

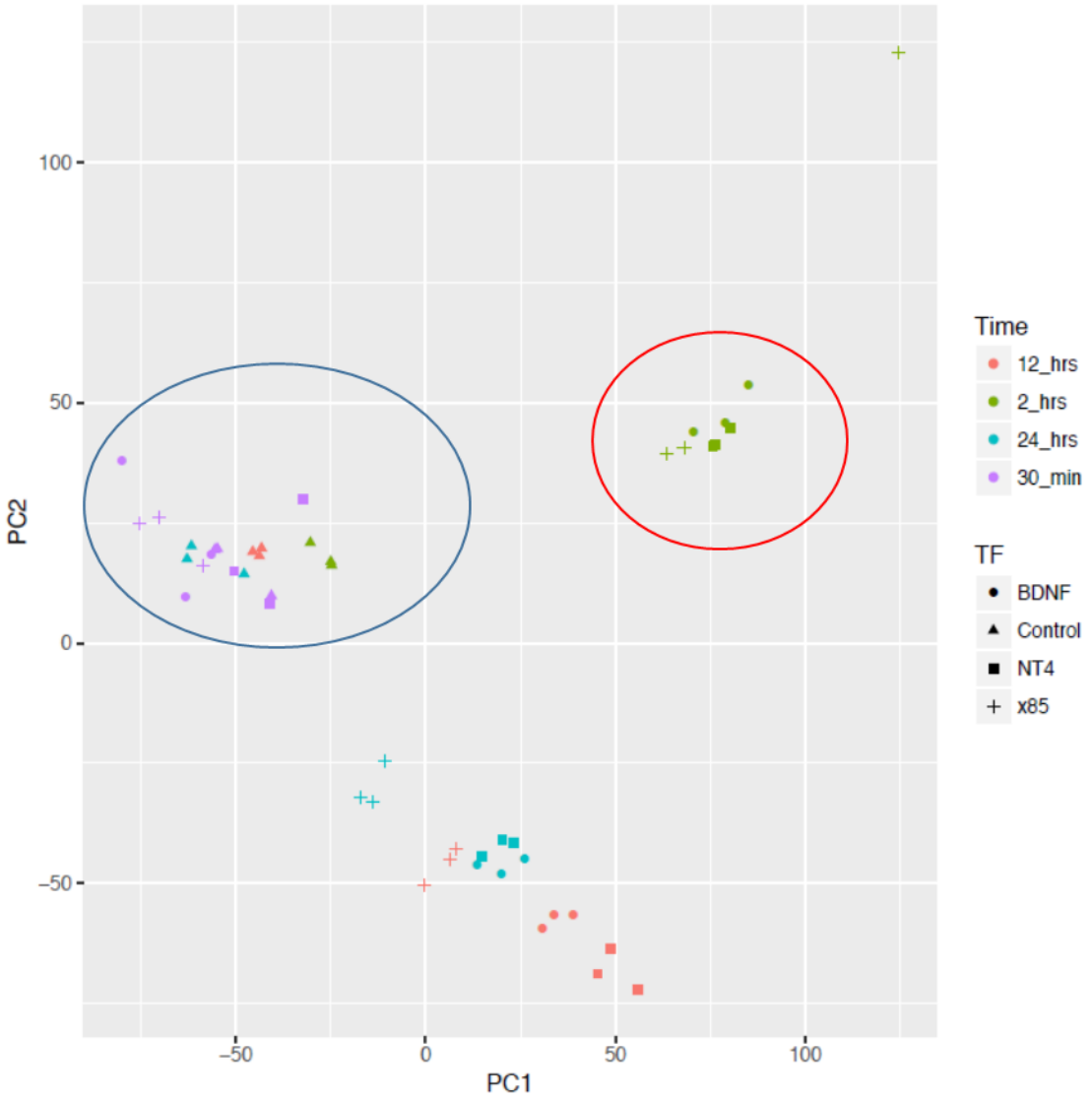

Figure 5.8. PCA on 30 DIV neurons treated with BDNF, NT4 and #85 for 4 different time points. *Each scheme represents the gene expression profile of a well. Different time points are illustrated with different colours and the 4 treatment conditions are presented with 4 schemes*

5.4.2 Differential gene expression analysis with limma-voom

The focus of this analysis was on the genes that are differentially expressed between the cell cultures treated with BDNF, AB85 and NT4 and control samples at time-points 30 minutes, 2 hours, 12 hours and 24 hours. Towards this direction limma, which is a R/Bioconductor package was used (Gentleman et al., 2004, Ritchie et al., 2015). The software package offers a differential expression pipeline which involves linear modeling for the analysis of complex experiments with multiple treatment factors and empirical Bayes statistical methods (Law et al., 2016). Under this approach the mean-variance relationship of the log-counts is estimated in a non-parametric way from the log-counts per million (log-cpm) that are normalized for sequence depth. Under the voom (variance modeling at the observational method) method the mean-variance trend is incorporated into a precision weight for each individual normalized observation. Since the same linear model is fitted to each gene it is possible to moderate the residual variances by borrowing strength between genes using the empirical Bayes method. The global variance estimate from this method can also incorporate a mean-variance trend and the gene-wise variances are compressed towards a mean-variance trend curve. The major advantage of the limma voom pipeline is the accurate detection of type I error rate regardless of the number of RNA-seq samples (Law et al., 2014).

A matrix of expression values was set up, where each row corresponds to the expression of one gene measured in raw counts and each column belongs to an RNA sample. Additionally, contrasts for pairwise comparisons between conditions were set up using the makeContrasts function. Limma uses log-CPM values which are assumed to be normally distributed, while the mean-variance relationship is calculated empirically. Initially the gene-wise linear models are fitted to the normalized log-cpm values considering each condition (treatment and timepoint). Thus, a residual standard deviation for each gene is produced and subsequently the mean-variance trend is fitted to the residual standard deviations in correlation to the average log-count measurement of each gene. In Figure 5.9 the mean-variance relationship of log-CPM values is displayed. The voom plot is characterized by a decreasing trend between the means and variances that is attributed to the technical variation in the sequencing experiment together with the biological variation among the triplicate samples from

different conditions. The sharp decreasing trend that was observed in this analysis showed that the biological variation was low and the major source of variation is due to technical variation (Law et al., 2014).

Linear modelling in limma package deploys the lmFit and constrasts.fit functions which can fit a separate model to the expression values for each gene. Subsequently empirical Bayes moderation through eBayes function uses information from all genes to get more accurate calculations for their variability. The residual variances obtained from the model are plotted against average expression values in Figure 5.10. It can be observed that upon the linear transformation the variance of the genes is independent of the mean expression level.

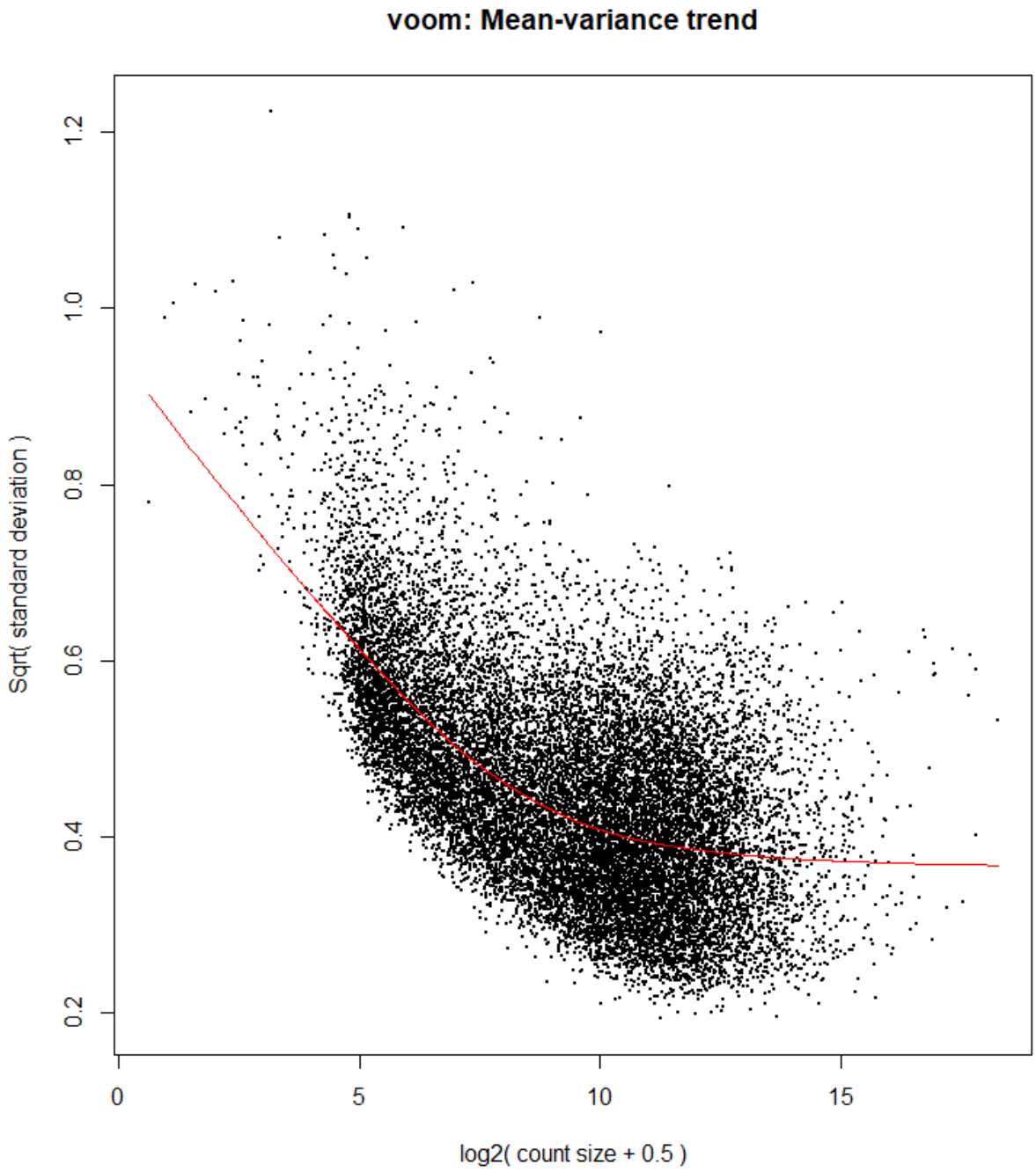

Figure 5.9: *Means (x-axis) and variances (y-axis) of each gene detected in the RNA seq experiment are plotted to describe the dependence between the two before voom is applied to the data. This plot is created using the voom function of the limma package and it extracts residual variances from fitting linear models to log-CPM transformed data. The variances are then transformed to the square-root of standard deviations and plotted against the mean expression of each gene. The means are log_2-transformed mean-counts with an offset of 0.5. Each black dot represents a gene, while the mean-variance trend is presented with a LOWESS (locally weighted regression) curve.*

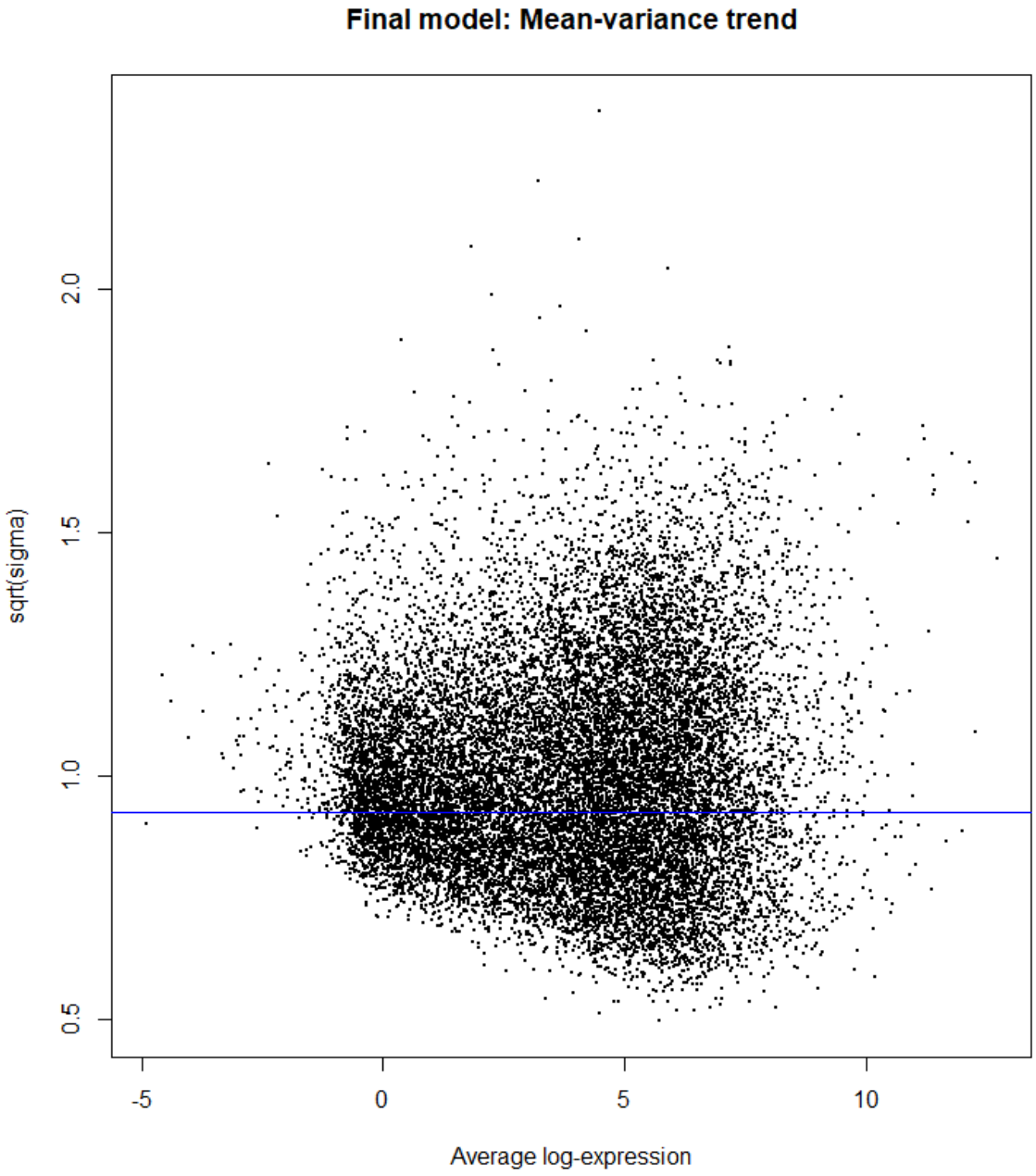

Figure 5.10: *The LOWESS trend (red line in figure 5.9) is removed after voom precision weights are applied to the data. The plot is created using plotSA which plots square root of the residual standard deviations against mean log-CPM values. The average square root of the residual standard deviations is marked by a horizontal blue line. Each black dot represents a gene.*

5.4.3 Top 20 upregulated genes upon treatment with TrkB ligands

Amongst the thousands of genes found to be upregulated over time, a subset of 20 genes was selected based on the significance of the change in their transcription levels throughout the 4 time points (adjusted p value <1.14E-88) and plotted in Figures 5.11 (for time-points 30 minutes and 2 hours) and 5.12 (time-points 12 and 24 hours) . The list of these genes with the p adjusted values and the fold of change across the 4 times points upon ANOVA test is shown at Table 5.2.

At the first timepoint, 30 minutes upon treatment the 20 most upregulated genes through conditions and time-points were not yet upregulated more than 2 times with the exception of *GEM* in cultures treated with NT4, which was upregulated 2.2 fold in comparison to the control. (Figure 5.11 A-C). At the second timepoint tested, 2 hours upon treatment the 20 genes were significantly upregulated with the exception of *STC1* (Figure 5.11 D-F). Interestingly 8 of these genes reached the peak of their expression 2 hours after treatment. More specifically, *FAM83G* was upregulated 16.6 fold by BDNF, 14.9 fold by AB85 and 16.89 fold by NT4. *GEM* was the gene with the highest upregulation, as it was upregulated 142 fold by BDNF, 96 fold by AB85 and 139 fold by NT4. *SPRY4* was upregulated 21 fold by BDNF, 18 fold by AB85 and 23 fold by NT4. *CD55* was upregulated 7 fold by BDNF and AB85 and 7.5 fold by NT4. *TACR1* was upregulated 19 fold by BDNF, 17 fold by AB85 and 19 fold by NT4. *DLK1* was upregulated 16 fold by BDNF and NT4 and 15 fold by AB85. HS3ST1 was upregulated 4 fold by BDNF and AB85 and 5 fold by NT4. *TNFRS12A* was upregulated 62 fold by BDNF, 65 fold by AB85 and 58 fold by NT4. At the third timepoint all 20 genes maintained high expression levels. Additionally 7 of these genes reached the peak of their expression (Figure 5.12 A-C). In more detail, *PALD1* was upregulated 55 fold by BDNF, 35 fold by AB85 and 38 fold by NT4. *LOXHD1* was upregulated 36 fold by BDNF, 23 fold by AB85 and 32 fold by NT4. *MMP1* was upregulated 42 fold by BDNF, 18 fold by AB85 and 108 fold by NT4. *C3orf52* was upregulated 30 fold by BDNF, 11 fold by AB85 and 93 fold by NT4. *SYTL5* was upregulated 12 fold by BDNF, 7 fold by AB85 and 10 fold by NT4. *SPATS2L* was upregulated 5 fold by BDNF, 3 fold by AB85 and 6 fold by NT4. *ARHGAP36* was upregulated 7 fold by BDNF, 5 fold by AB85 and NT4. At the last timepoint, 24 hours after treatment all 20 genes retained high expression levels and 4 of them reached their maximum expression (Figure 5.12

D-F). Indeed, *SPOCD1* was upregulated 128 fold by BDNF, 40 fold by AB85 and 126 fold by NT4. *PDYN* was upregulated 15 fold by both BDNF and NT4 and 7 fold by NT4. *ETV5* was upregulated 16 fold by BDNF, 14 fold by AB85 and 17 fold by NT4. *STC1* was upregulated 6 fold by BDNF and NT4 and 3 fold by AB85.

Paladin or *Pald1* is a phosphatase-domain containing protein which is highly expressed in endothelial cells during the early stages of embryonic development (Wallgard et al., 2012). It was also detected in hematopoietic cells and neural crest cells, while it was demonstrated that *Pald1* is essential for neural crest cell formation and migration (Roffers-Agarwal et al., 2012). Since mutations of cysteines in the putative phosphatase active motifs do not eliminate *Pald1* function and it does not appear to have phosphatase activity *in vitro* (Huang et al., 2009), it was suggested that *Pald1* is an antiphosphatase that controls the phosphorylation levels of the target proteins during neural crest development . Interestingly *Pald1* was also shown to be necessary for lung development and adult lung function in females, as *Pald1* knock-out females showed increased endothelial apoptosis and reduced endothelial cell number in the vascular compartment (Egana et al., 2017). *Spocd1* (Spen Paralog and Ortholog C-terminal Domain containing 1) encodes a transcription factor of the TFIIS family. It is known to interact with testis protein phoshatase 1 (PP1) which is an important serine/threnonine-specific phoshatase implicated in cellular singaling (Fardilha et al., 2011). It was also suggested that it is involved in developmental regulation due to the SPOC domain being usually part of developmental signaling (Ariyoshi and Schwabe, 2003). A recent study claimed that it also enhances proliferation and metastasis of glioma cells via positive regulation of Pentracix 3 (*PTX3*), while knockdown of *SPOCD1* with shRNA inhibited proliferation of glioma cells both *in vitro* and *in vivo* (Liu et al., 2018). Another study found *SPOCD1* to be expressed in tissues from osteosarcoma patients, while knockdown of *SPOCD1* by transfecting with shRNA human osteosarcoma cells blocked cell proliferation and increased apoptosis. Interestingly *SPOCD1* exerted its role in cell proliferation and apoptosis via expression of *VEGF-A* and knockdown of *VEGF-A* had similar effect on cell proliferation and apoptosis as knockdown of *SPOCD1* (Liang et al., 2018). *LOXHD1* is a highly conserved protein composed of 15 PLAT (polycystin/lipoxygenase/alpha-toxin) domains and it is involved in targeting proteins to the plasma membrane (Aleem et al., 2008). A missense mutation (4025T>A) in

Loxhd1 caused hearing loss and degeneration of hair cells in animal models, while a homozygous stop mutation in humans (2008C>T) led to progressive hearing loss in humans and the onset of hairing loss occurred during childhood, accompanied by balance disorders and vertigo (Grillet et al., 2009). Furthermore mutations in *LOXHD1* had been associated with late-onset-FCD (Fuchs corneal dystrophy) and the corneas of carriers of these mutations were found to display aggregate staining of LOXDH1. In the same study it was hypothesized that increased transcription of *LOXDH1* regardless of mutations could contribute to late-onset FCD (Riazuddin et al., 2012). *FAM38G* (Family with Sequence Similarity 83 Member G) also known as *PAWS1* (Protein Associated With Smad 1) was discovered using a proteomic approach as a novel regulator of non- canonical BMP pathway and a substrate of ALK3. It was shown that it acts through formation of a macromolecular complex with SMAD1 and BMP-induced phosphorylation of *Fam38g* controls the expression of BMP target genes *NEDD9* and *ASNS* (Vogt et al., 2014). Additionally experiments in *Xenopus* embryos and human cells (U20S) showed that *Fam38g* is indispensable for Wnt signaling and it acts through association with the a isoform of casein kinase 1 (CK1), although the precise mechanism is still under investigation (Bozatzi et al., 2018). *Gem* is an immediate early response gene (Maguire et al., 1994) and member of a group of small GTP-binding proteins of the Ras superfamily, which is known as RGK (Rad, Gem, Kir) family. Additionally it has been shown that *Gem* controls the reshaping of the actin cytoskeleton through binding to Rho kinase (Ward et al., 2002). In the same study *Gem* expression in N1E-115 neuroblastoma cells stimulated neurite extension through binding to ROK. Additionally Gem binds to Calmodulin (Cam) in a Ca^{2+} - dependent manner *in vitro* and it acts as a substrate for calmodulin-dependent protein kinase 2 (CaMKII), indicating that it *Gem* could be involved in Ca^{2+} activated signaling cascades and subsequent activation of serine/threonine kinases (Moyers et al., 1997). In line with these evidence a study using mouse primary hippocampal cultures showed that *Rem 2,* which is a GTP-binding protein identified based on its homology with Gem and other members of the RGK family of Ras-related small GTP-binding proteins (Finlin et al., 2000) is abundantly expressed in mouse primary neurons controls dendritic branching and synapse formation through signal transduction pathways (Ghiretti and Paradis, 2011). *Spry4* has been described as a TrkA-induced gene that downregulates Erk/MAPK pathway and inhibits *Rac1*, albeit not Akt singalling upon treatment of DRG and PC12 cells with NGF, through a negative feedbback loop.

Interestingly *Spry4* limits neurite outgrowth without influencing survival (Alsina et al., 2012). *Spry4* has also been shown to be downregulated during development of hippocampal neurons both *in vivo* and *in vitro* during development. Additionally shRNA against *Spry4* led to elongative axong growth in hippocampal cultures suggesting that this gene plays an important role in regulation of developmental axon growth (Hausott et al., 2012). *Lrrtm1* (Leucine rich repeat transmembrane neuronal proteins) is an immediate early gene that binds to neurexin in a calcium-dependent manner (Siddiqui et al., 2010) and its mRNA expression is increased upon increase of synaptic activity in hippicampal neurons. This upregulation demands nuclear calcium signaling, the activation of CaM kinases and CBP function (Hayer and Bading, 2015). The same study suggested that nuclear calcium singaling may regulate neuronal network activity through the *Lrrtm1*, which is a synaptic organizer. Additionally a study of a group of siblings that were diagnosed with famililial schizophrenia found a strong linkage of hypomethylation at the paternally inherited allele of the *LRRTM1* promoter with schizophrenia (Brucato et al., 2014). Interestingly *Lrrtm1* knockout mice presented reduction of the hippocampus size and impaired synaptic density and integrity highlighting the role of the gene in these functions (Takashima et al., 2011). *MMP1* (Matrix Metalloproteinase 1) is a zinc-dependent endopeptidase involved in different stages of neuroplasticity and it has been shown that hippocampi derived from mice overexpressing *Mmp1* had increased percentage of neural progenitor cells, which display augmented differentiation to neurons. The same study showed that *Mmp1* acts through its substrate PAR- (protease-activated receptor-1) which is G-protein coupled receptor (Valente et al., 2015). The pathway of MMP1/ PAR1 had also been shown to orchestrate neuronal dendritic organisation and synaptic plasticity, while overexpression of human *MMP1 in vivo* upregulated denditic spine density and complexity in CA1 hippocampal neurons. Additionally the *Hmmp-1* transgenic animals presented behavior changes that are linked with synaptic plasticity, such as memory and learning problems, decreased anxiety and sociability (Allen et al., 2016). *Cd55* (Cromer Blood Group) also known as Decay Accelarting Factor for Complement (*DAF*) is a ubiquitously expressed intrinsic complement regulatory protein which is reduced upon severe hypoxia, while higher expression of *Daf* reduced the cerebral damage upon traumatic brain injury (VanLandingham et al., 2007). Additionally *Daf* has neuroprotective effects to chemical hypoxia through down regulation of *Src* and caspases 3 and 9 (Wang et al., 2010). Interestingly another study showed that

downgregulation of *Cd55* was implicated in neuropathic pain (NPP) (Nie et al., 2015). *C3ORF52* or TPA-induced transmembrane protein (*TTMP*) was found to be upregulated upon treatment of the pancreatic cancer cell line CD18 and based on silico analysis predicted that it is a single-pass transmembrane protein of 217 residues targeting the endoplasmatic reticulum (Chan et al., 2005). The function of this gene is unknown. Prodynorphin (*Pdyn*) is a precursor protein that produces upon cleavage with proprotein convertase 2 (*PC2*), dynorphin opioiod neuropeptides α and β-neoendorphin and dynoprhins A and B (Day et al., 1998) that act through κ-opioid receptor (Chavkin et al., 1982). Importantly the amygdalohippocampal area of patients with major depression or bipolar disorder showed singificant reduction in prodynorhpin levels (Hurd, 2002). Another study demonstrated the reduced mRNA expression in postmortem periamydgaloid cortex (PAC) tissue in patiens with major depressive dissorder (MDD) and heroin users (Anderson et al., 2013). Missense mutations in the *PDYN* gene have been found to to lead to Spinocerebellar Ataxia Type 23 (SCA23), which is a neurodegenerative disease characterized by a somewhat slowly developing cerebellar ataxia (Bakalkin et al., 2010). Surprisingly treatment of striatal neurons with ethanol had as a consequence the activation of TrkB and the subsequent activation of MAPK signaling pathway which stimulated increase of PDYN. The same study demonstrated that dynorphin receptor (*Kor*) was necessary for the decrease of ethanol intake through BDNF. Therefore *Pdyn* is one of the downstream effectors of BDNF (Logrip et al., 2008). A recent study discovered that peripheral blood mono-nuclear cells from patients diagnosed with bipolar disorder type II (BD-II) had reduced mRNA levels of *PDYN* and lower DNA methylation levels at the promoter of *PDYN* gene. Additionally there was a positive correlation in promoter methylation of *PDYN* and *BDNF* (D'Addario et al., 2018). *Etv5* is a member of the polyomavirus enhanceractivator 3 (PEA3)/Etv4-subfamily and a transcriptional activator of MAPK signaling (Willardsen et al., 2014). *Etv5* mRNA levels were found to be upregulated upon treatment of different neuronal cells with NGF, while siRNA experiments targeting *Etv5* in rat sensory neurons inhibited neurite outgrowth, suggesting that *Etv5* acts a a link between neurotrophin signaling and sensory neuron differentiation (Fontanet et al., 2013). Another study provided supporting evidence to the role of *Etv5* in neurite development, by showing that treatment of DRG with BDNF increased mRNA levels of *Etv5*. Additionally overexpression of *Etv5* mediated BDNF-induced neurite outgrowth in DRG neurons (Liu et al., 2016). A recent study suggested that

Etv5 is necessary in hippocampal dendrite development and plasticity, as shown by both *in vitro* shRNA knockdown experiments for *Etv5* in rat hippocampal neurons and *Etv5* conditional knockout mice. These experiments demonstrated that *Etv5* deficient neurons and mice had smaller dendritic arbor length and limited complexity. Interestingly ETV5 mutant mice presented social and cognitive defects (Fontanet et al., 2018). The tachykinin receptor 1 (*TACR1*) also mentioned as neurokinin 1 receptor (NK1R) or substance P receptor (*SPR)* is a G protein coupled receptor located in the central nervous system and the peripheral nervous system (Takeda et al., 1991, Pinto et al., 2004). The endogenous ligand for this receptor is Substance P, which is a neuropeptide, a neurotransmitter and neuromodulator (Harrison and Geppetti, 2001). Spinal neurons that express this receptor are indispensable for sensing various types of pain and deletion of the spinal neurons that express *Tacr1* resulted in analgesia (Iadarola et al., 2017). In line with this injection of rodents with BDNF prior to intrathecal NMDA was found to induce TACR1 internalization during neuropathic pain, and treatment with a BDNF scavenger limited the rate of TACR1 internalization (Chen et al., 2014a). *Tacr1*-/- female mice had higher body mass and fat content, indicating the involvement of the receptor in body weight regulation in a sex dependent manner (Pillidge et al., 2016) . On the opposite a study using iPSC-derived neurons from human females suffering from anorexia nervosa discovered higher mRNA and protein levels of TACR1 (Negraes et al., 2017). Synaptotagmin-like protein 5 (*Sytl5*) is a member of the carboxyl-terminal-type (C-type) tandem proteins and an effector of the Ras-related protein Rab27A (Kuroda et al., 2002). Knockdown of *SYTL5* with shRNA in aSyn H4 neuroglial human lines was shown to enhance cell to cell transfer of aSyn and decrease oligomerization (Goncalves et al., 2016). Furthermore, whole transcriptome analysis of late-onset Alzheimer's Disease patients revealed a 2 fold-decrease of mRNA levels of *SYTL5* (Annese et al., 2018). Staniochallin 1 (*Stc1*) is expressed in terminally differentiated brain neurons and it has been described as a regulator of calcium homeostasis (Zhang et al., 1998, Gerritsen and Wagner, 2005). It was upregulated in neurons upon ischemic episods in human and mouse brain and its overexpression was shown to enhance survival of human neural-crest derived Paju cells treated with thapsigargin (Zhang et al., 2000). *Stc1* expression is induced upon activation of cAMP and ERK1/2 in rat primary cortical neurons and regulated by the neuroprotective agent PACAP (pituitary adenylate cyclase-activating polypeptide) (Holighaus et al., 2012). Delta-like 1 homolog (*DLK1*) is an EGF-like membrane-bound

protein encoded by a maternally imprinted gene (Laborda, 2000). It is a Notch related transmembrane protein that induces the generation of neurons from mouse and human neural progenitors by forcing exit from cell cycle. *DLK1* was found to suppress the SMAD pathway and Hes1-mediated Notch singalling in hESC derived neural progenitors (Surmacz et al., 2012). *Dlk1* has also been described as indispensable for the promotion of a fast biophysical signature in motor neurons and necessary for motor neuron type-specific gene expression (Muller et al., 2014). *DLK1* was also suggested to be a marker for hESC dopanimergic progenitor cells suitable for transplantation (Kikuchi et al., 2017). Furthermore *Dlk1* was shown to be necessary for proper myogenesis and regeneration of myofibers (Waddell et al., 2010). *SPATS2L* (Spermatogenesis Associated Serine Rich 2 Like) is a relatively unknown protein which has been linked to Bronchodilator response (BDR) in asthmatic patients (Himes et al., 2012). Heparan sulfate D-glucosaminyl 3-O-sulfotransferase 1 (*HS3ST1*) is expressed on cerebellar cortex and primary visual cortex (Miller et al., 2014) and its transcript levels were found to be decreased in AD brains (Desikan et al., 2015). In line with this notion, the genomic region that contains the gene has been associated with AD (Witoelar et al., 2018). *TNFRSF12A* also known as *TWEAKR* (TNF-related weak inducer of apoptosis receptor) or fibroblast growth factor-inducible 14 (*Fn14*) has been shown to be involved in tissue regeneration. More specifically TWEAK/TWEAKR pathway is implicated in the proliferative and differentiating commitment of skeletal muscle progenitor cells and it enhances muscle myoblast cell proliferation and differentiation upon injury *in vivo* (Girgenrath et al., 2006). Additionally TWEAK/TWEAKR signaling has shown to be indispensable for regeneration of adult liver in mice that underwent partial hepatectomy (Karaca et al., 2014). Traumatic brain injury or injection of a mini-osmotic pump in the rat brain led to an increase of about 2 fold of mRNA levels of *Tweakr* (Malik et al., 2011). TWEAKR has also been suggested to regulate different pathways of TWEAK-induced cell death in both human and mice cell lines (Nakayama et al., 2003). Interestingly treatment of neuronal progenitor cells from the SVZ with TWEAKR ligand, TWEAK induced the differentiation to neurons, while *Tweakr* -/- adult mice had significantly fewer neuroblasts (Scholzke et al., 2011). Additionally TWEAK was shown to promote astrocyte proliferation through TGF-α/EGFR singaling (Rousselet et al., 2012). *ARHGAP36* (Rho GTPase Activating Protein 36) is a positive regulator of hedgehog and an inhibitor of protein kinase A

(PKA) through binding to the catalytic subunit PKAC that blocks PKA activity and promoting the ubiquitylation of PKAC (Eccles et al., 2016).

gene symbol	gene name	Ensembl gene	Fold Change	pvalue	padj
PALD1	phosphatase domain containing, paladin 1	ENSG00000107719	35.22314214	5.1E-248	1.2E-243
SPOCD1	SPOC domain containing 1	ENSG00000134668	35.53774981	3.7E-192	4.5E-188
LOXHD1	lipoxygenase homology domains 1	ENSG00000167210	26.55144698	2.6E-177	2E-173
FAM83G	family with sequence similarity 83 member G	ENSG00000188522	4.079822467	4.6E-170	2.7E-166
GEM	GTP binding protein overexpressed in skeletal muscle	ENSG00000164949	14.86589484	7.9E-153	3.1E-149
SPRY4	sprouty RTK signaling antagonist 4	ENSG00000187678	11.64376143	9.2E-148	3.1E-144
LRRTM1	leucine rich repeat transmembrane neuronal 1	ENSG00000162951	5.978066232	1.3E-128	3.5E-125
MMP1	matrix metallopeptidase 1	ENSG00000196611	23.84104635	1.5E-126	3.7E-123
CD55	CD55 molecule (Cromer blood group)	ENSG00000196352	5.162474878	3.1E-115	6.7E-112
C3orf52	chromosome 3 open reading frame 52	ENSG00000114529	19.74979022	2.9E-114	5.8E-111
PDYN	prodynorphin	ENSG00000101327	5.181080434	6.7E-114	1.1E-110
ETV5	ETS variant 5	ENSG00000244405	10.3511701	7.5E-113	1.2E-109
TACR1	tachykinin receptor 1	ENSG00000115353	7.830128849	3.4E-109	5E-106
SYTL5	synaptotagmin like 5	ENSG00000147041	6.100408916	1.7E-108	2.4E-105
STC1	stanniocalcin 1	ENSG00000159167	4.56675838	2.5E-108	3.3E-105
DLK1	delta like non-canonical Notch ligand 1	ENSG00000185559	3.669883341	1.5E-100	1.7E-97
SPATS2L	spermatogenesis associated serine rich 2 like	ENSG00000196141	3.675586589	3.43E-96	3.73E-93
HS3ST1	heparan sulfate-glucosamine 3-sulfotransferase 1	ENSG00000002587	3.38993868	2.85E-94	2.96E-91
TNFRSF12A	TNF receptor superfamily member 12A	ENSG00000006327	11.26918606	1.14E-92	1.13E-89
ARHGAP36	Rho GTPase activating protein 36	ENSG00000147256	6.322714151	1.14E-88	1.05E-85

Table 5.2 List of 20 most upregulated genes across the 3 treatments with BDNF, AB85 and NT4 and the 4 time-points 30 minutes, 2 hours, 12 hours and 24 hours sorted by adjusted p value

Figure 5.11 *Top 20 upregulated genes after 30 minutes (A-C) and 2 hours (D-F), selected by the statistical significance of the change in their transcription levels across the 4 time-points analyzed. Log2FC in the X axis represent log2 fold of change.*

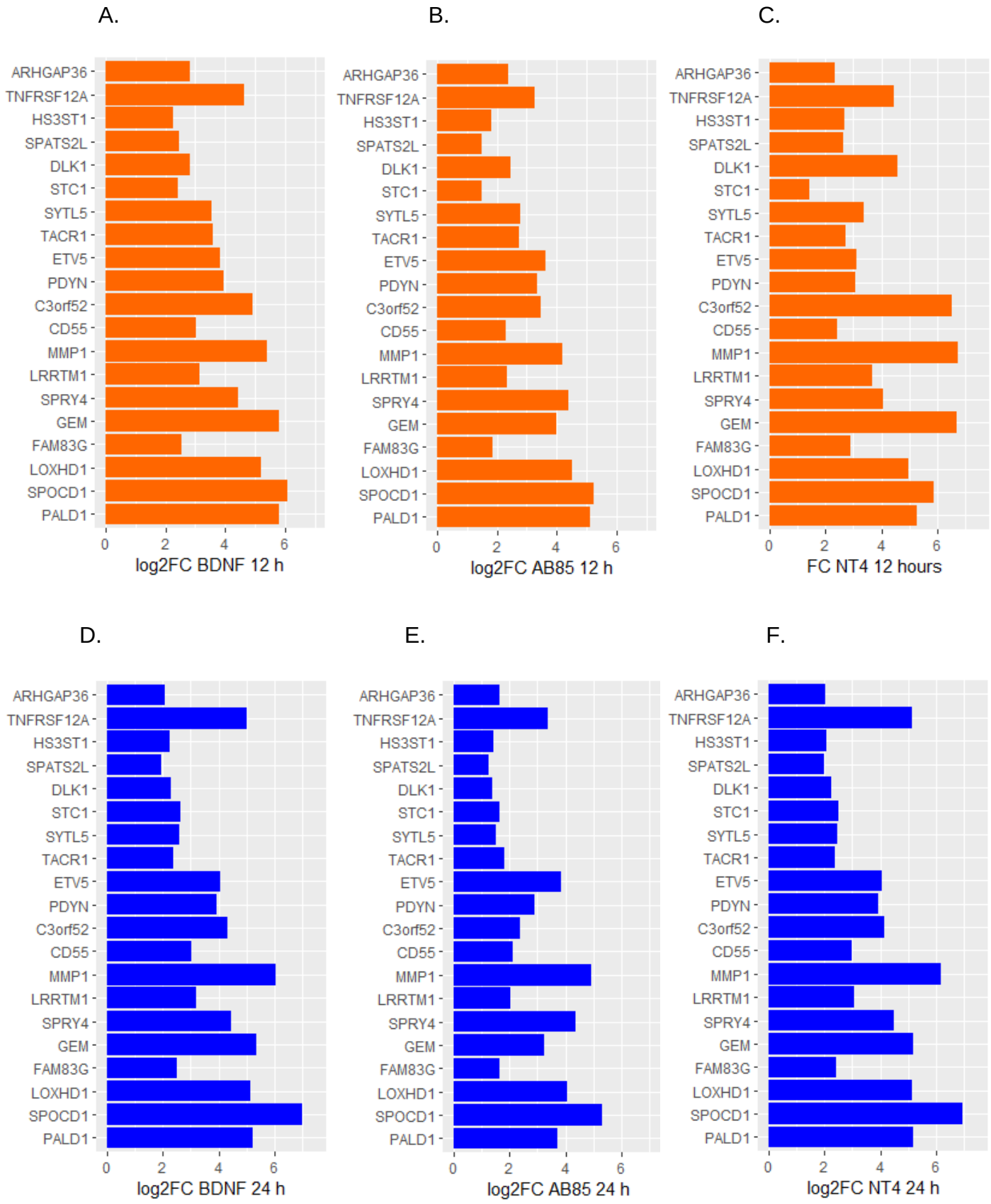

Figure 5.12 *Top 20 upregulated genes after 12 hours (A-C) and 24 hours (D-F), selected by the statistical significance of the change in their transcription levels across the 4 time-points analyzed. Log2FC in the X axis represent log2 fold of change.*

5.4.4 Top 20 downregulated genes upon treatment with TrkB ligands

Amongst the thousands of genes found to be downregulated over time, a subset of 20 genes was selected based on the significance of the change in their transcription levels throughout the 4 time points (adjusted p value <4.52E-51) and plotted in Figures 5.13 (for time-points 30 minutes and 2 hours) and 5.14 (time-points 12 and 24 hours) . The list of these genes with the p adjusted values and the fold of change across the 4 times points upon ANOVA test is shown at Table 5.3. At the time-point 30 minutes there was no gene of this subset overexpressed more than 2 fold (Figure 5.11 A-C).

At the first time-point, 30 minutes upon treatment the 20 most downregulated genes through conditions and time-points did not display changes in expression of more than 2-fold with the exception of *SOCS3* in cultures treated with NT4, which was upregulated 2.2-fold in comparison to the control. (Figure 5.13 A-C). At the second time-point, 2 hours upon treatment, 11 genes were significantly downregulated and 5 of them were downregulated more than in the other 3 time-points (Figure 5.13 D-F). More specifically, *KLF11* was downregulated by 4-fold by all three ligands, *PDZRN3* was downregulated 7-fold by BDNF, 7.5-fold by AB85 and 6-fold by NT4. *SIAH3* was downregulated 3.6-fold by BDNF and NT4 and 3.7-fold by AB85. *GALR1* was downregulated 5-fold by BDNF and 4.4-fold by AB85 and NT4. *CDH20* was downregulated 8-fold by BDNF, 7-fold by AB85 and 7.5-fold by NT4. At the third time-point, 12 hours upon treatment all 20 genes were significantly downregulated and 14 of them were downregulated more than in the other 3 time-points (Figure 5.14 A-C). In more detail, *STK32A* was downregulated 4-fold by BDNF, 2.4-fold by AB85 and 6-fold by NT4. *WNT7B* was downregulated 8.5-fold by BDNF, 3.8-fold by AB85 and 19-fold by NT4. *VSTM2A* was downregulated 4-fold by BDNF, 2.5-fold by AB85 and 7-fold by NT4. *SOCS3* was downregulated 2.5-fold by BDNF, 2-fold by AB85 and 2.3-fold by NT4. *YPEL1* was downregulated 2.7-fold by BDNF, 2-fold by AB85 and 2.5-fold by NT4. *MAP2K6* was downregulated 5-fold by BDNF, 2-fold by AB85 and 5-fold by NT4. *PZD2* was downregulated 9-fold by BDNF, 5-fold by AB85 and 5-fold by NT4. *UNC5B* was downregulated 6-fold by BDNF, 4-fold by AB85 and 6-fold by NT4. *KLHL29* was downregulated 2.8-fold by BDNF, 2-fold by AB85 and 4-fold by NT4. *PCSK2* was downregulated 3-fold by BDNF, 2.2-fold by AB85 and 3.3-fold by NT4.

GPR179 was downregulated 5.3-fold by BDNF, 3-fold by AB85 and 3.3-fold by NT4. *ROR1* was downregulated 3-fold by BDNF, 2-fold by AB85 and 4-fold by NT4. *UST* was downregulated 5.3-fold by BDNF, 3-fold by AB85 and 3.8-fold by NT4. *VSTM2A-OT1* was downregulated 3.7-fold by BDNF, 2.3-fold by AB85 and 6.39-fold by NT4. At the last time-point of 24 hours after treatment, 16 genes remained significantly downregulated. The genes that were not significantly upregulated were *SOCS3*, *YPEL1*, *KLHL29*, and *UST* (Figure 5.14 D-F). Additionally, *HUNK* was downregulated more than in the other 3 time-points, 2.5-fold by BDNF, 1.5-fold by AB85 and 2.4-fold by NT4.

Kruppel like factor 11 (*KLF11*) is a zinc finger transcription factor that binds to SP1-like sequences in gene promoters leading to inhibition of cell growth and apoptosis induction (Cook et al., 1998). Also, *Klf11* was shown to regulate the expression of neurotransmitter receptor *Drd2* (Dopamine Receptor D2) in DRG and PC12 cells (Seo et al., 2012). Dysregulation of *DRD2* has been linked with several neurological diseases including Parkinson's disease (Paus et al., 2008). Its expression levels are elevated in neurons and astrocytes in the prefrontal cortex of human brain (Udemgba et al., 2014). The protein levels of *Klf11* are upregulated in the thalamus, hypothalamus and amygdala following chronic exposure of rats to stress or alcohol, leading to activation of signaling cascades responsible for cellular stress and apoptosis (Duncan et al., 2015). Another study showed that KLF11 protein level was significantly increased in the postmortem prefrontal cortex of humans with MDD (Major Depressive Disorder) and this increase does not correlate with any other characteristic. The same study found increased levels of *Klf11* in a murine model of MDD. Additionally, it was demonstrated that *Klf11*$^{-/-}$ mice display considerably less depressive-like behavior upon exposure to chronic stress (Harris et al., 2015).

The E3 ubiquitin ligase PDZ domain-containing protein RING finger protein 3 (*PDZRN3*) is a ubiquitin ligase which has been shown to be involved in Wnt PCP signaling and necessary for vascular morphogenesis (Sewduth et al., 2014). *PDZRN3* also controls endothelial intercellular junction integrity and endothelial cell-specific overexpression of this protein resulted to early embryonic death accompanied by impaired organization of endothelial intercellular junctions. On the other hand specific loss of *Pdzrn3* in endothelial cells inhibited the vascular leakage in a mouse model of transient ischemic stroke (Sewduth et al., 2017). Interestingly *PDZRN3* has been

characterized as a key player in synaptic growth and regulation in mammalian neuromuscular junction (NMJ), through binding to muscle-specific receptor tyrosine kinase (MuSK) which is a major organizer of postsynaptic development of NMJ (Lu et al., 2007). It has to be noted that enhanced expression of *Pdzrn3* by deletion of the histone methyltransferase *Prdm16* (Positive Regulatory Domain 16) limited the capacity of newly generated neurons to migrate towards the upper layers of the cerebral cortex (Baizabal et al., 2018). *STK32A* (Serine/Threonine Kinase 32A) or *YANK1* (Yet Another Novel Kinase) belongs to the superfamily of serine/threonine protein kinases and it is composed of a catalytic domain and metal ion binding domain and participates in the phosphorylation of serine and threonine residues on different protein substrates (Strausberg et al., 2002). Additionally, *STK32A* has been characterized as a novel target gene of Wnt/*β*-catenin pathway which is involved in brain development and function and is disrupted in neurodegenerative disorders.

WNT7B (Wnt Family Member 7B) is a member of the WNT gene family and it has been implicated in oncogenesis as it was shown to enhance Wnt signaling in pancreatic cancer cell lines PDAC) and to augment cell growth (Arensman et al., 2014). Additionally, *WNT7B* expression is necessary for the amplification of prostate cancer cell lines and it promotes osteoblast differentiation *in vitro* through a cell-cell interaction (Zheng et al., 2013). It also has to be noted that *WNT7B* plays a key role in breast cancer and its progression. The deletion of the gene in myeloid cells decreased the mass and volume of the tumors caused by the absence of angiogenic switch (Yeo et al., 2014). *WNT7B* has also a role in brain development, as it regulates dendritic development through a non-canonical pathway via its effect in Rho GTPases and JNK (Rosso et al., 2005). A recent study demonstrated that the receptor of WNT7B, the seven-transmembrane frizzled-7 (Fz7) and the scaffold protein Dvl1 coactivate CAMKII and JNK leading to the formation of elaborate dendrites (Ferrari et al., 2018). The VSTM2A (V-Set and Transmembrane Domain Containing 2A) protein was found to be expressed and secreted by commited preadipocytes, while it controls the determination of adipocytes through regulation of BMP signaling and activation of PPARγ2 (Secco et al., 2017). Furthermore, its overexpression is a biomarker for mucinous tubular and spindle cell carcinoma (*MTSCC*) of the kidney (Wang et al., 2018a).

SOCS3 (Suppressor of Cytokine Signaling) or STAT-Induced Inhibitor 3 is a negative regulator of cytokine signalling of the JAK/STAT3 pathway through binding to tyrosine kinase receptors (Nicholson et al., 2000). The activation of the JAK/STAT3 signal transduction pathway is initiated in the spinal cord upon peripheral nerve injure (CCI), and its blockage by SOCS3 could lessen spinal cord neuroinflammation and the subsequent neuropathic pain. On the other hand, overexpression of *SOSC3* in T cells decreased IL-17 levels and enhanced atherosclerosis, when *in vivo* treatment with anti-sense oligodeoxynucleotides targeting *SOCS3* augmented atherosclerotic effect in *ApoE*$^{-/-}$ mice (Taleb et al., 2009). Interestingly *SOCS3* expression levels in the CNS are increased in animal models of obesity (Bjorbaek et al., 1998) and SOCS3 binds to the leptin receptor thus interfering with leptin functionality (Bjorbak et al., 2000). In line with this haploinsufficiency of *SOCS3* (Howard et al., 2004) or neural cell- specific *Socs3* conditional knockout mice (Mori et al., 2004) protected the animals from diet-induced obesity and sustain Leptin activity. Intriguingly the levels of *SOSC3* in the brain tissues of patients with AD were found to be increased (Walker et al., 2015) and they correlated with the deposition of Aβ (Iwahara et al., 2017). Additionally, accumulation of Aβ in postmortem human brains and rodent models of AD was identified as the cause of deficiencies in insulin signaling (Bomfim et al., 2012). Conditional deletion of *Socs3* promotes cell survival and axon regeneration in retinal ganglion cells upon optic nerve injury through a gp130-dependent pathway. It was shown that in *Socs3*-deleted RGCs mTOR levels quickly increase upon injury in contrast to the control cells, enhancing axonal growth (Smith et al., 2009)

YPEL1 (Yippee Like 1) belongs to the large family of YPEL genes and it has subcellular localization in association with centrosome, therefore it had been proposed that it is a component of cell division machinery (Hosono et al., 2004). Furthermore, in humans *YPEL1* is found at chromosome 22q11.2, in a genome region that is connected with various symptoms that comprise malformation of the craniofacial complex. It is also expressed in the ventral half of early embryos and it is implicated in face formation (Farlie et al., 2001). More recently *Ypel1* expression was shown to be controlled by BMP signaling and its overexpression leads to abnormal morphogenesis due to enhanced apoptosis (Tan et al., 2015).

MAP2K6 (Mitogen-Activated Protein Kinase 6) or *MKK6* (MAP kinase kinase 6) belongs to the dual specificity protein kinase family and acts as a mitogen-activated

protein (MAP) kinase kinase (Moriguchi et al., 1996, Raingeaud et al., 1996). It activates p38 MAP kinase upon inflammatory cytokines or environmental stress (Han et al., 1996). The p38 MAPK pathway was shown to be dysregulated in AD and it plays an important role in disease pathogenesis. *MAP2K6* was increased in hippocampal and cortex tissue from AD patients, while phospho-MAP2K6 was specifically localized in neurofibrillary tangles, senile plagues, neuropil threads and granual structures, i.e. the pathological alterations (Zhu et al., 2001). Interestingly activation of p38 by MAP2K6 cause phosphorylation of tau at particular sites and it co-immunoprecipitates with phosphorylated tau in hippocampal extracts from AD patients. The model proposed is that MAP2K6 and p38 are recruited to tau and together lead to the phosphorylation of C-terminal tau epitopes that are a hallmark of AD (Peel et al., 2004). On the same direction another study described that under high β-Amyloid levels MAP2K6 led to increased ROS production and apoptotic cell death (Bashir et al., 2014). Notably knockdown of MAPK11 which is activated by MAP2K6 significantly reduced *Htt* mRNA in mouse striatal HD cells and reduces disease-relevant behavioral phenotypes in a knockin HD mouse model (Yu et al., 2017).

PDZD2 (PDZ domain-containing protein 2) contains PDZ domains that bind to the C-termini of transmembrane receptors and ion channels. They can also bind to other proteins that contain PDZ domains and are involved in intracellular signaling (Lee and Zheng, 2010, Harris and Lim, 2001). *Pdzd2* is expressed in large and small diameter sensory neurons and its binding to the sensory neuron-specific TTX-resistant sodium channel Na$_V$1.8 is indispensable for the functional expression of Na$_V$1.8 current in DRG neurons (Shao et al., 2009).

UNC5B (UNC-5 Netrin Receptor B) is a member of the dependence receptor family. It is a single pass transmembrane protein that is composed of an extracellular region, a transmembrane region and a cytoplasmic region. UNC5B signaling is implicated in a wide range of different functions (Bhat et al., 2019). It promotes cell death in the absence of its ligand-Netrin-1 (NTN1) and the presence of its ligands leads to cell survival (Llambi et al., 2001). NTN1 acts a survival cue during the development of the nervous system through binding to UNC5B which initiates PI3K cascade which blocks apoptosis (Tang et al., 2008). Notably overexpression of *Unc5b* in wild type (WT) MGE interferes with the interneuron migration to the cortex, and reduction of *Unc5b* levels rescue the migration deficit in *Sip1* (SMAD Interacting Protein) mutant interneurons

(van den Berghe et al., 2013). *KLHL29* (Kelch Like Family Member 29) is a protein coding gene that belongs to the Kelch-like (KLHL) family with no known function. The members of this family contain a BTP/POZ domain, a BACK domain and 5-6 Kelch motifs (Dhanoa et al., 2013). The BTP/POZ domain is named after the amino acids motifs that comprise it (Zollman et al., 1994, Bardwell and Treisman, 1994) and it is known to facilitate protein binding (Albagli et al., 1995). Kelch-containing proteins are involved in extracellular communication and cell morphology (Adams et al., 2000). The BACK domain is a 130-residue region, whose mutations are known to cause disease in humans (Bomont et al., 2000, Liang et al., 2004).

SIAH3 (Seven in Absentia Homolog 3) or Siah E3 Ubiquitin Protein Ligase Family Member 3 is localized in mitochondria and it inhibits PINK1 (PTEN-induced kinase 1) accumulation in damaged mitochondria (Hasson et al., 2013).

PCSK2 (Proprotein Convertase Subtisilin/Kexin Type 2) or Neuroendocrine Convertase 2 (*NEC2*) is a member of the subtisilin-like proprotein convertase family and upon cleavage of the proregion it generates PC2 (Muller and Lindberg, 1999). *Pc2* is necessary for the first step of maturation of several neuroendocrine peptides from their precursors , for example the conversion of proinsulin to insulin intermediates (Smeekens et al., 1992) and the first step of glucagon biosynthesis (Rouille et al., 1994). Interestingly the brain and stomach of genetically obese or diet-induced mice were shown to contain significantly higher *Pcsk2* mRNA than the controls, while *Pcsk2*$^{-/-}$ mice weighted less than the wild type and were resistant to diet-induced obesity. Thus *Pcsk2* is implicated in body mass gain via the different regulatory peptides that it generates (Anini et al., 2010). In line with this a causal link between some SNPs of *PCSK2* in a Chinese cohort and diabetes was described (Chang et al., 2015).

GALR1 (Galanin Receptor 1) is one of the three-transmembrane proteins that bind the neuropeptide galanin (Habert-Ortoli et al., 1994) which interact with G-protein coupled receptors and has been implicated in various functions such as the regulation of sleep, energy metabolism and as a growth factor in the pituitary glands (Mechenthaler, 2008). (Mechenthaler, 2008). *Galr1*$^{-/-}$ mice are viable but present lower circulating levels of IGF-1 (insulin-like growth factor-I) and suffer from spontaneous tonic-clonic seizures indicating a role of *Galr1* in neuroendocrine regulation (Jacoby et al., 2002). Both *Galanin* and *Galr1* are expressed in the brain and highly expressed in the

noradrenergic neurons of the locus coeruleus (LC) (Williams et al., 2001) and *Galr1* is upregulated in a cyclic AMP-dependent manner (Hawes et al., 2005). Notably inhibition of *Galr1* with siRNA injected in the bilateral Prefrontal Cortex (PFC) improves the depressive-like behavior in postpartum depressed (PPD) rats and reversed the downregulation of CREB-BDNF signaling and 5-HT levels in the PFC of PPD rats (Li et al., 2018). In line with this *Galr1* mRNA levels were found to be increased in the ventral periaqueductal gray (vPAG) of rats exposed to chronic mild stress (CMS), a rodent model of depression and knocking down *Galr1* in the vPAG eliminated the depression-like behavior (Wang et al., 2016).

GPR179 (G Protein-Coupled Receptor 179) is a transmembrane protein with large extracellular segments that contain an EGF-like Ca^{2+} binding domain and a leucine repeat sequence (Orlandi et al., 2012) and it has been involved in autosomal-recessive complete congenital stationary night blindness (CSNB) as various mutations in *GPR179* in patients with CSNB were established as the cause of the disease. Additionally, GPR179 was highly concentrated in horizontal cells and Muller cell endfeet (Audo et al., 2012, Peachey et al., 2012). Another study found that *Grp179* is expressed in the inner nuclear layer of the retina and the protein is located at the dendritic tips of ON-bipolar cells in the retina, while the CNSB phenotype occurs due to the mislocalization of GPR179 (Orhan et al., 2013). The mechanism behind *Gpr179* role in vision was unraveled by a publication which demonstrated that GPR179 forms coimmunoprecipitates with mGluR6 and TRRM1 *in vivo*, and the formation of these macromolecular complexes are essential for the signal transduction of mGluR6 singlaling cascade (Orlandi et al., 2013). A recent study established GPR179 as direct binding partners of HSPGs (heparan sulfate proteoglycan) in the nervous system. HSPGs are a family of extracellular matrix proteins that are present in the synaptic cleft and are key players in the formation and maintenance of synaptic contacts. Furthermore, Pikachurin a member of the HSPGs interact with GRP179 in photoreceptor synapses and knockout of *Pikachurin* in mice impaired the post synaptic targeting of GRP179 subsequently affecting the function of photoreceptor synapses (Orlandi et al., 2018).

CDH20 (Cadherin 20) is a type II cadherin belonging to the cadherin superfamily and it is a calcium dependent cell-cell adhesion glycoprotein that contains five extracellular cadherin (EC) repeats, a transmembrane region and a highly conserved cytoplasmatic

tail (Kools et al., 2000). In rats *cad20* mRNA was expressed in the anterior neural region and rhombomere 2 in the early neural plate and later in the ventral cells of the hindbrain (Takahashi and Osumi, 2008).

ROR1 (Receptor Tyrosine Kinase Like Orphan Receptor 1) or *NTRKR1* (Neurotrophic Tyrosine Kinase receptor related 1) contain one extracellular Frizzled-like cysteine-rich domain and membrane proximal kringle domains and it was detected in the anterior part of day E7.5 mice embryos (Matsuda et al., 2001). Interestingly, ROR1 and its ligand Wnt5a were shown to be highly expressed in neocortical neural progenitor cells (NPCs) and siRNA suppression of *Ror1* or *Wnt5a* in NPCs isolated from embryonic neocortex led to the reduction of βIII-tubulin-positive neurons that were generated from NPCs and increased the proportion of GFAP-positive cells. The same study demonstrated that Wnt5a-Ror1 pathway act through DVL2 phosphorylation in a β-catenin independent manner in NPCs. Additionally, *Ror1* expression in the NPCs within the neocortical VZ *in vivo* was shown to be indispensable for the maintenance of the progenitors in the undifferentiated states, as miRNA against *Ror1* led to differentiation of progenitors to neurons, while forced expression of *Ror1* increased the proportion of Pax6-positive NPCs. Therefore, Wnt5a-Ror1 signaling pathway has a key role in maintaining proliferative NPCs during neurogenesis of the developing neocortex (Endo et al., 2012). Notably expression of *Ror1* was shown to be involved in glioblastoma stem cell maintenance and silencing of *Ror1* led to down-regulation of EMT (epithelial-mesenchymal transition) and reduced the migration and invasion in glioblastoma stem cells (Jung et al., 2016).

HUNK (Hormonally Up-Regulated Neu-Associated Kinase) is a protein kinase closely related to the SNF1 family of serine/threonine kinases (Gardner et al., 2000). It has to be noted that HUNK was found to promote cell survival in the mammary gland and regulate *myc* expression in a kinase-dependent manner through Akt signaling and to be required for PIEK-Akt-induced mammary tumorigenesis. Indeed, mammary tumor development was significantly delayed in Hunk$^{-/-}$ mice (Yeh et al., 2013). In line with this *HUNK* was shown to be overexpressed in aggressive subsets of human primary cancers of the colon and ovary as well as breast cancer while its overexpression was associated with metastasis of human breast cancers (Wertheim et al., 2009).

UST (Uronyl 2-Sulfotransferase) transfers sulfate to the 2-position of uronyl residues (Kobayashi et al., 1999) and it is involved in neuronal migration in the cerebral cortex. Indeed, *Ust* knockdown using in utero electroporation caused impaired migration of cortical neurons and accumulation of neurons in the lower intermediate zone (Ishii and Maeda, 2008). Interestingly knockdown of *UST* in human melanoma cells impaired melanoma cell migration and adhesion (Nikolovska et al., 2017). *VSTM2A-OT1* is a non-coding RNA of unknown function.

gene symbol	gene name	Ensembl gene	Fold Change	pvalue	padj
KLF11	Kruppel like factor 11	ENSG00000172059	-3.497443754	3.87E-114	7.11E-111
PDZRN3	PDZ domain containing ring finger 3	ENSG00000121440	-3.330307939	1.2E-101	1.44E-98
STK32A	serine/threonine kinase 32A	ENSG00000169302	-3.411414215	4.54E-88	3.88E-85
WNT7B	Wnt family member 7B	ENSG00000188064	-4.700267072	7.11E-87	5.48E-84
VSTM2A	V-set and transmembrane domain containing 2A	ENSG00000170419	-2.255341956	1.89E-81	1.29E-78
SOCS3	suppressor of cytokine signaling 3	ENSG00000184557	-3.750942483	5.54E-77	3.31E-74
YPEL1	yippee like 1	ENSG00000100027	-2.343097042	4.13E-74	2.29E-71
MAP2K6	mitogen-activated protein kinase kinase 6	ENSG00000108984	-4.755504559	1.36E-70	6.49E-68
PDZD2	PDZ domain containing 2	ENSG00000133401	-9.874405461	3.45E-70	1.59E-67
UNC5B	unc-5 netrin receptor B	ENSG00000107731	-4.547108273	4.96E-64	1.88E-61
KLHL29	kelch like family member 29	ENSG00000119771	-2.103209552	4.07E-60	1.39E-57
SIAH3	siah E3 ubiquitin protein ligase family member 3	ENSG00000215475	-2.751365816	1.27E-56	3.85E-54
PCSK2	proprotein convertase subtilisin/kexin type 2	ENSG00000125851	-2.609410639	1.76E-56	5.21E-54
GALR1	galanin receptor 1	ENSG00000166573	-5.617233442	1.41E-55	3.91E-53
GPR179	G protein-coupled receptor 179	ENSG00000277399	-5.114876928	6.19E-55	1.7E-52
CDH20	cadherin 20	ENSG00000101542	-2.951167305	1.45E-53	3.89E-51
ROR1	receptor tyrosine kinase like orphan receptor 1	ENSG00000185483	-4.330264632	1.9E-53	5.05E-51
HUNK	hormonally up-regulated Neu-associated kinase	ENSG00000142149	-2.28361519	3.71E-52	9.52E-50
UST	uronyl 2-sulfotransferase	ENSG00000111962	-5.121842753	1.48E-51	3.69E-49
VSTM2A-OT1	VSTM2A overlapping transcript 1	ENSG00000224223	-3.481258954	4.52E-51	1.1E-48

Table 5.3 List of 20 most downregulated genes across the 3 treatments with BDNF, AB85 and NT4 and the 4 time-points 30 minutes, 2 hours, 12 hours and 24 hours sorted by adjusted p value

Figure 5.13 *Top 20 downregulated genes after 30 minutes (A-C) and 2 hours (D-F), selected by the statistical significance of the change in their transcription levels across the 4 time-points analyzed. Log2FC in the X axis represent log2 fold of change.*

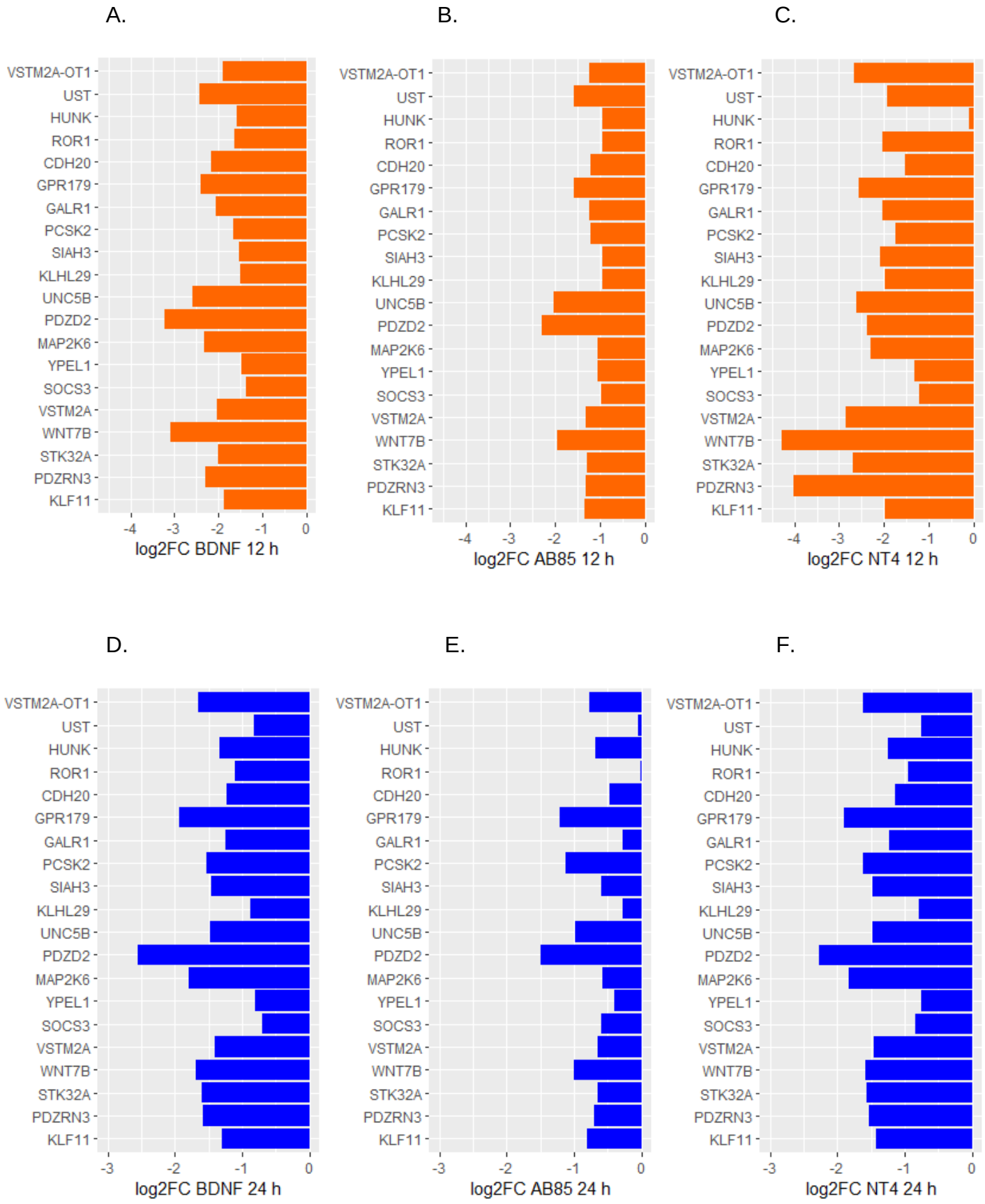

Figure 5.14 *Top 20 downregulated genes after 12 hours (A-C) and 24 hours (D-F), selected by the statistical significance of the change in their transcription levels across the 4 time-points analyzed Log2FC in the X axis represent log2 fold of change.*

5.4.5 Volcano plots comparing differentially regulated genes between TrkB ligands and controls

Volcano plots offer an informative way of visualizing the RNA-seq results. This type of plot is used to visualize changes in large datasets. A volcano plot is a scatterplot that has the –log 2 - fold change values for all genes on the horizontal (x) axis, and the –log 10- transformed p- value on the vertical (y) axis. Each dot corresponds to one gene. The scale of x and y axes is logarithmic in order to represent the whole population within a smaller space. It is named after a volcano, because it resembles a volcano that is erupting. The volcano plots presented in this Thesis were generated using R studio and the function res.

In order to determine the genes that are of statistical significance the p adjusted value was used instead of p value in order to avoid as much as possible the inclusion of false positives, i.e., genes that appear to be differentially expressed when they are not statistically significant. The threshold for the significant genes of interest was set to padj-value<0.01 and |log2 fold change| >1 or |fold change > 2. These genes appear as green dots. The non-significant genes are marked with three different colours. Black color marks the genes with p adjusted value >0.01 and |log2foldchange|<1. Red color marks the genes with p adjusted value <0.01 and |log2foldchange|<1. Orange color marks the genes with p adjusted value > 0.01 and |log2foldchange|>1. Plotting genes in this way results in two regions of interest in the plot: the top left and top right side, where the dots corresponding to either significantly downregulated or upregulated genes and low p-values are displayed.

Initially the control cultures have been compared to the cultures that were treated with one of the three TrkB ligands. After 30 minutes of treatment only few genes are differentially expressed after treatment with BDNF, AB85 or NT4. Interestingly the expression pattern is quite similar with all ligands (Figure 5.15 A-C). Upon treatment with BDNF 57 genes are upregulated and 4 genes are downregulated, whereas 59 genes are upregulated upon treatment with AB85 and 66 genes are upregulated upon treatment with NT4. Most of the genes expressed by the neurons are below the significance threshold for p-value and log2 fold change, whereas few genes are above the significance threshold for p-value but are below the significance threshold for log2

fold change and are colored with red. The genes that are above the significance threshold for log2 fold change and below the significance threshold for p-value are colored with orange (Figure 5.15 A-C). At the time-point of 2 hours many more genes appear to be differentially expressed. There are 1011 that are upregulated upon treatment with BDNF and 716 that are downregulated, 903 genes that are upregulated upon treatment with AB85 and 778 genes that are downregulated, 1026 genes that are upregulated upon treatment with NT4 and 663 genes are downregulated. It is also clear that the gene expression patterns observed in the three volcano plots at this time-point are very similar (Figure 5.16 A-C). After 12 hours the number of upregulated genes is decreased for all three ligands, when compared to time-point 2 hours, whereas the number of downregulated genes is increased for BDNF and NT4 (Figure 5.17 A-C)**.** More specifically there are 684 genes that are upregulated upon treatment with BDNF and 1052 that are downregulated, 458 genes that are upregulated upon treatment with AB85 and 700 genes that are downregulated, 932 genes that are upregulated upon treatment with NT4 and 1375 genes that are downregulated. The volcano plots for the time-point of 24 hours indicate that treatment with BDNF and NT4 led to differential expression of about the same number of genes, whereas treatment with AB85 changed the expression of smaller number of genes (Figure 5.18 A-C). Additionally, after 24 hours the number of both upregulated and downregulated genes is decreased in comparison to the time-point of 12 hours. In cultures treated with BDNF for 24 hours the number of upregulated genes is slightly reduced to 615 whereas the number of downregulated genes is reduced to about half (533 genes). The number of genes upregulated by AB85 is reduced to 293 when compared to 12 hours, and it is interesting that the number of downregulated genes is reduced to 109 from 700 genes in 12 hours. Additionally, the number of genes upregulated by NT4 at 24 hours is 590 and the number of downregulated genes is sharply decreased to 440 from 1375 at time-point 12 hours.

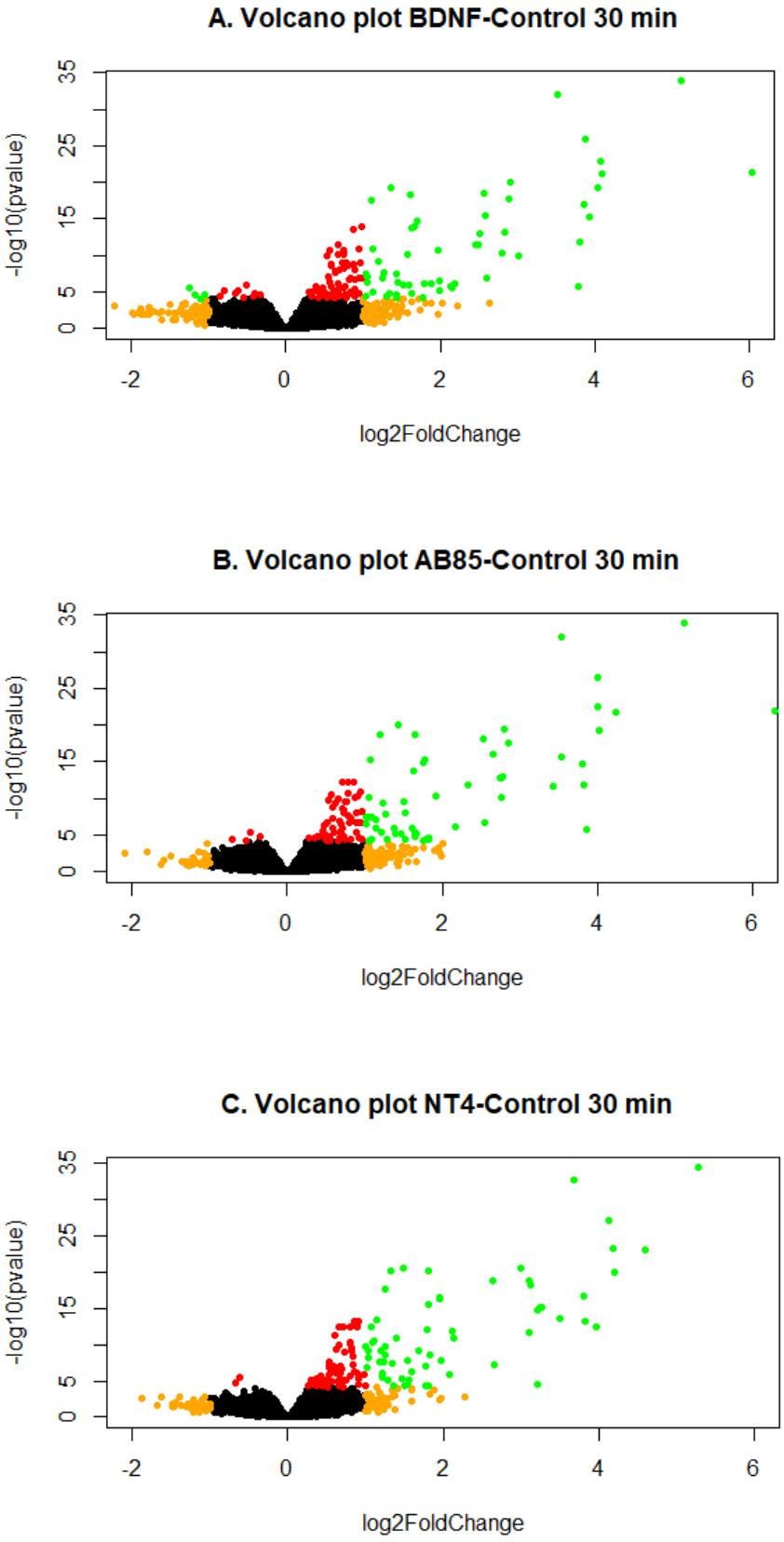

Figure 5.15: *Volcano plot (scatterplot) comparing the three TrkB ligands BDNF (A), AB85 (B) and NT4 (C) with untreated (control cultures) at time-point 30 minutes*

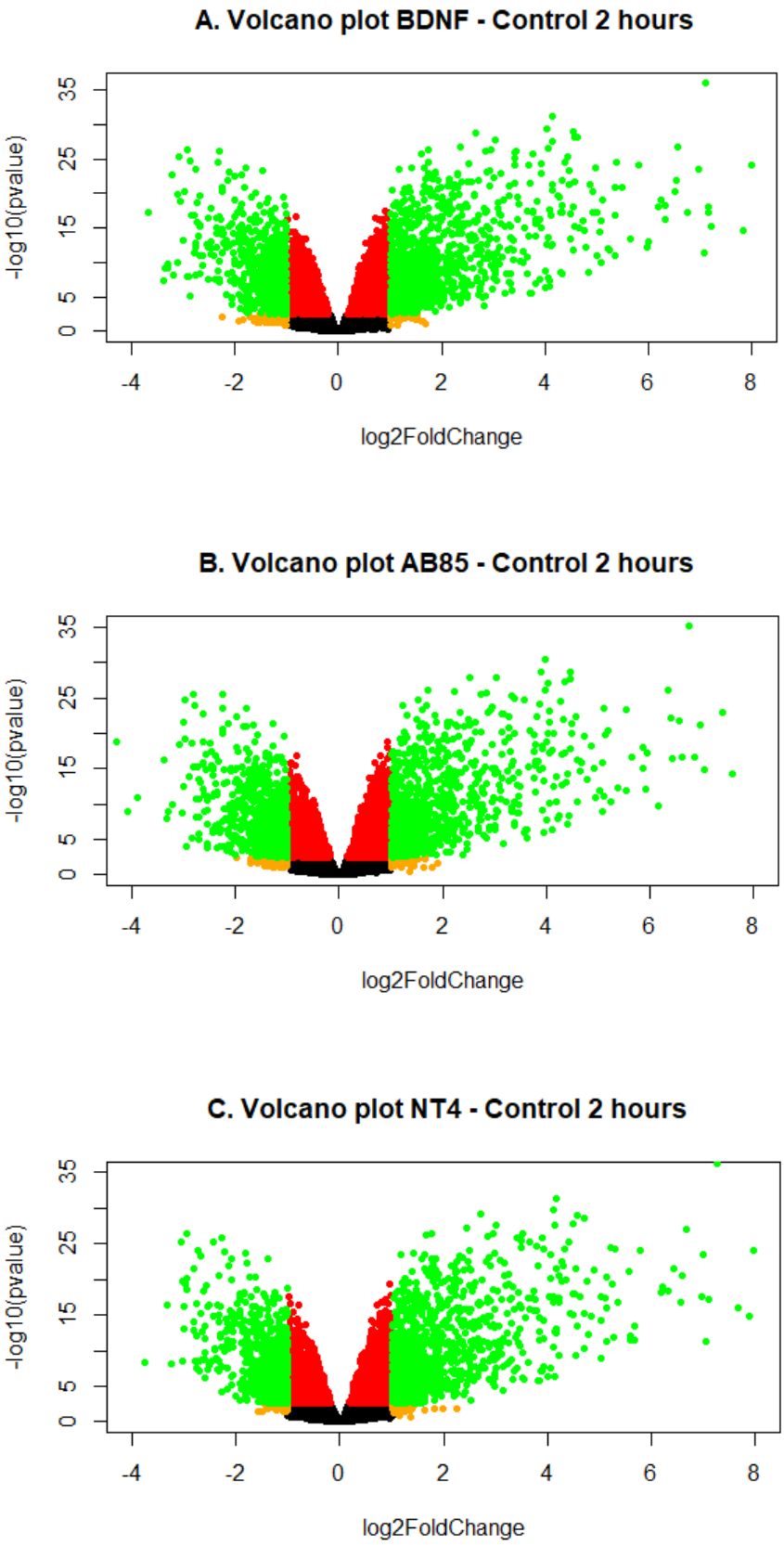

Figure 5.16: Volcano plot (scatterplot) comparing the three TrkB ligands BDNF (A), AB85 (B) and NT4 (C) with untreated (control cultures) at time-point 2 hours.

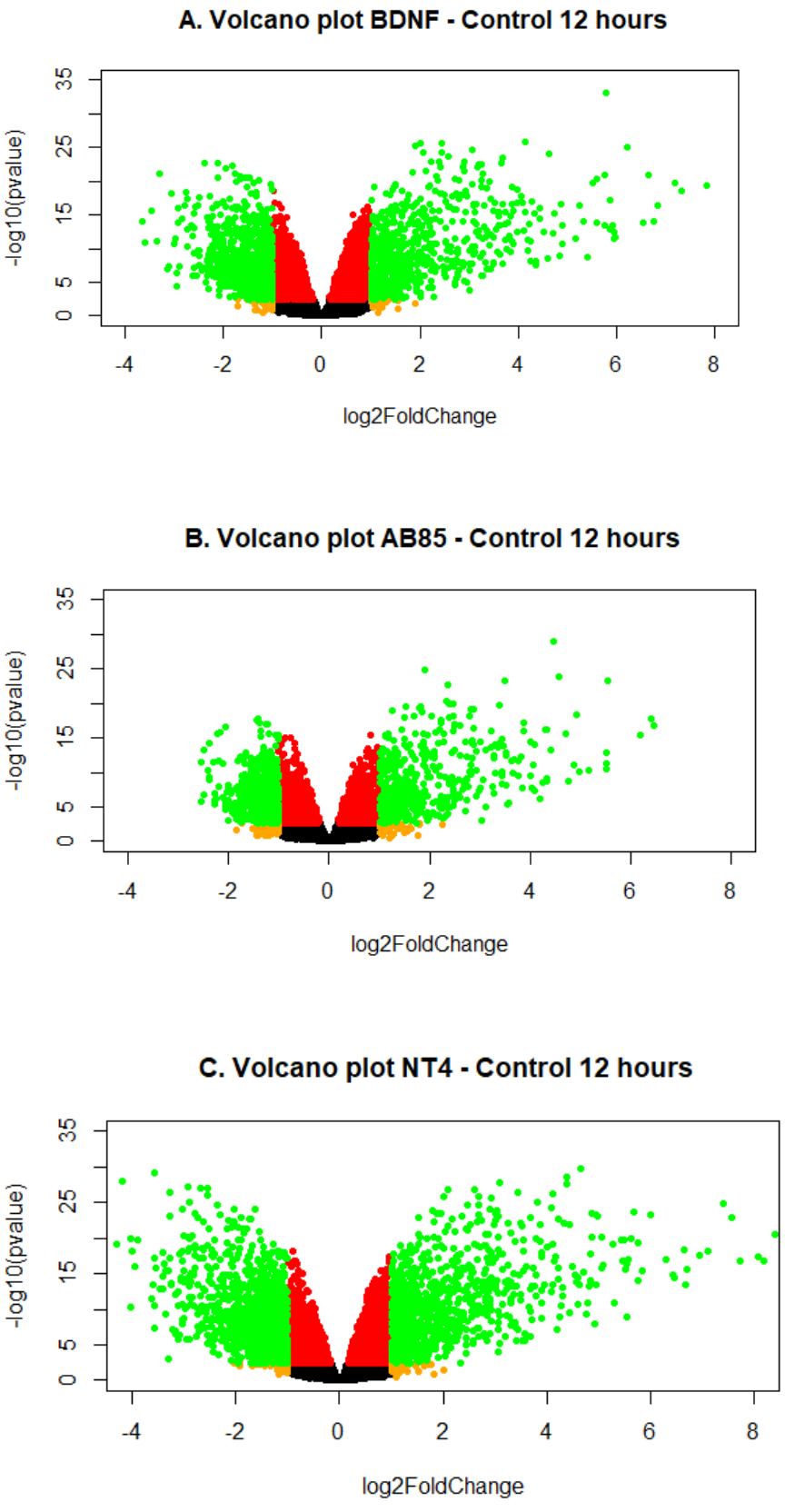

Figure 5.17: *Volcano plot (scatterplot) comparing the three TrkB ligands BDNF (A), AB85 (B) and NT4 (C) with untreated (control cultures) at time-point 12 hours*.

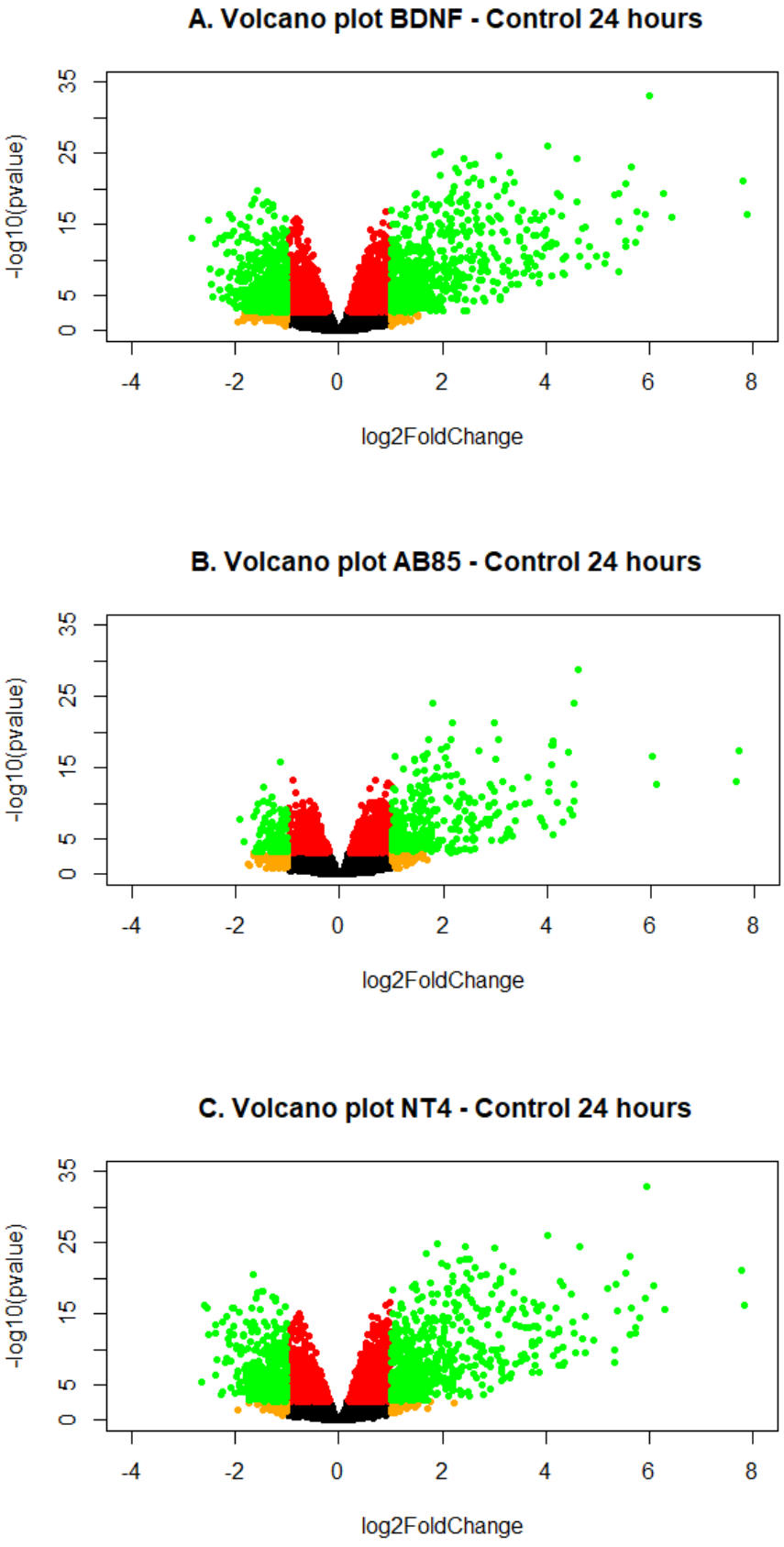

Figure 5.18: *Volcano plot (scatterplot) comparing the three TrkB ligands BDNF (A), AB85 (B) and NT4 (C) with untreated (control cultures) at time-point 24 hours.*

Figure 5.15-5.18: Volcano plot (scatterplot) comparing the three TrkB ligands BDNF (A), AB85 (B) and NT4 (C) with untreated (control cultures) at time-points 30 minutes, 2hours, 12 hours and 24 hours. On the horizontal (x) axis it has the log2foldchange values for all genes and on the vertical (y) axis it has the –log10 transformed p-value. Each dot represents a gene. Black color marks the genes with p adjusted value >0.01 and |log2foldchange|<1. Red color marks the genes with p adjusted value <0.01 and |log2foldchange|<1. Orange color marks the genes with p adjusted value > 0.01 and |log2foldchange|>1. Green color marks the genes that are differentially expressed between the two conditions that are compared, with p adjusted value <0.01 and |log2foldchange|>1.

5.4.6 Interactive MD plots generated with Glimma package for pairwise comparisons between TrkB ligands and controls

While volcano plot mentioned above summarize results visually it is a static plot that could not offer information for single genes in cases where the total number of differentially expressed genes is in the scale of hundreds or even thousands. Using the Glimma package in R it is possible to extend the common static R plots generated with the limma package and allow individual genes to be searched over multiple data points. Glimma provides an interactive mean-different plot using the **glMDPlot** function. The output is an html page, with summarized results in the left panel (similar to the output of a static MD plot), and the right panel displays the log-CPM values for a selected gene from the different samples. A table of results is displayed below the plots and it includes information about the geneID, symbol, gene name, log-CPM and logFC values as well as the p-adjusted value for each observation. The interactive display allows the user to select any dot that correspond to one gene or search for any particular gene using the search function. The differentially expressed genes were selected based on p adjusted value < 0.01 and fold change <-2 for downregulated genes and fold change > 2 for upregulated genes. Grey color corresponds to genes that were not found to be statistically significant, while red corresponds to genes that were found to be upregulated and blue to genes that were found to be downregulated (Figure 5.19). The example plot presented in this figure is a print screen from the interactive plot from the pairwise comparison between cultures treated with AB85 for 2 hours versus the corresponding control. Here glimma plots for 12 pairwise comparisons between TrkB ligands in the 4 time-points versus the corresponding controls are presented.

The links below correspond to the interactive MD plot for the cultures treated with any of the three TrkB ligands in comparison with the controls. In order for the MD plot to be displayed the corresponding whole folder need to be downloaded and unzipped. Then the HTML document will present the interactive MD plot for each pairwise comparison.

Cultures treated with BDNF for 30 minutes

https://www.dropbox.com/sh/bnprahgqqrlrh0y/AAC8f7-OkP-JLVm23UxfuT8na?dl=0

Cultures treated with AB85 for 30 minutes

https://www.dropbox.com/sh/x4hyqgab853f7lo/AACg1IUyjOVjoH2UCkIXHx6wa?dl=0

Cultures treated with NT4 for 30 minutes

https://www.dropbox.com/sh/jjf23j729u6zxxm/AADEyL7XFBEGWX_9jhmp_GTla?dl=0

Cultures treated with BDNF for 2 hours:

https://www.dropbox.com/sh/2w7jz1gogcjp67i/AAD0wMnuPvYmMQtzshtCxGSja?dl=0

Cultures treated with AB85 for 2 hours:

https://www.dropbox.com/sh/gpo7hbbdds3glf4/AAAomrIPKmiMVTfUH4Zjr2b9a?dl=0

Cultures treated with NT4 for 2 hours:

https://www.dropbox.com/sh/7d3a6i5n998576g/AABzswBtnI7YbTlhyLRHn_Eya?dl=0

Cultures treated with BDNF for 12 hours

https://www.dropbox.com/sh/ljx32tkmsk96o7o/AACw3Nl_K0ej4vT7ltswc_tMa?dl=0

Cultures treated with AB85 for 12 hours

https://www.dropbox.com/sh/x8lsvioekxajb6q/AAALa9-tPV73km8JaV3QFFuqa?dl=0

Cultures treated with NT4 for 12 hours

https://www.dropbox.com/sh/u335ysz3zko1r5e/AACXnRO-R08Uh2JrFNf4SCdoa?dl=0

Cultures treated with BDNF for 24 hours

https://www.dropbox.com/sh/fe7qzqkb6hqq150/AAAz5vVbIiDgGFggsbDWgl_ja?dl=0

Cultures treated with AB85 for 24 hours

https://www.dropbox.com/sh/st24w94clo9wlrp/AAA5oYS6BAVhDpdES1NSEmLPa?dl=0

Cultures treated with NT4 for 24 hours

https://www.dropbox.com/sh/ky77t8qe4ux3ju3/AAC2JwP7xl1Qa16UseCdOE44a?dl=0

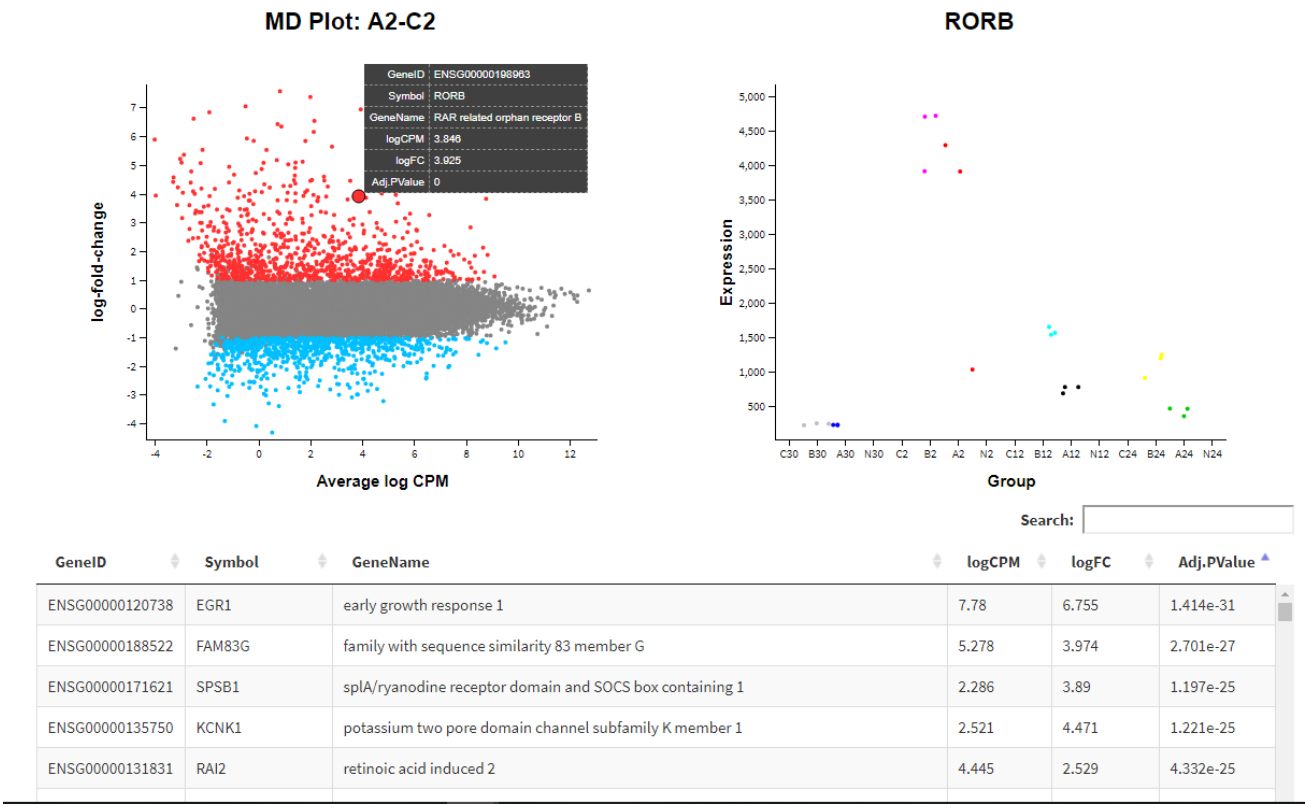

Figure 5.19: Interactive MD plot generated with the Glimma package of Bioconductor displaying all genes that are differentially expressed between AB85 (A2) and Control (C2) at time-point of 2 hours*. On the top left diagram, the genes are plotted against log 10-fold change and average log CPM, On the y axis there is log fold change of gene expression and on the x axis there is average log CPM (counts per million). Each dot corresponds to a single gene. Upregulated genes (fold change > 2 and padj < 0.01) are colored with red and downregulated genes are colored with blue (fold change < -2 and padj < 0.01), while genes that do not significantly change between the two conditions are colored with grey (|fold change| < 2 and padj > 0.01). By selecting a dot with the cursor a panel appears on the right displaying the changes in the expression of the particular gene (y axis) across the different conditions (x axis, group). It is also possible to search for any gene using the search function, which will return information for the GeneID, symbol of the gene, gene name, logCPM values, logFC (log Fold Change) and adj. P value.*

5.4.7 Volcano plots comparing differentially regulated genes between TrkB ligands

Subsequently volcano plots were used in order to compare the differential gene expression between the three TrkB ligands, and detect possible genes whose expression is uniquely (or preferentially) regulated by each of them. The threshold for the significant genes of interest was set to padj-value<0.01 and |log2 fold change| >1 or |fold change > 2. The positive log2fold change in each comparison corresponds to genes that are preferentially increased more than 2 fold by the ligand in the left side of the pair, for example BDNF in the comparison BDNF-AB85, whereas the negative log2fold change in each comparison corresponds to genes that are preferentially downregulated more than 2 fold by the ligand in the left side of the pair. However, some of the genes are selectively increased or downregulated only by one ligand and not the others in comparison to the control cultures. More details on these genes can be found in sections 5.4.15-5.4.18 and 5.4.21-5.4.24. The color code is the same as mentioned in 5.4.5. Whereas at the time-point 30 minutes there are few genes that are upregulated or downregulated with a |log2 fold change| more than 1, they are located below the p-value threshold of 0.01 (orange color) and they are therefore not significant. In the comparison of cultures treated with BDNF and AB85 there are only 5 such genes, whereas in the comparison of BDNF to NT4 there are 102 (71 upregulated with BDNF and 31 genes upregulated with NT4) such genes, but only 1 have a padj-value less than 0.05, MALAT1. Furthermore 79 genes (67 upregulated and 12 genes downregulated) with |fold change| > 2 and padj > 0.01 are present in the comparison of AB85 and NT4, and none of them has a padj-value less than 0.05. Overall, at the time-point 30 minutes there is no gene that is differentially expressed based on the significance threshold of padj vaule <0.01 and |fold change|>2 (Figure 5.20)

Similarly, to time-point 30 minutes, at time-point 2 hours there are few genes that are upregulated or downregulated more than 1, they are located below the p-value threshold of 0.01 (orange color) and they are therefore not significant. In the comparison of BDNF to AB85 there are 65 such genes (58 upregulated by BDNF and 7 upregulated with AB85), and there is also a gene with padj <0.01 but log2fold change

= 0.8 and it is colored with red, whereas in the comparison of BDNF to NT4 there are 22 such genes (12 upregulated with BDNF and 10 upregulated with NT4) and none of them has a padj <0.05. Furthermore 88 genes (26 upregulated with AB85 and 62 genes upregulated with NT4) with |fold change| > 2 and padj > 0.01 are present in the comparison of AB85 and NT4, and 40 of them has a padj-value less than 0.05. There is also one gene with padj-value < 0.01 and log2fold change = -0.87 which is colored with red (Figure 5.21).

At time-point 12 hours there are several genes that are differentially expressed and statistically significant between the three TrkB ligands. Between BDNF and AB85 there are 64 differentially expressed genes, 49 of them are upregulated with BDNF and 15 are upregulated with AB85. The number of differentially expressed genes between AB85 and NT4 is much higher as 360 genes are upregulated with AB85 and 406 genes are upregulated with NT4, a total of 766. Additionally, 1042 genes are differentially expressed between AB85 and NT4, with 499 genes upregulated by AB85 and 543 genes upregulated by NT4 (Figure 5.22).

The number of differentially expressed genes between BDNF, AB85 and NT4 is sharply decreased at time-point 24 hours. More specifically, between BDNF and AB85 there are 125 genes that are differentially expressed, with 114 genes upregulated with BDNF and 11 genes upregulated with AB85. There are no statistically significant genes that are differentially expressed between BDNF and NT4, but there are 40 genes with |log2 fold change| < 1 and p adj>0.01 colored with orange. Furthermore, there are 122 genes that are differentially expressed between AB85 and NT4, with 10 genes upregulated by AB85 and 112 genes upregulated by NT4 (Figure 5.23).

Therefore, it has been shown that there are no differences at the genes that are differentially expressed at the first two time-points upon treatment with any of the three TrkB ligands, whereas at time-point 12 hours there are several genes that differ between them. At time-point 24 hours the differences are located exclusively between AB85 and the other two TrkB ligands, as BDNF and NT4 express the same genes.

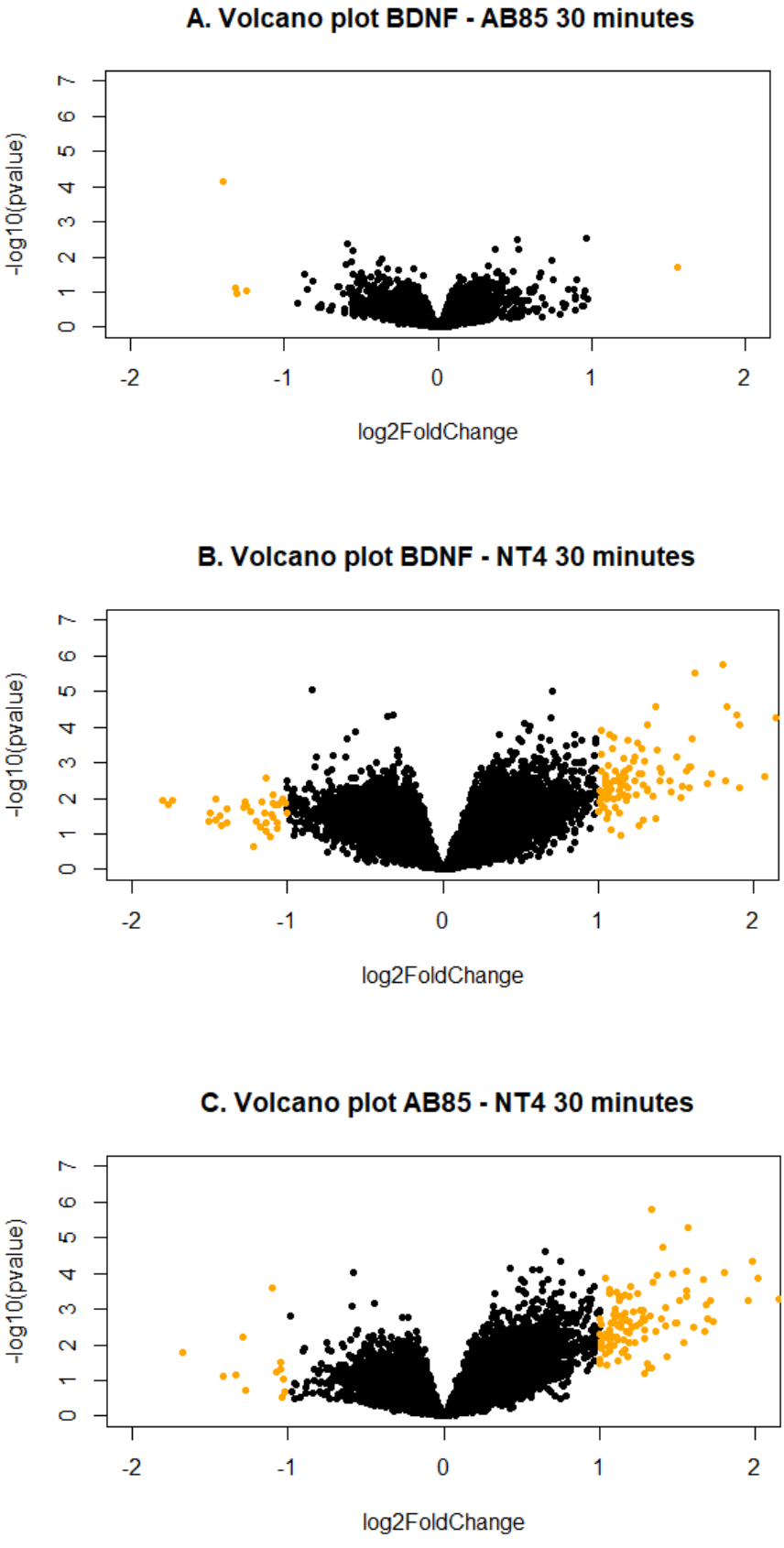

Figure 5.20: *Volcano plot (scatterplot) comparing the three TrkB ligands in pairwise comparisons, BDNF vs AB85 A), BDNF vs NT4 B), AB85 vs NT4 C), at time-point 30 minutes*

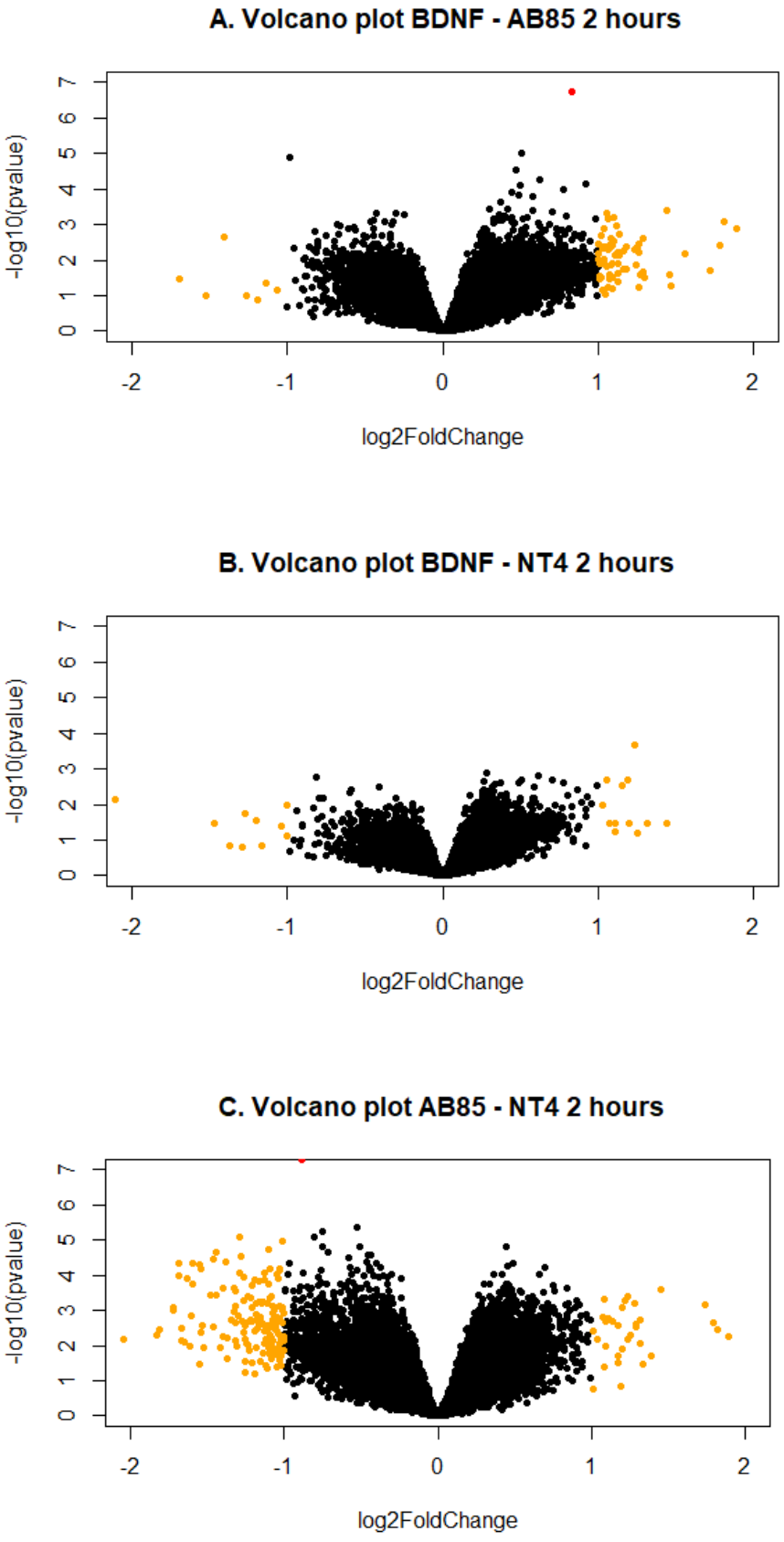

Figure 5.21: *Volcano plot (scatterplot) comparing the three TrkB ligands in pairwise comparisons, BDNF vs AB85 A), BDNF vs NT4 B), AB85 vs NT4 C), at time-point 2 hours*

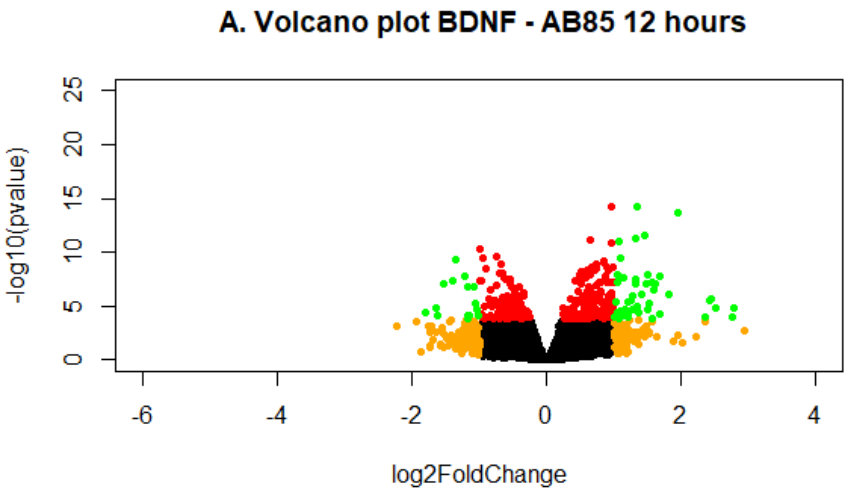

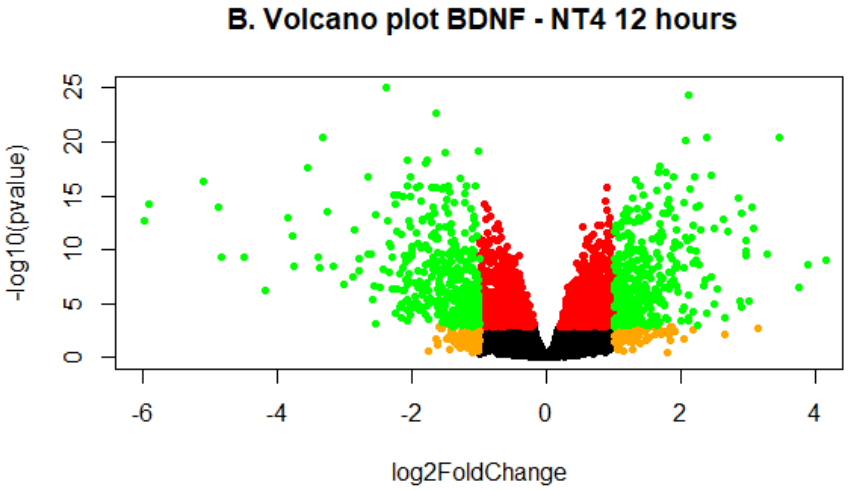

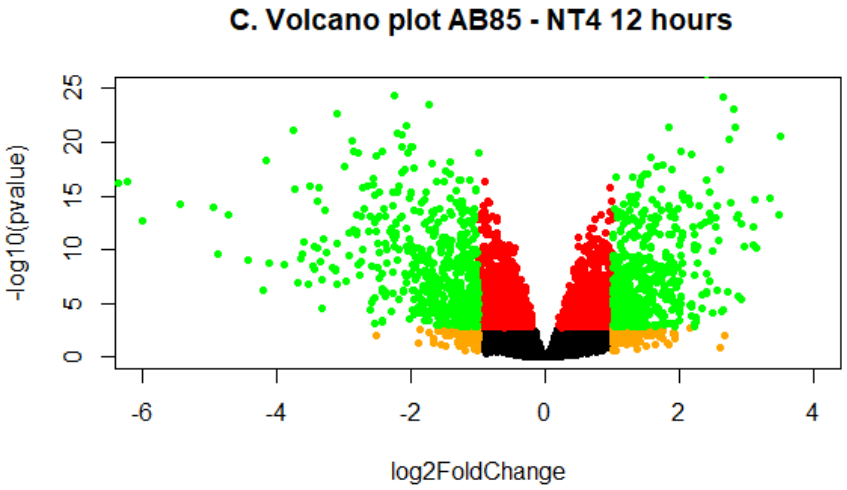

Figure 5.22: *Volcano plot (scatterplot) comparing the three TrkB ligands in pairwise comparisons, BDNF vs AB85 A), BDNF vs NT4 B), AB85 vs NT4 C), at time-point 12 hours*

A. Volcano plot BDNF - AB85 24 hours

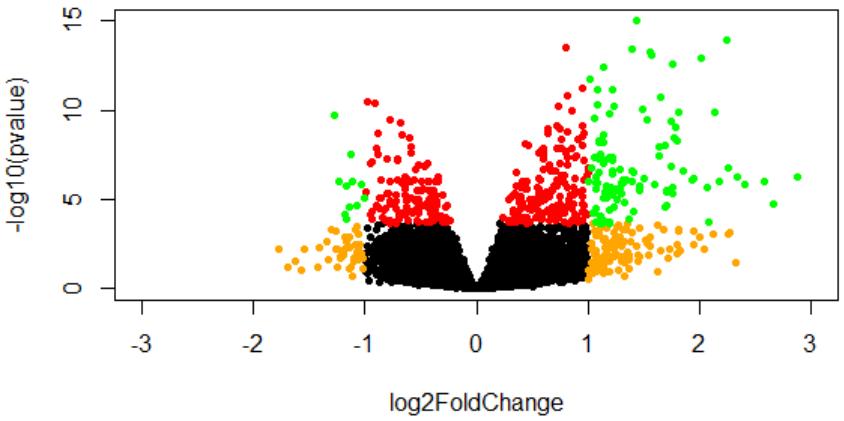

B. Volcano plot BDNF - NT4 24 hours

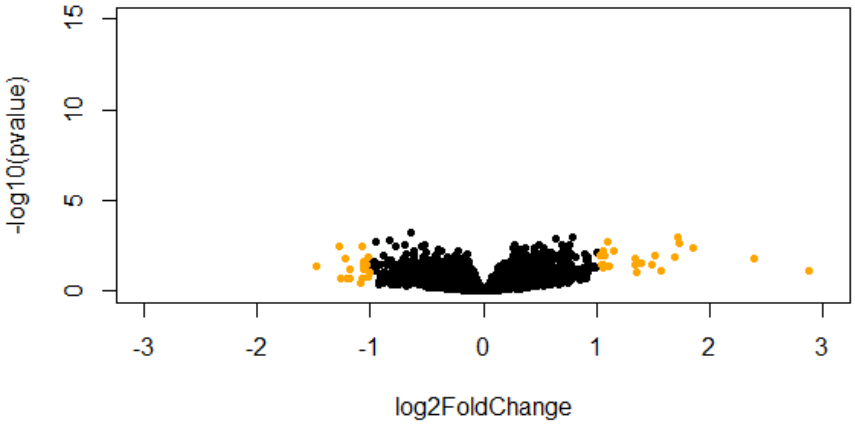

C. Volcano plot AB85 - NT4 24 hours

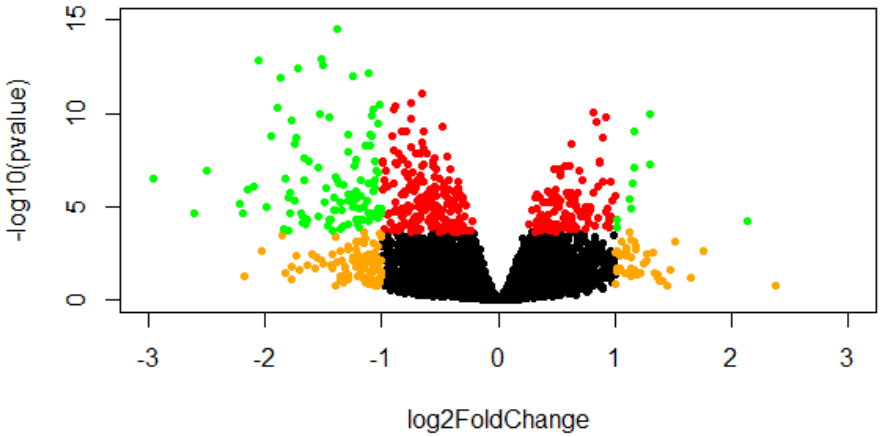

Figure 5.23: *Volcano plot (scatterplot) comparing the three TrkB ligands in pairwise comparisons, BDNF vs AB85 A), BDNF vs NT4 B), AB85 vs NT4 C), at time-point 24 hours*

Figure 5.20-5.23: Volcano plot (scatterplot) displaying pair-wise comparisons of the three TrkB ligands BDNF vs AB85 (A), AB85 (B) and NT4 (C) at time-points 30 minutes, 2hours, 12 hours and 24 hours. On the horizontal (x) axis it has the log2foldchange values for all genes and on the vertical (y) axis it has the –log10 transformed p-value. Each dot represents a gene. Black color marks the genes with p adjusted value >0.01 and |log2foldchange|<1. Red color marks the genes with p adjusted value <0.01 and |log2foldchange|<1. Orange color marks the genes with p adjusted value > 0.01 and |log2foldchange|>1. Green color marks the genes that are differentially expressed between the two conditions that are compared, with p adjusted value <0.01 and |log2foldchange|>1. Positive log2FoldChange values correspond to genes that are preferentially upregulated by the ligand in the left part of the pair (for example BDNF in BDNF-AB85), but also genes that are upregulated selectively by one ligand and not the other compared to the control cultures. Negative log2FoldChange values correspond to genes that are preferentially downregulated by the ligand in the left part of the pair, but also genes that are downregulated selectively by one ligand and not the other compared to the control cultures.

5.4.8 Interactive MD plots generated with Glimma package for pairwise comparisons between TrkB ligands.

Glimma provides an interactive mean-different plot using the **glMDPlot** function. The output is an html page, with summarized results in the left panel (similar to the output of a static MD plot), and the right panel displays the log-CPM values for a selected gene from the different samples. A table of results is displayed below the plots and it includes information about the geneID, symbol, gene name, log-CPM and logFC values as well as the p-adjusted value for each observation. The interactive display allows the user to select any dot that correspond to one gene or search for any particular gene using the search function. The differentially expressed genes were selected based on p adjusted value < 0.01 and fold change <-2 for genes that are downregulated more (compared to control cultures) by BDNF compared to AB85 and fold change > 2 for genes that are upregulated more (compared to control cultures) by BDNF compared to AB85. Grey color corresponds to genes that were not found to be statistically significant, while red corresponds to genes that were found to be upregulated and blue to genes that were found to be downregulated (Figure 5.24). The example plot presented in this figure is a print screen from the interactive plot from the pairwise comparison between cultures treated with BDNF for 24 hours versus the cultures treated with AB85 for 24 hours. As mentioned in the volcano plot section above only few genes are shown to be differentially expressed. Here glimma plots for 12 pairwise comparisons between TrkB ligands in the 4 time-points are presented.

The links below correspond to the interactive MD plot for the cultures treated with any of each of the TrkB ligands with the other TrkB ligands at each time point. In order for the MD plot to be displayed the corresponding whole folder need to be downloaded and unzipped. Then the HTML document will present the interactive MD plot for each pairwise comparison.

Cultures treated with BDNF versus cultures treated with AB85 for 30 minutes

https://www.dropbox.com/sh/oejfgldwlpjot9i/AABN25K-oIBa3344Fvz15Zm0a?dl=0

Cultures treated with BDNF versus cultures treated with NT4 for 30 minutes

https://www.dropbox.com/sh/xhyzbba7erpr5mq/AACE6F2DPIRdam6JYmlyNQqAa?dl=0

Cultures treated with AB85 versus cultures treated with NT4 for 30 minutes

https://www.dropbox.com/sh/tf1xz8icci4gpa6/AADNt9Z6SR859t9Zd9j4OqFLa?dl=0

Cultures treated with BDNF versus cultures treated with AB85 for 2 hours

https://www.dropbox.com/sh/1scqapgd703tcyi/AABypvSMd1byoJbZMt1M0XOaa?dl=0

Cultures treated with BDNF versus cultures treated with NT4 for 2 hours

https://www.dropbox.com/sh/qqr4yziaty4d9w0/AAAhVJuydnt6UQffRgAL63Sra?dl=0

Cultures treated with AB85 versus cultures treated with NT4 for 2 hours

https://www.dropbox.com/sh/35kkiasmyr9x21a/AAASTCOdM030yK-PiLziOLSta?dl=0

Cultures treated with BDNF versus cultures treated with AB85 for 12 hours

https://www.dropbox.com/sh/3b1d9fmtvfj9aa4/AACk5qKu9WFJsI8OXE_hjSv5a?dl=0

Cultures treated with BDNF versus cultures treated with NT4 for 12 hours

https://www.dropbox.com/sh/wctdwiobzbsq7dw/AACKFGNyDww-ugP_ZElKPoQEa?dl=0

Cultures treated with AB85 versus cultures treated with NT4 for 12 hours

https://www.dropbox.com/sh/pz66jztwq33suty/AACYlQluCfxMx7RQ0VK9NxVRa?dl=0

Cultures treated with BDNF versus cultures treated with AB85 for 24 hours

https://www.dropbox.com/sh/v6expc5rj0xxhcq/AACpg-WSfZk7c6S8xWxD4cDaa?dl=0

Cultures treated with BDNF versus cultures treated with NT4 for 24 hours

https://www.dropbox.com/sh/k7ysstowcbnpvu1/AAAgSNRu1Lh9_utO7hss8ihea?dl=0

Cultures treated with AB85 versus cultures treated with NT4 for 24 hours

https://www.dropbox.com/sh/rbhu2gj7mg5lwpp/AABUL7jI2y5lLmgwwkL-TgUba?dl=0

Search:

GeneID	Symbol	GeneName	logCPM	logFC	Adj.PValue
ENSG00000120738	EGR1	early growth response 1	7.78	1.428	2.001e-11
ENSG00000164949	GEM	GTP binding protein overexpressed in skeletal muscle	1.983	2.24	1.126e-10
ENSG00000135750	KCNK1	potassium two pore domain channel subfamily K member 1	2.52	1.391	1.951e-10
ENSG00000198648	STK39	serine/threonine kinase 39	5.025	0.7968	1.951e-10
ENSG00000107719	PALD1	phosphatase domain containing, paladin 1	1.862	1.55	2.349e-10

Figure 5.24: Interactive MD plot generated with the Glimma package of Bioconductor displaying all genes that are differentially expressed between BDNF (B24) and AB85 (A24) at time-point of 24 hours*. On the top left diagram, the genes are plotted against log 10-fold change and average log CPM, On the y axis there is log fold change of gene expression and on the x axis there is average log CPM (counts per million). Each dot corresponds to a single gene. Genes that are upregulated more (compared to control cultures) by BDNF compared to AB85 (fold change > 2 and padj < 0.01) are colored with red and genes that are upregulated more (compared to control cultures) by AB85 compared to BDNF are colored with blue (fold change < -2 and padj < 0.01), while genes that do not significantly change between the two conditions are colored with grey (|fold change| < 2 and padj > 0.01). By selecting a dot with the cursor, a panel appears on the right displaying the changes in the expression of the particular gene (y axis) across the different conditions (x axis, group). It is also possible to search for any gene using the search function, which will return information for the GeneID, symbol of the gene, gene name, logCPM values, logFC (log Fold Change) and adj. P value.*

5.4.9 Volcano plots comparing differentially regulated genes between TrkB ligands

Another point of the analysis included testing the genes that are differentially expressed by each TrkB ligand at the 4 time-points. Volcano plots for BDNF, AB85 and NT4 were constructed and the comparisons included cultures treated with the same TrkB ligand at successive time-points. In cultures treated with BDNF for 30 minutes or 2 hours important changes were noticed, as 1172 genes were found to be upregulated at 30 minutes, and 1115 genes were found to be upregulated at 2 hours (Figure 5.25 A). In cultures treated with BDNF for 2 hours or 12 hours 986 genes were found to be upregulated at 2 hours and 514 genes to be upregulated at 12 hours (Figure 5.25 B). Few changes were noticed in cultures treated with BDNF for 12 hours or 24 hours as 37 genes were found to be upregulated at 12 hours and 96 genes to be upregulated at 24 hours (Figure 5.25 C)

Similarly, to the cultures treated with BDNF, cultures treated with AB85 showed important changes in the number of genes expressed between time-points 30 minutes, 2 hours and 12 hours and fewer changes between cultures treated for 12 hours and 24 hours. More specifically, between cultures treated with AB85 for 30 minutes and 2 hours 1525 genes were upregulated at 30 minutes and 1108 genes were upregulated at 2 hours (Figure 5.26 A). Additionally, between cultures treated with AB85 for 2 hours and 12 hours 1023 genes were upregulated at 2 hours and 875 genes were upregulated at 12 hours (Figure 5.26 B). Between cultures treated with AB85 for 12 hours and 24 hours, 42 genes were upregulated at 12 hours and 65 genes were upregulated at 24 hours (Figure 5.26 C)

In contrast to cultures treated with BDNF and AB85, cultures treated with NT4 show changes in the number of genes differentially expressed between all 4 time-points. More specifically, between cultures treated with NT4 at 30 minutes and 2 hours, 850 genes were upregulated at 30 minutes and 1135 genes were upregulated at 2 hours (Figure 5.27 A). Additionally, between cultures treated with NT4 at 2 hours and 12 hours, 1194 genes were upregulated at 2 hours and 722 genes were upregulated at 12 hours (Figure 5.27 B). Between cultures treated with NT4 at 12 and 24 hours, 381 genes were upregulated at 12 hours and 607 genes were upregulated at 24 hours (Figure 5.27 C).

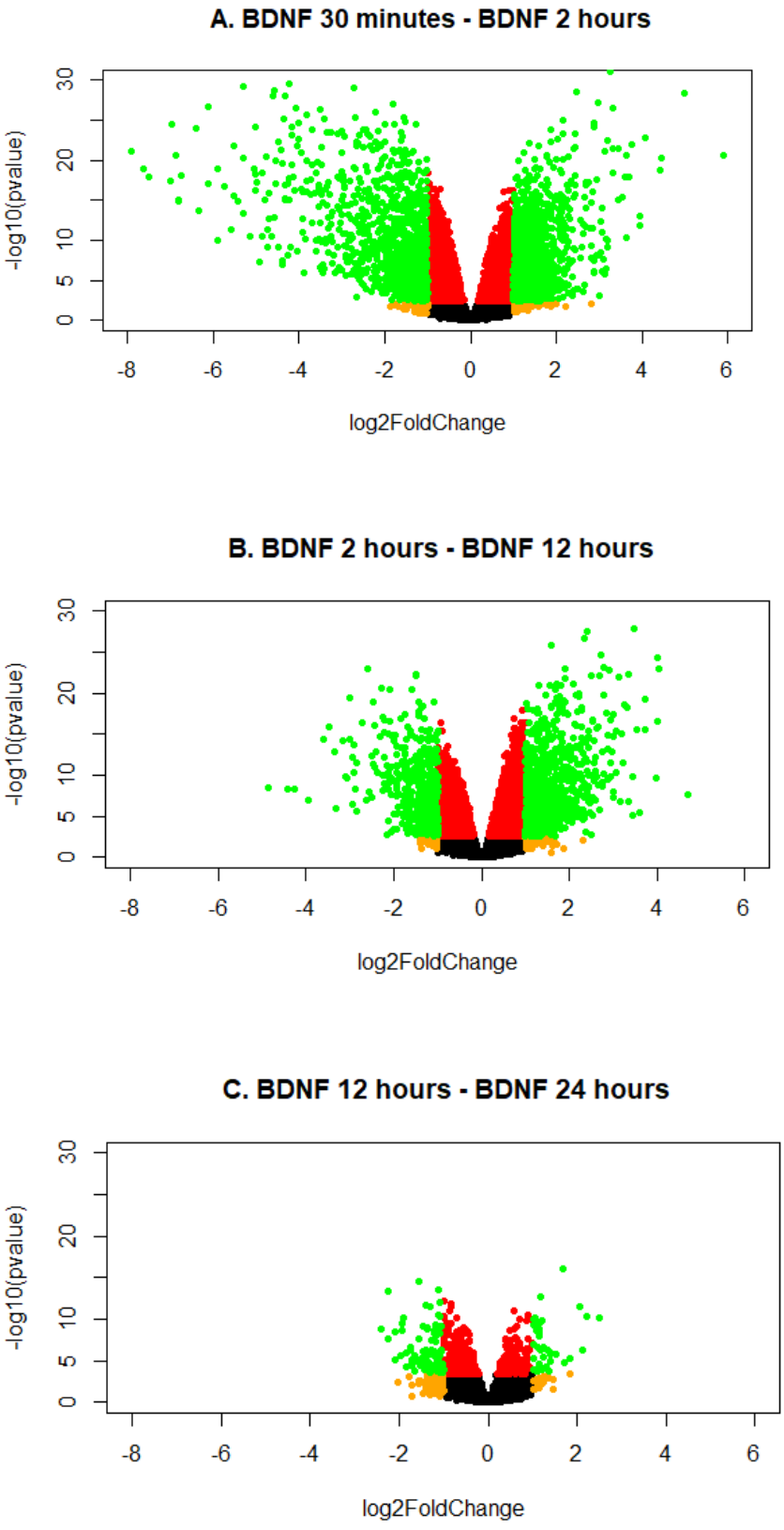

Figure 5.25: *Volcano plot (scatterplot) displaying pair-wise comparisons of cultures treated with BDNF at 4 timepoints (30 minutes, 2 hours, 12 hours and 24 hours).*

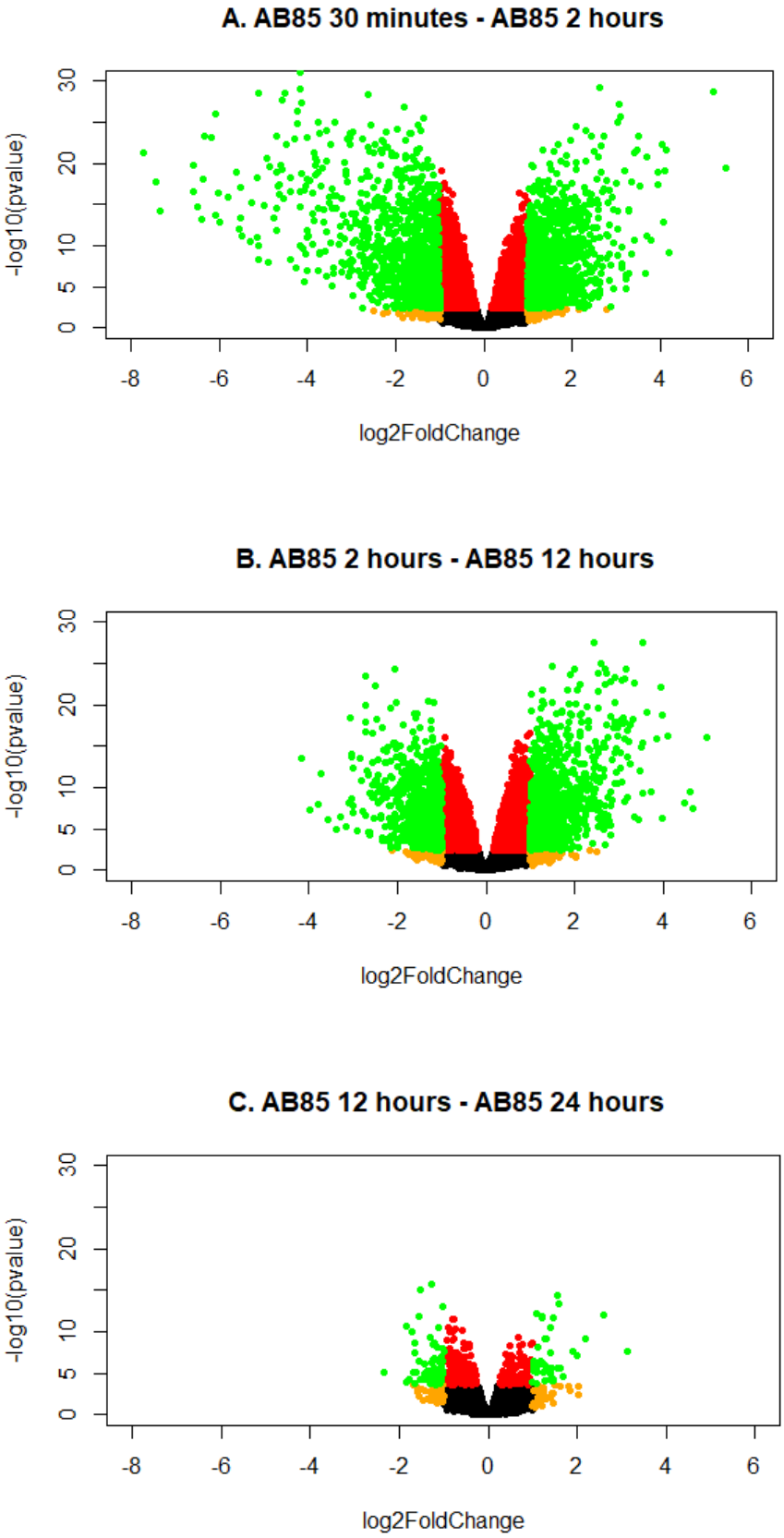

Figure 5.26: *Volcano plot (scatterplot) displaying pair-wise comparisons of cultures treated with AB85 at 4 timepoints (30 minutes, 2 hours, 12 hours and 24 hours).*

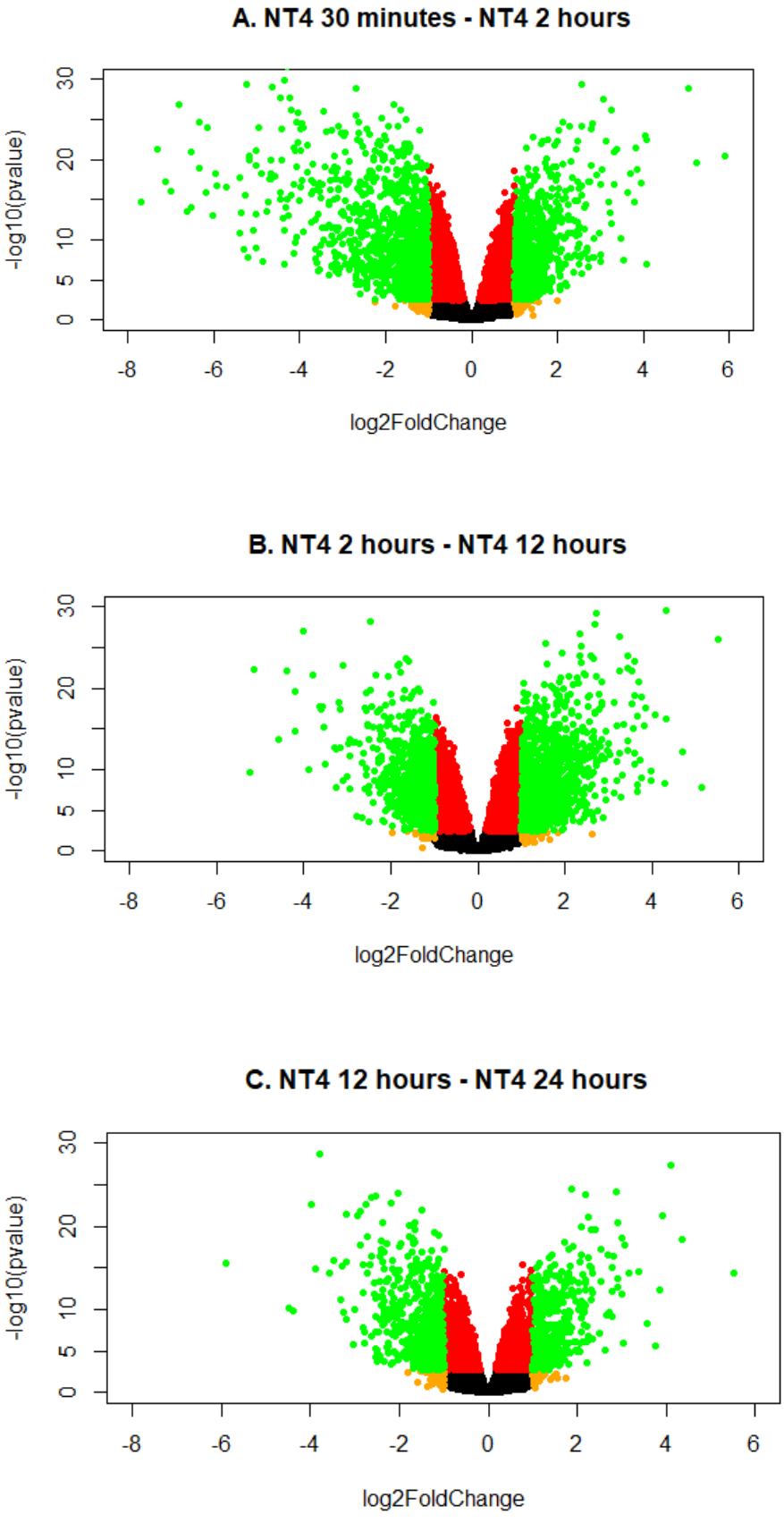

Figure 5.27: *Volcano plot (scatterplot) displaying pair-wise comparisons of cultures treated with NT4 at 4 timepoints (30 minutes, 2 hours, 12 hours and 24 hours).*

Figure 5.25-5.27: Volcano plot (scatterplot) displaying pair-wise comparisons of the time-points 30 minutes, 2hours, 12 hours and 24 hours for each one of the three TrkB ligands, BDNF, AB85 and NT4. On the horizontal (x) axis it has the log2foldchange values for all genes and on the vertical (y) axis it has the –log10 transformed p-value. Each dot represents a gene. Black color marks the genes with p adjusted value >0.01 and |log2foldchange|<1. Red color marks the genes with p adjusted value <0.01 and |log2foldchange|<1. Orange color marks the genes with p adjusted value > 0.01 and |log2foldchange|>1. Green color marks the genes that are differentially expressed between the two conditions that are compared, with p adjusted value <0.01 and |log2foldchange|>1.

5.4.10 Interactive MD plots generated with Glimma package for pairwise comparisons between TrkB ligands at the four timepoints.

Glimma provides an interactive mean-different plot using the **glMDPlot** function. The output is an html page, with summarized results in the left panel (similar to the output of a static MD plot), and the right panel displays the log-CPM values for a selected gene from the different samples. A table of results is displayed below the plots and it includes information about the geneID, symbol, gene name, log-CPM and logFC values as well as the p-adjusted value for each observation. The interactive display allows the user to select any dot that correspond to one gene or search for any particular gene using the search function. The differentially expressed genes were selected based on p adjusted value < 0.01 and fold change <-2 for downregulated genes and fold change > 2 for upregulated genes. Grey color corresponds to genes that were not found to be statistically significant, while red corresponds to genes that were found to be upregulated and blue to genes that were found to be downregulated (Figure 5.28). The example plot presented in this figure is a print screen from the interactive plot from the pairwise comparison between cultures treated with NT4 for 2 hours versus the cultures treated with NT4 for 12 hours. As mentioned in the volcano plot section above hundreds of genes are shown to differentially expressed. Here glimma plots for 12 pairwise comparisons between TrkB ligands in the 4 time-points versus the corresponding controls are presented.

The links below correspond to the interactive MD plot for the cultures treated with any of the three TrkB ligands in comparison with the controls. In order for the MD plot to be displayed the corresponding whole folder need to be downloaded and unzipped. Then the HTML document will present the interactive MD plot for each pairwise comparison.

Cultures treated with BDNF for 30 minutes versus cultures treated with BDNF for 2 hours

https://www.dropbox.com/sh/bxxlwsy4lbzxefu/AAAluy2n0P9n5WA_FLBuvNuRa?dl=0

Cultures treated with BDNF for 2 hours versus cultures treated with BDNF for 12 hours

https://www.dropbox.com/sh/vg0icq1nw0bywqk/AACW7FzEIlqQGZHQMkEdPGzUa?dl=0

Cultures treated with BDNF for 12 hours versus cultures treated with BDNF for 24 hours

https://www.dropbox.com/sh/m51u5novv7gjrsl/AAAjqVF9yqgSKArOgBsByxx_a?dl=0

Cultures treated with AB85 for 30 minutes versus cultures treated with AB85 for 2 hours

https://www.dropbox.com/sh/q0hxhqp2fmlm5b9/AAAehC-Y855klJD-QI1iFA8Ia?dl=0

Cultures treated with AB85 for 2 hours versus cultures treated with AB85 for 12 hours

https://www.dropbox.com/sh/c86xh0a1y6ci2ri/AAAbwFKW_U7no4IgbEKSLc-na?dl=0

Cultures treated with AB85 for 12 hours versus cultures treated with AB85 for 24 hours

https://www.dropbox.com/sh/ozpwhf352wxoevw/AADm7Dgh1S_K9oib_KQ0v4cha?dl=0

Cultures treated with NT4 for 30 minutes versus cultures treated with NT4 for 2 hours

https://www.dropbox.com/sh/tpiweemfzxkwonx/AACj6OuaPYQXkRQzW5Z_2Tm6a?dl=0

Cultures treated with NT4 for 2 hours versus cultures treated with NT4 for 12 hours

https://www.dropbox.com/sh/tfl1628x02f7r9g/AADBss-jDd5GvAglsDpqpctBa?dl=0

Cultures treated with NT4 for 12 hours versus cultures treated with NT4 for 24 hours

https://www.dropbox.com/sh/6nk58mpny0g3iyv/AACKRvvLqXgpdhF2N6nAREx-a?dl=0

.

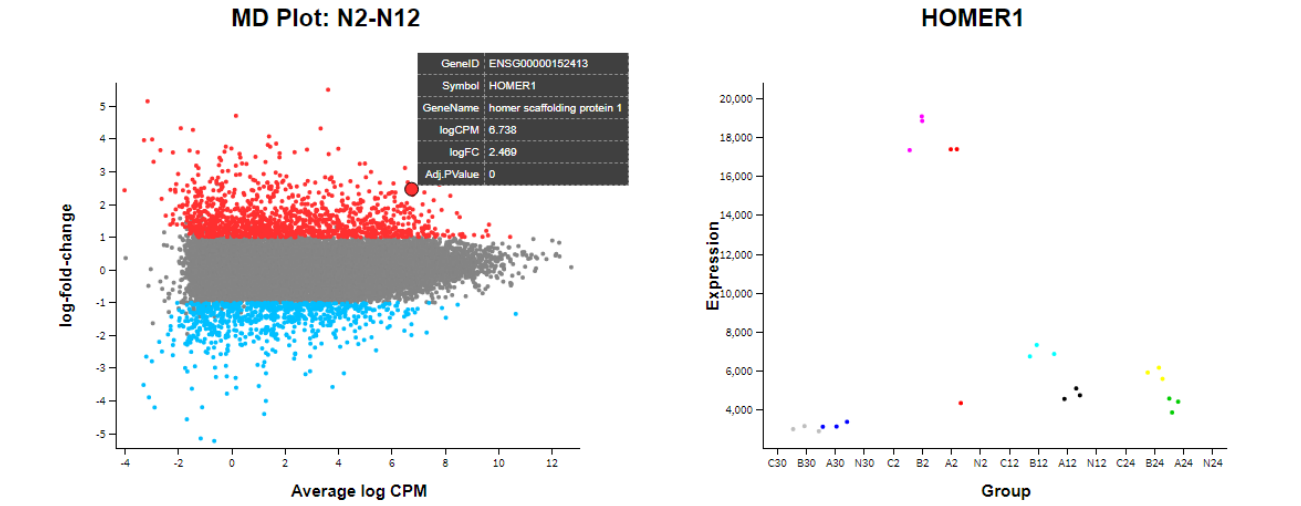

Search:

GeneID	Symbol	GeneName	logCPM	logFC	Adj.PValue
ENSG00000143858	SYT2	synaptotagmin 2	3.328	4.324	4.841e-26
ENSG00000131831	RAI2	retinoic acid induced 2	4.445	2.713	6.76e-26
ENSG00000152954	NRSN1	neurensin 1	5.405	-2.454	3.764e-25
ENSG00000149571	KIRREL3	kirre like nephrin family adhesion molecule 3	6.592	2.677	6.945e-25
ENSG00000144821	MYH15	myosin heavy chain 15	1.277	-3.998	3.052e-24

Figure 5.28: Interactive MD plot generated with the Glimma package of Bioconductor displaying all genes that are differentially expressed between cultures treated with NT4 for 2 (N2) and 12 hours (N12). *On the top left diagram, the genes are plotted against log 10-fold change and average log CPM, On the y axis there is log fold change of gene expression and on the x axis there is average log CPM (counts per million). Each dot corresponds to a single gene. Upregulated genes (fold change > 2 and padj < 0.01) are colored with red and correspond to genes that are upregulated by NT4 at 2 hours compared to NT4 at 12 hours and downregulated genes are colored with blue and correspond to genes that are downregulated by NT4 at 2 hours compared to NT4 at 12 hours (fold change < -2 and padj < 0.01), while genes that do not significantly change between the two conditions are colored with grey (|fold change| < 2 and padj > 0.01). By selecting a dot with the cursor, a panel appears on the right displaying the changes in the expression of the particular gene (y axis) across the different conditions (x axis, group). It is also possible to search for any gene using the search function, which will return information for the GeneID, symbol of the gene, gene name, logCPM values, logFC (log Fold Change) and adj. P value.*

5.4.11 Hierarchical clustered heatmap of the top 1000 differentially expressed genes

An analysis of the top 1000 differentially expressed genes was performed using pair-wise multiple comparisons between experimental conditions testing for differentially expressed genes. All of the 1000 genes tested had an adjusted P value equal or lower to 0.01 ($p \leq 0.01$) and a |log2fold| value higher than 1 relative to control for at least one experimental condition. A hierarchical clustering of the top 1000 differentially expressed genes identified time point specific gene clusters and similarities in genome-wide expression between the 12 different experimental sets (Figure 5.11). Whilst at 30 minutes comparatively few changes were detected, at 2 h the changes observed were strikingly similar following the addition of the three TrkB ligands. After 12 and 24-hour treatment, the transcriptional changes induced by BDNF and NT4 were similar, whilst the neurons treated with #85 for 12 and 24 hours showed fewer genes differentially expressed compared to the corresponding controls. A Gene Ontology analysis (GO) classified the observed changes in gene expression in 9 different categories. Among the most interesting groupings was the first “Ion Channel, Axon growth regulation, BDNF, MAPK, calcium signalling and shared RTK signalling “. Interestingly most of the genes belonging to this category were upregulated already at 2 hours. Whilst this was not unexpected it represents an important validation of the method as well as an indication that #85 activates very similar pathways compared to BDNF and NT4. The second category “Growth factors, calcium signalling, protein glycosylation, cell adhesion, G protein regulators” included genes that were mainly upregulated after 12 hours. The grouping “Ion Channels, including hyperpolarization-activated cyclic nucleotide-gated, sodium and potassium channels, TRP, PIEZO, and channel-like proteins, transporters” contained subset of genes that were differentially upregulated at 2- 12- and 24- hour time points. Although the number of the down-regulated genes (463) were approximately equal to the number of the genes that were up-regulated, those with increased expression were involved into a greater diversity of biological processes. The genes that were mainly downregulated belonged to 3 groupings with the largest one being “Lipid signalling, TGF pathway, Potassium channels and channel-like membrane proteins, taste receptors”.

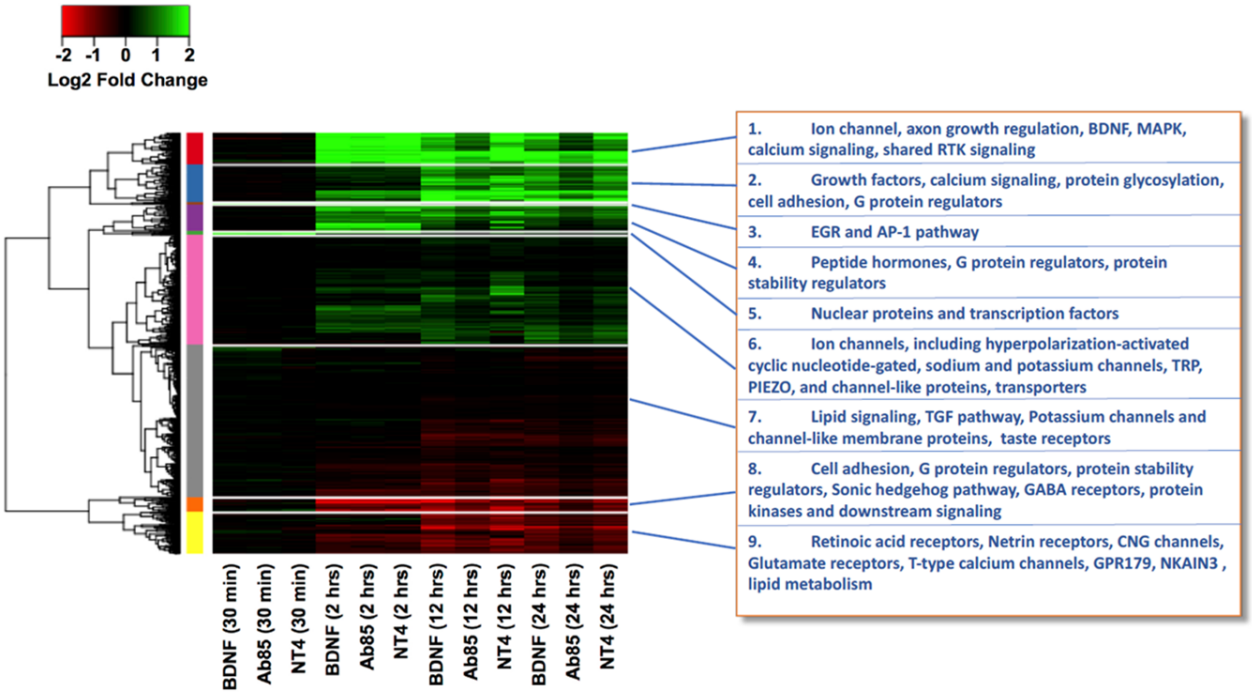

Figure 5.29. Heat map of hierarchical cluster analysis with GO annotation for the top 1000 differentially expressed genes with absolute fold change >2 and p < 0.01. The differentially expressed genes were clustered by using a Gene Ontology analysis of expression in nine different functional categories.

5.4.12 Gene analysis and GO description of differentially regulated genes in the 4 time-points, comparing the TrkB agonists to control cultures

As a next step of the RNA seq analysis the number of shared genes upon treatment with BDNF, #85 or NT4 was calculated for the 4 different time points using a threshold with adjusted p value < 0.01 and absolute fold change >2. In order to better understand the dynamics of gene expression in the time-points of 2 hours, 12 hours and 24 hours, Gene Ontology (GO) analysis was performed using the shinyGO platform.

5.4.12.1 TIMEPOINT 30 MINUTES

In the first time-point of 30 minutes the small number of genes that are expressed do not allow reliable GO analysis. At this time-point 36 genes were found to be upregulated more than 2-fold by all three TrkB ligands with p adjusted value <0.01 (table 5.4). Interestingly 23 of these genes belong to the family of immediate-early response genes (IEGs). Immediate-early genes (IEGs) are activated and transcribed within few minutes after stimulation, and do not require de novo protein synthesis. This large group of genes is known to be activated upon mitogen stimulus. Interestingly, NGF was shown to activate the transcription of IEGs (Curran and Morgan, 1985, Angelastro et al., 2000). Importantly 8 genes were upregulated more than 10-fold by all three TrkB ligands and all of them belong to the IEG family. The 4 members of the EGR (early growth response) family of zing finger transcription factor proteins belong to this subset of 8 genes and three EGR members are the top 3 upregulated genes at the time-point of 30 minutes. *EGR1, EGR2 and EGR3* were upregulated to a similar extend by all three TrkB ligands but not *EGR4*. More specifically *EGR2* was upregulated more than 70-fold, EGR1 more than 30-fold, EGR3 more than 12-fold while EGR4 is upregulated 44-fold by BDNF, 52-fold by AB85 and 78-fold by NT4. It has to be noted that *Egr1*, *Egr2* and *Fos* have been identified as transcriptional targets of BDNF/TrkB signalling pathway and the BDNF mediated induction of these genes through the transcription factors C/EBP and NeuroD is important for neuronal function (Calella et al., 2007) *Egr3* is upregulated in brain neurons upon neuronal activity (Yamagata et al., 1994) and BDNF induces EGR3 expression via PKC/MAPK-dependent pathway (Roberts et al., 2006). Furthermore, expression of EGR4 has been shown to be increased upon treatment of immature hippocampal neurons with BDNF in an ERK 1/2 dependent manner (Ludwig et al., 2011). Additionally, *Arc* is known to be transcribed during LTP and learning and BDNF was shown to induce selective

translation of Arc in synaptoneurosomal preparation (Wibrand et al., 2006, Yin et al., 2002). *FOSB* is an inducible transcription factor and an inactivating mutation of this gene renders the mice deficient in nurturing their offspring (Brown et al., 1996). Interestingly a truncated version of FosB (ΔFosB) was found to be important in hippocampus cellular morphology and hippocampus dependent learning and memory. Upon silencing of its transcriptional activity in hippocampus learning and memory were impaired (Eagle et al., 2015). Furthermore, FosB is important for hippocampus development, as the hippocampus in *FosB* knock-out mice was malformed and the hippocampal neurogenesis was reduced. Additionally, the adult animals suffered from spontaneous epileptic seizures (Yutsudo et al., 2013) . It has to be noted that FosB is also implicated in depression and addiction, as multiple *FosB* isoforms were found to be downregulated in hippocampus of human patients with depression and cocaine addiction, while the decreased levels have been linked with cognitive deficits linked with chronic cocaine abuse and depression (Gajewski et al., 2016). The *FOS* gene (c-FOS proto-oncogene) encodes a DNA-binding protein that binds to c-jun and forms a heterodimeric transcriptional factor, activator protein-1 (AP-1) (Curran and Morgan, 1985)(Curran 1995). It is also used as a marker of neuronal activity (Dragunow and Robertson, 1988, Sagar et al., 1988). It is implicated in transcription regulation and potentiates the long-term effects of growth factors and membrane-depolarising signals of neural activity (Sheng and Greenberg, 1990, Miyashita et al., 2018). Additionally, BDNF was shown to be one of the upstreams signals for c-FOS expression and activation of BDNF/c-FOS cascade in the retrosplenial cortex has been found to be essential for memory persistence (Katche et al., 2010, Katche and Medina, 2017).

B-cell translocation gene 2 (BTG2), a member of the BTG/TOB gene family was characterized as a gene upregulated within few minutes upon treatment with growth factors and mitogens (Bradbury et al., 1991). The transcription of BTG2 is controlled by miRNAs, and the 3’ untranslated region contains 17 binding sites (Fei et al., 2014).

Importantly BTG2 has an important role in cell cycle progression and possess antiproliferative effect through downregulation of cyclin D1 that leads to inhibition of retinoblastoma (Rb) phosphorylation and G1 arrest (Guardavaccaro et al., 2000, Montagnoli et al., 1996). It has also been shown that BTG2 could induce a G2/M arrest without the involvement of p53, while its expression could promote cellular senescence in fibroblasts. Notably BTG2 expression was shown to promote cellular

senescence in normal fibroblasts by interfering with the cell-cycle regulator Pin1 (Wheaton, Muir, Ma, & Benchimol, 2010). Interestingly it has been shown that a key element of drug-induced cellular senescence in human tumor cell lines is the upregulation of BTG1 and BTG2 (Chang et al., 2002). Remarkably, BTG2 is important in neurogenesis during adulthood, as its expression level is upregulated during neurogenesis and the inhibition of its expression results in programmed cell death of differentiated neurons *in vitro* (el-Ghissassi et al., 2002). *In vivo* data demonstrated that mice with impaired expression of *Btg2* display accretion of undifferentiated neurons and impaired contextual memory (Farioli-Vecchioli et al., 2009). BTG2 has been shown to control neurite outgrowth through regulation of arginine methylation in the nucleus (Miyata et al., 2008). Additionally, BTG2 is an effector of the transcription factor CREB and is essential in neuroprotection (Tan et al., 2012). Most importantly reduced expression of BTG2 in solid tumors correlates with poor outcome. In breast carcinoma BTG2 downregulation increases cyclin D expression and enhanced AKT phosphorylation. Therefore, low level of BTG2 in breast tumor links to disease progression and decreased survival (Kawakubo et al., 2004, Kawakubo et al., 2006, Takahashi et al., 2011). In liver cancer reduced amount of BTG2 results to increased amount of cyclin D1/ cyclin E which cause increased tumor grade (Zhang et al., 2011) In prostate cancer. BTG2 is downregulated by *miR-32* and *miR-21*, and its downregulation leads to disease onset and progression, therapy resistance and eventually metastasis (Coppola et al., 2013, Jalava et al., 2012). *In vivo* studies of knockout and overexpression of *Btg2* in mice models established the function of this gene as a tumor suppressor in medulloblastoma.

GPR50 also known as melatonin-related receptor is coded by an X-linked gene and an orphan receptor with high sequence homology with melatonin receptors (Dufourny et al., 2008). It has been suggested that GPR50 interacts with human melatonin receptor MT1 via its transmembrane domain, leading to inhibition of MT1 receptor signalling (Levoye et al., 2006). The large carboxyl terminal tail (C-tail) of the receptor serves as a scaffold for interacting partners (Grunewald et al., 2009). A common sequence variant that lacks four amino acids (GPR50Δ4) correlates with mental disorders (Thomson et al., 2005) and impaired lipid metabolism (Bhattacharyya et al., 2006). Type 1 TGFβ receptor (TβR1) forms a molecular complex with GPR50 which activates Smad2/3 and non-canonical pathways. Reduced GPR50 levels are related

to poor survival prognosis in human breast cancer, while *in vivo* GPR50 protects against tumour development in animal models (Wojciech et al., 2018). It has also been suggested that *GPR50* is a genetic rick factor for major depressive disorder and bipolar affective disorder, which are linked to abnormality of cortical development in females (Macintyre et al., 2010, Gogtay et al., 2007, Thomson et al., 2005). Additionally, *GPR50* promoter methylation level was found to be significantly downregulated in Alzheimer's disease male patients in comparison to healthy male volunteers (Chen et al., 2019b).

GPR50 was found to be expressed in NPCs in the ventricular zone of E14 mouse brain, which is enriched with NPCs. The same study demonstrated that knockdown of GPR50 with siRNA impaired self-renewal and neuronal differentiation of NPCs, while overexpression of GPR50 upregulated neuronal differentiation of NPCs (Ma et al., 2015). Interestingly yeast-two hybrid studies found that neurite outgrowth inhibitor NOGO-A interacts with GPR50, and both of them are located in the synapse in the adult mouse brain. Additionally, overexpression of GPR50 increased neurite length and filopodia-like structures in differentiated Neuroscreen-1 cells.

NPAS4 is an activity-dependent transcription factor and its expression is regulated by activity-dependent Ca2+ signalling (Choy et al., 2015) and PI3K-Akt signalling (Ooe et al., 2009). In terms of posttranslational level regulation, it was described that MAPK directly phosphorylates NPAS4. This transcription factor regulates inhibitory synapse number and function in cortical and hippocampal neurons of mice and rats through regulation of activity-dependent genes, which mediate the formation of GABA-releasing synapses on excitatory neurons. Interestingly BDNF mediates at least a part of the effect of NPAS4 on inhibitory synapse number, as siRNA against BDNF reduced the potential of NPAS4 to increase GABAergic synapses. Furthermore, BDNF expression was shown to be downregulated by approximately two-fold in cultures expressing Npas4-RNAi, while cultures from *Npas4*$^{-/-}$ mice also displayed a decrease in depolarization-induced BDNF expression (Lin et al., 2008). Another study from the same group described three binding sites of NPAS4 within the the *Bdnf* gene, and demonstrated that in *Npas4*$^{-/-}$ mice the transcription of several *Bdnf* isoforms is reduced. NPAS4 expression in mouse hippocampus is upregulated upon sensory stimuli and NPAS4 is responsible for the redistribution of inhibitory synapses in CA1 pyramidal neurons, which is partly mediated by BDNF which specifically regulates

somatic but not dendritic inhibition (Bloodgood et al., 2013). Notably *Npas4* and *Bdnf* expression was reduced upon overexpression of Histone deacetyase-3 (HDAC3) which promotes degeneration (Louis Sam Titus et al., 2019).

Npas4 has also a role in memory, as it regulates the number of functional synaptic contacts between CA3 contacts between CA3 pyramidal neurons and mossy fibers, that are necessary for learning-induced modification of MF-CA3 synapses during contextual memory formation. *Npas4* deletion blocks learning-induced strengthening of MF inputs (Weng et al., 2018). It is also remarkable that reduced *Npas4* expression within paravalbumin interneurons lead to deficits in short-term memory, and suggest that *Npas4* could be a major contributor to PV+ neurons dysfunction in neurodevelopmental disorders such as schizophrenia (Shepard et al., 2019). In line with this observation, Npas4$^{-/-}$ mice display behavioural deficits such as hyperactivity and long-term memory and cognitive deficits that were suggested to replicate schizophrenia-related symptomatology. The same study described upregulation of Npas4 expression in the hippocampus of wt mice after a social encounter, together with Npas4 dependent upregulation of c-Fos in the CA1 and CA3 regions of hippocampus after cognitive tasks (Coutellier et al., 2012).

NR4A2 belongs to the nuclear receptor subfamily 4A (NR4A) and it has described as necessary for the normal development and maintenance of midbrain dopaminergic (mDA) neurons (Kadkhodaei et al., 2009). Two mutations in this gene (-291Tdel and -245T-->G) led to decrease in *NR4A2* mRNA levels in transfected cell lines and lymphocytes of carriers, and impaired transcription of TH. Therefore, these two mutations have been correlated with dopaminergic dysfunction and Parkinson disease (Le et al., 2003). Additionally, loss-of-function mutations of *NR4A2* have been linked with early-onset dopa-responsive dystonia parkinsionism (Wirth et al., 2020). It has also been involved in various brain functions such as neuroprotection and cognitive functions. Interestingly, NR4A2 expression in glutamatergic neurons was markedly reduced in 5XFAD mice, an animal model of AD, in an age-dependent manner. The same study described reduced expression of NR4A2 expression in post-mortem human AD brains (Moon et al., 2019).

NR4A1 also belongs to the nuclear receptor subfamily 4A (NR4A) and it is crucial for the development of striatal striosomal compartment, and impairment of this gene

expression decrease the expression of striosome markers *in vivo* and *in vitro* (Cirnaru et al., 2019). It is an orphan receptor which is induced by various stimuli like growth factors, cytokines and miRNA and it is implicated in glucose homeostasis, lipid metabolism and energy balance (Zhang et al., 2018). *Nr4a1* has also shown to regulate the density and distribution of CA1 pyramidal neurons and knockdown of *Nr4a1* in hippocampal slice cultures lessend synaptic potentiation stimulated by chronic hyperactivity (Chen et al., 2014b).

IER2 is an immediate early response gene that has been linked to the regulation of tumor progression and metastasis, and its ectopic expression in metastatic pancreatic tumor cells induces their metastatis *in vivo* and increases their motility in culture (Chen et al., 2014b). In a mouse model of ALS (Hur deficient) *Ier2* mRNA levels were reduced in brain tissues (Sun et al., 2018a) and in line with this result *IER2* mRNA levels were also reduced in the brain and spinal cord of ALS patients (Dangond et al., 2004).

JunB is a member of the Jun family and it is a component of AP-1 transciption factor. JunB was shown to increase upon BDNF treatment of primary cortical neurons for 2 hours (Tuvikene et al., 2016). Neuronal activation of rat hippocampal neurons increased JunB expression (Rylski et al., 2009). Transgenic mice ovexpressing JunB displayed enhanced survival of neurons of the substancia nigra pars comacta (SNC) through inhibition of axotomy induced c-Jun (Winter et al., 2002). Interestingly, knockout of *Pten* and *JunB* in adult prostate epithelial cells led to invasive tumor formation, while high-grade and metastatic tumors from patients with prostate cancer were lacking JUNB (Birner et al., 2015).

CYR61 is a secreted extracellular matrix (ECM) associated signalling protein of the CCN family. It regulates various cellular activities such as cell adhesion, migration, proliferation, differentiation, apoptosis, senescence via interaction with cell surface integrin receptors and heparan sulfate proteoglycans (Lau, 2011, Jun and Lau, 2011). Iinterestingly, Cyr61 was described as a regulator of dendritic growth, sufficient to induce dendritic growth in both developing and mature neurons (Malik et al., 2013). Moreover, Cyr61 was found to be secreted by GDNF stimulated Muller glial cells and to enhance survival of photoreceptor (PR) cells (Kucharska et al., 2014) .

Activating transcription factor 3 (ATF3) is a member of the ATF/CREB family of transcription factors. Upon stress stimuli it forms dimers to activate or repress gene

expression. It is also implicated in immune response, atherogenesis, cell cycle and glucose homeostasis. It is a repressor of inflammation and it has been suggested that it may be an oncogene or tumor suppressor depending in different tissues (Jadhav and Zhang, 2017). Upon normal conditions *ATF3* mRNA and protein levels are low in neurons and glia cells but their levels are swiftly upregulated after injury. ATF3 expression correlates with survival and regeneration after axotomy, and in peripheral nerves it associates with the generation of Schwann cell phenotype which is a marker of axonal regeneration (Hunt et al., 2012).

Symbol	GeneName	BDNF-FC	AB85-FC	NT4-FC	adj.P.Val
EGR2	early growth response 2	72,1185469	70,3245081	73,5341166	2,36E-45
EGR4	early growth response 4	44,7126339	52,3646874	78,3719692	4,63E-80
EGR1	early growth response 1	31,1077328	31,1757203	35,2426075	2,94E-07
ARC	activity regulated cytoskeleton associated protein	14,0176504	15,4976945	20,2149105	3,6E-17
FOSB	FosB proto-oncogene, AP-1 transcription factor subunit	13,4909032	12,8654052	14,7294194	1,28E-140
FOS	Fos proto-oncogene, AP-1 transcription factor subunit	11,7325264	11,5877185	13,2934918	2,35E-07
EGR3	early growth response 3	12,9465541	14,1280421	15,6785581	1,15E-88
BTG2	BTG anti-proliferation factor 2	10,8167655	10,9859712	12,3211849	3,05E-157
GPR50	G protein-coupled receptor 50	11,0145881	10,2430034	8,58831833	0,0000162
NPAS4	neuronal PAS domain protein 4	10,3980684	8,45380157	10,0750095	7,72E-39
AF003625.3	lincRNA	9,5823978	9,61762547	10,8475078	5,74E-08
RP11-459E5.1	lincRNA	5,9674406	7,43555702	9,75842205	7,39E-23
CTC-250I14.6	lincRNA	4,65156863	5,51683972	8,07249386	1,19E-07
NR4A2	nuclear receptor subfamily 4 group A member 2	6,73698408	6,31443717	7,33908533	5,31E-76
NR4A1	nuclear receptor subfamily 4 group A member 1	6,23031243	6,08398117	7,30333483	1,62E-83
IER2	immediate early response 2	5,26634539	5,57864969	7,81151174	6,58E-10
JUNB	JunB proto-oncogene, AP-1 transcription factor subunit	4,66467037	5,47654226	7,65581548	2,37E-14
RP11-1100L3.8	lincRNA	5,47291621	5,29564862	7,30392299	3,92E-32
CYR61	cysteine rich angiogenic inducer 61	5,45012204	5,30055202	6,64112545	6,78E-20
ATF3	activating transcription factor 3	5,31838406	5,16300149	5,63269228	8,07E-85
RP11-667K14.3	lincRNA	4,90681276	4,50341591	3,93838569	3,75E-17
ASCL1	achaete-scute family bHLH transcription factor 1	3,41383356	3,30599596	3,93272385	8,62E-23
FOSL1	FOS like 1, AP-1 transcription factor subunit	3,46300853	3,34213968	3,63772464	0,0000102
NR4A3	nuclear receptor subfamily 4 group A member 3	3,05695477	3,24160421	3,37622936	1,59E-58
AC003104.1	lincRNA	3,26027882	3,24130771	3,18089282	6,76E-07
JUN	Jun proto-oncogene, AP-1 transcription factor subunit	2,93401289	3,21673771	3,71855984	2,2E-47
DUSP5	dual specificity phosphatase 5	2,94892618	3,02639549	3,44891312	0,00883764
EPOP	elonginBC polycomb repressive complex2 assoc. protein	2,78879785	2,6604148	3,31391206	1,34E-24
SNORA48	small nucleolar RNA, H/ACA box 48	3,14651064	2,5719308	2,29977217	0,00255887
LAG3	lymphocyte activating 3	3,00468123	2,65141245	2,60647003	1,94E-09
MAFF	MAF bZIP transcription factor F	2,42154292	2,59646826	2,90389964	0,00124467
RP11-867G23.10	lincRNA	2,18615429	2,03590434	2,35303673	0,00000119
MCL1	MCL1, BCL2 family apoptosis regulator	2,50269193	2,62105717	2,77694135	0,0018128
TIPARP	TCDD inducible poly (ADP-ribose) polymerase	2,27136019	2,28904268	2,26230846	0,00866926
DUSP1	dual specificity phosphatase 1	2,09298187	2,23707687	2,47983891	3,69E-49
FOSL2	FOS like 2, AP-1 transcription factor subunit	2,19914207	2,24583129	2,24497284	1,92E-09

Table 5.4 list with the genes upregulated by all three TrkB ligands in the timepoint 30 minutes with adjusted p value <0.01 and fold change > 1.5

5.4.12.2 TIMEPOINT 2 HOURS

At the time-point 2 hours 1199 genes are upregulated more than 2-fold in a statistically significant manner (p adjusted value p <0.01) (Table 5.5). Many GO categories relevant to BDNF-TrkB signalling are detected, such as MAPK cascade, signal transduction by protein phosphorylation, regulation of MAPK cascade. Additionally, several genes belonging to the regulation of protein phosphorylation, cell-cell signalling, regulation of intracellular signal transduction, regulation of cell signalling are upregulated. Additionally,1844 downregulated genes are detected at the same time-point, no significant enrichment for GO was detected.

5.4.12.3 TIMEPOINT 12 HOURS

At the time-point 12 hours 1103 genes are upregulated more than 2-fold in comparison to the control cultures and in a statistically significant manner (p adjusted value p <0.01) (Table 5.6). Many GO categories are relevant to synapses such as synaptic signaling, trans-synaptic signaling, chemical synaptic transmission, regulation of trans-synaptic signaling, implying that at this time-point the machinery for synaptic transmission is activated. The categories “regulation of cell communication” and “regulation of signaling” are also present with 268 and 270 genes respectively. The category positive regulation of phosphorus metabolic process with 102 genes is also detected. This category is linked with DNA synthesis, ATP synthesis, membrane synthesis, and protein phosphorylation.

Furthermore 1844 genes are downregulated more than 2-fold in comparison to the control cultures and in a statistically significant manner (p adjusted value p <0.01) (Table 5.7). Many GO categories detected are relevant to neurons such as neuron projection guidance, axon guidance, axonogenesis, neuron differentiation, regulation of nervous system development, neuron projection development, generation of neurons.

5.4.12.4 TIMEPOINT 24 HOURS

At the time-point 24 hours 671 genes are upregulated more than 2-fold in comparison to the control cultures and in a statistically significant manner (p adjusted value p <0.01) (Table 5.8). GO categories relevant to synapses are detected, such as synaptic

signaling, trans-synaptic signaling, anterograde trans-synaptic signaling, regulation of trans-synaptic signaling and modulation of chemical synaptic transmission. Additionally, more than one fourth of these genes belong to the categories “regulation of cell communication” and “regulation of cell-cell signaling”. Although 614 genes are downregulated at this time-point, no significant enrichment was detected.

Enrichment FDR	Genes in list	Total genes	Functional Category
7,37E+01	272	3382	Regulation of multicellular organismal process
8,43E+04	75	603	Regulation of system process
1,88E+05	287	3903	Regulation of cell communication
1,88E+05	290	3952	Regulation of signaling
3,57E+05	108	1077	Circulatory system development
6,87E+04	216	2763	Regulation of developmental process
4,93E+06	84	793	Regulation of MAPK cascade
6,11E+06	149	1756	Regulation of cell proliferation
7,79E+05	212	2785	Anatomical structure morphogenesis
7,79E+05	132	1503	Regulation of protein phosphorylation
1,06E+07	141	1653	Regulation of phosphorylation
1,30E+07	157	1911	Positive regulation of multicellular organismal process
1,36E+07	171	2138	Regulation of multicellular organismal development
1,50E+07	254	3529	Regulation of signal transduction
2,06E+07	147	1774	Cell-cell signaling
2,06E+07	153	1870	Regulation of phosphate metabolic process
2,06E+07	76	723	Regulation of ion transport
2,06E+07	125	1433	Positive regulation of developmental process
2,06E+07	153	1872	Regulation of phosphorus metabolic process
2,06E+07	115	1286	Negative regulation of multicellular organismal process
2,06E+07	76	724	Cardiovascular system development
2,07E+07	125	1440	Negative regulation of cell communication
2,07E+07	96	1007	MAPK cascade
2,19E+07	162	2027	Regulation of intracellular signal transduction
2,19E+07	73	687	Blood vessel development
2,19E+07	75	715	Vasculature development
2,19E+07	125	1444	Negative regulation of signaling
2,91E+07	96	1018	Signal transduction by protein phosphorylation
3,43E+07	96	1022	Positive regulation of cell proliferation
3,58E+07	66	603	Blood vessel morphogenesis

Table 5.5 GO biological process for the 1199 upregulated genes that are upregulated upon treatment with all three TrkB ligands (BDNF, AB85 and NT4) at time-point 2 hours.

Enrichment FDR	Genes in list	Total genes	Functional Category
7,40E+03	86	762	Synaptic signaling
7,40E+03	86	756	Trans-synaptic signaling
7,40E+03	83	723	Regulation of ion transport
7,61E+02	84	746	Anterograde trans-synaptic signaling
7,61E+02	153	1774	Cell-cell signaling
7,61E+02	84	746	Chemical synaptic transmission
1,76E+05	61	485	Regulation of ion transmembrane transport
2,11E+05	67	566	Regulation of transmembrane transport
7,63E+05	268	3903	Regulation of cell communication
9,69E+04	270	3952	Regulation of signaling
3,34E+06	46	336	Regulation of cation transmembrane transport
5,29E+05	56	467	Modulation of chemical synaptic transmission
5,30E+05	56	468	Regulation of trans-synaptic signaling
5,40E+06	40	273	Regulation of transporter activity
5,40E+06	208	2905	Regulation of localization
5,71E+06	139	1725	Response to oxygen-containing compound
8,62E+05	91	975	Response to organic cyclic compound
1,47E+07	30	173	Regulation of cation channel activity
2,17E+07	37	253	Regulation of ion transmembrane transporter activity
3,15E+07	77	793	Regulation of MAPK cascade
4,29E+07	102	1183	Positive regulation of phosphorus metabolic process
4,29E+07	102	1183	Positive regulation of phosphate metabolic process
4,31E+07	37	261	Regulation of transmembrane transporter activity
5,91E+07	95	1082	Response to drug
7,58E+07	93	1057	Positive regulation of protein phosphorylation
8,93E+07	94	1077	Circulatory system development
9,10E+06	18	73	Regulation of neurotransmitter receptor activity
1,26E+08	194	2785	Anatomical structure morphogenesis
1,95E+08	89	1018	Positive regulation of cell differentiation
2,57E+08	61	603	Regulation of system process

Table 5.6 GO biological process for the 1103 upregulated genes that are upregulated upon treatment with all three TrkB ligands (BDNF, AB85 and NT4) at time-point 12 hours.

Enrichment FDR	Genes in list	Total genes	Functional Category
0.000687616472926894	47	275	Neuron projection guidance
0.000687616472926894	47	274	Axon guidance
0.00252719920373112	67	474	Axonogenesis
0.00270348373423844	71	517	Axon development
0.0108767578733426	13	42	Negative chemotaxis
0.0172468732716724	89	746	Anterograde trans-synaptic signaling
0.0172468732716724	90	756	Trans-synaptic signaling
0.0172468732716724	83	680	Plasma membrane bounded cell projection morphogenesis
0.0172468732716724	89	746	Chemical synaptic transmission
0.0172468732716724	82	666	Neuron projection morphogenesis
0.0172468732716724	83	682	Cell projection morphogenesis
0.0199508072560614	90	762	Synaptic signaling
0.0199508072560614	74	598	Cell morphogenesis involved in neuron differentiation
0.0244415678383175	118	1067	Cell morphogenesis
0.0275302823427436	149	1412	Neuron differentiation
0.027658089923378	83	701	Cell part morphogenesis
0.0352563052365394	241	2474	Nervous system development
0.0352563052365394	106	953	Regulation of nervous system development
0.0426949720179953	87	756	Cell morphogenesis involved in differentiation
0.046933986403829	21	115	Regulation of calcium ion-dependent exocytosis
0.046933986403829	110	1008	Neuron projection development
0.046933986403829	161	1575	Generation of neurons

Table 5.7 GO biological process for the 1844 downpregulated genes that are downregulated upon treatment with all three TrkB ligands (BDNF, AB85 and NT4) at time-point 12 hours.

Enrichment FDR	Genes in list	Total genes	Functional Category
2,36E+04	62	762	Synaptic signaling
2,36E+04	62	756	Trans-synaptic signaling
3,96E+04	60	746	Anterograde trans-synaptic signaling
3,96E+04	60	746	Chemical synaptic transmission
3,96E+04	184	3903	Regulation of cell communication
4,93E+04	185	3952	Regulation of signaling
1,55E+04	103	1774	Cell-cell signaling
3,26E+05	100	1725	Response to oxygen-containing compound
1,69E+06	55	723	Regulation of ion transport
1,69E+06	71	1077	Circulatory system development
4,79E+06	163	3547	Response to organic substance
5,74E+06	41	468	Regulation of trans-synaptic signaling
5,74E+06	67	1019	Response to organonitrogen compound
5,74E+06	46	566	Regulation of transmembrane transport
5,74E+06	41	467	Modulation of chemical synaptic transmission
7,31E+06	156	3382	Regulation of multicellular organismal process
1,16E+07	64	975	Response to organic cyclic compound
1,19E+07	29	263	G protein-coupled receptor signaling pathway, coupled to cyclic nucleotide second messenger
1,27E+07	138	2905	Regulation of localization
1,27E+07	41	485	Regulation of ion transmembrane transport
1,62E+07	68	1082	Response to drug
1,72E+07	93	1704	Response to endogenous stimulus
1,83E+07	159	3529	Regulation of signal transduction
2,13E+07	29	273	Regulation of transporter activity
2,53E+07	46	603	Regulation of system process
2,79E+07	69	1126	Response to nitrogen compound
3,89E+07	17	99	Response to cAMP
5,23E+07	131	2785	Anatomical structure morphogenesis
5,71E+07	49	687	Blood vessel development
5,71E+07	27	253	Regulation of ion transmembrane transporter activity

Table 5.8 GO biological process for the 671 upregulated genes that are upregulated upon treatment with all three TrkB ligands (BDNF, AB85 and NT4) at time-point 24 hours.

5.4.13 Venn diagram analysis of the genes upregulated between BDNF, AB85, NT4 and control cultures

In the data presented below the differences in the transcriptome of the untreated neurons versus neurons treated with either BDNF, AB85 or NT4 are examined using pairwise comparisons. In order to examine the number of genes that are differentially expressed by a particular TrkB agonist, venn diagram illustrations have been used. Venn diagram comparisons also illustrate the overlap of expressed genes among cultures treated with BDNF, AB85 and NT4. Initially untreated cultures (controls) were compared to cultures treated with one of three TrkB agonists and the comparisons were made using 3 levels of statistical significance (p- adjusted values, 0.05, 0.01 and 0.001) and 4 levels of change (fold change, 1.5, 2, 4 and 10). Upregulated and downregulated genes compared to corresponding control were examined separately. Overall few dozens of genes change their expression at the first 30 minutes, whereas the maximum number of differentially expressed genes is observed at 2 hours. Subsequently fewer genes are altered at 12 and 24 hours.

5.4.13.1 UPREGULATED GENES AT TIME-POINT 30 MINUTES

At the first time point examined, 30 minutes after treatment 85 genes are upregulated by BDNF, AB85 and NT4 more than 1.5-fold with a p-adjusted value of 0.05. Additionally, 27 genes are differentially expressed by BDNF, 13 genes by AB85 and 22 by NT4. Upon shifting the p-adjusted value to 0.01 the number of genes shared between the three TrkB ligands is decreased to 77, and the number of genes upregulated by each of the three TrkB ligands is also decreased to 12 genes by BDNF, 7 genes by AB85 and 17 genes by NT4. The number of shared upregulated genes in cultures treated with the three TrkB ligands versus untreated samples is further decreased by shifting further the p-adjusted value to 0.001 to 64. The number of genes upregulated by each of the three TrkB ligands is also decreased to 6 genes by BDNF, 2 genes by AB85 and 14 genes by NT4. When the level of change is set to 2-fold and the p-adjusted value to 0.05, 49 genes are found to be upregulated by the three TrkB ligands, and this number is slightly decreased to 46 upon sifting the p-adjusted value to 0.01 and further decreased to 38 upon shifting the p-adjusted value to 0.001. The number of differentially upregulated genes by BDNF and AB85 by more than 2-fold is reduced when the p-adjusted value is shifted to 0.01 and 0.001, but the number of

genes differentially upregulated by NT4 is only reduced by 1. Additionally, 24 genes are upregulated by the three TrkB ligands more than 4-fold when the p adjusted value was set to 0.05 or 0.01 and 23 when it was set to 0.001. However very few genes are differentially increased by any of the three TrkB ligands more than 4-fold. More specifically 2 genes were upregulated by BDNF, 1 gene was upregulated by NT4 and no gene was upregulated by AB85 with p adjusted value 0.001. Interestingly 11 genes are upregulated more than 10-fold by BDNF, AB85 and NT4 and this observation is significant in the three p-adjusted values tested. Also, no gene is differentially increased more than 10-fold by any single TrkB agonist.

5.4.13.2 UPREGULATED GENES AT TIME-POINT 2 HOURS

Interestingly after 2 hours 1387 genes are upregulated more than 1.5-fold by all TrkB ligands with a p-adjusted value 0.05, while 1255 genes are upregulated by more than 1.5-fold when the p-adjusted value is shifted to 0.01 (90% of the genes upregulated with p-adj at 0.05). By shifting the p-adjusted value to 0.001 1096 genes are found to be upregulated by more than 1.5-fold with all ligands (79% of the genes upregulated with p-adj at 0.001). Notably there are many more genes (523) upregulated more than 1.5-fold selectively by AB85 with a p-adjusted value of 0.05 in comparison to the genes upregulated by BDNF (158) and NT4 (195), but this number is reduced by 50% when the p-adjusted value is shifted to 0.001. Only 20% of the genes (113 genes) are upregulated more than 1.5-fold with AB85 are detected when the level of change is shifted to 2, therefore the other 80% of the genes is upregulated between 1.5 and 2-fold. On the other hand, about 50% of the genes upregulated by BDNF or NT4 more than 1.5-fold are also upregulated more than 2-fold, 57 and 79 genes respectively. The number of shared genes expressed more than 2-fold with p-adjusted value 0.05 is 780, and this number does not change much when the threshold of p-adjusted value is shifted to 0.01 and 0.001, 759 and 705 genes respectively. The number of genes selectively upregulated more than 2-fold by BDNF or NT4 is also quite consistent between the three levels of p-adjusted value, whereas the number of genes selectively expressed by AB85 at p-adjusted 0.001 is 63 compared to 113 at p-adjusted 0.05. By shifting the level of increase at 4-fold and p-adjusted at 0.05, 291 genes or 37% of the genes increased at 2-fold and p-adjusted 0.05, are increased upon treatment with the three ligands. This number remains essentially unchanged upon shifting the p-adjusted value at 0.01 and 0. 001. Only 12, 6 and 13 genes are respectively selectively

upregulated by BDNF, AB85 and NT4 with p-adjusted value at 0.05. These numbers do not change significantly upon application of p-adjusted value to 0.1 or 0.001, highlighting the significance of this observation. Additionally, the level of increase was set to fold change 10 and the number of genes (104) upregulated by three TrkB ligands was the same in three different p adjusted values. Interestingly only 2 genes were selectively upregulated more than 10-fold by any of the three TrkB ligands across the three significance levels.

5.4.13.3 UPREGULATED GENES AT TIME-POINT 12 HOURS

At time point 12 hours the number of genes upregulated by BDNF, AB85 and NT4 more than 1.5-fold with a p-adjusted value 0.05 is 738. This number equals to 53% of the genes upregulated at 2 hours with the same p-adjusted value, and upon shifting the p adjusted value to 0.01 and 0.001 this number is reduced to 648 and 515 genes respectively. Interestingly the number of genes selectively upregulated more than 1.5-fold by NT4 with p-adjusted value 0.01 is much larger than the genes selectively upregulated by BDNF (799 versus 315), and very few genes are selectively upregulated by AB85 (36). By shifting the level of increase to 2-fold and keeping the p-adjusted value at 0.01 the number of shared genes by the three ligands is 366 or 56% of those shared at the level of increase at 1.5-fold. Therefore 282 genes shared between BDNF, AB85 and NT4 are upregulated between 1.5 and 2-fold in comparison to the control. Also 91 genes are selectively upregulated more than 2-fold by BDNF, 18 by AB85 and 392 by NT4. Subsequently 224 genes are selectively upregulated between 1.5 and 2-fold by BDNF, 18 genes by AB85 and 407 by NT4. When the level of increase is shifted to 4 and the p-adjusted value is maintained to 0.01, 138 genes are found to be increased by the three ligands. Hence 228 genes shared between BDNF, AB85 and NT4 are increased between 2 and 4-fold. Moreover 36 genes are selectively upregulated more than 4-fold by BDNF, 2 by AB85 and 147 genes by NT4. Thus 55 genes are selectively upregulated between 2 and 4-fold by BDNF, 16 genes by AB85 and 245 genes by NT4. Furthermore 43 genes were increased more than 10-fold by the three TrkB ligands and 19 genes were selectively upregulated by BDNF, 1 gene by AB85 and 50 genes by NT4. Thus 17 genes are selectively upregulated between 4 and 10-fold by BDNF, 1 gene by AB85 and 97 genes by NT4. It has to be noticed that not only NT4 selectively upregulates many more genes than AB85 and

NT4, but 18% of these genes are upregulated more than 4-fold and 6% of these genes more than 10-fold.

5.4.13.4 UPREGULATED GENES AT TIME-POINT 24 HOURS

At time point 24 hours the number of genes upregulated by BDNF, AB85 and NT4 more than 1.5-fold with a p-adjusted value 0.05 is 610. This number equals to 44% of the genes upregulated at 2 hours and 82% of the genes upregulated at 12 hours, and upon shifting the p adjusted value to 0.01 and 0.001 this number is reduced to 483 and 374 genes respectively. Interestingly the number of genes selectively upregulated more than 1.5-fold by BDNF with p-adjusted value at 0.01 is similar to the number selectively upregulated by NT4 (162 versus 172), whereas very few genes are selectively upregulated by AB85 (23). By shifting the level of increase to 2-fold and keeping the p-adjusted value at 0.01 the number of shared genes by the three ligands is 279 or 58% of those shared at the level of increase of 1.5-fold. Therefore 204 genes shared between BDNF, AB85 and NT4 are upregulated between 1.5 and 2-fold in comparison to the control. Also 70 genes are selectively upregulated more than 2-fold by BDNF, 11 by AB85 and 45 by NT4. Subsequently 92 genes are selectively upregulated between 1.5 and 2-fold by BDNF, 12 genes by AB85 and 127 genes by NT4. When the level of increase is shifted to 4 and the p-adjusted value is maintained to 0.01, 108 genes are found to be increased by the three ligands. Hence 171 genes shared between BDNF, AB85 and NT4 are increased between 2 and 4-fold. Moreover 14 genes are selectively upregulated more than 4-fold by BDNF, 0 by AB85 and 8 genes by NT4. Thus 56 genes are selectively upregulated between 2 and 4-fold by BDNF, 11 genes by AB85 and 37 genes by NT4. Furthermore 28 genes were increased more than 10-fold by the three TrkB ligands and 80 genes were upregulated by the three TrkB ligands between 4 and 10-fold in comparison to the control. Additionally, 8 genes are selectively upregulated more than 10-fold by BDNF, 0 by AB85 and 1 by NT4. Thus 6 genes are selectively upregulated between 4 and 10-fold by BDNF, 0 genes by AB85 and 7 genes by NT4. It has to be noticed that although BDNF and NT4 selectively upregulate several genes less than 9% and 5% of these genes respectively are upregulated more than 4-fold.

5.4.13.5 DOWNREGULATED GENES AT TIME-POINT 30 MINUTES

At the first time point examined, 30 minutes after treatment there are no genes that are downregulated by all three TrkB ligands more than 1.5-fold with a p-adjusted value of 0.05. However, 31 genes were differentially decreased by BDNF, 1 gene by AB85 and 2 genes by NT4. By shifting the p-adjusted value to 0.01 only 6 genes were differentially decreased by BDNF, 0 genes by AB85 and 1 gene by NT4. Similarly, when the p-adjusted value was shifted to 0.001 only 1 gene was differentially decreased by BDNF, 0 genes by AB85 and only 1 gene by NT4. Interestingly 13 genes were differentially downregulated more than 2-fold by BDNF, 0 genes by AB85 and 1 gene by NT4 and p-adjusted value at 0.05. However, no gene is decreased more than 2-fold compared to the control, when the p-adjusted is shifted at 0.01. Additionally, only 1 gene is selectively downregulated more than 4-fold by BDNF with p adjusted value of 0.05 and 1 genes with NT4, while no gene is selectively downregulated by AB85. Upon shifting the p-adjusted value to 0.01 there was no gene detected that was downregulated more than 4-fold.

5.4.13.6 DOWNREGULATED GENES AT TIME-POINT 2 HOURS

Interestingly after 2 hours 1221 genes are downregulated more than 1.5-fold by all TrkB ligands with a p-adjusted value 0.05, while 1048 genes are downregulated by more than 1.5-fold when the p-adjusted value is shifted to 0.01 or 85% of the genes downregulated at p-adjusted 0.05. By shifting the p-adjusted value to 0.001, 831 genes are found to be downregulated by more than 1.5-fold with all ligands or 68% of the genes downregulated at p-adjusted 0.05. Notably there are many more genes (707) downregulated more than 1.5-fold selectively by AB85 with a p-adjusted value of 0.05 in comparison to the genes downregulated by BDNF (200) and NT4 (255). Upon shifting the p-adjusted value at 0.01 less genes were selectively downregulated more than 1.5-fold by BDNF (157), AB85 (488) and NT4 (198). When the p-adjusted value was set to 0.001 even less genes were selectively downregulated by BDNF (108), AB85 (324) and NT4 (163).

When the level of decrease was set to 2-fold it was noticed that there were small differences in the number of genes downregulated by all three TrkB ligands between the three p-adjusted values. It was observed that 432 genes were downregulated by BDNF, AB85 and NT4 at p adjusted value 0.01 or 41% of the genes downregulated more than 1.5-fold. Thus 616 genes were downregulated between 1.5 and 2-fold.

Additionally, 92 genes were selectively downregulated more than 2-fold with p-adjusted value 0.01 by BDNF, 240 by AB85 and 90 by NT4. Therefore 65 genes were selectively downregulated by BDNF between 1.5 and 2-fold, 248 genes were selectively downregulated by AB85 between 1.5 and 2-fold and 108 genes were selectively downregulated by NT4. Upon shifting the level of decrease to 4-fold and the p adjusted value to 0.01 the number of genes downregulated by the three ligands was significantly lower than the number of genes downregulated more than 2-fold. More specifically only 63 genes were downregulated more than 4-fold by the three TrkB ligands, consequently 369 genes were downregulated between 2 and 4-fold by BDNF, AB85 and NT4. Additionally, 8 genes were selectively downregulated by BDNF, 34 genes were selectively downregulated by AB85 and 6 genes were specifically downregulated by NT4. Subsequently 84 genes were selectively downregulated by BDNF between 2 and 4-fold, 206 genes were selectively downregulated by AB85 between 2 and 4-fold and 84 genes were selectively downregulated by NT4. It has to be noted that almost no genes were found to be downregulated more than 10-fold by the three TrkB ligands. Indeed 1 gene was downregulated more than 10-fold with p-adjusted value=0.01 by the three ligands, thus 62 genes were downregulated between 4 and 10-fold. Additionally, 1 gene was selectively downregulated by BDNF, 2 genes by AB85 and no gene was selectively downregulated by NT4. Therefore 7 genes were selectively upregulated by BDNF between 4 and 10-fold, 32 genes by AB85 and 6 genes by NT4.

5.4.13.7 DOWNREGULATED GENES AT TIME-POINT 12 HOURS

Notably 12 hours after treatment 1287 genes are downregulated more than 1.5-fold by all TrkB ligands with a p-adjusted value 0.05, while 991 genes are downregulated by more than 1.5-fold when the p-adjusted value is shifted to 0.01 or 77% of the genes downregulated at p-adjusted 0.05. By shifting the p-adjusted value to 0.001, 657 genes are found to be downregulated by more than 1.5-fold with all ligands or 51% of the genes downregulated at p-adjusted 0.05. Notably there are many more genes (1118) downregulated more than 1.5-fold selectively by NT4 with a p-adjusted value of 0.05 in comparison to the genes downregulated by BDNF (536) and AB85 (240). Upon shifting the p-adjusted value at 0.01 less genes were selectively expressed by BDNF (438), AB85 (208) and NT4 (1020). When the p-adjusted value was set to 0.001 even less genes were selectively expressed by BDNF (315), AB85 (118) and NT4 (868).

The difference in the proportion of downregulated genes between the three TrkB ligands is maintained in the three p-adjusted thresholds, highlighting its significance.

When the level of decrease was set to 2-fold it was noticed that there were some differences in the number of genes downregulated by all three TrkB ligands between the three p-adjusted values. The number of the genes downregulated was decreased as the p-adjusted threshold was becoming stricter, and the most severe difference relied between AB85 at p-adjusted values 0.01 and 0.001 where only 50% of the genes downregulated with 0.01 are also downregulated with the latter. It was also observed that 384 genes were downregulated more than 2-fold by BDNF, AB85 and NT4 at p adjusted value 0.01 or 38% of the genes downregulated more than 1.5-fold. Thus 607 genes were downregulated between 1.5 and 2-fold. Additionally, 243 genes were selectively downregulated more than 2-fold with p-adjusted value 0.01 by BDNF, 142 by AB85 and 644 by NT4. Therefore 195 genes were selectively downregulated by BDNF between 1.5 and 2-fold, 66 genes were selectively downregulated by AB85 between 1.5 and 2-fold and 376 genes were selectively downregulated by NT4. Upon shifting the level of decrease to 4-fold and the p adjusted value to 0.01 the number of genes downregulated by the three ligands was much less than the number of genes downregulated more than 2-fold. More specifically only 19 genes were downregulated more than 4-fold by the three TrkB ligands, consequently 365 genes were downregulated between 2 and 4-fold by BDNF, AB85 and NT4. Additionally, 34 genes were selectively downregulated by BDNF, 4 genes were selectively downregulated by AB85 and 172 genes were specifically downregulated by NT4. Subsequently 209 genes were selectively downregulated by BDNF between 2 and 4-fold, 138 genes were selectively downregulated by AB85 between 2 and 4-fold and 472 genes were selectively downregulated by NT4. It has to be noted that no genes were found to be downregulated more than 10-fold by the three TrkB ligands, thus 19 genes were downregulated between 4 and 10-fold. Additionally, 3 genes were selectively downregulated by BDNF, 0 genes by AB85 and 24 genes were selectively downregulated by NT4. Therefore 31 genes were selectively downregulated by BDNF between 4 and 10-fold, 4 genes by AB85 and 148 genes by NT4.

5.4.13.8 DOWNREGULATED GENES AT TIME-POINT 24 HOURS

Finally, 24 hours after treatment 531 genes are downregulated more than 1.5-fold by all TrkB ligands with a p-adjusted value 0.05, while 293 genes are downregulated by more than 1.5-fold when the p-adjusted value is shifted to 0.01 or 55% of the genes downregulated at p-adjusted 0.05. By shifting the p-adjusted value to 0.001, 160 genes are found to be downregulated by more than 1.5-fold with all ligands or 54% of the genes downregulated at p-adjusted 0.01. Interestingly there are far less genes (55) downregulated more than 1.5-fold selectively by AB85 with a p-adjusted value of 0.05 in comparison to the genes downregulated by BDNF (403) and AB85 (242). Upon shifting the p-adjusted value at 0.01 less genes were selectively expressed by BDNF (321), AB85 (29) and NT4 (160). When the p-adjusted value was set to 0.001 even less genes were selectively downregulated by BDNF (199), AB85 (10) and NT4 (97).

When the level of decrease was set to 2-fold it was noticed that there were differences in the number of genes downregulated by all three TrkB ligands between the three p-adjusted values. The number of the genes downregulated was decreased as the p-adjusted threshold was becoming stricter. It was also observed that 84 genes were downregulated by BDNF, AB85 and NT4 at p adjusted value 0.01 or 28% of the genes downregulated more than 1.5-fold. Thus 209 genes were downregulated between 1.5 and 2-fold. Additionally, 155 genes were selectively downregulated more than 2-fold with p-adjusted value 0.01 by BDNF, 9 by AB85 and 71 by NT4. Therefore 166 genes were selectively downregulated by BDNF between 1.5 and 2-fold, 20 genes were selectively downregulated by AB85 between 1.5 and 2-fold and 89 genes were selectively downregulated by NT4. Upon shifting the level of decrease to 4-fold and the p adjusted value to 0.01 the number of genes downregulated by the three ligands was zero. More specifically no genes were found to be downregulated more than 4-fold by the three TrkB ligands, consequently 84 genes were downregulated between 2 and 4-fold by BDNF, AB85 and NT4. Additionally, 13 genes were selectively downregulated by BDNF, 0 genes were selectively downregulated by AB85 and 8 genes were specifically downregulated by NT4. Subsequently 142 genes were selectively downregulated by BDNF between 2 and 4-fold, 9 genes were selectively downregulated by AB85 between 2 and 4-fold and 63 genes were selectively

downregulated by NT4. It has to be noted that no genes were found to be downregulated more than 10-fold by any of the three TrkB ligands.

A.

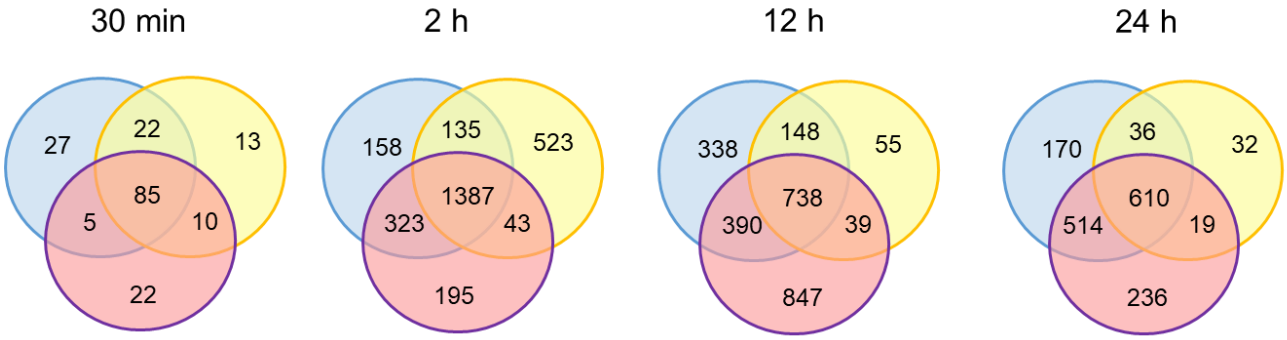

B.

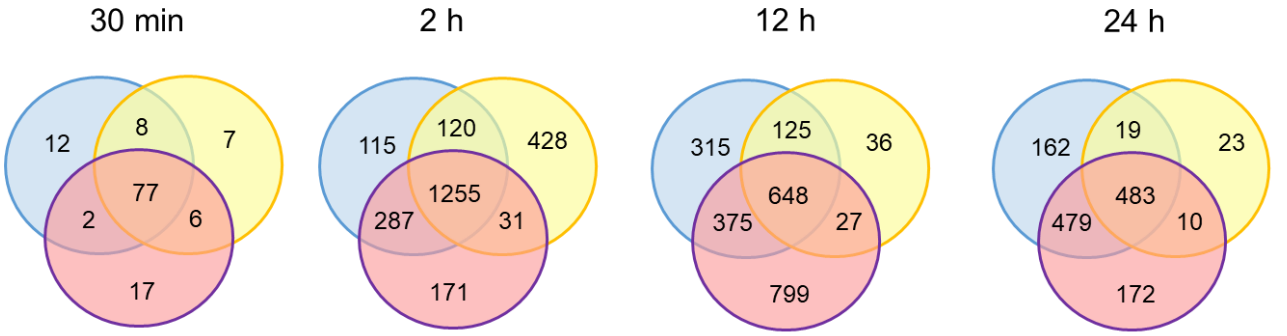

C.

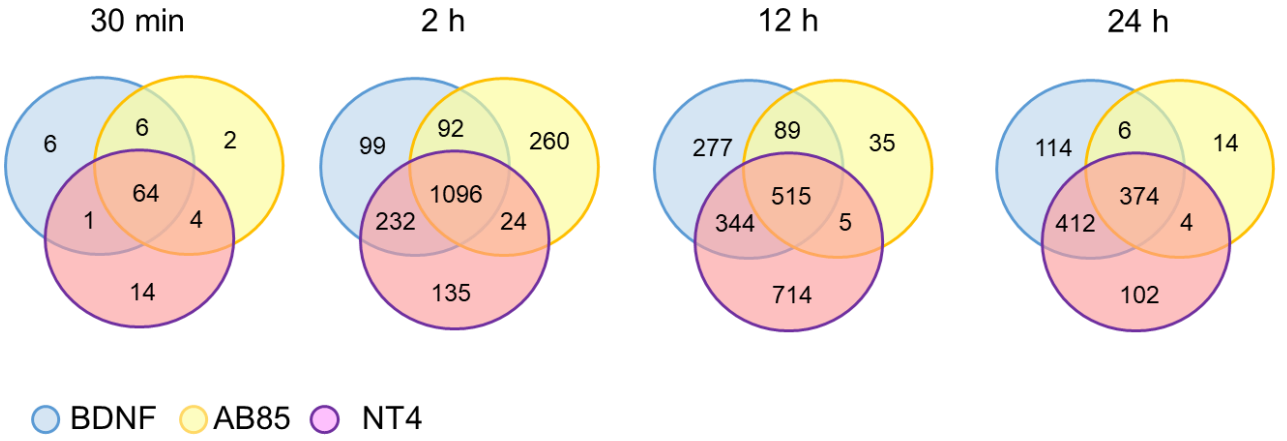

Figure 5.30 Venn diagrams illustrating the number of genes that are upregulated in the 3 treatment conditions (BDNF, AB85 and NT4) and 4 time points (30 min, 2 hours, 12 hours and 24 hours) in comparison to the untreated (control) cultures. The genes presented in this illustration are selected based on fold change > 1.5 and adjusted p value < 0.05 (A.), adjusted p value <0.01 (B.), adjusted p value < 0.001 (C.).

A.

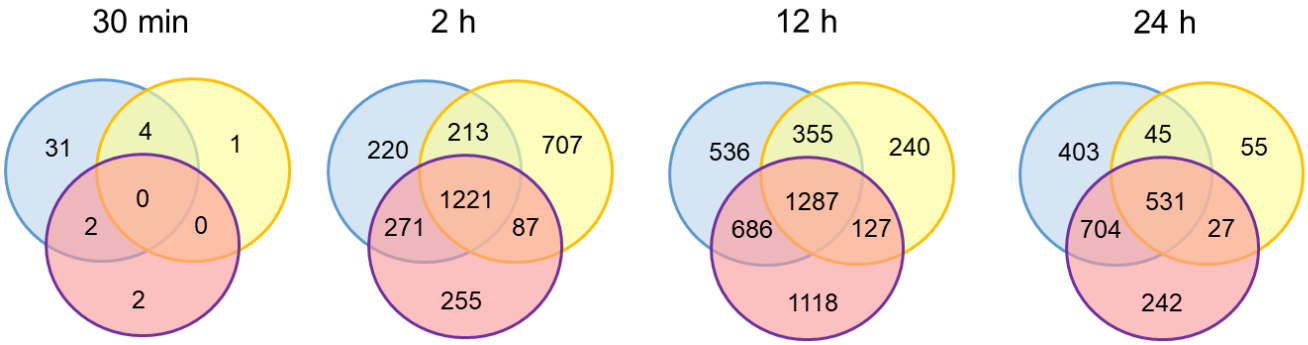

B.

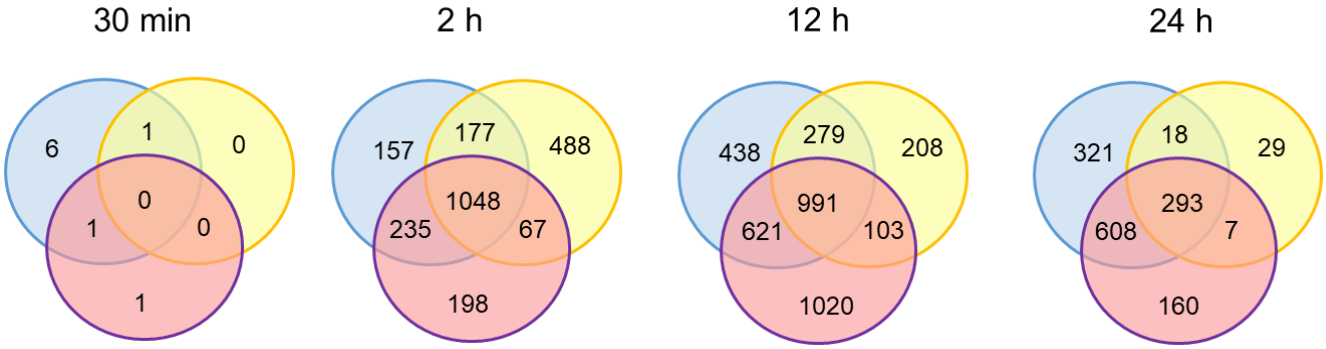

C.

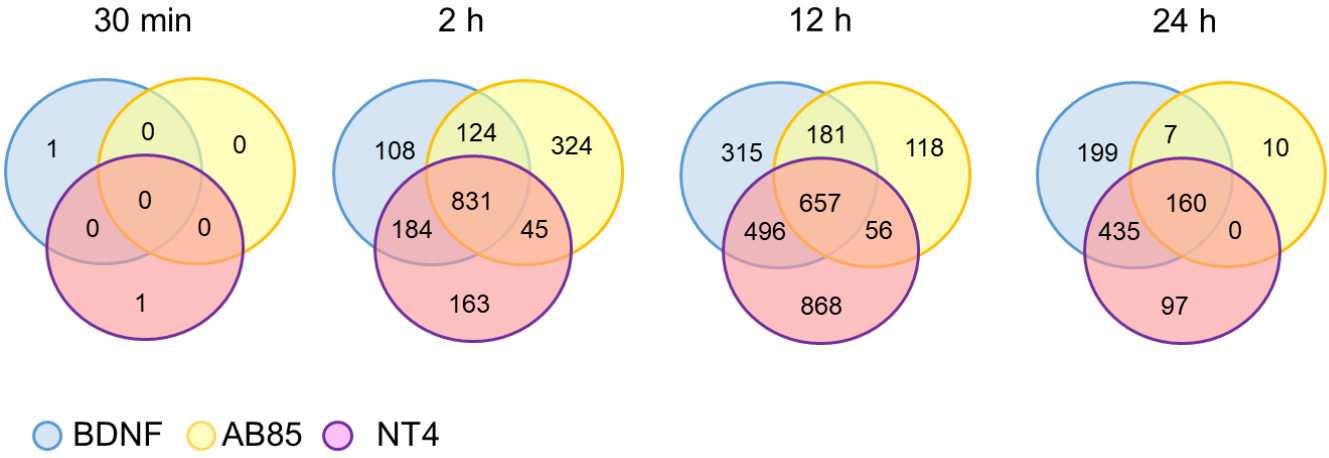

Figure 5.31 Venn diagrams illustrating the number of genes that are downregulated in the 3 treatment conditions (BDNF, AB85 and NT4) and 4 time points (30 min, 2 hours, 12 hours and 24 hours) in comparison to the untreated (control) cultures. The genes presented in this illustration are selected based on fold change < -1.5 and adjusted p value < 0.05 (A.), adjusted p value <0.01 (B.), adjusted p value < 0.001 (C.).

A.

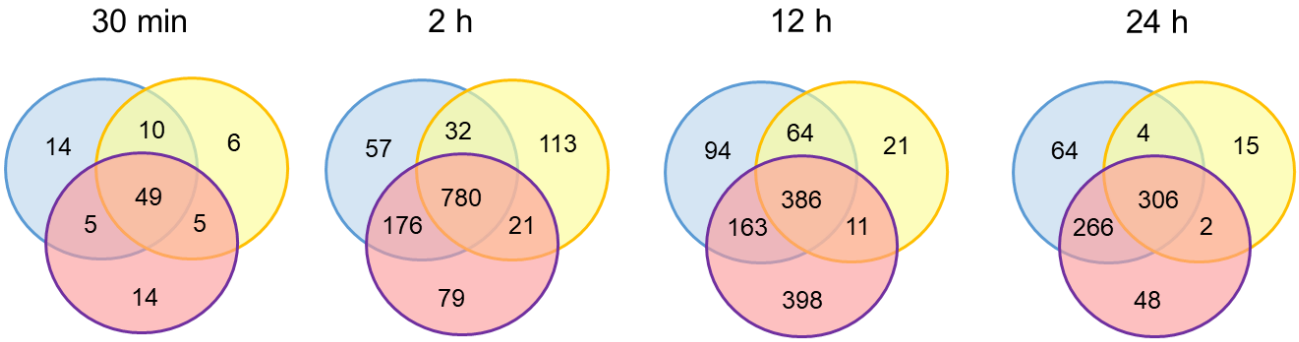

B.

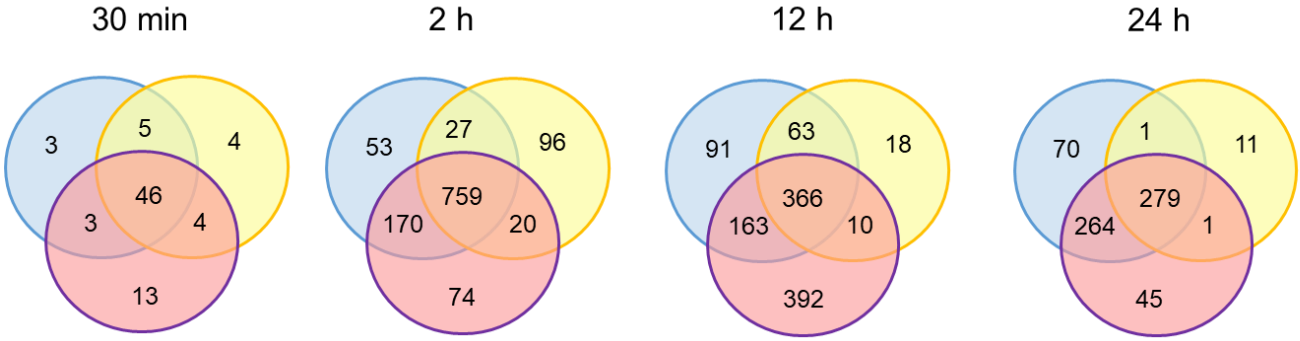

C.

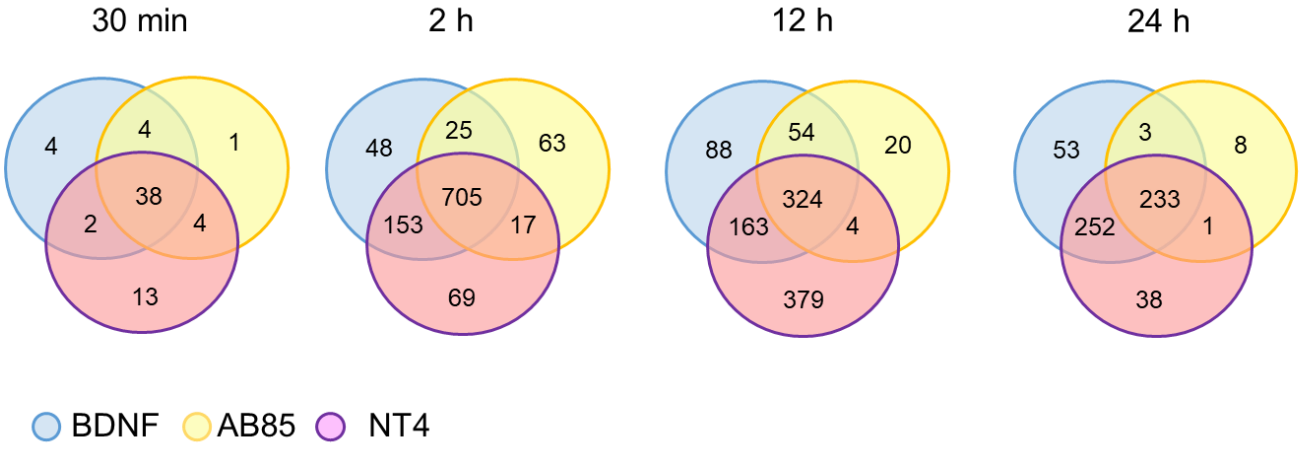

Figure 5.32. Venn diagrams illustrating the number of genes that are upregulated in the 3 treatment conditions (BDNF, AB85 and NT4) and 4 time points (30 min, 2 hours, 12 hours and 24 hours) in comparison to the untreated (control) cultures. The genes presented in this illustration are selected based on fold change > 2 and adjusted p value < 0.05 (A.), adjusted p value <0.01 (B.), adjusted p value < 0.001 (C.).

A.

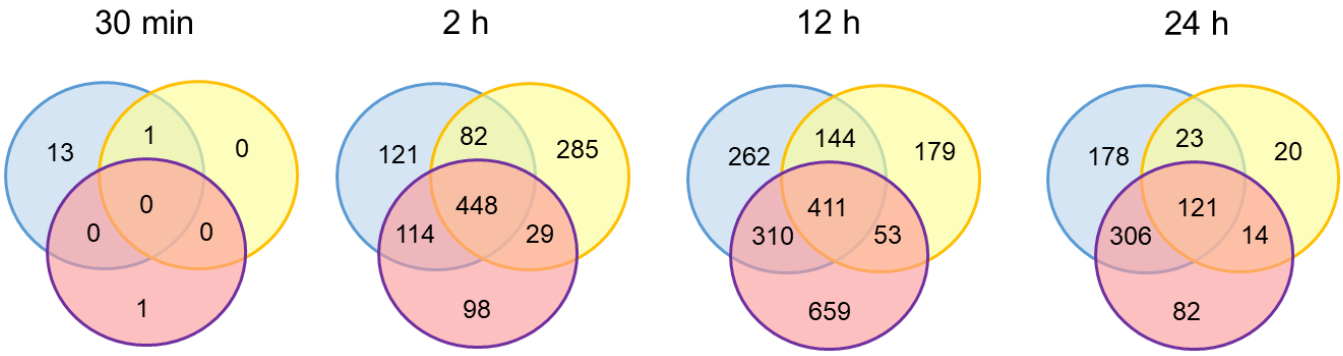

B.

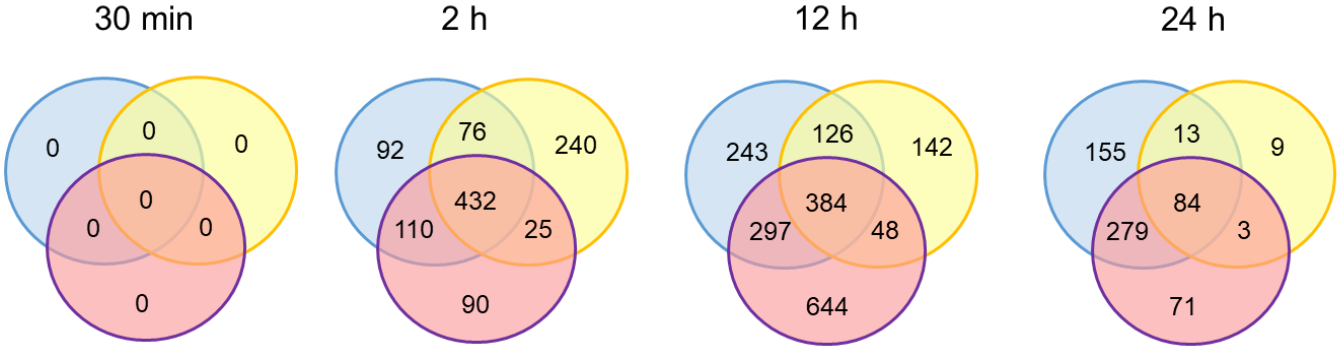

C.

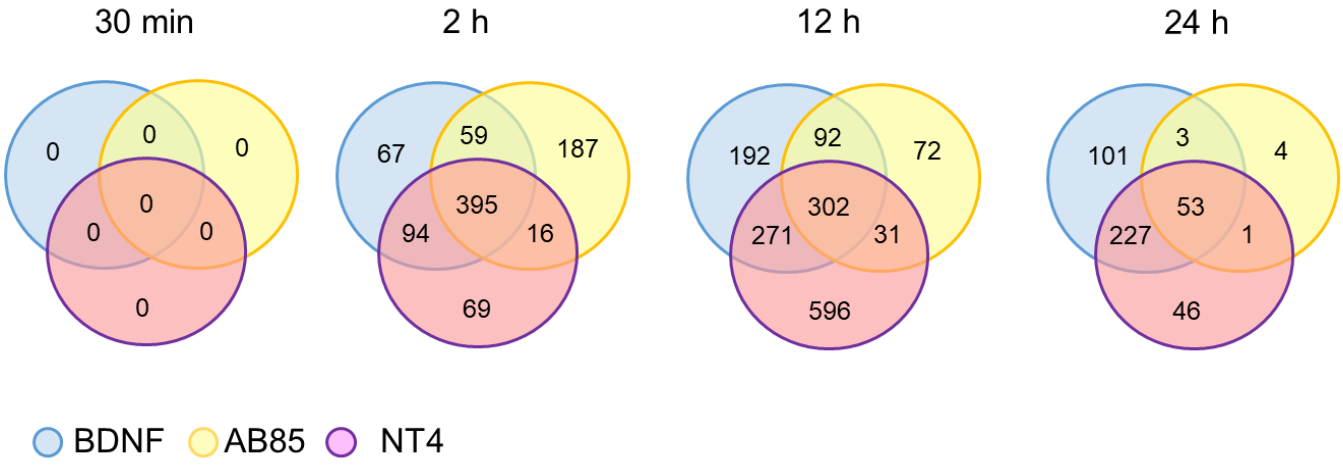

Figure 5.33 Venn diagrams illustrating the number of genes that are downregulated in the 3 treatment conditions (BDNF, AB85 and NT4) and 4 time points (30 min, 2 hours, 12 hours and 24 hours) in comparison to the untreated (control) cultures. The genes presented in this illustration are selected based on fold change < -2 and adjusted p value < 0.05 (A.), adjusted p value <0.01 (B.), adjusted p value < 0.001 (C.).

A.

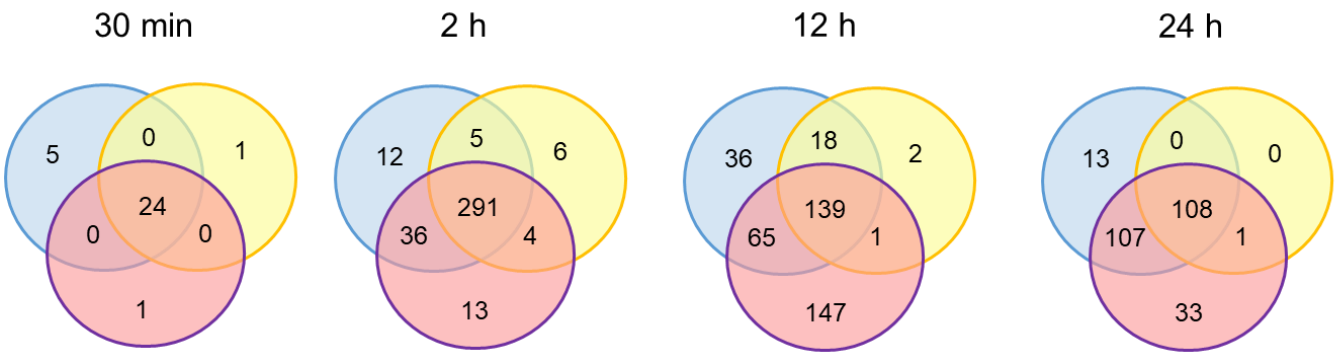

B.

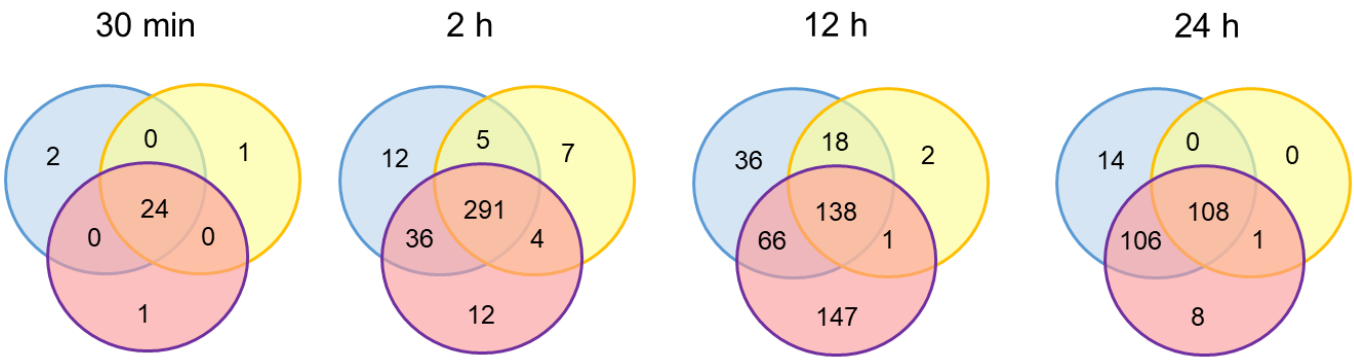

C.

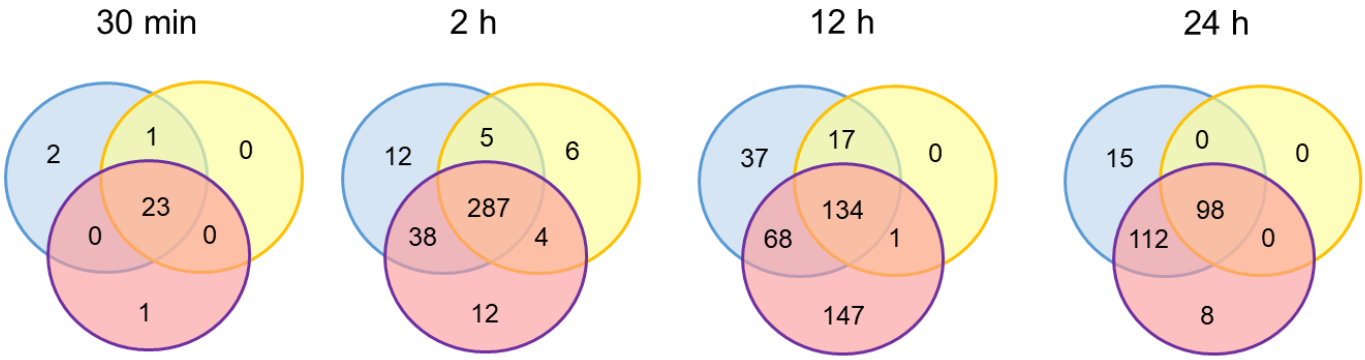

Figure 5.34 Venn diagrams illustrating the number of genes that are upregulated in the 3 treatment conditions (BDNF, AB85 and NT4) and 4 time points (30 min, 2 hours, 12 hours and 24 hours) in comparison to the untreated (control) cultures. The genes presented in this illustration are selected based on fold change > 4 and adjusted p value < 0.05 (A.), adjusted p value <0.01 (B.), adjusted p value < 0.001 (C.).

A.

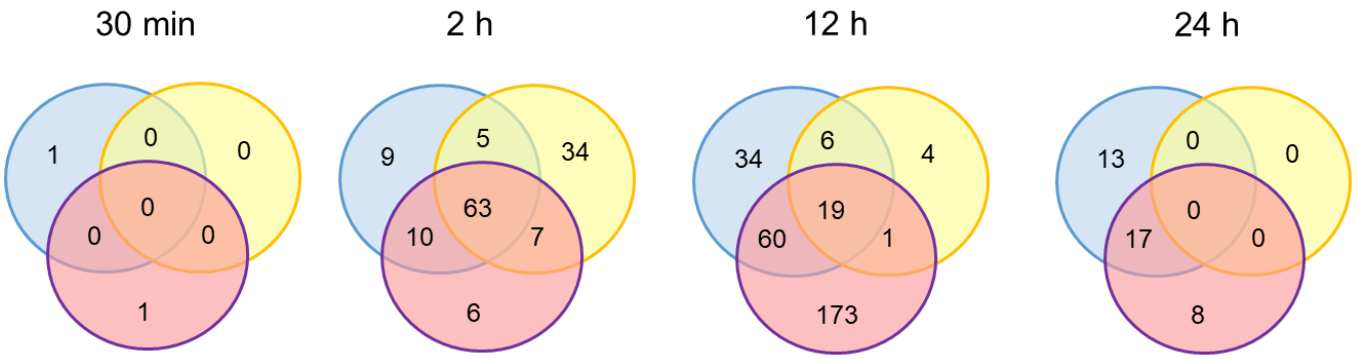

B.

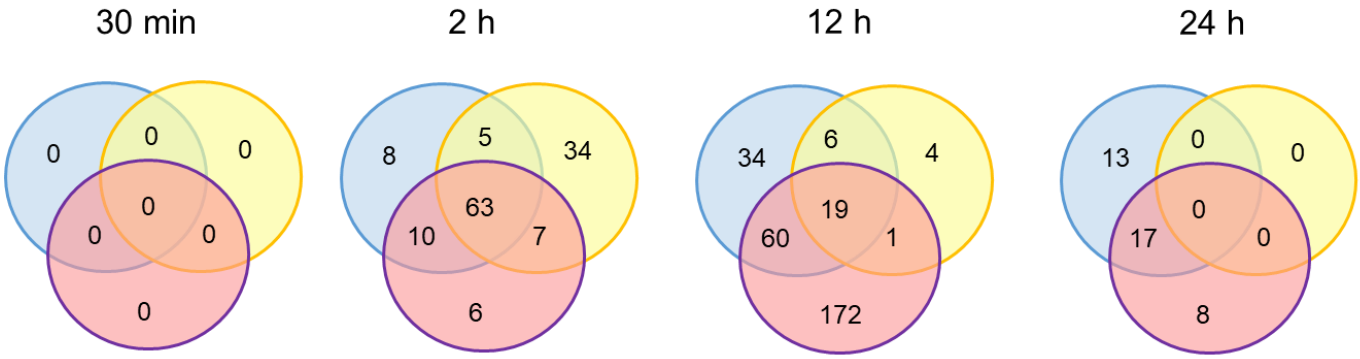

C.

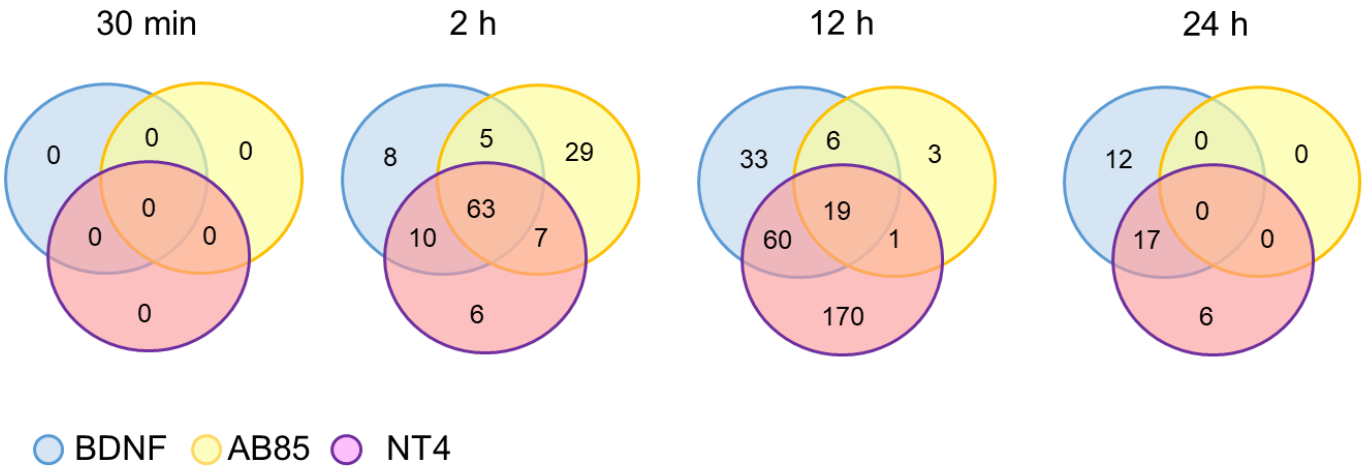

Figure 5.35 Venn diagrams illustrating the number of genes that are downregulated in the 3 treatment conditions (BDNF, AB85 and NT4) and 4 time points (30 min, 2 hours, 12 hours and 24 hours) in comparison to the untreated (control) cultures. The genes presented in this illustration are selected based on fold change < -4 and adjusted p value < 0.05 (A.), adjusted p value <0.01 (B.), adjusted p value < 0.001 (C.).

A.

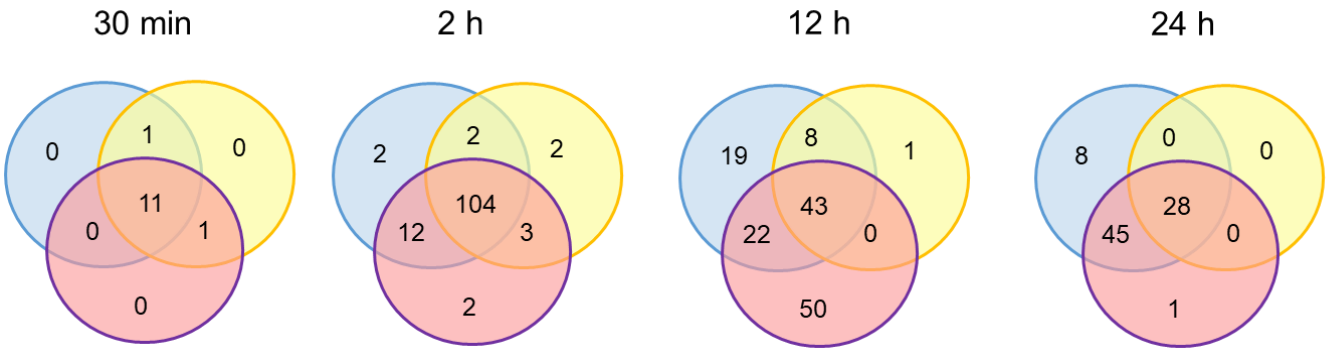

B.

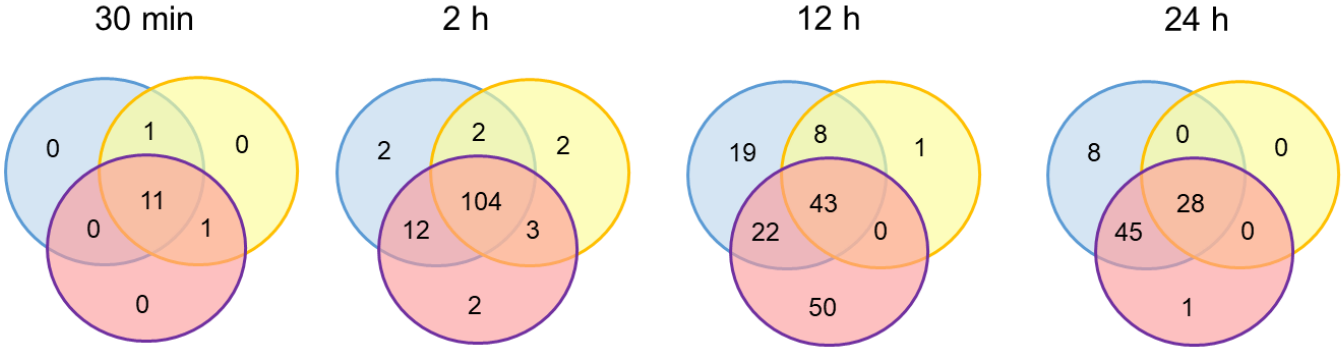

C.

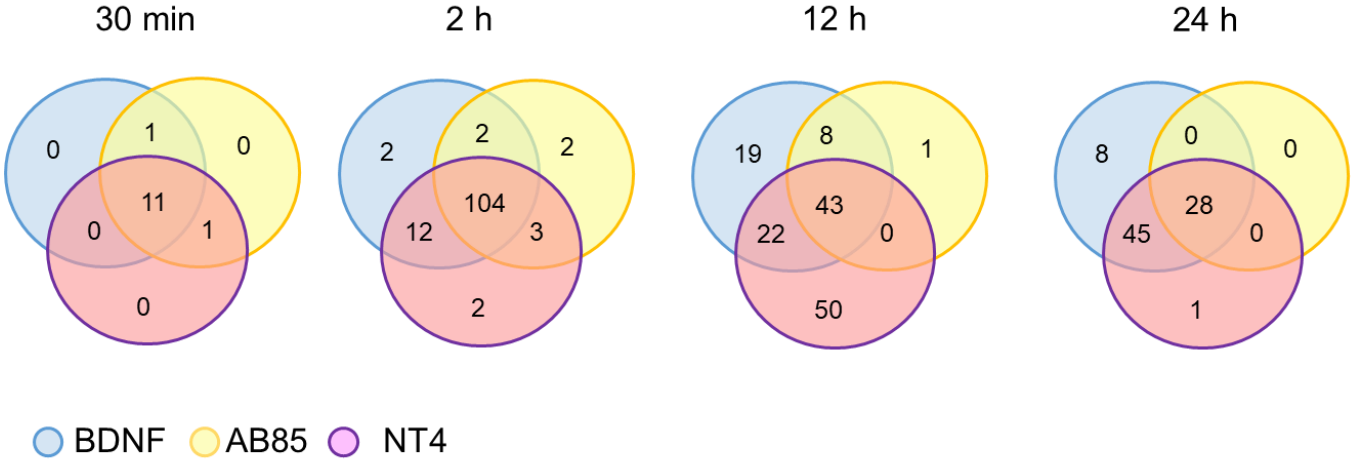

Figure 5.36 Venn diagrams illustrating the number of genes that are upregulated in the 3 treatment conditions (BDNF, AB85 and NT4) and 4 time points (30 min, 2 hours, 12 hours and 24 hours) in comparison to the untreated (control) cultures. The genes presented in this illustration are selected based on fold change > 10 and adjusted p value < 0.05 (A.), adjusted p value <0.01 (B.), adjusted p value < 0.001 (C.).

A.

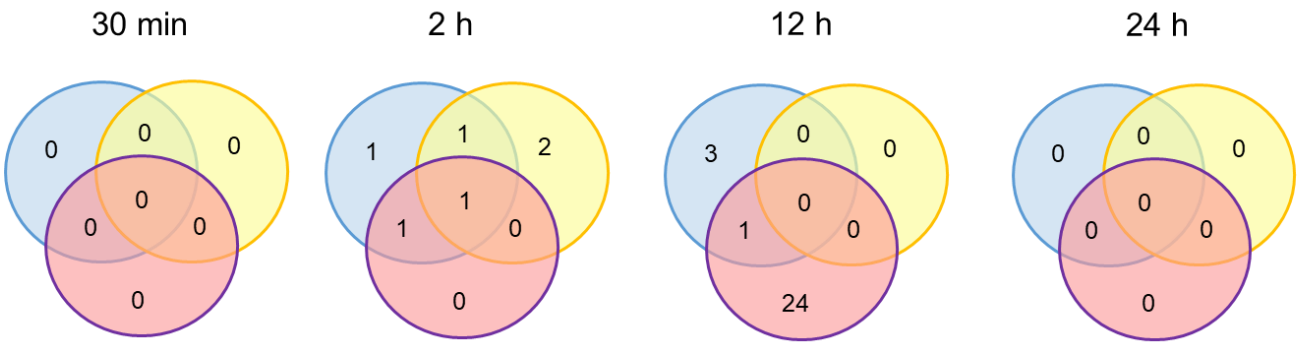

B.

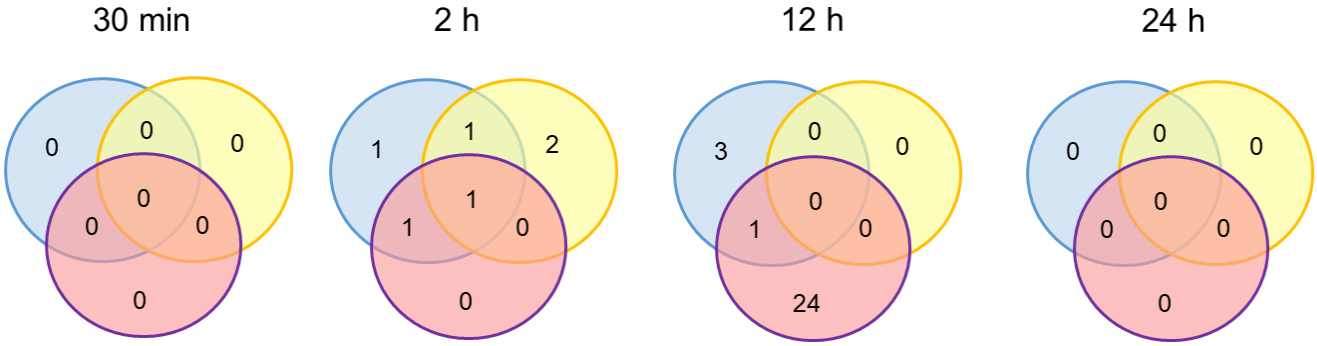

C.

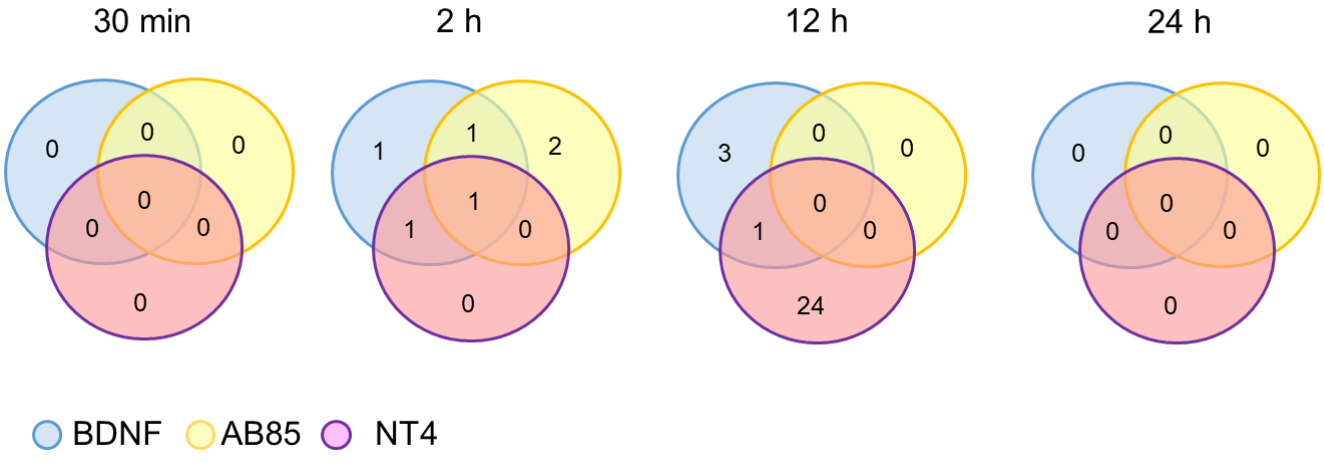

Figure 5.37 Venn diagrams illustrating the number of genes that are downregulated in the 3 treatment conditions (BDNF, AB85 and NT4) and 4 time points (30 min, 2 hours, 12 hours and 24 hours) in comparison to the untreated (control) cultures. The genes presented in this illustration are selected based on fold change < -10 and adjusted p value < 0.05 (A.), adjusted p value <0.01 (B.), adjusted p value < 0.001 (C.).

5.4.14 Venn diagram analysis of the genes upregulated between BDNF, AB85, NT4 in pairwise comparisons

So far, the cultures treated with one of the TrkB ligands have been compared to untreated cultures (controls). However, in this way it is not feasible to identify the number of genes that are differentially expressed in a significant manner between the TrkB ligands. For example, if gene A at 2 hours is upregulated by BDNF 0.9-fold compared to the control, 0.85-fold by AB85 and 1.2-fold by NT4, it will appear that this gene is uniquely upregulated by NT4, although the difference in the expression levels between the TrkB ligands are not more than 1.5 or 2-fold. In order to identify the genes that are truly differently regulated by each of the three TrkB ligands, limma voom comparisons were used in order to directly compare the cultures treated with BDNF, AB85 and NT4. The pair-wise comparisons of cultures treated with BDNF-AB85, BDNF-NT4, and AB85-NT4 were used to generate venn diagrams. Based on the literature and publications on RNA seq the p-adjusted value for these comparisons were set to 0.01. This value secures that there will be low number of false positives and it is not very strict that would result with false discard of positive results. Additionally, 3 levels of increase or decrease were applied, 1.5-fold, 2-fold and 4 -fold. At time-points 30 minutes and 2 hours no gene was found to be differentially upregulated between any of the pair-wise comparisons more than 1.5-fold with p-adjusted value 0.01. Therefore, there was no gene specifically increased by any of the three TrkB ligands at the first two time-points.

5.4.14.1 UPREGULATED GENES IN PAIRWISE COMPARISONS AT TIME-POINT 12 HOURS

On the contrary several hundred genes were found to be upregulated in the pair-wise comparisons at time-point 12 hours. Interestingly the number of genes that are shared between the three TrkB ligands increased upon increasing the threshold of change. More specifically 2578 genes were shared between BDNF, AB85 and NT4 at 12 hours when the fold change was set to 1.5, while 3250 genes were shared at fold change 2 and 3756 genes were shared at fold change 4. Interestingly when the fold change was set to 1.5 there are far more genes increased by NT4 (604) than with BDNF (34) or AB85 (44). Upon shifting the threshold of change at 2-fold the number of genes specifically increased by any of the three TrkB ligands was reduced. Indeed, 9 genes

were upregulated more than 2-fold by BDNF, 12 were upregulated more than 2 -fold by AB85 and 327 were upregulated more than 4-fold by NT4. Subsequently 25 genes were upregulated by BDNF between 1.5 and 2-fold, 32 genes were upregulated by AB85 between 1.5 and 2-fold and 277 genes were upregulated by NT4 between 1.5 and 2-fold. No genes are found to be upregulated more than 4-fold by BDNF or AB85, and 61 genes are upregulated more than 4-fold by NT4. Thus 9 genes are increased by BDNF between 2 and 4-fold, 12 genes are increased by AB85 between 2 and 4-fold and 266 genes are increased by NT4 between 2 and 4-fold.

5.4.14.2 UPREGULATED GENES IN PAIRWISE COMPARISONS AT TIME-POINT 24 HOURS

At the last time-point 24 hours the number of genes differentially upregulated by the three TrkB ligands is greatly reduced compared to the corresponding number in the time-point of 12 hours. Additionally, there is almost no difference in the number of genes specifically by BDNF, AB85 or NT4. More specifically no gene is upregulated by BDNF or NT4 more than 1.5-fold and 50 genes are upregulated more than 1.5-fold by AB85 compared to BDNF and NT4. Upon shifting the threshold of change to 2, only 4 genes are upregulated more than 2-fold by AB85. Thus 46 genes were upregulated by AB85 between 1.5 and 2-fold. No gene is upregulated more than 4-fold by any of the three TrkB agonists.

A.

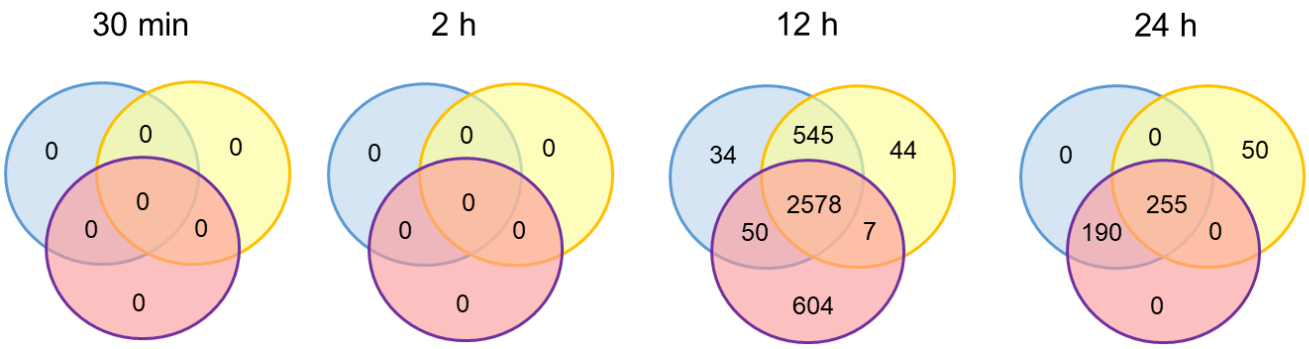

B.

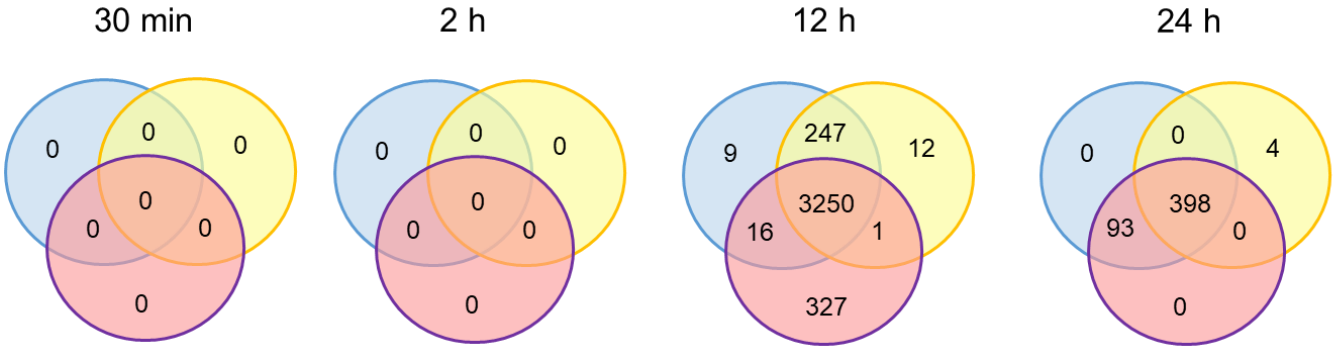

C.

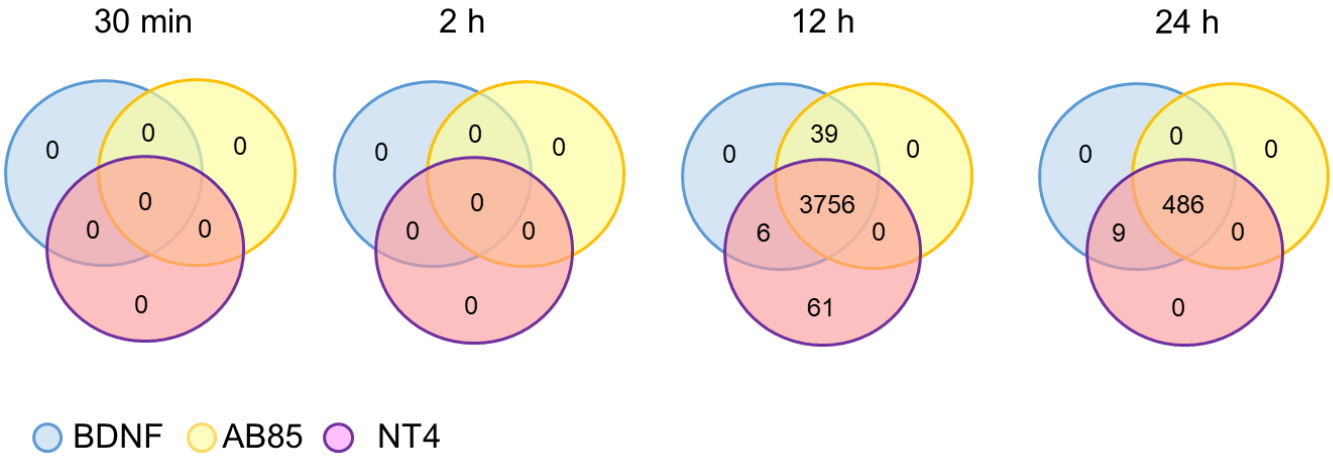

Figure 5.38 Venn diagrams illustrating the number of genes that are upregulated in the 3 treatment conditions (BDNF, AB85 and NT4) and 4 time points (30 min, 2 hours, 12 hours and 24 hours) upon comparison of the three TrkB ligands with each other. The genes presented in this illustration are selected based on adjusted p value < 0.01 and fold change > 1.5 (A.), fold change > 2 (B.), fold change > 4 (C.).

5.4.15 Genes upregulated more than 2-fold by BDNF in pairwise comparisons with AB85 and NT4 at time-point 12 hours

9 genes were upregulated more than 2-fold by BDNF in pairwise comparisons with AB85 and NT4 at time-point 12 hours (Table 5.9). EGR1 is an immediate early response gene and was discussed above. It is upregulated more than 51-fold by BDNF, about 20-fold by NT4 and about 19-fold by AB85. EGR2 is also an immediate early response gene discussed above and it is upregulated more than 16-fold by BDNF, 6-fold by AB85 and 5-fold by NT4. XIPR1 (xin-actin-binding repeat containing 1) is a striated muscle-specific protein located at the myotendinous junction in skeletal muscle and it is a marker of muscle damage and it is found upregulated in myopathies (Nilsson et al., 2013). XIPR1 has an important role in cardial conduction and rare variants of the gene were linked with sudden unexplained nocturnal death (Huang et al., 2018). NPY2R is a member of the neuropeptide Y receptor family of G-protein coupled receptors. SNPs in *NPY2R* have been associated with alcohol dependence, alcohol and cocaine dependence, alcohol withdrawal and cocaine dependence in a study with a sample of 1,923 people (Wetherill et al., 2008). Notably an SNP in *NPY2R* promoter has been associated with later onset of HD disease in humans, and activation of the receptor in PC12 mutant htt cells had neuroprotective effect (Kloster et al., 2014). LRRC70 (Leucine Rich Repeat Containing 70) also known as synleurin is a single span transmembrane leucine-rich repeat protein with involvement in cytokine stimulation (Wang et al., 2003). *AMIGO2* or amphoterin induced gene is a downstream target of calcium-dependent signals and enhances neuronal survival. AMIGO2 mRNA was located in the CA2/CA3 hippocampal region in mouse brain and it had a similar localization pattern with growth factors and proteins linked to neuronal survival signaling (Laeremans et al., 2013). Another study found that AMIGO2 is expressed by starbust amacrine cells (SACs) and rod bipolar cells, two retinal interneurons and controls their dendritic arborization (Laeremans et al., 2013). CMKLR1 (Chemerin receptor chemokine-like Receptor 1) is a G protein-coupled receptor expressed by dorsal root ganglion and spinal cord neuronal cells. It is also a functional receptor of $A\beta_{42}$ and it is implicated in microglia-mediated Aβ degradation and clearance (Haque et al., 2018). $A\beta_{42}$ promoted CMKLR1- dependent cell migration via activation of ERK1/2, PKA and Akt pathways (Peng et al., 2015). Rac2 (Ras-

related C3 botulinum toxin substrate 2) is a member of the Rac subfamily of the family of Rho family of GTPases. It is mainly expressed in the hematopoietic system and Rac2 $^{-/-}$ mice are viable and fertile but present defects in the hematopoietic system (Pedersen and Brakebusch, 2012). CD82 (Cluster of Differentiation 82) is a glycoprotein transmembrane protein and a suppressor of metastasis in various solid tumors (Pehkonen et al., 2018). In human metastatic cancer CD82 was downregulated and CD82+ positive tumors of the lung had good prognosis (Dong et al., 1996, Adachi et al., 1996). CD82 was found to be coexpressed with CC1 and olig2 and overexpression of CD82 in immature cells of the neonatal forebrain SVZ forced them into differentiation to $CC1^{+}$ and MBP^{+} myeninating oligodentrocytes. In line with this result, shRNA against CD82 targeting CD82 in SVZ cells *in vivo* diminished their differentiation potential into myelinating oligodendrocytes (Mela and Goldman, 2009).

GeneID	Symbol	GeneName	adj.P.Val B/A	adj.P.Val B/N	FC BDNF 12h	FC AB85 12 h	FC NT4 12 h
ENSG00000120738	EGR1	early growth response 1	5,27433E-11	4,05478E-13	51,07560598	20,58720655	19,30685181
ENSG00000122877	EGR2	early growth response 2	2,83163E-05	2,43418E-07	16,8715902	6,020746771	5,034896775
ENSG00000168334	XIRP1	xin actin binding repeat containing 1	9,19142E-05	0,000183801	21,83217662	7,863949235	9,886994565
ENSG00000185149	NPY2R	neuropeptide Y receptor Y2	0,000193461	1,90815E-08	9,096754292	2,809270715	1,379722653
ENSG00000186105	LRRC70	leucine rich repeat containing 70	0,002086024	8,37447E-05	6,929508627	2,628316514	2,336066682
ENSG00000139211	AMIGO2	adhesion molecule with Ig like domain 2	0,002215848	1,03992E-07	1,269866476	-1,585684719	-2,78345446
ENSG00000174600	CMKLR1	chemerin chemokine-like receptor 1	0,002665341	1,87839E-05	3,444182464	1,723527806	1,392577146
ENSG00000128340	RAC2	Rac family small GTPase 2	0,004231045	6,21586E-08	8,540941671	3,058653522	1,241644264
ENSG00000085117	CD82	CD82 molecule	0,007047963	3,39293E-05	3,089259875	1,449610088	1,286319909

TABLE 5.9 Table with genes preferentially upregulated only by BDNF at time point 12 hours with adjusted p value <0.01 and fold change > 2.

5.4.16 Genes preferentially downregulated more than 2-fold by BDNF and NT4 together in pairwise comparisons with AB85 at time-point 12 hours

Next the genes selectively upregulated more than 2-fold by AB85 compared to BDNF and NT4 at the time-point of 12 hours were examined. 12 genes were detected and all of them were down-regulated by all three TrkB ligands in comparison with the control cultures, and these genes were downregulated more than 2-fold (padj<0.01) by both BDNF and NT4 compared to AB85. MAP2K6 (dual specificity mitogen-activated protein kinase kinase 6) is a member of the dual specificity protein kinase family and its expression in cultured cells led to increase in p38 MAP kinase activity and enhanced gene expression controlled by the transcription factors ATF2 and Elk-1 (Raingeaud et al., 1996). It was also shown to act as a upstream regulator of Rho family GTPases (Kim et al., 2010). WNT7B (Wnt Family Member 7B) is expressed in the hippocampus during dendritogenesis and it is involved in denditric arborization (Rosso et al., 2005) , which is achieved through phosphorylation of CAMKII and JNK proteins (Ferrari et al., 2018) SMPDL3B (Sphingomyelin Phosphodiesterase Acid Like 3B) is a lipid-modulating phosphodiesterase expressed on macrophages and it is involved in membrane lipid composition and fluidity (Heinz et al., 2015). SCML4 (Scm Polycomb Group Protein Like 4) is a putative polycomb group (PcG) protein. PcC proteins are known to compose multiprotein complexes that are necessary for the preservation of the transcriptionally repressive state of homeotic genes in development (Heinz et al., 2015). SHH (Sonic Hedgehog Signaling) is a protein with key role in early embryo patterning. It is the major signal for the patterning of the ventral neural tube, the anterior-posterior limb axis and it interacts with several pathways such as Wnt/ β-catenin and BMP. It is also involved in neural regeneration upon injury of facial motor neurons upon facial nerve axotomy (Belgacem et al., 2016). FREM 2 (FRAS1-related extracellular matrix protein 2) is an extracellular matrix protein that is indispensable for the preservation of skin epithelium *in utero* and for the maintenance of renal epithelium structure in adult mice. A missense mutation in this gene was also linked to Fraser syndrome, a recessive multisystem disorder of syndactyly and renal defects (Jadeja et al., 2005) . DACT2 (Dishevelled Binding Antagonist Of Beta Catenin 2) is described as a tumor suppressor, and DACT2 methylation was observed in colon cancer tissues and was correlated with decrease in overall survival (Wang et al.,

2015). Five long non-coding RNA are also included in the 12 genes that are differentially upregulated more than 2-fold by AB85 compared to BDNF and NT4, with unknown function.

GeneID	Symbol	GeneName	adj.P.Val A/B	adj.P.Val A/N	FC BDNF 12 h	FC AB85 12h	FC NT4 12 h
ENSG00000108984	MAP2K6	mitogen-activated protein kinase kinase 6	8,52431E-07	4,81473E-08	-5,047673327	-2,05915691	-4,93675946
ENSG00000188064	WNT7B	Wnt family member 7B	8,60147E-06	1,37417E-12	-8,565552361	-3,86627269	-19,4977187
ENSG00000130768	SMPDL3B	sphingomyelin phosphodiesterase acid like 3B	1,81325E-05	6,70615E-05	-6,632223486	-2,86767349	-6,42949805
ENSG00000267194	RP1-193H18.2	lincRNA	3,0291E-05	1,10809E-06	-5,996531886	-2,28432605	-6,28039402
ENSG00000146285	SCML4	Scm polycomb group protein like 4	5,24251E-05	1,34415E-11	-5,086182543	-2,4136207	-11,0837836
ENSG00000164690	SHH	sonic hedgehog	0,000781075	1,17953E-07	-6,419559642	-3,08565053	-8,56844733
ENSG00000227050	RP11-460I13.2	lincRNA	0,001887875	0,003635514	-4,380579244	-2,18389087	-4,75645833
ENSG00000278934	CTD-2006M22.2	lincRNA	0,00229416	5,09077E-09	-4,035210047	-1,96547738	-8,24083028
ENSG00000255402	RP11-696P8.2	lincRNA	0,00399965	0,000144634	-3,713119568	-1,63470841	-3,92669751
ENSG00000150893	FREM2	FRAS1 related extracellular matrix protein 2	0,005154274	1,5906E-05	-3,592067852	-1,45563126	-5,36721065
ENSG00000253878	RP11-347C18.3	lincRNA	0,005154274	1,82107E-06	-2,455527954	-1,20679021	-3,21880387
ENSG00000164488	DACT2	dishevelled binding antagonist of beta catenin 2	0,008294565	0,002596425	-4,873958862	-2,40821484	-4,95859849

TABLE 5.10 Table with genes preferentially downregulated by BDNF and NT4 in comparison to AB85 at time point 12 hours with adjusted p value <0.01 and fold change > 2.

5.4.17 Genes upregulated more than 2-fold by NT4 in pairwise comparisons with BDNF and AB85 at time-point 12 hours

Next, the genes upregulated more than 2-fold by NT4 at time-point of 12 hours were examined. Since 327 genes were detected, the best approach to characterise this result was GO analysis (Table 5.11). 80 genes were classified as relevant to animal organ development, 62 genes to anatomical structure morphogenesis, 27 to tube development, and 27 to embryo development. Interestingly, 65 genes belong to the cell surface receptor signalling pathway.

Enrichment FDR	Genes in list	Total genes	Functional Category
2,28E+09	80	3779	Animal organ development
0.000162567239951614	62	2785	Anatomical structure morphogenesis
0.00167140306459228	65	3287	Cell surface receptor signaling pathway
0.00167140306459228	31	1099	Animal organ morphogenesis
0.00167140306459228	49	2168	Tissue development
0.00167140306459228	32	1164	Anatomical structure formation involved in morphogenesis
0.00184423940471473	66	3382	Regulation of multicellular organismal process
0.0027921352256556	10	152	Response to purine-containing compound
0.00306185165536494	16	392	Extracellular matrix organization
0.00522717179484694	46	2165	Cell proliferation
0.00522717179484694	17	460	Extracellular structure organization
0.00522717179484694	9	137	Response to organophosphorus
0.00747108587421049	11	218	Osteoblast differentiation
0.00885666425738474	13	307	Renal system development
0.00924991778702818	35	1541	Cell adhesion
0.00924991778702818	27	1054	Embryo development
0.00924991778702818	33	1412	Neuron differentiation
0.00924991778702818	41	1911	Positive regulation of multicellular organismal process
0.00924991778702818	31	1286	Negative regulation of multicellular organismal process
0.00948599802829298	35	1548	Biological adhesion
0.00948599802829298	27	1062	Tube development
0.00949294976232595	18	565	Sensory organ development
0.0115915376980393	35	1575	Generation of neurons
0.0118372650196076	10	205	Muscle cell proliferation
0.0123245304991082	7	99	Response to cAMP
0.0123762993684236	23	860	Tube morphogenesis
0.0123762993684236	13	339	Cell chemotaxis
0.0138944579851198	63	3547	Response to organic substance
0.0140746017196578	13	346	Urogenital system development
0.0149091368487253	36	1683	Neurogenesis

TABLE 5.11 G0 analysis of 327 genes preferentially upregulated by NT4 compared to BDNF and AB85 at time-point 12 hours

5.4.18 Genes upregulated more than 4-fold by NT4 in pairwise comparisons with BDNF and AB85 at time-point 12 hours

Next the genes selectively upregulated more than 4-fold in the pairwise comparisons of the TrkB ligands between each other were examined. No genes are upregulated more than 4-fold by BDNF or AB85 in these pairwise comparisons. 42 genes are upregulated more than 4-fold by NT4 in comparison to BDNF and AB85 and they are listed in table 5.12. Amongst them are 10 lincRNA genes and 1 pseudogene. The gene with the highest difference in the mRNA expression levels between the three TrkB ligands in this subset of genes is PMCH (Pro-Melanin Concentrating Hormone) which is expressed 25.8- fold more in NT4 treated cultures, than BDNF treated cultures, and 42.9- fold more in NT4 treated cultures than AB85 treated cultures. Upon cleavage, MCH neuropeptide (Melanin-concentrating hormone) is produced, and it is expressed in CNS and PNS with involvement in the regulation of energy metabolism and feeding behaviors (An et al., 2001). The next gene in terms of the magnitude of expression preferentially induced by NT4 treatment compared to BDNF and AB85 treatment is RP11-472I20.3, which is expressed 26.4- fold more in NT4 than in BDNF treated cultures, and 22.6- fold more in NT4 than in AB85 treated cultures. The function of this lncRNA is unknown. MYH15 (Myosin Heavy Chain 15) is classified as a genetic risk factor for ALS, and it was found to control the toxicity of dipeptides produced from expanded G_4C_2 repeat (Kim et al., 2019). It is expressed 12.8- fold more in NT4 than in BDNF treated cultures, and 16.3-fold more in NT4 than in AB85 treated cultures. WBSCR17 is a N-acetylgalactosaminyltransferase and it is located in the genomic area that is deleted in the Williams-Beuren syndrome (WBS), a developmental disorder. TSHR (thyrotropin receptor) is a member of the G protein-coupled receptor superfamily and it is the receptor for the thyroid-stimulating hormone and it enhances the stimulation of thyroxine (T4) and thriodothyronine (T3) (Szkudlinski et al., 2002). PARPBP (PARP1 Binding Protein) is a replisome associated protein, which is necessary for the suppression of replication stress in proliferating undifferentiated cells and PARI knockout led to stochastic chromosome instability in mouse ES cells but not in fibroblasts(Mochizuki et al., 2017). GABRQ is the theta subunit of the GABA A receptor, which is the major inhibitory neurotransmitter in the CNS (Watanabe et al.,

2002). ANXA3 (Annexin A3) is known to bind to membrane phospholipids in a Ca^{2+} dependent manner and participate in cell differentiation and migration (Gerke et al., 2005). Overexpression of this gene promotes tumor proliferation and metastasis in lung, liver, ovarian carcinoma, and knockdown in *in vivo* and vitro blocked breast cancer cell invasion (Du et al., 2018) GLSTN2 (Calsyntenin 2) is mainly expressed in motorneurons and in the late stages of cerebellar development it is expressed in a subset of Purkinje cells (de Ramon Francas et al., 2017). Furthermore, Clstn2 $^{-/-}$ mice were hyperactive and had deficits in spatial learning and memory (Lipina et al., 2016) In line with this results, *CLSTN2* alleles in humans were related with delayed word recall (Papassotiropoulos et al., 2006, Jacobsen et al., 2009). MCUB (Mitochondrial Calcium Uniporter Dominant Negative Subunit Beta) is involved in calcium homeostasis, through regulation of the activity of the mitochondrial inner membrane calcium uniporter (MCU) by modulation of the calcium uptake into the mitochondria (Jacobsen et al., 2009). NDRG1 (N-myc downstream regulated gene 1) is an intracellular protein with a role in cell differentiation. The overexpression of this protein was associated with enhanced cell proliferation, migration and invasion in bladder cancer. DHRS9 (Dehydrogenase/Reductase 9) is identified as a specific marker for *in vitro* generated regulatory Macrophages (Mregs) (Riquelme et al., 2017). It is upregulated 18.7-fold in NT4 treated cultures compared to BDNF treated cultures, and 21-fold compared to AB85 treated cultures. GNAS-AS1 (GNAS Antisense RNA 1) was found to be involved in proliferation, migration and cell invasion of nasopharyngeal cancer cells *in vitro* and it acts through Wnt/β-catenin pathway (Wang et al., 2020b). PLPP4 (Phospholipid Phosphatase 4) is a phoshatidate phosphatase expressed in the brain, kidney and testis (Takeuchi et al., 2007) and higher levels of this protein have been described in lung carcinoma cells (Zhang et al., 2017). KRT75 (Keratin 75) belongs to the keratin family and is important in hair and nair formation, as mice expressing a mutant form of the gene developed hair and nail defects (Chen et al., 2008). It is upregulated 15.3-fold in NT4 treated cultures compared to BDNF treated cultures, and 15,4-fold in AB85 treated cultures. GPAT3 (Glycerol-3-Phosphate Acyltransferase 3) is an enzyme that is essential in adipogenesis and lipid formation (Yu et al., 2018). HSPB3 Heat Shock Protein Family B (Small) Member 3 is important in myogenic differentiation (Sugiyama et al., 2000) and it was discovered that it enhances survival of motoneurons in chick embryo upon lesion-induced degeneration (Sugiyama et al., 2000). GPC6 (Glypican Proteoglycan 6) belongs to the family of

glycosylphosphatidylinositol-anchored heparan sulfate proteoglycans and it is involved in skeletal growth, as mutations in this gene cause omodysplasia (Campos-Xavier et al., 2009) CHST3 (Carbohydrate Sulfotransferase 3) is an enzyme that catalyzes the sulfation of chondroitin, a proteoglycan of the extracellular matrix and mutations in this gene were linked with spondyloepiphyseal dysplasia and hearing loss in humans (Waryah et al., 2016). MET codes for a receptor tyrosine-kinase c-MET that binds hepatocyte growth factor (HGF) and upon binding activates downstream signaling pathways involved in cell migration, profileration and angiogenesis. MET is a proto-oncogene with high expression in various cancers, such as non-small cell lung cancer (NSCLC), gastrointestinal (GI) cancer, and hepatocellular carcinoma (HCC) (Mo and Liu, 2017).NR5A2 (Nuclear Receptor Subfamily 5 Group A Member 2) controls glucose and lipid metabolism but is also necessary for T cell maturation (Seitz et al., 2019). GCSAM (Germinal Center Associated Signaling And Motility) is expressed in lung cell carcinoma, and hypomethylation of this gene is linked with longer survival (Li et al., 2019). IL1R1 (Interleukin 1 Receptor Type 1) is a cytokine receptor that is part of immune and inflammatory responses and it mediates celastrol metabolism. *Il1r1*$^{-/-}$ mice had lower levels of phosphorylated p38 and phosphorylated Erk1 and Erk2 compared to wild-type mice and were obese *(Feng et al., 2019)*.TMEM233 (Transmembrane Protein 233) is a protein coding gene with unknown function. CDCP1 (CUB Domain Containing Protein 1) is a transmembrane protein which is expressed in highly aggressive triple-negative breast cancer cells (Turdo et al., 2016). CNGA3 (Cyclic Nucleotide Gated Channel Subunit Alpha 3) is a member of the cyclic nucleotide-gated cation channel protein family and it is indispensable for normal vision and olfactory signal transduction. Mutations of this gene are correlated with achromatopsia (Zobor et al., 2017). PMP22 (Peripheral Myelin Protein 22) is a transmembrane glycoprotein and an important component of myelin in the peripheral nervous system. It is dysregulated in several neuropathies, including Charcot–Marie–Tooth type 1A (CMT1A), Dejerine–Sottas disease, and Hereditary Neuropathy with Liability to Pressure Palsy (HNPP)(Li et al., 2013). *RGS20* (Regulator of G Protein Signaling 20) belongs to the family of regulator of G protein signaling (RGS) proteins, it selectively binds to G(z)-alpha and G(alpha)-i2 subunits, and controls their downstream signaling (Wang et al., 2002). *TFPI2* (Tissue Factor Pathway Inhibitor 2) is a member of the Kunitz-type serine proteinase inhibitor family and it is a tumor suppressor gene, which is commonly silenced in gastric cancer

(Takada et al., 2010). *MIR431* (MicroRNA 431) is a microRNA with unknown function. SLC16A6 (Solute Carrier Family 16 Member 6) transports monocarboxylic acids in various tissues and is linked with height regulation in humans (Karanth and Schlegel, 2018). SERTM2 (Serine Rich and Transmembrane Domain Containing 2) is a protein coding gene with unknown function. MMP12 (Matrix Metallopeptidase 12) is a peptidase of the family of matrix metalloproteinases, which is involved in macrophage migration and is also known to regulate inflammation though cleavage of IFNγ, that makes the cytokine unable to transfer the signal via its receptor (Dufour et al., 2018). *APCDD1L* (APC Down-Regulated 1 Like) is a protein coding gene with unknown function.

GeneID	Symbol	adj.P.Val N/B	adj.P.Val N/A	FC BDNF 12 h	FC AB85 12	FC NT4 12 h
ENSG00000144821	MYH15	1,62272E-23	3,33013E-24	1,504926667	1,184307343	19,40739392
ENSG00000185274	WBSCR17	5,69849E-22	2,24606E-21	-1,883984017	-1,717782888	2,671552868
ENSG00000165409	TSHR	9,97903E-18	1,33668E-18	1,993856083	1,508781068	18,80645284
ENSG00000185480	PARPBP	3,14153E-15	2,84132E-16	1,291687977	-1,139728472	13,15001448
ENSG00000268089	GABRQ	1,68543E-14	1,04987E-15	-1,131286652	-1,391765577	5,11599736
ENSG00000183395	PMCH	3,29041E-14	1,62953E-14	1,806785933	1,086507325	46,68856098
ENSG00000138772	ANXA3	3,8556E-13	2,85929E-14	2,251372507	1,859752943	10,36558689
ENSG00000158258	CLSTN2	4,05478E-13	1,11504E-13	1,154218747	1,104789738	4,876898166
ENSG00000005059	MCUB	4,4473E-13	1,04346E-14	5,246594236	3,914778718	21,9670988
ENSG00000104419	NDRG1	1,75138E-12	4,71659E-14	1,211045414	-1,083862459	5,405293686
ENSG00000283217	RP11-472I20.3	1,87697E-12	1,06493E-12	-1,800704456	-1,539558636	14,68801285
ENSG00000073737	DHRS9	3,42061E-12	1,73703E-12	1,584255128	1,410459189	29,67598546
ENSG00000235590	GNAS-AS1	6,87671E-12	3,33845E-12	2,223360476	2,206895595	19,09858485
ENSG00000203805	PLPP4	1,20153E-11	9,58657E-12	1,226241512	1,286860207	6,179255308
ENSG00000171889	MIR31HG	2,02565E-11	1,88768E-14	2,050345062	1,080521671	22,2666625
ENSG00000170454	KRT75	3,5975E-11	1,85983E-11	1,08673156	1,083929793	16,72130349
ENSG00000138678	GPAT3	4,11875E-11	6,84007E-14	5,676700006	2,473885066	26,61713742
ENSG00000169271	HSPB3	2,27817E-10	1,48472E-10	1,674295076	1,6165929	9,32248826
ENSG00000183098	GPC6	5,17151E-10	1,03433E-10	1,716688063	1,583863601	6,969432049
ENSG00000238271	IFNWP19	6,42679E-10	7,38516E-14	1,809469206	1	15,14048108
ENSG00000122863	CHST3	4,92478E-09	1,8649E-09	2,111301614	2,029886956	9,464469737
ENSG00000105976	MET	1,94656E-08	6,26378E-10	1,743812955	1,145527335	9,464390356
ENSG00000116833	NR5A2	1,97924E-08	1,88594E-09	1,638267657	1,278315524	7,889180728
ENSG00000174500	GCSAM	2,86471E-08	1,98697E-10	9,10571047	5,430641233	38,1009076
ENSG00000115594	IL1R1	3,00301E-08	6,50917E-12	3,56779635	1,078567785	16,32312831
ENSG00000253161	LINC01605	3,16105E-08	1,15305E-08	1,530949687	1,291120315	20,06510237
ENSG00000224982	TMEM233	3,54466E-08	1,19523E-08	1,003222028	1,042991776	7,167634825
ENSG00000282849	RP11-121P12.1	3,54466E-08	1,50606E-09	1,488315041	-1,000451028	23,32697907
ENSG00000163814	CDCP1	4,41958E-08	1,63874E-08	1,352086558	1,255136611	7,15933004
ENSG00000144191	CNGA3	1,83379E-07	2,94715E-08	-1,089926497	-1,252958894	6,0066998
ENSG00000109099	PMP22	1,91885E-07	6,34559E-08	1,415572244	1,218688171	11,93649243
ENSG00000147509	RGS20	2,52806E-07	1,3213E-07	1,266748351	1,170303093	9,017503342
ENSG00000239218	RPS20P22	3,36908E-07	4,75352E-08	1,644398021	1,375222788	7,297850228
ENSG00000105825	TFPI2	4,60469E-07	4,90374E-08	4,271378276	3,233258157	24,72313709
ENSG00000260186	LINC02137	5,81134E-07	4,00914E-09	1,176762229	-1,370723093	4,75341366
ENSG00000208001	MIR431	7,57924E-07	1,14544E-09	3,718855689	1,834816327	15,06870977
ENSG00000125148	MT2A	5,24911E-06	1,40073E-06	1,035216024	-1,064760924	5,163700951
ENSG00000108932	SLC16A6	7,14355E-06	8,23887E-06	-1,318874583	-1,207931699	3,504149938
ENSG00000260802	SERTM2	9,86854E-06	2,28556E-07	2,257130117	1,448936766	10,4337861
ENSG00000262406	MMP12	1,22466E-05	2,47161E-07	2,184062379	1,626068134	8,940005547
ENSG00000198768	APCDD1L	1,76614E-05	1,25587E-05	1,137965408	1,133967316	6,886097831
ENSG00000105989	WNT2	9,43112E-05	2,8803E-06	1,104381949	-1,300821625	4,583053947

TABLE 5.12 Table with genes preferentially upregulated by NT4 at time point 12 hours with adjusted p value <0.01 and fold change > 4.

GeneID	Symbol	GeneName
ENSG00000144821	MYH15	myosin heavy chain 15
ENSG00000185274	WBSCR17	polypeptide N-acetylgalactosaminyltransferase 17
ENSG00000165409	TSHR	thyroid stimulating hormone receptor
ENSG00000185480	PARPBP	PARP1 binding protein
ENSG00000268089	GABRQ	gamma-aminobutyric acid type A receptor theta subunit
ENSG00000183395	PMCH	pro-melanin concentrating hormone
ENSG00000138772	ANXA3	annexin A3
ENSG00000158258	CLSTN2	calsyntenin 2
ENSG00000005059	MCUB	mitochondrial calcium uniporter dominant negative beta
ENSG00000104419	NDRG1	N-myc downstream regulated 1
ENSG00000283217	RP11-472I20.3	lncRNAs
ENSG00000073737	DHRS9	dehydrogenase/reductase 9
ENSG00000235590	GNAS-AS1	GNAS antisense RNA 1
ENSG00000203805	PLPP4	phospholipid phosphatase 4
ENSG00000171889	MIR31HG	MIR31HG
ENSG00000170454	KRT75	keratin 75
ENSG00000138678	GPAT3	glycerol-3-phosphate acyltransferase 3
ENSG00000169271	HSPB3	heat shock protein family B (small) member 3
ENSG00000183098	GPC6	glypican 6
ENSG00000238271	IFNWP19	Interferon Omega 1 Pseudogene 19,
ENSG00000122863	CHST3	carbohydrate sulfotransferase 3
ENSG00000105976	MET	MET proto-oncogene, receptor tyrosine kinase
ENSG00000116833	NR5A2	nuclear receptor subfamily 5 group A member 2
ENSG00000174500	GCSAM	germinal center associated signaling and motility
ENSG00000115594	IL1R1	interleukin 1 receptor type 1
ENSG00000253161	LINC01605	lncRNAs
ENSG00000224982	TMEM233	transmembrane protein 233
ENSG00000282849	RP11-121P12.1	lncRNAs
ENSG00000163814	CDCP1	CUB domain containing protein 1
ENSG00000144191	CNGA3	cyclic nucleotide gated channel alpha 3
ENSG00000109099	PMP22	peripheral myelin protein 22
ENSG00000147509	RGS20	regulator of G protein signaling 20
ENSG00000239218	RPS20P22	Ribosomal Protein S20 Pseudogene 22
ENSG00000105825	TFPI2	tissue factor pathway inhibitor 2
ENSG00000260186	LINC02137	lncRNAs
ENSG00000208001	MIR431	microRNA 431
ENSG00000125148	MT2A	metallothionein 2A
ENSG00000108932	SLC16A6	solute carrier family 16 member 6
ENSG00000260802	SERTM2	serine rich and transmembrane domain containing 2
ENSG00000262406	MMP12	matrix metallopeptidase 12
ENSG00000198768	APCDD1L	APC down-regulated 1 like
ENSG00000105989	WNT2	Wnt family member 2

TABLE 5.13 Table with gene names and description for genes that are preferentially upregulated by NT4 at time point 12 hours with adjusted p value <0.01 and fold change > 4.

5.4.19 Genes upregulated more than 2-fold by AB85 in pairwise comparisons with BDNF and NT4 at time-point 24 hours

Next the genes selectively upregulated more than 2-fold and p adjusted value <0.01 by BDNF, AB85 and NT4 in pairwise comparisons at 24 hrs were examined. There is no gene selectively upregulated by BDNF and NT4 under these criteria. However, 4 genes were upregulated by AB85 compared to BDNF and NT4, MAP2K6, NWD2, SHH and SERTM1. MAP2K6 and SERTM1 were also upregulated more than 2-fold by AB85 compared to BDNF and NT4 in the time-point of 12 hours. In cultures treated with AB85 MAP2K6 is upregulated 2.41-fold compared to BDNF and 2.46-fold compared to AB85. SHH is upregulated 2.16-fold by ABB85 compared to BDNF and 2.17-fold compared to NT4. NWD2 is upregulated 2.3-fold by AB85 compared to BDNF and 2.3-fold compared to NT4. NWD2 (NACHT And WD Repeat Domain Containing 2) is a protein coding gene with unknown function. SERTM1 (Serine Rich and Transmembrane Domain Containing 1) is a protein coding gene with unknown function.

5.4.20 Venn diagram analysis of the genes downregulated between BDNF, AB85, NT4 in pairwise comparisons

At time-points 30 minutes and 2 hours no gene is differentially downregulated by a specific ligand more than 1.5-fold with a p-adjusted value of 0.01 in any of the pair-wise comparisons between ligands. Therefore, there were no genes whose expression was preferentially decreased by any of the three TrkB ligands at the first two time-points. On the contrary several hundred genes are differentially downregulated in the pair-wise comparisons at time-point 12 hours. Interestingly the number of genes that are shared between the three TrkB ligands increased upon increasing the threshold of change. More specifically 2580 genes were shared between BDNF, AB85 and NT4 at 12 hours when the fold change was set to 1.5, while 3248 genes were shared at fold change 2 and 3814 genes were shared between the 3 TrkB ligands at fold change 4. Interestingly when the fold change was set to 1.5 there are far more genes whose expression was preferentially decreased by NT4 (569) than with BDNF (10) or AB85 (82). Upon shifting the threshold of change at 2-fold the number of genes whose expression was preferentially decreased by any of the three TrkB ligands was reduced. Indeed, 1 gene is downregulated more than 2 -fold by BDNF, 32 are downregulated more than 2-fold by AB85 and 252 are downregulated more than 4-fold by NT4. Subsequently 9 genes are downregulated by BDNF between 1.5 and 2-fold, 50 genes are downregulated by AB85 between 1.5 and 2-fold and 317 genes are downregulated by NT4 between 1.5 and 2-fold. Noticeably, few genes are differentially expressed by any of the three TrkB ligands more than 4-fold. In particular, no genes are selectively decreased by BDNF more than 4-fold, 6 by AB85 and 39 by NT4. Thus, no gene is decreased by BDNF between 2 and 4-fold, 26 genes were decreased by AB85 and 213 genes by NT4.

At the last time-point 24 hours the number of genes differentially downregulated by 1.5-fold by either of the three TrkB ligands is greatly reduced compared to the corresponding number in the time-point of 12 hours. Additionally, there are no genes whose expression is preferentially downregulated by BDNF or NT4 compared to the other two TrkB ligands, but 190 genes are preferentially downregulated compared by AB85 compared to BDNF and NT4. Upon shifting the threshold of change to 2 only 93 genes are preferentially downregulated by AB85. Thus 97 genes are downregulated

by AB85 between 1.5 and 2-fold. Additionally, only 9 genes are downregulated by AB85 more than 4-fold in comparison to BDNF and NT4. Subsequently 84 genes are downregulated by AB85 between 2 and 4-fold.

A.

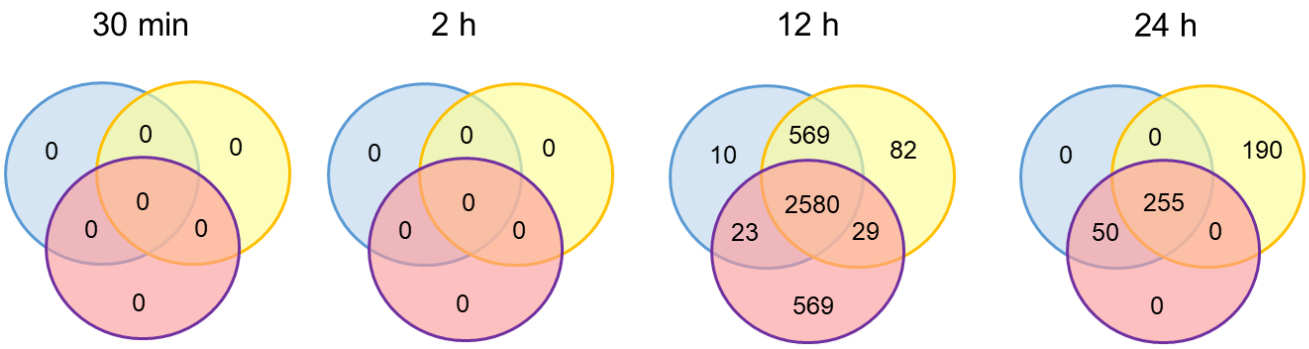

B.

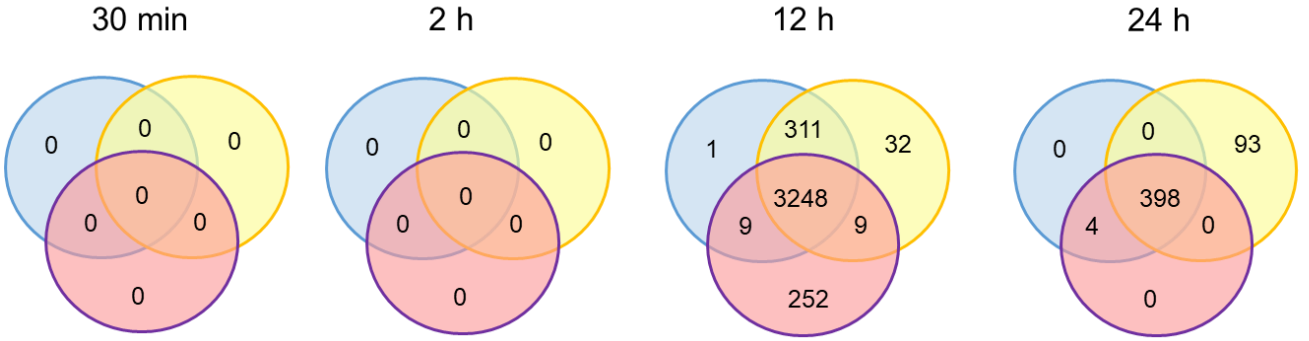

C.

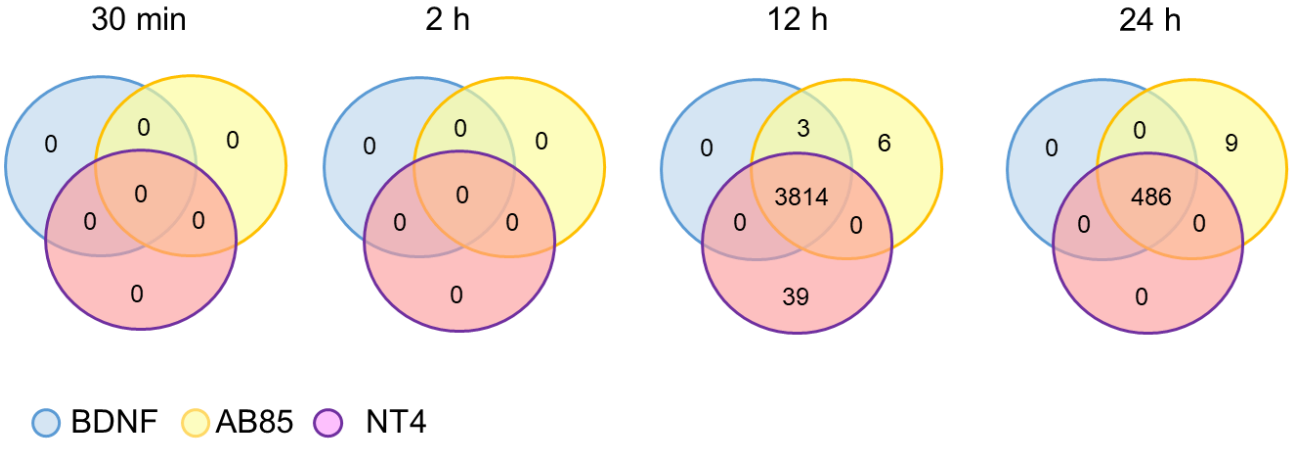

Figure 5.39 Venn diagrams illustrating the number of genes that are downregulated in the 3 treatment conditions (BDNF, AB85 and NT4) and 4 time points (30 min, 2 hours, 12 hours and 24 hours) upon comparison of the three TrkB ligands with each other. The genes presented in this illustration are selected based on adjusted p value < 0.01 and fold change > 1.5 (A.), fold change > 2 (B.), fold change > 4 (C.).

5.4.21 Genes downregulated more than 2-fold in pairwise comparisons of the three TrkB ligands with each other at time-point 12 hours

No genes are differentially expressed in the three pairwise comparisons of the three TrkB ligands with each other at the time-points of 30 minutes and 2 hours with p adjusted value <0.01. At 12 hours, 10 genes are downregulated more than 1.5-fold by BDNF compared to AB85 and NT4, 82 genes are downregulated more than 1.5-fold by AB85 compared to BDNF and NT4 and 569 genes are downregulated more than 1.5-fold by NT4 compared to BDNF and AB85. 1 gene is downregulated more than 2-fold by BDNF compared to AB85 and NT4. This gene is PNMA6F and it is downregulated 2.12-fold by BDNF compared to AB85 and 2.04-fold compared to NT4. 26 genes are downregulated more than 2-fold with padj<0.01 by AB-85 compared to BDNF and NT4 (table 5.14). All these genes, except MIR222HG which is downregulated in AB85 compared to control cultures, are upregulated by the three TrkB ligands, but are less upregulated by AB85. Additionally, 252 genes are downregulated more than 2-fold with padj<0.01 by NT4 compared to BDNF and AB85. These 252 genes were analyzed using GO analysis (Table 5.16)

GeneID	Symbol	adj.P.Val A/B	adj.P.Val A/N	FC BDNF 12 h	FC AB85 12 h	FC NT4 12 h
ENSG00000164949	GEM	1,45728E-10	5,81811E-17	56,655211	15,80152598	103,209963
ENSG00000114529	C3orf52	1,30315E-08	4,83821E-20	30,53251472	11,21835608	92,9050822
ENSG00000112773	FAM46A	1,79314E-08	1,16477E-13	9,446930365	3,85335083	12,7256668
ENSG00000135750	KCNK1	2,56412E-08	2,53813E-17	8,563406229	4,102993438	15,9602244
ENSG00000006327	TNFRSF12A	7,19071E-06	4,39048E-06	24,74837599	9,614510123	21,8840539
ENSG00000168685	IL7R	8,41803E-06	4,12647E-10	24,03898541	7,983621449	34,5266944
ENSG00000150961	SEC24D	1,03957E-05	2,39003E-09	5,755707081	2,719269652	7,11154069
ENSG00000106366	SERPINE1	2,28229E-05	3,42292E-09	15,08960152	5,389431284	21,0364083
ENSG00000269993	AF003625.3	2,58539E-05	0,000116833	34,1113283	13,40071166	27,8373211
ENSG00000156804	FBXO32	2,64394E-05	5,91495E-09	6,444473421	2,723587866	8,30925081
ENSG00000142627	EPHA2	0,000195929	9,35573E-12	6,383344463	2,668688223	13,9423128
ENSG00000134853	PDGFRA	0,000224049	4,05689E-09	4,190315318	1,828931722	6,38117281
ENSG00000138271	GPR87	0,00039612	2,21236E-07	8,812667746	2,232337183	14,0865971
ENSG00000115594	IL1R1	0,000531272	6,50917E-12	3,56779635	1,078567785	16,3231283
ENSG00000196611	MMP1	0,00055191	2,75557E-12	41,96432623	18,28553759	107,709617
ENSG00000102195	GPR50	0,000697198	1,72117E-05	31,23770036	14,50597765	33,388376
ENSG00000197261	C6orf141	0,00075482	7,08406E-13	14,15991518	5,313259599	48,2886487
ENSG00000261488	RP11-757F18.5	0,001272757	4,41851E-14	15,46369595	6,242890163	61,5968215
ENSG00000254656	RTL1	0,002356178	3,88234E-14	15,09559973	6,816643335	60,2019341
ENSG00000118785	SPP1	0,002597282	0,000409886	9,856499775	4,649161746	9,64153523
ENSG00000138678	GPAT3	0,004143297	6,84007E-14	5,676700006	2,473885066	26,6171374
ENSG00000158270	COLEC12	0,004240774	8,03393E-12	2,697452468	1,225973318	7,50245601
ENSG00000099860	GADD45B	0,004603222	1,5682E-10	4,871163639	2,434778334	10,721238
ENSG00000122641	INHBA	0,005154274	1,84403E-07	9,790383734	4,57342879	15,6610007
ENSG00000019991	HGF	0,006391868	9,36795E-08	3,633458067	1,431671731	9,23115852
ENSG00000270069	MIR222HG	0,006748443	0,00402067	2,509184132	-1,270130082	2,21859891

TABLE 5.14 Table with genes preferentially upregulated by both BDNF and NT4 compared to AB85 at time point 12 hours with adjusted p value <0.01 and fold change > 2.

GeneID	Symbol	GeneName
ENSG00000164949	GEM	GTP binding protein overexpressed in skeletal muscle
ENSG00000114529	C3orf52	chromosome 3 open reading frame 52
ENSG00000112773	FAM46A	family with sequence similarity 46 member A
ENSG00000135750	KCNK1	potassium two pore domain channel subfamily K member 1
ENSG00000006327	TNFRSF12A	TNF receptor superfamily member 12A
ENSG00000168685	IL7R	interleukin 7 receptor
ENSG00000150961	SEC24D	SEC24 homolog D, COPII coat complex component
ENSG00000106366	SERPINE1	serpin family E member 1
ENSG00000269993	AF003625.3	lincRNA
ENSG00000156804	FBXO32	F-box protein 32
ENSG00000142627	EPHA2	EPH receptor A2
ENSG00000134853	PDGFRA	platelet derived growth factor receptor alpha
ENSG00000138271	GPR87	G protein-coupled receptor 87
ENSG00000115594	IL1R1	interleukin 1 receptor type 1
ENSG00000196611	MMP1	matrix metallopeptidase 1
ENSG00000102195	GPR50	G protein-coupled receptor 50
ENSG00000197261	C6orf141	chromosome 6 open reading frame 141
ENSG00000261488	RP11-757F18.5	lincRNA
ENSG00000254656	RTL1	retrotransposon Gag like 1
ENSG00000118785	SPP1	secreted phosphoprotein 1
ENSG00000138678	GPAT3	glycerol-3-phosphate acyltransferase 3
ENSG00000158270	COLEC12	collectin subfamily member 12
ENSG00000099860	GADD45B	growth arrest and DNA damage inducible beta
ENSG00000122641	INHBA	inhibin beta A subunit
ENSG00000019991	HGF	hepatocyte growth factor
ENSG00000270069	MIR222HG	lincRNA

TABLE 5.15 Table with gene names preferentially downregulated by AB85 at time point 12 hours with adjusted p value <0.01 and fold change > 2.

Enrichment FDR	Genes in list	Total genes	Functional Category
1,33E+01	36	746	Anterograde trans-synaptic signaling
1,33E+01	36	762	Synaptic signaling
1,33E+01	36	756	Trans-synaptic signaling
1,33E+01	36	746	Chemical synaptic transmission
1,32E+05	48	1774	Cell-cell signaling
2,83E+05	13	103	Synaptic transmission, glutamatergic
9,68E+05	23	468	Regulation of trans-synaptic signaling
9,68E+05	56	2474	Nervous system development
9,68E+05	23	467	Modulation of chemical synaptic transmission
1,85E+06	26	627	Behavior
1,93E+07	38	1412	Neuron differentiation
1,95E+07	42	1683	Neurogenesis
2,90E+07	40	1575	Generation of neurons
2,90E+07	10	79	Regulation of synaptic transmission, glutamatergic
2,90E+07	75	4319	Regulation of biological quality
1,44E+07	38	1541	Cell adhesion
1,46E+08	38	1548	Biological adhesion
1,46E+08	32	1154	Neuron development
3,24E+08	29	1008	Neuron projection development
6,81E+08	53	2785	Anatomical structure morphogenesis
7,61E+08	29	1054	Central nervous system development
1,45E+09	23	723	Regulation of ion transport
2,90E+08	9	102	Glutamate receptor signaling pathway
2,97E+08	28	1067	Cell morphogenesis
3,37E+09	17	434	Synapse organization
3,59E+09	26	953	Regulation of nervous system development
5,15E+09	17	450	Regulation of membrane potential
0.000106031584785064	51	2905	Regulation of localization
0.000106031584785064	14	325	Cognition
0.00011179848968806	13	282	Cell-cell adhesion via plasma-membrane adhesion molecules

TABLE 5.16 Table with G0 analysis for the 252 genes preferentially downregulated by NT4 at time point 12 hours compared to BDNF and AB85 with adjusted p value <0.01 and fold change > 2.

5.4.22 Genes downregulated more than 4-fold in pairwise comparisons of the three TrkB ligands with each other at time-point 12 hours

No genes are downregulated more than 4-fold by BDNF compared to AB85 and NT4. 6 genes are downregulated more than 4-fold by AB85 compared to BDNF and NT4 with a p adjusted value <0.01. GPR87 (G Protein-Coupled Receptor 87) is G-protein coupled receptor and overexpression of this gene has been shown to enhance pancreatic cancer aggressiveness through activation of NF-kB signaling pathway (Wang et al., 2017). It is downregulated 5.45-fold by AB85 compared to BDNF and 8.77 compared to NT4. IL1R1 was described above, as it was upregulated more than 4-fold by NT4. It is also downregulated 5.3-fold by AB85 compared to BDNF and 26.25-fold compared to NT4. *IFNWP19* (Interferon Omega 1 Pseudogene 19) is a pseudogene. It is downregulated 6.87-fold by AB85 compared to BDNF and 94-fold compared to NT4. MIR31HG is a long-non coding RNA that is implicated in head and neck squamous cell carcinoma, through interaction with HIF1A (Hypoxia-inducible factor 1-alpha) (Wang et al., 2018b). Additionally, overexpression of *MIR31HG* is a poor prognostic factor for this cancer. It is downregulated 5.11-fold by AB85 compared to BDNF and 6.36-fold compared to NT4. HGF (Hepatocyte Growth Factor) is a paracrine morphogenic factor that promotes cancer cell migration and invasion (Xiang et al., 2017). Interestingly cancer -associated fibroblasts expressing HGF are resistant to anti-cancer therapy through activation of pro-survival signaling pathways such as ERK and AKT (Owusu et al., 2017). Interestingly HGF is involved in the pathophysiology of IR (Insulin Resistance), with high expression levels in various IR conditions such as obesity. It is downregulated 5.11-fold by AB85 compared to BDNF and 14.82-fold compared to NT4. *MIR222HG* is a long-non coding RNA that binds to Argonaute-mediated RNA-induced silencing complex and its increase is linked with the progression of hormone-sensitive prostate cancer (PCa) (HSPC) to castration-resistant PCa (CRPC) (Sun et al., 2018b). It is downregulated 2.76-fold by AB85 compared to BDNF and 5.42-fold compared to NT4.

16 genes were downregulated more than 4-fold by NT4 compared to BDNF and AB85 and 21 genes were preferentially downregulated more than 4-fold by NT4 compared

to the two other TrkB ligands. 9 of the genes included in the table are lincRNAs. The highest difference is observed in *ACKR3* (Atypical Chemokine Receptor 3) which is as member of the G-protein coupled receptor family and it is acts as a co-receptor for HIV-1 and HIV-2 entry *in vitro* (D'Huys et al., 2018). Glioblastoma tumors with high expression of ACKR3 are linked with poor prognosis and a monoclonal antibody against it increased survival in mice models of glioblastoma (Salazar et al., 2018). It is downregulated 9.9-fold in NT4 treated cultures in comparison to BDNF and 11.69-fold in AB85 treated cultures. *NTNG1* (Netrin G1) is involved in axon growth during neuronal development, and mutations in this gene have been linked with Rett Syndrome (Archer et al., 2006). It is downregulated 4.2-fold in NT4 treated cultures compared to BDNF and 5.2-fold compared to AB85 treated cultures. *BRINP2* (BMP/Retinoic Acid Inducible Neural Specific 2) is expressed in the mammalian CNS during development, and mutations in this gene has been linked with ADHD in humans, while *Brinp2*$^{-/-}$ mice are hyperactive (Berkowicz et al., 2016) . *NRP2* (Neuropilin 2) is a prognostic marker for reduced survival in bladder cancer (Schulz et al., 2019). *MATN2* (Matrilin 2) is a component of extracellular filamentous networks and it is a member of the von Willebrand factor A domain containing protein family (Piecha et al., 2002). *PCSK5* (Proprotein Convertase Subtilisin/Kexin Type 5) is a protease that is indispensable for early cranio-cardiac mesoderm formation and appropriate heart development (Szumska et al., 2017). *ISM1* (Isthmin 1) suppressed in tumor growth and angiogenesis in mice by inhibiting VEGF (Xiang et al., 2011). NMBR (Neuromedin B Receptor) is a transmembrane G protein-coupled receptor that binds neuromedin B and variants of this gene is implicated in schizophrenia (Porcelli et al., 2016). MITF (Melanocyte Inducing Transcription Factor) is a transcription factor that is involved in melanin synthesis and its dysregulation is known to affect eye function (Garcia-Llorca et al., 2019). C6 (complement C6) is part of the complement system that is important for innate and adaptive immune system and heterozygous mutations in this gene have been linked to recurrent infections of meningococcal disease (Westra et al., 2014). FAM198B (Family With Sequence Similarity 198, Member B) is a predicted to be a membrane-bound glycoprotein localized on Golgi apparatus and is a downstream signal of FGF receptor pathway. High expression of this gene is linked with prolonged survival in lung cancer patients (Hsu et al., 2018). LDB2 (LDB2) is involved in cell migration (Storbeck et al., 2009) . *NMBR-AS1* is the antisense transcript of NMBR. *FAM198B-AS1* is the antisense transcript of FAM198B.

SST (somatostatin) is expressed in the whole body and it blocks the secretion of pituitary hormones, and is therefore an important regulator of the endocrine system. It also controls the rate of neurotransmission in the CNS (Eigler and Ben-Shlomo, 2014). *C1orf115* is a protein coding gene with unknown function. *SPRY1* (Sprouty, Drosophila, Homolog Of, 1) plays an important role in cancer progression, as it is markedly expressed in triple-negative breast cancer, while suppression of this gene led to slower growth of cancer cells and fewer lung metastases (He et al., 2016). PIEZO2 (Piezo Type Mechanosensitive Ion Channel Component 2) is a protein with several transmembrane domains that act as mechanically-activated cation channels, which controls sensitivity to mechanical pain in mice (Murthy et al., 2018). VSIG2 (V-Set And Immunoglobulin Domain Containing 2) is a protein with no clear function. ESAM (Endothelial Cell Adhesion Molecule) is a maker of hematopoietic stem cells (HSCs) and its deficiency has an impact in adult-type hemoglobin synthesis (Ueda et al., 2019). EMCN (endomucin) is a marker for hematopoietic stem cells during development (Matsubara et al., 2005).ERBB4 (Erb-B2 Receptor Tyrosine Kinase 4) is a member of the Tyr protein kinase family and the subfamily EGF receptor subfamily which is activated by neuregulins, and it defines the timing of astrogenesis in the developing brain (Sardi et al., 2006). SOSTDC1 (Sclerostin Domain Containing 1) is a N-glycosylated secreted protein that acts a BMP antagonist, which is reduced in breast cancer. High levels of its mRNA are linked to increased patient survival (Clausen et al., 2011). PDE1A (Phosphodiesterase 1A) is implicated in signal transduction and it is increased upon traumatic brain injury (Oliva et al., 2012). NCR2 (Natural Cytotoxicity Triggering Receptor 2) is involved in endosomal transport of cholesterol and mutations in this gene are associated with Niemann-Pick type C (NP-C) disease, a fatal autosomal recessive neurodegenerative disorder (Vanier and Millat, 2003).CHST9 (Carbohydrate Sulfotransferase 9) is located at the golgi membrane and catalyzes the transfer of sulfate to position 4 of non-reducing N-acetylgalactosamine (GalNAc) residues in N-glycans and O-glycans. A frameshift mutation of this gene is associated with schizophrenia (Chen et al., 2019a). CKK (Cholecystokinin) is a regulated peptide expressed in human gut and brain tissues, but also expressed in primary human tumors, such as renal, neuronal and myogenic stem cell tumors (Chen et al., 2019a). WNT9B (Wnt Family Member 9B) regulates progenitor cell expansion and differentiation in mesenchymal progenitor cell population (Karner et al., 2011). PRTN3 (Proteinase 3) is necessary for the synthesis and degradation of collagen in the tumor

microenvironment and high expression of the gene correlates with poor survival in patients with pancreatic cancer (Hu et al., 2019).

GeneID	Symbol	adj.P.Val N/A	adj.P.Val N/B	FC BDNF 12 h	FC AB85 12 h	FC NT4 12 h
ENSG00000144476	ACKR3	2,40376E-24	1,62272E-23	1,143046212	1,340560877	-8,7239493
ENSG00000162631	NTNG1	2,91841E-23	2,47586E-21	1,184236074	1,449307707	-3,593667223
ENSG00000198797	BRINP2	2,42626E-21	9,97903E-18	-2,721182576	-1,803551333	-11,79058159
ENSG00000118257	NRP2	2,36228E-20	9,97903E-18	-1,069529911	1,266739552	-5,261398162
ENSG00000132561	MATN2	3,37495E-18	1,7651E-17	1,441635128	1,47440185	-6,45841141
ENSG00000099139	PCSK5	7,09958E-18	1,33489E-14	-2,026967349	-1,386153782	-8,792247156
ENSG00000101230	ISM1	1,20065E-14	1,63425E-14	2,083992417	2,000715745	-2,347752126
ENSG00000135577	NMBR	1,28859E-13	5,98445E-13	-1,172456837	-1,035021287	-5,197667212
ENSG00000187098	MITF	3,27342E-13	1,38147E-12	-2,864753982	-1,835264484	-12,71097344
ENSG00000039537	C6	4,26748E-13	2,20466E-12	-1,778489083	-1,710350949	-7,349722677
ENSG00000164125	FAM198B	5,41327E-13	3,4287E-12	1,613398029	1,886305014	-3,749115061
ENSG00000169744	LDB2	7,19745E-13	8,76384E-12	-3,073504718	-2,234223089	-13,14046518
ENSG00000236822	NMBR-AS1	5,45425E-12	9,96456E-11	-1,32272205	-1,029592003	-5,317472825
ENSG00000248429	FAM198B-AS1	8,34831E-12	1,5564E-10	1,123100387	1,610558185	-4,784827514
ENSG00000157005	SST	1,13142E-11	1,66323E-10	3,408231018	2,996098487	-1,968817223
ENSG00000162817	C1orf115	2,08604E-11	2,29338E-10	1,032279484	-1,248845758	-5,820151276
ENSG00000164056	SPRY1	2,84841E-11	2,69127E-10	1,245913261	1,450077092	-3,306515767
ENSG00000225216	AC007362.3	3,46401E-11	8,11086E-10	-1,157190471	1,344213206	-4,698806292
ENSG00000154864	PIEZO2	5,9257E-11	8,36191E-10	3,785625954	3,889625133	-1,249309397
ENSG00000019102	VSIG2	7,24487E-11	1,40036E-09	1,014212639	1,033428381	-5,594647241
ENSG00000149564	ESAM	3,42446E-10	7,99715E-09	-1,046689996	-1,138761742	-4,752387548
ENSG00000164035	EMCN	5,18019E-10	1,16276E-08	-2,5256582	-1,495823638	-11,05480276
ENSG00000178568	ERBB4	8,02665E-10	2,50553E-08	-1,225795065	1,138660268	-4,976994209
ENSG00000265533	RP11-638L3.1	1,96045E-09	6,07122E-08	2,72377846	3,004872093	-1,734053089
ENSG00000171243	SOSTDC1	3,86029E-09	6,21586E-08	-1,108154121	1,002157144	-5,126658192
ENSG00000115252	PDE1A	1,58754E-08	1,46904E-07	1,233307868	1,169537412	-3,467152983
ENSG00000264843	RP11-856M7.2	1,92659E-06	2,30786E-07	2,443901643	2,985595905	-1,649942614
ENSG00000096264	NCR2	1,16674E-05	1,29811E-06	-1,331699134	1,022863979	-5,447072107
ENSG00000280135	RP1-47M23.3	1,71498E-05	9,21267E-06	-4,56291603	-3,416879955	-21,77284493
ENSG00000154080	CHST9	1,9456E-05	1,36938E-05	-1,765926456	-1,460380021	-7,348762788
ENSG00000075429	CACNG5	6,93635E-05	0,000122672	-1,04828524	-1,019392916	-4,461699505
ENSG00000249484	LINC01470	0,000156613	0,000125472	3,366355873	2,664976264	-1,510866593
ENSG00000158955	WNT9B	0,000332841	0,000172651	-1,483338579	-1,703927613	-7,022047415
ENSG00000254746	RP11-958J22.1	0,001265106	0,000614047	-3,140062699	-2,63195331	-13,33086289
ENSG00000196415	PRTN3	0,001548371	0,000697718	-1,401083658	-1,381107601	-5,721831042
ENSG00000259937	RP11-438D14.2	0,004110059	0,004096158	2,024428791	1,34269685	-3,255057878
ENSG00000144015	TRIM43	0,009960514	0,004115394	4,030419504	1,768771528	-2,544130471

TABLE 5.17 Table with genes downregulated and preferentially downregulated by NT4 at time point 12 hours with adjusted p value <0.01 and fold change > 4.

GeneID	Symbol	GeneName
ENSG00000144476	ACKR3	atypical chemokine receptor 3
ENSG00000162631	NTNG1	netrin G1
ENSG00000198797	BRINP2	BMP/retinoic acid inducible neural specific 2
ENSG00000118257	NRP2	neuropilin 2
ENSG00000132561	MATN2	matrilin 2
ENSG00000099139	PCSK5	proprotein convertase subtilisin/kexin type 5
ENSG00000101230	ISM1	isthmin 1
ENSG00000135577	NMBR	neuromedin B receptor
ENSG00000187098	MITF	melanogenesis associated transcription factor
ENSG00000039537	C6	complement C6
ENSG00000164125	FAM198B	family with sequence similarity 198 member B
ENSG00000169744	LDB2	LIM domain binding 2
ENSG00000236822	NMBR-AS1	NMBR antisense RNA 1
ENSG00000248429	FAM198B-AS1	FAM198B antisense RNA 1
ENSG00000157005	SST	somatostatin
ENSG00000162817	C1orf115	chromosome 1 open reading frame 115
ENSG00000164056	SPRY1	sprouty RTK signaling antagonist 1
ENSG00000225216	AC007362.3	lincRNA
ENSG00000154864	PIEZO2	piezo type mechanosensitive ion channel component 2
ENSG00000019102	VSIG2	V-set and immunoglobulin domain containing 2
ENSG00000149564	ESAM	endothelial cell adhesion molecule
ENSG00000164035	EMCN	endomucin
ENSG00000178568	ERBB4	erb-b2 receptor tyrosine kinase 4
ENSG00000265533	RP11-638L3.1	uncharacterized LOC643542
ENSG00000171243	SOSTDC1	sclerostin domain containing 1
ENSG00000115252	PDE1A	phosphodiesterase 1A
ENSG00000264843	RP11-856M7.2	lincRNA
ENSG00000096264	NCR2	natural cytotoxicity triggering receptor 2
ENSG00000280135	RP1-47M23.3	lincRNA
ENSG00000154080	CHST9	carbohydrate sulfotransferase 9
ENSG00000075429	CACNG5	calcium voltage-gated channel auxiliary subunit gamma 5
ENSG00000249484	LINC01470	long intergenic non-protein coding RNA 1470
ENSG00000158955	WNT9B	Wnt family member 9B
ENSG00000254746	RP11-958J22.1	lincRNA
ENSG00000196415	PRTN3	proteinase 3
ENSG00000259937	RP11-438D14.2	lincRNA
ENSG00000144015	TRIM43	tripartite motif containing 43

TABLE 5.18 Table with the names of genes preferentially downregulated by NT4 at time point 12 hours with adjusted p value <0.01 and fold change > 4.

5.4.23 Genes downregulated more than 2-fold in pairwise comparisons of the three TrkB ligands with each other at time-point 24 hours

No genes were preferentially downregulated more than 2-fold by BDNF or NT4 at the time-point of 24 hours. However, 93 genes were downregulated more than 2-fold by AB85 compared to BDNF and NT4 and the GO analysis is presented in Table 5.19.

Enrichment FDR	Genes in list	Total genes	Functional Category
0.000714770555465559	13	746	Anterograde trans-synaptic signaling
0.000714770555465559	13	762	Synaptic signaling
0.000714770555465559	13	756	Trans-synaptic signaling
0.000714770555465559	13	746	Chemical synaptic transmission
0.000714770555465559	26	2785	Anatomical structure morphogenesis
0.000714770555465559	16	1099	Animal organ morphogenesis
0.000716879004229936	20	1774	Cell-cell signaling
0.00105333735501281	15	1077	Circulatory system development
0.0013955410012756	7	207	Locomotory behavior
0.00192677902118897	4	42	Regulation of sensory perception of pain
0.00192677902118897	4	43	Regulation of sensory perception
0.00212057685553913	4	45	Rhythmic behavior
0.00326289498005502	2	3	Embryonic genitalia morphogenesis
0.00326289498005502	29	3779	Animal organ development
0.00337850494462474	9	468	Regulation of trans-synaptic signaling
0.00337850494462474	5	108	Neuropeptide signaling pathway
0.00337850494462474	5	107	Sensory perception of pain
0.00337850494462474	9	467	Modulation of chemical synaptic transmission
0.00417345080470299	26	3287	Cell surface receptor signaling pathway
0.00417345080470299	29	3903	Regulation of cell communication
0.00477791153929467	29	3952	Regulation of signaling
0.00477791153929467	27	3536	Cellular response to chemical stimulus
0.00578298819487744	26	3382	Regulation of multicellular organismal process
0.0060240841893931	16	1541	Cell adhesion
0.00609503813312836	16	1548	Biological adhesion
0.00734710122374839	4	75	Inositol phosphate metabolic process
0.00792798314906789	10	687	Blood vessel development
0.00792798314906789	2	6	Positive regulation of dopamine secretion
0.00792798314906789	2	6	Positive regulation of glomerular mesangial cell proliferation
0.00832969233826649	3	32	Positive regulation of smooth muscle contraction

TABLE 5.19 Table with G0 analysis for the 93 genes preferentially downregulated by AB85 at time point 24 hours compared to BDNF and NT4 with adjusted p value <0.01 and fold change > 2.

5.4.24 Genes downregulated more than 4-fold in pairwise comparisons of the three TrkB ligands with each other at time-point 24 hours

At the time-point of 24 hours no genes were downregulated selectively by BDNF or NT4. 2 genes were downregulated more than 4-fold by AB85 compared to BDNF and AB85 with padj<0.01 and 7 genes were upregulated by all three TrkB, but they were upregulated more than 4-fold by both BDNF and NT4 compared to AB85 with padj<0.01 (table 5.20). *GEM* is an immediate early response gene that is upregulated at the 30-minute time-point and it is the most highly expressed gene at this point. *MIR431* is a lincRNA with unknown function. *GCSAM* (Germinal Center Associated Signaling And Motility) is expressed in lung cell carcinoma, and hypomethylation of this gene is linked with longer survival (Li et al., 2019). *HAPLN3* (Hyaluronan And Proteoglycan Link Protein 3) is expressed in a glia-dependent manner (Li et al., 2019). *AQP3* (Aquaporin 3) is a glycerol channel (Dzyubenko et al., 2016). *GPR87* (G Protein-Coupled Receptor 87) is G-protein coupled receptor and overexpression of this gene has been shown to enhance pancreatic cancer aggressiveness through activation of NF-kB signaling pathway (Wang et al., 2017). *ITK* (IL2 Inducible T Cell Kinase) functions downstream of the T-cell receptor to control phospholipase C-gamma.

GeneID	Symbol	adj.P.Val A/B	adj.P.Val A/N	FC BDNF 24 h	FC AB85 24 h	FC NT4 24 h
ENSG00000164949	GEM	1,13E-10	1,06E-09	40,78135158	9,311376994	36,0352772
ENSG00000261488	lincRNA	3,40E-05	0,00012919	7,082565448	1,618057219	6,39678276
ENSG00000128340	RAC2	9,21E-05	2,90E-05	8,897851257	2,179803303	10,0161903
ENSG00000208001	MIR431	9,53E-05	6,76E-05	4,764156798	1,150830957	5,0884748
ENSG00000174500	GCSAM	0,000128617	0,00156082	7,066091785	1,353983627	5,66404786
ENSG00000140511	HAPLN3	0,000135317	0,00018004	6,958700984	1,620053527	6,90567313
ENSG00000165272	AQP3	0,000166777	0,0006633	4,511854197	1,012332233	4,01605283
ENSG00000138271	GPR87	0,00022097	0,00024985	3,977665042	-1,22991491	4,03987056
ENSG00000113263	ITK	0,001222504	0,00173085	4,494619076	-1,08144356	4,12429798

TABLE 5.20 Table with genes upregulated by both BDNF and NT4 compared to AB85 at time point 24 hours with adjusted p value <0.01 and fold change > 4.

5.4.25 Verification of selected genes with RT-qPCR

In order to verify the results obtained with RNA-seq 7 genes were selected to be verified by RT-qPCR. The genes were selected based on the knowledge from literature that they are regulated by BDNF and the availabillity of commercialy available primers. A separate differentiation experiment was performed with the same set up of the RNA-seq experiment and three triplicate wells were used per each condition. Day 30 neurons were lysed and RNA was extracted as detailed in the Materials and Methods. The genes tested included 4 immediate early response genes *EGR1, EGR2, EGR3 and NPAS4* , as well as *VGF, SYNPO,* and *PALD1*. *VGF* or VGF nerve growth factor inducible codes for a secreted neuropeptide precursor and is known to be induced by NGF, CREB and BDNF (Mandolesi et al., 2002). *SYNPO* or Synaptopodin has been found to be essential for the formation of spine apparatuses (Mundel et al., 1997). *VGF* is found to be increased in a much greater extent in RT-qPCR across time-points and treatments, with the exception of cultures treated with NT4 for 24 hours. *SYNPO* expression patterns are more complex, but the differences in the fold of increase between the two expreriments are more moderate. *EGR1, EGR2* and *EGR3* are expressed to a much greater extent in the first time-point of 30 minutes in the RT-qPCR experiment, but at the later time-points *EGR1* and *EGR2* are increased to a much greater extent in the RNA seq experiment. On the other hand EGR3 is expressed at similar levels at the later time-points Although the fold of change of gene transcription was different between RNA seq and RT-PCR the direction of the increase was replicated. The divergence between the level of increase between the two methods could be attributed to the higher sensitivity of the RT-PCR when single genes are tested. Alternatively the transcript detected by RT-PCR may not reflect the total amount of mRNA produced by a gene (Figure 5.40)

RNA SEQ

	control	BDNF 2hours	85 2 hours	NT4 2 hours	BDNF 12 hours	85 12 hours	NT4 12 hours	BDNF 24 hours	85 24 hours	NT4 24 hours
VGF	1	11.12553	11.47981	13.69162	9.166249	8.070024	12.48189	11.22239	5.911638	11.04779
SYNPO	1	3.536657	3.553304	3.25568	3.730512	2.266579	1.526659	4.357505	2.30254	4.252506
PALD1	1	18.21311	14.42535	15.60574	55.36195	34.89185	38.5003	37.13649	13.0022	36.00145
NPAS4	1	1.572657	1.752579	1.507478	1.383254	1.134646	2.103847	1.552378	1.411142	1.567278
EGR2	1	41.98955	29.38706	41.78642	16.87159	6.020747	5.034897	22.92731	8.09602	22.91591
EGR1	1	119.456	93.79974	131.4484	51.07561	20.58721	19.30685	57.49846	21.96506	55.49012
EGR3	1	3.865209	2.280036	4.016863	0.955274	0.833743	1.273922	1.062505	0.854867	0.951907

RT PCR

	Control	BDNF 2 hours	85 2 hours	NT4 2 hours	BDNF 12 hours	82 12 hours	NT4 12 hours	BDNF 24 hours	85 24 hours	NT4 24 hours
VGF	1	89.49749	48.80335	88.87485	31.65007	17.21166	23.92868	18.86757	12.3247	13.21893
SYNPO	1	1.477038	1.550493	2.148402	3.215218	1.743339	3.076413	2.700783	1.499575	1.276744
PALD1	1	1.340964	1.975361	1.323478	1.59215	3.029628	3.14633	2.781714	2.057258	3.100351
NPAS4	1	1.569999	2.051551	1.986389	1.059321	1.090617	1.875732	1.080317	0.748359	1.342858
EGR2	1	123.1514	69.74303	128.6792	2.87307	1.172338	2.305262	2.511411	0.952028	1.401877
EGR1	1	205.4651	120.6123	237.1226	6.188929	4.277431	4.545224	9.425117	2.348305	3.069043
EGR3	1	16.63489	13.69184	20.72739	1.715272	0.811117	0.845238	0.672455	0.456954	0.39501

Figure 5.40 Expression fold changes relative to the control of 7 genes obtained with RNA SEQ and RT PCR. *Green colour indicates higher level of increase and bright yellow indicates intermediate level of change. The numbers presented in this figure correspond to increase/decrease in comparison to the control cultures. For the RT-qPCR experiment 18s RNA was used as a control*

.

5.5 Discussion

As it was described in chapter 4, a novel monoclonal antibody, AB85, was found to act as an efficient TrkB agonist in terms of phosphorylation of pTrkB and some components of the downstream signalling such as c-FOS. In order to provide an in-depth comparison of the efficiency of AB85 to BDNF and NT4, cultures of human neurons were treated with either BDNF, AB85 and NT4 at 4 different time-points. At the first time-point of 30 minutes 43 genes were upregulated more than 2-fold and with a p-adjusted value <0.01, and most of them are immediate early response genes and transcription factors that initiate the signalling cascades downstream of TrkB pathway. A global and unbiased transcriptome analysis identified 1199 genes that are upregulated after 2-hour treatment of day 30 neurons with either BDNF, NT4 or AB85, whereas 1103 and 671 genes remain upregulated after 12 and 24 hours of treatment respectively. Furthermore, 1065 genes are downregulated after 2 hours of treatment with either one of the TrkB agonists, 1844 genes are downregulated after 12 hours of treatment and 614 are downregulated after 24 hours of treatment. These genes were analysed with Gene Ontology analysis (GO) and relevant gene categories were discovered. Additonally, PCA analysis of differentially expressed genes revealed that samples clustered according to experimental condition and time of treatment. This finding highlights the reproducibility of the differentiation protocol used across different wells. A great number of these differentially regulated genes are shared between the three ligands and hierarchical clustering with gene ontology placed them in relevant categories. One of the most intriguing categories of upregulated genes was calcium signalling. Interestingly, calcium signalling and increased BDNF expression are linked in striatal neurons (Hasbi et al., 2009).

A large cluster that contains genes coding for sodium and potassium channels was found to be upregulated mainly at the 12-hour time-point and are subsequently downregulated at the 24-hour time-point. Interestingly BDNF has been shown to negatively regulate the G protein-activated inwardly rectifying potassium channels (Rogalski et al., 2000). Another gene cluster that was found to be downregulated includes protein kinases and protein stability regulators such as the proto-oncogene *JUN*, the zing finger transcription factor *KLF11* and the mitogen-activated protein (MAP) kinase kinase *MAP2K6*. Notably treatment with BDNF, NT4 and to a lesser extend #85 were found to decrease transcription of genes belonging to the lipid

metabolism cluster. This finding fits well with the notion that chronic administration of BDNF in obese db/db mice leads to significant reductions in serum concentrations of free fatty acid, total cholesterol and phospholipids (Tsuchida et al., 2002). It is notable that all three ligands increased the transcription of immediate early response genes that have been extensively reported to be upregulated upon BDNF treatment. Indeed, *cFOS* which is an indirect marker of neuronal activity was upregulated 11.73-fold by BDNF, 11.58-fold by AB85 and 13.29-fold by NT4 at the time-point 30 minutes and the activity dependent transcription factor *NPAS4*, was increased 10.3-fold by BDNF, 8,45-fold by AB85 and 10-fold by NT4. *Arc* which is also known to be regulated by BDNF was increased more than 11-fold by BDNF, 15.49-fold by AB85 and 20.2-fold by AB85. It has to be mentioned that various genes were found to be differentially regulated specifically by NT4 after treatment for 12 hours. The atypical chemokine receptor 3 *(ACKR3)* was the most significantly downregulated gene of this category and was decreased by 8.72-fold, whereas the Pro-Melanin Concentrating Hormone *(PMCH)* was the most significantly upregulated gene and was increased by 46.68-fold.

The great number of genes that are detected in this experiment and the multiple parameters examined prohibits extensive in-depth analysis of the data obtained. Therefore, the Glimma package of the Bioconductor package that generates interactive graphs was used. Using this package several pairwise comparisons have been made. Each one of the three TrkB ligands is compared to itself over the 4 time-points, to the other 2 TrkB ligands in each time-point and to control cultures over the 4 time-points. In this way it is possible to examine any gene expressed in this setup in every possible combination. A basic goal of this experiment was to identify which genes are specifically regulated by any of the three TrkB ligands. In the previous version of this Thesis, p adjusted value and Fold-change values from an ANOVA analysis on the 48 different samples have been used. However, in these comparisons, each sample was compared to the control culture in the appropriate time-point. In this case several genes were classified as differentially regulated even though this was not necessarily the case. For example, when the threshold was set at 2-fold change, a gene expressed 1.8-fold by BDNF, 1.7-fold by AB85 and 2.2-fold by NT4 would be counted as a gene upregulated by NT4 more than 2-fold. Now, limma package of the Bioconductor was used to circumvent this problem. This package uses empirical

statistical methods in a linear model for the analysis of complex experiments with multiple treatment factors. Using these scripts it was found that no genes are differentially regulated by any of the three TrkB ligands in a statistically significant manner (p.adjusted <0.01) at the time-points 12 and 24 hours. After 12 hours of treatment the main difference in the pairwise comparisons between the ligands is located on the number of genes upregulated by NT4. 604 genes are upregulated more than 1.5-fold by NT4 in comparison to the other TrkB ligands, 327 genes were upregulated more than 2-fold and 61 are upregulated more than 4-fold. After 24 hours no genes are differentially regulated by BDNF or NT4 and 50 genes are upregulated by AB85 more than 1.5-fold in comparison to the other TrkB ligands. 4 of these genes are also upregulated more than 4-fold. It is observed that most of the genes upregulated in a statistically significant manner are upregulated between 1.5 and 2-fold. However, the consensus in the scientific literature of RNA-seq is that the threshold is widely used in 2-fold. Interestingly, there are no genes downregulated specifically by only one of the three TrkB ligands. After 12 hours of treatment the main difference is located again in the genes downregulated selectively by NT4. 569 genes are downregulated more than 1.5-fold in comparison to the other TrkB ligands, 252 genes are downregulated more than 2-fold and 39 genes are downregulated more than 4-fold. Notably, after 24 hours of treatment there are no genes downregulated by either BDNF or NT4. However, 190 genes are downregulated more than 1.5-fold by AB85 in comparison to the other TrkB ligands, 93 genes are downregulated more than 2-fold and 9 genes are downregulated more than 4-fold. It is also observed that the majority of the genes with altered expression that were examined remain significant in the three degrees of significance examined here. This is a further support for the validity of results presented here. It is worth emphasizing that AB85 is found to do downregulate more than 4-fold, compared to other TrkB ligands, 4 genes that are markedly upregulated in various cancers. This finding needs to be verified by RT-qPCR and animal models for potential therapeutic significance. Interestingly a number of genes are found to be preferentially upregulated or downregulated by NT4. There are 5 genes upregulated more than 4-fold by NT4 alone (WBSCR17, GABRQ, PR11-472120.3, CNGA3, SLC16A6) and 37 genes are upregulated by the three TrkB ligands but are preferentially upregulated more than 4-fold compared to the other TrkB ligands by NT4. These genes include genes involved in neurodegenerative diseases such as *MYH15* that is a risk factor for ALS, *WBSR17* which is deleted in Williams syndrome,

CHST3 which is impaired in skeletal dysplasia and hearing loss in humans, *PMP22* that is downregulated in several neuropathies. Another gene that is preferentially upregulated by NT4 is *CLSTN2* which is expressed in motor neurons and is proposed to have an impact on human memory and more specific word recall. *ANXA3* is another gene preferentially upregulated by NT4 and it has been shown to be involved in cellular growth and signal transduction. Two genes that are important in hunger regulation, homeostasis and sleep, were also upregulated significantly more by NT4 than BDNF and AB85, *PNOC* and *PMCH*. Intriguingly, TSHR, the thyrotropin receptor that responds to thyroid-stimulating hormone was found to be increased. Interestingly a study has found reduced levels of BDNF and NT4 in mice with hypothyroidism, suggesting a link between the neurotrophins and thyroid regulation (Bhroz et al.,2017). Genes that are upregulated to a greater extent by NT4 compared to BDNF and AB85 include genes involved in different cancers, such as C*DCP1* which is increased in triple negative cancer cells and *MIR136*, which is downregulated in the same type of cancer and is correlated with poor prognosis. *MET,* a proto onco-gene is also upregulated by a significantly greater amount by NT4 compared to BDNF and AB85, as is the case for PLPP4 which is increased in lung carcinoma. The results relevant to cancer would be meaningful to be replicated in a more appropriate model, such as cancer cell lines. There are 16 genes selectively downregulated more than 4-fold by NT4 compared to control cultures at 12 hours and 21 genes downregulated more than 4-fold by NT4 compared to BDNF and AB85 including interesting genes such as *ACK3* which is expressed in glioma cells and linked to MEK/ERK resistance to apoptosis and is a poor prognosis marker, *NTNG1* which mediates axon growth and in implicated in Rett syndrome, *BRINP2* which plays an important role in behaviour, as *BRINP2* $^{-/-}$ mice have increased anxiety and *SST* a hormone of endocrine system which is involved in neurotransmission. Two markers of hematopoietic stem cells, *ESAM* and *EMSN* were also downregulated by NT4, as is the case for *PDEA1* which is increased after traumatic brain injury and *NCR2* which is mutated in fatal neurodegenerative disease. *CHST9*, another gene downregulated by NT4 has been deleted in some schizophrenia cases. Some of the downregulated genes by NT4 compared to BDNF and AB85 are involved in cancer, such as *SOSTDC1* which is reduced in breast cancer.

RT-qPCR was used to test 7 of the genes upregulated with RNA-seq as a first-step validation. One differentiation experiment was used in triplicate wells for the RT-qPCR,

and therefore it was not possible to examine more than 7 genes at once. This is due to the fact that from each well of neurons about 400-700 ng of RNA is extracted, while a RT-qPCR reaction needs 50 ng. The differences observed between the RT-qPCR and the RNA seq data could be attributed to various reasons, such as the potential different specificity of the techniques or also some variability between differentiations. Future experiments could address this point by repeating RT-qPCR experiments from the same stage of numerous differentiations for a number of key genes. Different differentiation experiments could also be used to extract proteins from the same stage of the differentiation and examine the same genes in the protein level.

Overall, the two neurotrophins and the TrkB activating antibody have been found here to activate transcription of neurons in a similar manner, in particular at early time points (Merkouris et al 2018). Transcriptional changed induced by BDNF and NT4 remain similar at later time points but diverge from the changes induced by antibody #85. This divergence could be attributed to small differences in the first minutes of treatment that are subsequently amplified, or due to different kinetics of the antibody compared to the two neurotrophins.

Further experiments would shed light on the exact identity of the neurons used in this Thesis, with the use of immunostaining and RT-qPCR. Co-localisation of c-FOS with transcription factors expressed by a particular cell type could identify the cells that mediate BDNF-TrkB signaling. It would also be valuable to examine TrkB internalisation upon treatment with BDNF, AB85 and NT4 and examine any differences that will arise between the three TrkB ligands. RNA-seq experiments could be performed in single-pulse experiments, two or three-pulses with treatment for shorter and longer time-points in order to explore whether BDNF, AB85 and NT4 have major transcriptional differences in these conditions. A further confirmatory experiment for the existing similarities between BDNF, NT4 and AB85 would be X-ray crystallography studies to detect the binding point of AB85 to TrkB.

Some straightforward experiments that will offer new insights building on the data presented here could include the use of human iPSCs derived from Huntigton patients from the HD consortium, that have been differentiated from Nick Allen lab under the same protocol and found to be reliant on BDNF for their survival. It would be intriguing to perform RNA-seq experiments on control cultures together with cultures treated with

BDNF, AB85 and NT4 to compare the similarities between these TrkB ligands in the downstream survival signals. It would be important to examine whether AB85 has a survival effect on these neurons, and whether this effect is similar to BDNF. NT4 would also be used in this experiment, as it appears to act very similar to BDNF based on the RNA-seq experiment described above. A profound experimental strategy would include treatment of a mouse model of Huntigton's disease with AB85, as reduction of cortical BDNF mRNA levels has been shown to correlate with the progression of disease in a mouse model of HD (Zuccato et al., 2005) . Another possibility is treatment of a mouse model of Alzheimer Disease, as BDNF delivery from astrocytes has been shown to rescue memory deficit in such models.

Chapter 6: Discussion

The main results of this study are that a large proportion of inhibitory neurons generated from human ESCs respond to the addition of BDNF, NT4 and of a novel TrkB activating monoclonal antibody by phosphorylating TrkB in a time- and dose-dependent manner. Comparative RNA-seq analyses of the whole transcriptome indicated striking similarities at early time points between the changes observed following the addition of all 3 TrkB ligands. These findings were published in PNAS (Merkouris et al.2018). The difficulties encountered when exploring the biochemistry of BDNF in neurons derived from human embryonic stem cells are also discussed.

6.1 Modulation of BDNF/TrkB signaling as a theurapeutic strategy for brain disorders

BDNF and its main receptor, TrkB are key components in neuroplasticity during development and remain important in the adult nervous system. TrkB activation upon BDNF binding promotes neurogenesis, synaptogenesis and synaptic plasticity, with a direct impact in memory and cognition (Lu et al., 2014). Gene targeting experiments in the mouse have convincingly established that TrkB is essential to prevent the death of BDNF and NT4-responsive sensory neurons during development (Klein et al., 1993) as well as for functional synaptic plasticity (Minichiello et al., 1999). Given this background and the widely recognised roles of especially BDNF, but also NT4 during development as well as in the adult brain, attention initially focussed on the use of BDNF itself as potential therapeutic agent for neurological and neurodegenerative disease (reviewed in (Lu et al., 2013, Gupta et al., 2013). Rodent models of brain disorders have been used to demonstrate the possible therapeutic benefits of targeting BDNF signalling. Direct delivery of BDNF into the striatum diminished the symptoms in animal models of Huntigton’s disease (Zuccato and Cattaneo, 2014)

In line with this result overexpression of BDNF in the forebrain under the control of the promoter for α subunit of Ca2+/calmodulin-dependent protein kinase II increased to a great extent the protein levels in cerebral cortex and striatum and prohibited cell death of striatal neurons and motor dysfunction (Xie et al., 2010).

Interestingly BDNF levels were low in parietal cortices and hippocampi in post-mortem brains of Alzheimer's disease patients (Hock et al., 2000). Engineered astrocytes expressing BDNF under GFAP promoter were used to treat a mouse model that recapitulate some of AD hallmarks resulting in an increase in dendritic spine density and morphology and rescue of memory deficits (de Pins et al., 2019). Another paper showed that amyloid- peptide promotes truncation of TrkB and subsequent reduction of TrkB signaling (Jeronimo-Santos et al., 2015).

However, BDNF has very short half-life in the blood in the range of few minutes, and the physicochemical properties of BDNF (isoelectric point, pI approximately 10) makes it difficult to diffuse, and as such unsuitable for use as a drug. In addition, it does not penetrate the blood-brain barrier (Pardridge et al., 1994). Several alternative, indirect strategies have then been used to try and circumvent these problems and increase BDNF/NT4/TrkB signalling by using drugs penetrating the blood-brain barrier and increasing Bdnf transcription such as the sphingosine-1 phosphate analogue Fingolimod (Deogracias et al., 2012) or else directly activating TrkB. Fingolimod is extensively used in the context of multiple sclerosis (Kappos et al., 2010) and acts to prevent the exit of T lymphocytes from the lymph nodes. Whether or not this will limit its use in the context of neurodegenerative diseases is unclear at this point. Several TrkB agonists have been suggested to mimic BDNF, and at the end of 2017 over 200 papers were found through PubMed search. With regard to drugs activating TrkB directly, a number of reports have indicated that small molecules may activate TrkB such as 7,8-dihydroxyflavone or LM22A-4 (a small molecule designed to mimic part of BDNF's structure). However, a recent survey of such molecules testing their potential as TrkB agonists using multiplex quantitative assays measuring TrkB phosphorylation and downstream pathways failed to confirm that these drugs may activate TrkB in a manner analogous to BDNF(Boltaev et al., 2017). As an alternative to small chemical entities activating TrkB, monoclonal antibodies (generated by the traditional route involving immunising animals) have been developed and shown to activate TrkB. As immunoglobulins or fragments thereof are now widely used in humans, much is known about the tolerability of these reagents as well as their pharmaco-kinetic properties. These reagents have been convincingly shown to activate TrkB in either reporter systems or in neurons (Bai et al., 2010, Cazorla et al., 2011) and in one case even in neurons derived from induced-pluripotent cells (Traub et al., 2017). A very recent

study described a TrkB agonistic antibody (AS86) that promoted neurite outgrowth and prevented Aβ-induced cell death in mice hippocampal primary neurons, while it facilitated LTP in hippocampal slices. It was also shown to rescue spatial memory deficits in a 11-month but not in a 14-month-old AD mouse model (Wang et al., 2020a). Interestingly another recent study generated novel TrkB agonists using the NFAT assay described a TrkB antibody (Ab4B19) that induces a slower decline in plasma membrane expression of TrkB than BDNF, significantly increased length of neurites in mouse cortical neurons and rescued PC12 cells expressing human TrkB. This antibody was still detected after 3 days in the blood and 5 days in brain tissues and prevented motorneurons cell death in culture after serum deprivation. This study also used the spinal root avulsion model as a model of *in vivo* motorneuron damage, where BDNF and Ab4B19 largely prevented motorneuron degeneration. The TrkB antibody was found to be even more effective than BDNF (Guo et al., 2019) Excitingly, the same antibody has been tested in neurons derived from human embryonic stem cells expressing midbrain and hindbrain neuronal subtypes, where BDNF was shown to phosphorylate TrkB. Ab4b19 was also shown to phosphorylate TrkB, albeit to a much lower extent. However, the TrkB antibody had the same survival effect with BDNF in terms of pro-survival effect in human neurons under oxygen/glucose deprivation (Han et al., 2019). Future experiments could test Ab4B19 and AB85 side by side, together with BDNF both *in vitro* and *in vivo* models that are mentioned above in order to determine the potential utility of AB85 as a theurapeutic agent.

6.2 Studying TrkB signalling using human neurons

Most of the data presented in this thesis was derived from experiments using human embryonic stem cell-derived neurons that widely expressed the inhibitory neuron GABAergic marker, GAD65/67. Previous *in vitro* and *in vivo* work with rodents has indicated that such neurons typically express TrkB, depend on TrkB signalling during development and express the *Bdnf* gene at barely detectable levels, unlike excitatory neurons (Baquet et al., 2004; Rauskolb et al., 2010). It had been previously reported that hESCs and hiPSCs can differentiate to GABAergic medium-sized spiny neurons (MSNs), which are the principal projection neurons of the striatum (Arber et al., 2015). Indeed, Activin A was shown to promote what can be described as a “lateral ganglionic eminence identity” as evidenced by the expression of the transcription factors CTIP2,

GSX2 and FOXP2 typically expressed by basal ganglia neurons (Arber et al., 2015). The introduction of defined media containing small molecules regulating cell cycle exit and interfering with the notch, CREB and WNT pathways allowed the generation within about 37 days of neurons expressing the synaptic markers synaptophysin and PSD-95 (Telezhkin et al., 2016). In the studies within this thesis, using a combination of protocols, inhibitory neurons could be generated from H9 hESCs after a period of 30 days. Whilst similar results could be obtained with H7 hESCs, H9 cells were used in most experiments because H9 ESCs differentiate to neurons slightly faster than H7 ESCs. Beyond the efficient and reproducible generation of inhibitory neurons within an acceptable time frame it is the high proportion of neurons responding to TrkB ligands that made this system attractive for RNA seq analyses.

6.3 Comparing TrkB activation following the addition of BDNF, NT4 and #85

Preliminary studies indicated that 4 different TrkB agonistic antibodies selected using the procedure described in Material and Methods were able to phosphorylate TrkB. The antibody designated #85 was selected based on its ability to rapidly phosphorylate TrkB at relatively low concentrations. Detailed investigations with this antibody as well as with the natural ligands BDNF and NT4 indicated that whilst TrkB was phosphorylated in a dose-dependent manner, the range in ligand concentrations between levels of BDNF or NT4 that produce no detectable TrkB phosphorylation to levels of BDNF and NT-4 that led to maximal TrkB phosphorylation was remarkably narrow, being of the order of 3- to 4-fold. Moreover, increasing the levels of BDNF or NT4 greatly above those needed to maximally phosphorylate TrkB did not lead to a decrease in TrkB phosphorylation. As variability between experiments made accurate determinations of EC50 values difficult, these could only be roughly estimated to correspond to about 0.19 nM for BDNF, 0.45 nM for #85 and 1.92 nM for NT4. The reasons for the observed variability did not become entirely clear and were observed even when all samples were analysed on the same gels or originated from the same multiwell plates. It is conceivable that the slight differences in the density of the neurons between different wells or in the identity of the cultures could have a bigger

impact on the expression of TrkB. The use of AlphaLisa assay makes it possible to test several conditions in the same plate, and would be therefore more appropriate for EC50 determination using several more closely spaced concentrations. With regard to the time course of phosphorylation following ligand addition, 4 different times were analysed, with similar results following the addition of any of the 3 ligands: maximal levels of phosphorylation were detected after 30 minutes, followed by a decrease of signal intensity already after 2 hours followed by even stronger decrease by 12 and 24 hours. Previous experiments with rat cortical have provided strong evidenced for downregulation of cell surface TrkB by mechanisms involving proteasome-mediated degradation of TrkB (Sommerfeld et al., 2000, Proenca et al., 2016). The latter study with rodent neurons also indicates that both BDNF and NT4 induce a rapid loss of cell surface TrkB, but that in these neurons BDNF induce a more rapid downregulation than NT4. Whilst the down-regulation of TrkB has not been directly addressed here, and decreased phosphorylation of TrkB may not necessarily mean disappearance of TrkB from the cell surface, the detailed mechanisms could readily be addressed in future studies using the system described here. In particular, biotinylation of cell surface-exposed molecules followed by immunoprecipitation would shed light into the mechanisms leading to the marked decrease of the pTrkB signal with time. Such studies would be important in the context of the findings reported by Proenca and colleagues as the differences they observe between BDNF and NT4 with regard to the kinetics of cell surface reduction of TrkB levels may have important functional implications. Indeed, these authors suggested that NT4 may initiate a more long-lasting signalling cascade. However, it should be noted that the RNAseq data (see below) do not suggest tremendous differences between BDNF and NT4 with regard to transcriptional changes, even 24h after ligand addition.

Whilst the major goal of the study was to compare natural ligands with #85 using human neurons (given that #85 had been selected using human TrkB, see Material and Methods), it is interesting to note that using rodent systems, #85 seems to be less potent then BDNF in terms of the degree of TrkB phosphorylation (Merkouris et al 2018) . Whilst the extracellular domain of human and rat or mouse TrkB are more than 90% conserved these results suggest that small sequence differences may matter. Also, it should be noted that the extracellular domain of TrkB is heavily glycosylated

whereby nothing is known about possible differences between the glycosylation patterns of rodent versus human TrkB.

An intriguing question is if TrkB is re-exposed and re-activated at the cell surface following exposure to its ligand. Preliminary attempts indicated that upon treatment with BDNF, or NT4 or #85 for 12, 24, 48 and 72 hours followed by removal of the ligand for 5 minutes, TrkB phosphorylation could not be achieved by re-exposing the neurons to any of the three ligands for a period of 15 minutes. However, this experiment was done once and the media was not fully removed due to the fragile nature of the cultures. Since the neurons do not die in the absence of ligand it will be interesting in future experiments to delineate the duration of ligand deprivation required for TrkB to be again activated at the cell surface. A recent study using human neurons addressed a similar question (Traub et al., 2017). One of the two antibodies tested (designated AB20) was found to be again able to re-phosphorylate TrkB following 2 initial exposures of the cells to antibody for only 15 minutes. However, this effect was not seen with BDNF (see also below for further discussion of the Traub et al study).

6.4 Global transcriptome analyses following exposure of hESC-derived neurons to BDNF, #85 and NT4

Given the relative homogeneity of the cultures as well as the number of cells responding to the addition of TrkB ligands, it was of interest to explore at different time point the transcriptional changes downstream of TrkB activation. In order to minimise possible transcriptional changes due to neuronal maturation during the 24h time period, neurons were treated for periods of time that were as short as possible and as close as possible to the untreated controls. In addition, triplicate controls were used at 4 different times during the experiments (see Fig.5.2 for a summary of the treatment scheme). The results of all 48 samples were entered into a Principal Component Analysis (PCA) that was used to compare genome wide changes. One important result emerging from this analysis is that all controls, i.e., untreated samples grouped together in one cluster indicating that no significant global transcription changes occur during the experimental time period. The 30-min treated samples also grouped in the control cluster, indicating that there are too few significant changes at this early time

point to affect this type of global analysis. Remarkably, immaterial of the ligand used to activate TrkB, all data points neatly grouped at 2h following TrkB activation, with the single exception of one outlier that was subsequently left out of the analysis. These considerations also mean that the analysis encompassed in the end 47 samples out of 48. This PCA method represents a straightforward and comprehensive way to illustrate that with increasing time following ligand addition, BDNF and NT4 clearly segregate together whilst the #85 cluster increasingly distinguished itself from the natural TrkB ligand, and even more so at 24h than at 12 h. One possible explanation for this progressive segregation is that for example small differences in the activation of early transcription factors are progressively amplified over time by the secondary activation of other elements of the transcription machinery.

Out of the 48 samples used in the RNA seq analysis one triplicate culture that was treated with AB85 for 12 hours was an extreme outlies with many more differential regulated genes than the rest 47 cultures and was excluded from further analysis. This RNA seq analysis revealed that upon treatment for 2, 12 or 24 hours several hundreds of genes are differentially expressed compared with untreated neurons. Whilst this may not seem too surprising, it is interesting to note that during the course of this work, a highly relevant study came out that shares important similarities with the RNA seq analysis reported here, as well as the intent of the experiment overall (Traub et al., 2017). Briefly, this study compared the ability of BDNF and of two proprietary monoclonal antibodies activating TrkB and designated AB2 and AB20 originally raised in the mouse and subsequently humanized (Traub et al., 2017). Unlike here phosphorylation of TrkB was measured by an enzyme-linked immunoassay and EC50s were defined as 25, 67 and 530 pM for BDNF, AB2 and AB20 respectively, whilst efficacy only reached about 50% for both antibodies (compared with BDNF set at 100%). One difference is that neurons derived from hIPSCs were used as opposed to hESCs here but more importantly, the number of TrkB-responsive genes was far lower compared what has been observed in chapter five of this thesis using a related, but different differentiation protocol. Notably, the study by Traub and colleagues identified only 42 genes to be differentially expressed following the addition of either BDNF or 2 related monoclonal antibodies activating TrkB for a time-point of 6 hours. Thirty of these genes were also found to be upregulated in this study, but to a far larger extend than in the the Traub study. Only 2 genes showed similar changes whilst 10

genes were pseudogenes that were not taken into consideration in the analysis of RNA seq data in Chapter 5. Specifically, VGF, or nerve growth factor induced VGF was induced by more than 10-fold upon 2 hour or 12-hour treatment with all three ligands in the present study, whilst the increase was only about 4.5-fold in the Traub et al. study. VGF is a secreted protein and neuropeptide precursor with a role in metabolism (Hahm et al., 1999) and synaptic plasticity and *Vgf* mRNA levels are increased in cultured hippocampal neurons upon treatment with BDNF for 3 hours (Alder et al., 2003). The second most upregulated gene (4-fold) in the Traub study was *GPR50*, a G-protein coupled receptor 1 family member previously shown to inhibit melatonin receptor 1A function through hetero-dimerization. Following the addition of TrkB ligands, it was upregulated by more than 60-fold after 2 h and 14-fold after 12 h. In the work presented here more than 50 genes were found to be increased by more than 50-fold. Still, a close scrutiny of the data revealed that few genes are differentially regulated selectively upon treatment with NT4 for 12 h.

The most downregulated gene that was selectively regulated by NT4 only was atypical chemokine receptor 3 *(ACKR3)* which encodes a member of the G-protein coupled receptor family which was downregulated by 10-fold. It is an orphan receptor, as its endogenous ligands has not been identified yet and it acts as co-receptor for human immunodeficiency virus (HIV) (Balabanian et al., 2005). The most highly upregulated gene by NT4 at the 12-hour time point was the Pro-Melanin Concentrating Hormone *(PMCH)* which was upregulated by 45-fold. This gene encodes for a preprotein which upon proteolytical processing leads to Melanin-concentrating hormone, a short neuropeptide of 19 amino acids that stimulates hunger (Marsh et al., 2002). TSHR which encodes for thyrotrophin and thyrostimulin was also found to be increased by 18-fold upon stimulation with NT4.

Unfortunately, it has not been possible to directly compared antibodies AB2 and AB20 with #85 but based on the results obtained with BDNF in both studies it appears likely that the differences between the 2 sets of data may originate from the culture system used. Specifically, Traub et al. also used a protocol involving SMAD inhibition but also an inhibitor of the GSK3 pathway, phorbol ester and BMP4 as described previously (Reinhardt et al., 2013). This protocol gives rise to cultures that typically do not grow as monolayer and as a result it is exceedingly difficult to obtain reliable data on the proportion of TrkB-expressing and –responding neurons. It is thus conceivable that in

the study by Traub et al., the proportion of neurons responding to TrkB activation may be lower, thus explaining why the number of gene changes following ligand addition may be lower. With regard to the important question of the relative merits of the three antibodies in question (#85, AB2 and AB20) direct comparisons should be made using one and the same cellular assay and similar measurements methods so as to reach useful conclusions.

6.5. Use of human excitatory neurons to study *BDNF regulation*

In spite of the wealth of information regarding the role of BDNF not only in rodents but also in humans (see Introduction), most of the data related to the biochemistry and molecular biology of BDNF originate from mouse work, with the notable exception of those related to the organisation of the *BDNF* gene in humans (reviewed in West et al., 2014). It was therefore of interest to explore novel aspects of BDNF's biochemistry using neurons derived from human pluripotent cells, not least because of the description of the human antisense mRNA (West et al., 2014). Using a differentiation system based on triple SMAD imbibition, large number of excitatory neurons could be generated, with an unclear proportion of these neurons expressing some of the transcription factors expected to be expressed by cortical pyramidal neurons and therefore likely to express the BDNF gene. Indeed, most of the *BDNF* transcript variants described in the human cortex could be shown to be also present in hESC-derived neurons (see Fig 3.5). The levels of *BDNF* transcripts were found to increase about 10- fold between 33 and 82 DIV, suggesting that the increase in the expression of BDNF mRNA may follow the development of synaptic connectivity as reflected by a parallel increase in the levels of synaptophysin. As expected, the levels of *BDNF* mRNA levels were found to increase following depolarisation with elevated levels of KCl (see Fig 3.4). Whilst the long non-coding *BDNF* antisense transcript was found to be expressed in RNA extracted from these cultures, its levels remained unchanged throughout the differentiation procedure (see Fig 3.5). Interestingly, the levels of this antisense were also found to be regulated upon depolarization elicited by increased KCl levels whereby unlike sense transcripts, the antisense transcript was down-regulated (see Fig 3.5). This opens the possibility that this antisense transcript may have a role in regulating BDNF expression and that potentially, one of the explanations for the increased BDNF protein levels typically seen after depolarization may be a decrease of the antisense transcript. Further investigations will be needed to

understand the functional connections, if any, between *BDNF* sense and *BDNF*-antisense mRNA levels and their respective regulation. However, the extended culture times needed to achieve a reasonable degree of maturation of the neurons under the experimental conditions used turned out to be a major problem. Also, the heterogeneity of the cells generated as well as the formation of aggregates over time represented very significant obstacles, unlikely to be overcome during a reasonable time frame.

At this point very little is known about the potential role of the BDNF antisense transcript, perhaps unsurprisingly in view of the difficulties in reproducibly generating monolayer cultures of human neurons expressing significant levels of BDNF (see above). Interestingly, the same antisense transcript is also found in primate brain tissue (Pruunsild et al., 2007) and one study suggests that mouse cells also express a (significantly shorter) BDNF antisense transcript (Modarresi et al., 2012). The same study tested the impact of BDNF-AS on BDNF by using shRNA against BDNF-AS HEK293T cells that endogenously expressed BDNF. Modaressi and colleagues described that BDNF-AS knockdown has been found to increase BDNF protein levels *in vitro*.

Despite the differences in the length of these antisense mRNAs between mouse and human, the 225-bp overlapping region is 90% homologous. However, attempts to detect *BDNF* antisense transcripts failed during the course of the experiments detailed in this thesis failed, both in mouse neurons derived from embryonic stem cells or in RNA extracted from the mouse hippocampus (data not shown). The absence of *BDNF-AS* in rodents suggests a primate specific function, which could be investigated further by analysing RNA from other primates than human.

Despite progress in the development of differentiation protocols based on human pluripotent cells, it seems that the degree of neuronal maturation remains problematic. For example, recent, still unpublished experiments by Mariah Lelos (Brain Repair Group, Cardiff University) revealed that human foetal tissue generate more rapidly functionally relevant neurons when replacing dopaminergic neurons than cells derived from pluripotent human stem cells, even many months after transplantation in the striatum on the side ipsilateral to the lesion of Parkinsonian rats (unpublished data). It thus seems that the maturation of human neurons generated from pluripotent cells

may still represent a significant challenge, not just in the context of studying questions related to the biochemistry and molecular biology of BDNF.

6.6 Conclusions

Using neurons derived from hESCs grown under conditions favouring the development of neurons that express functional TrkB and respond to TrkB ligands, the experiments reported here indicate striking similarities in the changes caused by exposure of the neurons to two different physiological ligands of TrkB compared with a novel monoclonal antibody activating TrkB. These similarities were particularly striking at early time points and suggest that this novel antibody may be a useful tool to use in functional assays. Such assays are now needed to further delineate the potential of this new reagent in activating TrkB *in vitro* and *in vivo*, using animal models of disease that have previously suggested that the activation of TrkB may be potentially be therapeutically beneficial. In particular, the Huntington Disease (HD) consortium has generated iPSC lines from HD patients and demonstrated that the lines containing longer CAG repeats were the most vulnerable to BDNF withdrawal (Consortium, 2012). Whether or not #85 could substitute for BDNF would be an interesting first step. Furthermore, BDNF overexpression in the forebrain of mice engineered to express the *HUNTINGTIN* gene with CAG repeats has been shown to improve symptoms such as cognitive deficits and the loss of striatal neurons (Xie et al., 2010). Intra-striatal injections of reagents such as #85 into such mouse models would be an important next step in further delineating the therapeutic potential of this reagent.

7. REFERENCES

ADACHI, M., TAKI, T., IEKI, Y., HUANG, C. L., HIGASHIYAMA, M. & MIYAKE, M. 1996. Correlation of KAI1/CD82 gene expression with good prognosis in patients with non-small cell lung cancer. *Cancer Res,* 56**,** 1751-5.

ADAMS, J., KELSO, R. & COOLEY, L. 2000. The kelch repeat superfamily of proteins: propellers of cell function. *Trends Cell Biol,* 10**,** 17-24.

AHLSKOG, J. E., GEDA, Y. E., GRAFF-RADFORD, N. R. & PETERSEN, R. C. 2011. Physical exercise as a preventive or disease-modifying treatment of dementia and brain aging. *Mayo Clin Proc,* 86**,** 876-84.

AKIYAMA, T., SATO, S., CHIKAZAWA-NOHTOMI, N., SOMA, A., KIMURA, H., WAKABAYASHI, S., KO, S. B. H. & KO, M. S. H. 2018. Efficient differentiation of human pluripotent stem cells into skeletal

muscle cells by combining RNA-based MYOD1-expression and POU5F1-silencing. *Sci Rep,* 8**,** 1189.

ALBAGLI, O., DHORDAIN, P., DEWEINDT, C., LECOCQ, G. & LEPRINCE, D. 1995. The BTB/POZ domain: a new protein-protein interaction motif common to DNA- and actin-binding proteins. *Cell Growth Differ,* 6**,** 1193-8.

ALDER, J., THAKKER-VARIA, S., BANGASSER, D. A., KUROIWA, M., PLUMMER, M. R., SHORS, T. J. & BLACK, I. B. 2003. Brain-derived neurotrophic factor-induced gene expression reveals novel actions of VGF in hippocampal synaptic plasticity. *J Neurosci,* 23**,** 10800-8.

ALEEM, A. M., JANKUN, J., DIGNAM, J. D., WALTHER, M., KUHN, H., SVERGUN, D. I. & SKRZYPCZAK-JANKUN, E. 2008. Human platelet 12-lipoxygenase, new findings about its activity, membrane binding and low-resolution structure. *J Mol Biol,* 376**,** 193-209.

ALLEGRUCCI, C. & YOUNG, L. E. 2007. Differences between human embryonic stem cell lines. *Hum Reprod Update,* 13**,** 103-20.

ALLEN, M., GHOSH, S., AHERN, G. P., VILLAPOL, S., MAGUIRE-ZEISS, K. A. & CONANT, K. 2016. Protease induced plasticity: matrix metalloproteinase-1 promotes neurostructural changes through activation of protease activated receptor 1. *Sci Rep,* 6**,** 35497.

ALSINA, F. C., IRALA, D., FONTANET, P. A., HITA, F. J., LEDDA, F. & PARATCHA, G. 2012. Sprouty4 is an endogenous negative modulator of TrkA signaling and neuronal differentiation induced by NGF. *PLoS One,* 7**,** e32087.

ALTAR, C. A., CAI, N., BLIVEN, T., JUHASZ, M., CONNER, J. M., ACHESON, A. L., LINDSAY, R. M. & WIEGAND, S. J. 1997. Anterograde transport of brain-derived neurotrophic factor and its role in the brain. *Nature,* 389**,** 856-60.

AMARAL, M. D. & POZZO-MILLER, L. 2007. TRPC3 channels are necessary for brain-derived neurotrophic factor to activate a nonselective cationic current and to induce dendritic spine formation. *J Neurosci,* 27**,** 5179-89.

AMIR, R. E., VAN DEN VEYVER, I. B., WAN, M., TRAN, C. Q., FRANCKE, U. & ZOGHBI, H. Y. 1999. Rett syndrome is caused by mutations in X-linked MECP2, encoding methyl-CpG-binding protein 2. *Nat Genet,* 23**,** 185-8.

AN, S., CUTLER, G., ZHAO, J. J., HUANG, S. G., TIAN, H., LI, W., LIANG, L., RICH, M., BAKLEH, A., DU, J., CHEN, J. L. & DAI, K. 2001. Identification and characterization of a melanin-concentrating hormone receptor. *Proc Natl Acad Sci U S A,* 98**,** 7576-81.

ANASTASIA, A., DEINHARDT, K., CHAO, M. V., WILL, N. E., IRMADY, K., LEE, F. S., HEMPSTEAD, B. L. & BRACKEN, C. 2013. Val66Met polymorphism of BDNF alters prodomain structure to induce neuronal growth cone retraction. *Nat Commun,* 4**,** 2490.

ANDERS, S., MCCARTHY, D. J., CHEN, Y., OKONIEWSKI, M., SMYTH, G. K., HUBER, W. & ROBINSON, M. D. 2013. Count-based differential expression analysis of RNA sequencing data using R and Bioconductor. *Nat Protoc,* 8**,** 1765-86.

ANDERSON, S. A., MICHAELIDES, M., ZARNEGAR, P., REN, Y., FAGERGREN, P., THANOS, P. K., WANG, G. J., BANNON, M., NEUMAIER, J. F., KELLER, E., VOLKOW, N. D. & HURD, Y. L. 2013. Impaired periamygdaloid-cortex prodynorphin is characteristic of opiate addiction and depression. *J Clin Invest,* 123**,** 5334-41.

ANDREW, S. E., GOLDBERG, Y. P., KREMER, B., TELENIUS, H., THEILMANN, J., ADAM, S., STARR, E., SQUITIERI, F., LIN, B., KALCHMAN, M. A. & ET AL. 1993. The relationship between trinucleotide (CAG) repeat length and clinical features of Huntington's disease. *Nat Genet,* 4**,** 398-403.

ANGELASTRO, J. M., KLIMASCHEWSKI, L., TANG, S., VITOLO, O. V., WEISSMAN, T. A., DONLIN, L. T., SHELANSKI, M. L. & GREENE, L. A. 2000. Identification of diverse nerve growth factor-regulated genes by serial analysis of gene expression (SAGE) profiling. *Proc Natl Acad Sci U S A,* 97**,** 10424-9.

ANINI, Y., MAYNE, J., GAGNON, J., SHERBAFI, J., CHEN, A., KAEFER, N., CHRETIEN, M. & MBIKAY, M. 2010. Genetic deficiency for proprotein convertase subtilisin/kexin type 2 in mice is associated

with decreased adiposity and protection from dietary fat-induced body weight gain. *Int J Obes (Lond),* 34**,** 1599-607.

ANNESE, A., MANZARI, C., LIONETTI, C., PICARDI, E., HORNER, D. S., CHIARA, M., CARATOZZOLO, M. F., TULLO, A., FOSSO, B., PESOLE, G. & D'ERCHIA, A. M. 2018. Whole transcriptome profiling of Late-Onset Alzheimer's Disease patients provides insights into the molecular changes involved in the disease. *Sci Rep,* 8**,** 4282.

ARBER, C., PRECIOUS, S. V., CAMBRAY, S., RISNER-JANICZEK, J. R., KELLY, C., NOAKES, Z., FJODOROVA, M., HEUER, A., UNGLESS, M. A., RODRIGUEZ, T. A., ROSSER, A. E., DUNNETT, S. B. & LI, M. 2015. Activin A directs striatal projection neuron differentiation of human pluripotent stem cells. *Development,* 142**,** 1375-86.

ARCHER, H. L., EVANS, J. C., MILLAR, D. S., THOMPSON, P. W., KERR, A. M., LEONARD, H., CHRISTODOULOU, J., RAVINE, D., LAZAROU, L., GROVE, L., VERITY, C., WHATLEY, S. D., PILZ, D. T., SAMPSON, J. R. & CLARKE, A. J. 2006. NTNG1 mutations are a rare cause of Rett syndrome. *Am J Med Genet A,* 140**,** 691-4.

ARENSMAN, M. D., KOVOCHICH, A. N., KULIKAUSKAS, R. M., LAY, A. R., YANG, P. T., LI, X., DONAHUE, T., MAJOR, M. B., MOON, R. T., CHIEN, A. J. & DAWSON, D. W. 2014. WNT7B mediates autocrine Wnt/beta-catenin signaling and anchorage-independent growth in pancreatic adenocarcinoma. *Oncogene,* 33**,** 899-908.

ARIYOSHI, M. & SCHWABE, J. W. 2003. A conserved structural motif reveals the essential transcriptional repression function of Spen proteins and their role in developmental signaling. *Genes Dev,* 17**,** 1909-20.

ARMITAGE, R. J. 1994. Tumor necrosis factor receptor superfamily members and their ligands. *Curr Opin Immunol,* 6**,** 407-13.

ATWAL, J. K., MASSIE, B., MILLER, F. D. & KAPLAN, D. R. 2000. The TrkB-Shc site signals neuronal survival and local axon growth via MEK and P13-kinase. *Neuron,* 27**,** 265-77.

AUBRY, L., BUGI, A., LEFORT, N., ROUSSEAU, F., PESCHANSKI, M. & PERRIER, A. L. 2008. Striatal progenitors derived from human ES cells mature into DARPP32 neurons in vitro and in quinolinic acid-lesioned rats. *Proc Natl Acad Sci U S A,* 105**,** 16707-12.

AUDO, I., BUJAKOWSKA, K., ORHAN, E., POLOSCHEK, C. M., DEFOORT-DHELLEMMES, S., DRUMARE, I., KOHL, S., LUU, T. D., LECOMPTE, O., ZRENNER, E., LANCELOT, M. E., ANTONIO, A., GERMAIN, A., MICHIELS, C., AUDIER, C., LETEXIER, M., SARAIVA, J. P., LEROY, B. P., MUNIER, F. L., MOHAND-SAID, S., LORENZ, B., FRIEDBURG, C., PREISING, M., KELLNER, U., RENNER, A. B., MOSKOVA-DOUMANOVA, V., BERGER, W., WISSINGER, B., HAMEL, C. P., SCHORDERET, D. F., DE BAERE, E., SHARON, D., BANIN, E., JACOBSON, S. G., BONNEAU, D., ZANLONGHI, X., LE MEUR, G., CASTEELS, I., KOENEKOOP, R., LONG, V. W., MEIRE, F., PRESCOTT, K., DE RAVEL, T., SIMMONS, I., NGUYEN, H., DOLLFUS, H., POCH, O., LEVEILLARD, T., NGUYEN-BA-CHARVET, K., SAHEL, J. A., BHATTACHARYA, S. S. & ZEITZ, C. 2012. Whole-exome sequencing identifies mutations in GPR179 leading to autosomal-recessive complete congenital stationary night blindness. *Am J Hum Genet,* 90**,** 321-30.

BAI, Y., XU, J., BRAHIMI, F., ZHUO, Y., SARUNIC, M. V. & SARAGOVI, H. U. 2010. An agonistic TrkB mAb causes sustained TrkB activation, delays RGC death, and protects the retinal structure in optic nerve axotomy and in glaucoma. *Invest Ophthalmol Vis Sci,* 51**,** 4722-31.

BAIZABAL, J. M., MISTRY, M., GARCIA, M. T., GOMEZ, N., OLUKOYA, O., TRAN, D., JOHNSON, M. B., WALSH, C. A. & HARWELL, C. C. 2018. The Epigenetic State of PRDM16-Regulated Enhancers in Radial Glia Controls Cortical Neuron Position. *Neuron,* 99**,** 239-241.

BAKALKIN, G., WATANABE, H., JEZIERSKA, J., DEPOORTER, C., VERSCHUUREN-BEMELMANS, C., BAZOV, I., ARTEMENKO, K. A., YAKOVLEVA, T., DOOIJES, D., VAN DE WARRENBURG, B. P., ZUBAREV, R. A., KREMER, B., KNAPP, P. E., HAUSER, K. F., WIJMENGA, C., NYBERG, F., SINKE, R. J. & VERBEEK, D. S. 2010. Prodynorphin mutations cause the neurodegenerative disorder spinocerebellar ataxia type 23. *Am J Hum Genet,* 87**,** 593-603.

BALABANIAN, K., LAGANE, B., INFANTINO, S., CHOW, K. Y., HARRIAGUE, J., MOEPPS, B., ARENZANA-SEISDEDOS, F., THELEN, M. & BACHELERIE, F. 2005. The chemokine SDF-1/CXCL12 binds to and signals through the orphan receptor RDC1 in T lymphocytes. *J Biol Chem,* 280**,** 35760-6.

BAQUET, Z. C., GORSKI, J. A. & JONES, K. R. 2004. Early striatal dendrite deficits followed by neuron loss with advanced age in the absence of anterograde cortical brain-derived neurotrophic factor. *J Neurosci,* 24**,** 4250-8.

BARBACID, M. 1995. Structural and functional properties of the TRK family of neurotrophin receptors. *Ann N Y Acad Sci,* 766**,** 442-58.

BARDE, Y. A., EDGAR, D. & THOENEN, H. 1982. Purification of a new neurotrophic factor from mammalian brain. *EMBO J,* 1**,** 549-53.

BARDWELL, V. J. & TREISMAN, R. 1994. The POZ domain: a conserved protein-protein interaction motif. *Genes Dev,* 8**,** 1664-77.

BASHIR, M., PARRAY, A. A., BABA, R. A., BHAT, H. F., BHAT, S. S., MUSHTAQ, U., ANDRABI, K. I. & KHANDAY, F. A. 2014. beta-Amyloid-evoked apoptotic cell death is mediated through MKK6-p66shc pathway. *Neuromolecular Med,* 16**,** 137-49.

BAYDYUK, M., NGUYEN, M. T. & XU, B. 2011. Chronic deprivation of TrkB signaling leads to selective late-onset nigrostriatal dopaminergic degeneration. *Exp Neurol,* 228**,** 118-25.

BELGACEM, Y. H., HAMILTON, A. M., SHIM, S., SPENCER, K. A. & BORODINSKY, L. N. 2016. The Many Hats of Sonic Hedgehog Signaling in Nervous System Development and Disease. *J Dev Biol,* 4.

BEMELMANS, A. P., HORELLOU, P., PRADIER, L., BRUNET, I., COLIN, P. & MALLET, J. 1999. Brain-derived neurotrophic factor-mediated protection of striatal neurons in an excitotoxic rat model of Huntington's disease, as demonstrated by adenoviral gene transfer. *Hum Gene Ther,* 10**,** 2987-97.

BERCHTOLD, N. C., CASTELLO, N. & COTMAN, C. W. 2010. Exercise and time-dependent benefits to learning and memory. *Neuroscience,* 167**,** 588-97.

BERKEMEIER, L. R., WINSLOW, J. W., KAPLAN, D. R., NIKOLICS, K., GOEDDEL, D. V. & ROSENTHAL, A. 1991. Neurotrophin-5: a novel neurotrophic factor that activates trk and trkB. *Neuron,* 7**,** 857-66.

BERKOWICZ, S. R., FEATHERBY, T. J., WHISSTOCK, J. C. & BIRD, P. I. 2016. Mice Lacking Brinp2 or Brinp3, or Both, Exhibit Behaviors Consistent with Neurodevelopmental Disorders. *Front Behav Neurosci,* 10**,** 196.

BHAT, S. A., GURTOO, S., DEOLANKAR, S. C., FAZILI, K. M., ADVANI, J., SHETTY, R., PRASAD, T. S. K., ANDRABI, S. & SUBBANNAYYA, Y. 2019. A network map of netrin receptor UNC5B-mediated signaling. *J Cell Commun Signal,* 13**,** 121-127.

BHATTACHARYYA, S., LUAN, J., CHALLIS, B., KEOGH, J., MONTAGUE, C., BRENNAND, J., MORTEN, J., LOWENBEIM, S., JENKINS, S., FAROOQI, I. S., WAREHAM, N. J. & O'RAHILLY, S. 2006. Sequence variants in the melatonin-related receptor gene (GPR50) associate with circulating triglyceride and HDL levels. *J Lipid Res,* 47**,** 761-6.

BIBEL, M., RICHTER, J., SCHRENK, K., TUCKER, K. L., STAIGER, V., KORTE, M., GOETZ, M. & BARDE, Y. A. 2004. Differentiation of mouse embryonic stem cells into a defined neuronal lineage. *Nat Neurosci,* 7**,** 1003-9.

BIFFO, S., OFFENHAUSER, N., CARTER, B. D. & BARDE, Y. A. 1995. Selective binding and internalisation by truncated receptors restrict the availability of BDNF during development. *Development,* 121**,** 2461-70.

BINDER, D. K. & SCHARFMAN, H. E. 2004. Brain-derived neurotrophic factor. *Growth Factors,* 22**,** 123-31.

BIRNER, P., EGGER, G., MERKEL, O. & KENNER, L. 2015. JunB and PTEN in prostate cancer: 'loss is nothing else than change'. *Cell Death Differ,* 22**,** 522-3.

BJORBAEK, C., ELMQUIST, J. K., FRANTZ, J. D., SHOELSON, S. E. & FLIER, J. S. 1998. Identification of SOCS-3 as a potential mediator of central leptin resistance. *Mol Cell,* 1**,** 619-25.

BJORBAK, C., LAVERY, H. J., BATES, S. H., OLSON, R. K., DAVIS, S. M., FLIER, J. S. & MYERS, M. G., JR. 2000. SOCS3 mediates feedback inhibition of the leptin receptor via Tyr985. *J Biol Chem,* 275**,** 40649-57.

BLOODGOOD, B. L., SHARMA, N., BROWNE, H. A., TREPMAN, A. Z. & GREENBERG, M. E. 2013. The activity-dependent transcription factor NPAS4 regulates domain-specific inhibition. *Nature,* 503**,** 121-5.

BOLAND, M. J., HAZEN, J. L., NAZOR, K. L., RODRIGUEZ, A. R., MARTIN, G., KUPRIYANOV, S. & BALDWIN, K. K. 2012. Generation of mice derived from induced pluripotent stem cells. *J Vis Exp***,** e4003.

BOLGER, A. M., LOHSE, M. & USADEL, B. 2014. Trimmomatic: a flexible trimmer for Illumina sequence data. *Bioinformatics,* 30**,** 2114-20.

BOLTAEV, U., MEYER, Y., TOLIBZODA, F., JACQUES, T., GASSAWAY, M., XU, Q., WAGNER, F., ZHANG, Y. L., PALMER, M., HOLSON, E. & SAMES, D. 2017. Multiplex quantitative assays indicate a need for reevaluating reported small-molecule TrkB agonists. *Sci Signal,* 10.

BOMFIM, T. R., FORNY-GERMANO, L., SATHLER, L. B., BRITO-MOREIRA, J., HOUZEL, J. C., DECKER, H., SILVERMAN, M. A., KAZI, H., MELO, H. M., MCCLEAN, P. L., HOLSCHER, C., ARNOLD, S. E., TALBOT, K., KLEIN, W. L., MUNOZ, D. P., FERREIRA, S. T. & DE FELICE, F. G. 2012. An anti-diabetes agent protects the mouse brain from defective insulin signaling caused by Alzheimer's disease- associated Abeta oligomers. *J Clin Invest,* 122**,** 1339-53.

BOMONT, P., WATANABE, M., GERSHONI-BARUSH, R., SHIZUKA, M., TANAKA, M., SUGANO, J., GUIRAUD-CHAUMEIL, C. & KOENIG, M. 2000. Homozygosity mapping of spinocerebellar ataxia with cerebellar atrophy and peripheral neuropathy to 9q33-34, and with hearing impairment and optic atrophy to 6p21-23. *Eur J Hum Genet,* 8**,** 986-90.

BONNI, A., BRUNET, A., WEST, A. E., DATTA, S. R., TAKASU, M. A. & GREENBERG, M. E. 1999. Cell survival promoted by the Ras-MAPK signaling pathway by transcription-dependent and -independent mechanisms. *Science,* 286**,** 1358-62.

BOTHWELL, M. 1991. Keeping track of neurotrophin receptors. *Cell,* 65**,** 915-8.

BOYD, J. G. & GORDON, T. 2001. The neurotrophin receptors, trkB and p75, differentially regulate motor axonal regeneration. *J Neurobiol,* 49**,** 314-25.

BOZATZI, P., DINGWELL, K. S., WU, K. Z., COOPER, F., CUMMINS, T. D., HUTCHINSON, L. D., VOGT, J., WOOD, N. T., MACARTNEY, T. J., VARGHESE, J., GOURLAY, R., CAMPBELL, D. G., SMITH, J. C. & SAPKOTA, G. P. 2018. PAWS1 controls Wnt signalling through association with casein kinase 1alpha. *EMBO Rep,* 19.

BRADBURY, A., POSSENTI, R., SHOOTER, E. M. & TIRONE, F. 1991. Molecular cloning of PC3, a putatively secreted protein whose mRNA is induced by nerve growth factor and depolarization. *Proc Natl Acad Sci U S A,* 88**,** 3353-7.

BRADLEY, A., EVANS, M., KAUFMAN, M. H. & ROBERTSON, E. 1984. Formation of germ-line chimaeras from embryo-derived teratocarcinoma cell lines. *Nature,* 309**,** 255-6.

BROWN, J. R., YE, H., BRONSON, R. T., DIKKES, P. & GREENBERG, M. E. 1996. A defect in nurturing in mice lacking the immediate early gene fosB. *Cell,* 86**,** 297-309.

BRUCATO, N., DELISI, L. E., FISHER, S. E. & FRANCKS, C. 2014. Hypomethylation of the paternally inherited LRRTM1 promoter linked to schizophrenia. *Am J Med Genet B Neuropsychiatr Genet,* 165B**,** 555-63.

BRUNET, A., DATTA, S. R. & GREENBERG, M. E. 2001. Transcription-dependent and -independent control of neuronal survival by the PI3K-Akt signaling pathway. *Curr Opin Neurobiol,* 11**,** 297-305.

BUCHMAN, A. S., YU, L., BOYLE, P. A., SCHNEIDER, J. A., DE JAGER, P. L. & BENNETT, D. A. 2016. Higher brain BDNF gene expression is associated with slower cognitive decline in older adults. *Neurology,* 86**,** 735-41.

BUEKER, E. D. 1948. Implantation of tumors in the hind limb field of the embryonic chick and the developmental response of the lumbosacral nervous system. *Anat Rec,* 102**,** 369-89.

BULLITT, E. 1990. Expression of c-fos-like protein as a marker for neuronal activity following noxious stimulation in the rat. *J Comp Neurol,* 296**,** 517-30.

BUSTIN, S. A. 2000. Absolute quantification of mRNA using real-time reverse transcription polymerase chain reaction assays. *J Mol Endocrinol,* 25**,** 169-93.

CALELLA, A. M., NERLOV, C., LOPEZ, R. G., SCIARRETTA, C., VON BOHLEN UND HALBACH, O., BERESHCHENKO, O. & MINICHIELLO, L. 2007. Neurotrophin/Trk receptor signaling mediates C/EBPalpha, -beta and NeuroD recruitment to immediate-early gene promoters in neuronal cells and requires C/EBPs to induce immediate-early gene transcription. *Neural Dev,* 2**,** 4.

CAMPOS-XAVIER, A. B., MARTINET, D., BATEMAN, J., BELLUOCCIO, D., ROWLEY, L., TAN, T. Y., BAXOVA, A., GUSTAVSON, K. H., BOROCHOWITZ, Z. U., INNES, A. M., UNGER, S., BECKMANN, J. S., MITTAZ, L., BALLHAUSEN, D., SUPERTI-FURGA, A., SAVARIRAYAN, R. & BONAFE, L. 2009. Mutations in the heparan-sulfate proteoglycan glypican 6 (GPC6) impair endochondral ossification and cause recessive omodysplasia. *Am J Hum Genet,* 84**,** 760-70.

CATHOMAS, F., VOGLER, C., EULER-SIGMUND, J. C., DE QUERVAIN, D. J. & PAPASSOTIROPOULOS, A. 2010. Fine-mapping of the brain-derived neurotrophic factor (BDNF) gene supports an association of the Val66Met polymorphism with episodic memory. *Int J Neuropsychopharmacol,* 13**,** 975-80.

CAZORLA, M., ARRANG, J. M. & PREMONT, J. 2011. Pharmacological characterization of six trkB antibodies reveals a novel class of functional agents for the study of the BDNF receptor. *Br J Pharmacol,* 162**,** 947-60.

CHACON-FERNANDEZ, P., SAUBERLI, K., COLZANI, M., MOREAU, T., GHEVAERT, C. & BARDE, Y. A. 2016. Brain-derived Neurotrophic Factor in Megakaryocytes. *J Biol Chem,* 291**,** 9872-81.

CHAMBERS, S. M., FASANO, C. A., PAPAPETROU, E. P., TOMISHIMA, M., SADELAIN, M. & STUDER, L. 2009. Highly efficient neural conversion of human ES and iPS cells by dual inhibition of SMAD signaling. *Nat Biotechnol,* 27**,** 275-80.

CHAN, C. Y., SALABAT, M. R., DING, X. Z., KELLY, D. L., TALAMONTI, M. S., BELL, R. H., JR. & ADRIAN, T. E. 2005. Identification and in silico characterization of a novel gene: TPA induced trans-membrane protein. *Biochem Biophys Res Commun,* 329**,** 755-64.

CHAN, J. P., CORDEIRA, J., CALDERON, G. A., IYER, L. K. & RIOS, M. 2008. Depletion of central BDNF in mice impedes terminal differentiation of new granule neurons in the adult hippocampus. *Mol Cell Neurosci,* 39**,** 372-83.

CHAN, J. P., UNGER, T. J., BYRNES, J. & RIOS, M. 2006. Examination of behavioral deficits triggered by targeting Bdnf in fetal or postnatal brains of mice. *Neuroscience,* 142**,** 49-58.

CHANG, T. J., CHIU, Y. F., SHEU, W. H., SHIH, K. C., HWU, C. M., QUERTERMOUS, T., JOU, Y. S., KUO, S. S., CHANG, Y. C. & CHUANG, L. M. 2015. Genetic polymorphisms of PCSK2 are associated with glucose homeostasis and progression to type 2 diabetes in a Chinese population. *Sci Rep,* 5**,** 14380.

CHAVKIN, C., JAMES, I. F. & GOLDSTEIN, A. 1982. Dynorphin is a specific endogenous ligand of the kappa opioid receptor. *Science,* 215**,** 413-5.

CHEN, J., JAEGER, K., DEN, Z., KOCH, P. J., SUNDBERG, J. P. & ROOP, D. R. 2008. Mice expressing a mutant Krt75 (K6hf) allele develop hair and nail defects resembling pachyonychia congenita. *J Invest Dermatol,* 128**,** 270-9.

CHEN, J., WU, J. S., MIZE, T., MORENO, M., HAMID, M., SERVIN, F., BASHY, B., ZHAO, Z., JIA, P., TSUANG, M. T., KENDLER, K. S., XIONG, M. & CHEN, X. 2019a. A Frameshift Variant in the CHST9 Gene Identified by Family-Based Whole Genome Sequencing Is Associated with Schizophrenia in Chinese Population. *Sci Rep,* 9**,** 12717.

CHEN, W., JI, H., LI, L., XU, C., ZOU, T., CUI, W., XU, S., ZHOU, X., DUAN, S. & WANG, Q. 2019b. Significant association between GPR50 hypomethylation and AD in males. *Mol Med Rep,* 20**,** 1085-1092.

CHEN, W., WALWYN, W., ENNES, H. S., KIM, H., MCROBERTS, J. A. & MARVIZON, J. C. 2014a. BDNF released during neuropathic pain potentiates NMDA receptors in primary afferent terminals. *Eur J Neurosci,* 39**,** 1439-54.

CHEN, Y., WANG, Y., ERTURK, A., KALLOP, D., JIANG, Z., WEIMER, R. M., KAMINKER, J. & SHENG, M. 2014b. Activity-induced Nr4a1 regulates spine density and distribution pattern of excitatory synapses in pyramidal neurons. *Neuron,* 83**,** 431-443.

CHEN, Z. Y., JING, D., BATH, K. G., IERACI, A., KHAN, T., SIAO, C. J., HERRERA, D. G., TOTH, M., YANG, C., MCEWEN, B. S., HEMPSTEAD, B. L. & LEE, F. S. 2006. Genetic variant BDNF (Val66Met) polymorphism alters anxiety-related behavior. *Science,* 314**,** 140-3.

CHIARUTTINI, C., VICARIO, A., LI, Z., BAJ, G., BRAIUCA, P., WU, Y., LEE, F. S., GARDOSSI, L., BARABAN, J. M. & TONGIORGI, E. 2009. Dendritic trafficking of BDNF mRNA is mediated by translin and blocked by the G196A (Val66Met) mutation. *Proc Natl Acad Sci U S A,* 106**,** 16481-6.

CHOY, F. C., KLARIC, T. S., KOBLAR, S. A. & LEWIS, M. D. 2015. The Role of the Neuroprotective Factor Npas4 in Cerebral Ischemia. *Int J Mol Sci,* 16**,** 29011-28.

CIRNARU, M. D., MELIS, C., FANUTZA, T., NAPHADE, S., TSHILENGE, K. T., MUNTEAN, B. S., MARTEMYANOV, K. A., PLOTKIN, J. L., ELLERBY, L. M. & EHRLICH, M. E. 2019. Nuclear Receptor Nr4a1 Regulates Striatal Striosome Development and Dopamine D1 Receptor Signaling. *eNeuro,* 6.

CLAUSEN, K. A., BLISH, K. R., BIRSE, C. E., TRIPLETTE, M. A., KUTE, T. E., RUSSELL, G. B., D'AGOSTINO, R. B., JR., MILLER, L. D., TORTI, F. M. & TORTI, S. V. 2011. SOSTDC1 differentially modulates Smad and beta-catenin activation and is down-regulated in breast cancer. *Breast Cancer Res Treat,* 129**,** 737-46.

COHEN, M. S., BAS ORTH, C., KIM, H. J., JEON, N. L. & JAFFREY, S. R. 2011. Neurotrophin-mediated dendrite-to-nucleus signaling revealed by microfluidic compartmentalization of dendrites. *Proc Natl Acad Sci U S A,* 108**,** 11246-51.

COHEN, S. 1960. Purification of a Nerve-Growth Promoting Protein from the Mouse Salivary Gland and Its Neuro-Cytotoxic Antiserum. *Proc Natl Acad Sci U S A,* 46**,** 302-11.

COHEN, S. 1964. Isolation and Biological Effects of an Epidermal Growth-Stimulating Protein. *Natl Cancer Inst Monogr,* 13**,** 13-37.

COHEN, S., LEVI-MONTALCINI, R. & HAMBURGER, V. 1954. A Nerve Growth-Stimulating Factor Isolated from Sarcom as 37 and 180. *Proc Natl Acad Sci U S A,* 40**,** 1014-8.

CONOVER, J. C., ERICKSON, J. T., KATZ, D. M., BIANCHI, L. M., POUEYMIROU, W. T., MCCLAIN, J., PAN, L., HELGREN, M., IP, N. Y., BOLAND, P. & ET AL. 1995. Neuronal deficits, not involving motor neurons, in mice lacking BDNF and/or NT4. *Nature,* 375**,** 235-8.

CONSORTIUM, H. D. I. 2012. Induced pluripotent stem cells from patients with Huntington's disease show CAG-repeat-expansion-associated phenotypes. *Cell Stem Cell,* 11**,** 264-78.

COOK, T., GEBELEIN, B., MESA, K., MLADEK, A. & URRUTIA, R. 1998. Molecular cloning and characterization of TIEG2 reveals a new subfamily of transforming growth factor-beta-inducible Sp1-like zinc finger-encoding genes involved in the regulation of cell growth. *J Biol Chem,* 273**,** 25929-36.

COPPOLA, V., MUSUMECI, M., PATRIZII, M., CANNISTRACI, A., ADDARIO, A., MAUGERI-SACCA, M., BIFFONI, M., FRANCESCANGELI, F., CORDENONSI, M., PICCOLO, S., MEMEO, L., PAGLIUCA, A., MUTO, G., ZEUNER, A., DE MARIA, R. & BONCI, D. 2013. BTG2 loss and miR-21 upregulation contribute to prostate cell transformation by inducing luminal markers expression and epithelial-mesenchymal transition. *Oncogene,* 32**,** 1843-53.

CORDEIRA, J. W., FELSTED, J. A., TEILLON, S., DAFTARY, S., PANESSITI, M., WIRTH, J., SENA-ESTEVES, M. & RIOS, M. 2014. Hypothalamic dysfunction of the thrombospondin receptor alpha2delta-1 underlies the overeating and obesity triggered by brain-derived neurotrophic factor deficiency. *J Neurosci,* 34**,** 554-65.

COUTELLIER, L., BERAKI, S., ARDESTANI, P. M., SAW, N. L. & SHAMLOO, M. 2012. Npas4: a neuronal transcription factor with a key role in social and cognitive functions relevant to developmental disorders. *PLoS One,* 7**,** e46604.

CROLL, S. D., CHESNUTT, C. R., RUDGE, J. S., ACHESON, A., RYAN, T. E., SIUCIAK, J. A., DISTEFANO, P. S., WIEGAND, S. J. & LINDSAY, R. M. 1998. Co-infusion with a TrkB-Fc receptor body carrier enhances BDNF distribution in the adult rat brain. *Exp Neurol,* 152**,** 20-33.

CUNNINGHAM, M. E., STEPHENS, R. M., KAPLAN, D. R. & GREENE, L. A. 1997. Autophosphorylation of activation loop tyrosines regulates signaling by the TRK nerve growth factor receptor. *J Biol Chem,* 272**,** 10957-67.

CURRAN, T. & MORGAN, J. I. 1985. Superinduction of c-fos by nerve growth factor in the presence of peripherally active benzodiazepines. *Science,* 229**,** 1265-8.

D'ADDARIO, C., PALAZZO, M. C., BENATTI, B., GRANCINI, B., PUCCI, M., DI FRANCESCO, A., CAMURI, G., GALIMBERTI, D., FENOGLIO, C., SCARPINI, E., ALTAMURA, A. C., MACCARRONE, M. & DELL'OSSO, B. 2018. Regulation of gene transcription in bipolar disorders: Role of DNA methylation in the relationship between prodynorphin and brain derived neurotrophic factor. *Prog Neuropsychopharmacol Biol Psychiatry,* 82**,** 314-321.

D'HUYS, T., CLAES, S., VAN LOY, T. & SCHOLS, D. 2018. CXCR7/ACKR3-targeting ligands interfere with X7 HIV-1 and HIV-2 entry and replication in human host cells. *Heliyon,* 4**,** e00557.

DAHERON, L., OPITZ, S. L., ZAEHRES, H., LENSCH, M. W., ANDREWS, P. W., ITSKOVITZ-ELDOR, J. & DALEY, G. Q. 2004. LIF/STAT3 signaling fails to maintain self-renewal of human embryonic stem cells. *Stem Cells,* 22**,** 770-8.

DANGOND, F., HWANG, D., CAMELO, S., PASINELLI, P., FROSCH, M. P., STEPHANOPOULOS, G., STEPHANOPOULOS, G., BROWN, R. H., JR. & GULLANS, S. R. 2004. Molecular signature of late-stage human ALS revealed by expression profiling of postmortem spinal cord gray matter. *Physiol Genomics,* 16**,** 229-39.

DANJO, T., EIRAKU, M., MUGURUMA, K., WATANABE, K., KAWADA, M., YANAGAWA, Y., RUBENSTEIN, J. L. & SASAI, Y. 2011. Subregional specification of embryonic stem cell-derived ventral telencephalic tissues by timed and combinatory treatment with extrinsic signals. *J Neurosci,* 31**,** 1919-33.

DAVIDSON, K. C., MASON, E. A. & PERA, M. F. 2015. The pluripotent state in mouse and human. *Development,* 142**,** 3090-9.

DAVIES, A. M. & LINDSAY, R. M. 1985. The cranial sensory ganglia in culture: Differences in the response of placode-derived and neural crest-derived neurons to nerve growth factor. *Developmental Biology,* 111**,** 62-72.

DAY, R., LAZURE, C., BASAK, A., BOUDREAULT, A., LIMPERIS, P., DONG, W. & LINDBERG, I. 1998. Prodynorphin processing by proprotein convertase 2. Cleavage at single basic residues and enhanced processing in the presence of carboxypeptidase activity. *J Biol Chem,* 273**,** 829-36.

DE LOS ANGELES, A., LOH, Y. H., TESAR, P. J. & DALEY, G. Q. 2012. Accessing naive human pluripotency. *Curr Opin Genet Dev,* 22**,** 272-82.

DE PINS, B., CIFUENTES-DIAZ, C., FARAH, A. T., LOPEZ-MOLINA, L., MONTALBAN, E., SANCHO-BALSELLS, A., LOPEZ, A., GINES, S., DELGADO-GARCIA, J. M., ALBERCH, J., GRUART, A., GIRAULT, J. A. & GIRALT, A. 2019. Conditional BDNF Delivery from Astrocytes Rescues Memory Deficits, Spine Density, and Synaptic Properties in the 5xFAD Mouse Model of Alzheimer Disease. *J Neurosci,* 39**,** 2441-2458.

DE RAMON FRANCAS, G., ALTHER, T. & STOECKLI, E. T. 2017. Calsyntenins Are Expressed in a Dynamic and Partially Overlapping Manner during Neural Development. *Front Neuroanat,* 11**,** 76.

DECHANT, G. & BARDE, Y. A. 2002. The neurotrophin receptor p75(NTR): novel functions and implications for diseases of the nervous system. *Nat Neurosci,* 5**,** 1131-6.

DEOGRACIAS, R., YAZDANI, M., DEKKERS, M. P., GUY, J., IONESCU, M. C., VOGT, K. E. & BARDE, Y. A. 2012. Fingolimod, a sphingosine-1 phosphate receptor modulator, increases BDNF levels and

improves symptoms of a mouse model of Rett syndrome. *Proc Natl Acad Sci U S A,* 109**,** 14230-5.

DESIKAN, R. S., SCHORK, A. J., WANG, Y., THOMPSON, W. K., DEHGHAN, A., RIDKER, P. M., CHASMAN, D. I., MCEVOY, L. K., HOLLAND, D., CHEN, C. H., KAROW, D. S., BREWER, J. B., HESS, C. P., WILLIAMS, J., SIMS, R., O'DONOVAN, M. C., CHOI, S. H., BIS, J. C., IKRAM, M. A., GUDNASON, V., DESTEFANO, A. L., VAN DER LEE, S. J., PSATY, B. M., VAN DUIJN, C. M., LAUNER, L., SESHADRI, S., PERICAK-VANCE, M. A., MAYEUX, R., HAINES, J. L., FARRER, L. A., HARDY, J., ULSTEIN, I. D., AARSLAND, D., FLADBY, T., WHITE, L. R., SANDO, S. B., RONGVE, A., WITOELAR, A., DJUROVIC, S., HYMAN, B. T., SNAEDAL, J., STEINBERG, S., STEFANSSON, H., STEFANSSON, K., SCHELLENBERG, G. D., ANDREASSEN, O. A., DALE, A. M., INFLAMMATION WORKING GROUP, I. & DEMGENE, I. 2015. Polygenic Overlap Between C-Reactive Protein, Plasma Lipids, and Alzheimer Disease. *Circulation,* 131**,** 2061-2069.

DHANOA, B. S., COGLIATI, T., SATISH, A. G., BRUFORD, E. A. & FRIEDMAN, J. S. 2013. Update on the Kelch-like (KLHL) gene family. *Hum Genomics,* 7**,** 13.

DOBIN, A., DAVIS, C. A., SCHLESINGER, F., DRENKOW, J., ZALESKI, C., JHA, S., BATUT, P., CHAISSON, M. & GINGERAS, T. R. 2013. STAR: ultrafast universal RNA-seq aligner. *Bioinformatics,* 29**,** 15-21.

DONG, J. T., SUZUKI, H., PIN, S. S., BOVA, G. S., SCHALKEN, J. A., ISAACS, W. B., BARRETT, J. C. & ISAACS, J. T. 1996. Down-regulation of the KAI1 metastasis suppressor gene during the progression of human prostatic cancer infrequently involves gene mutation or allelic loss. *Cancer Res,* 56**,** 4387-90.

DOVEY, H. F., JOHN, V., ANDERSON, J. P., CHEN, L. Z., DE SAINT ANDRIEU, P., FANG, L. Y., FREEDMAN, S. B., FOLMER, B., GOLDBACH, E., HOLSZTYNSKA, E. J., HU, K. L., JOHNSON-WOOD, K. L., KENNEDY, S. L., KHOLODENKO, D., KNOPS, J. E., LATIMER, L. H., LEE, M., LIAO, Z., LIEBERBURG, I. M., MOTTER, R. N., MUTTER, L. C., NIETZ, J., QUINN, K. P., SACCHI, K. L., SEUBERT, P. A., SHOPP, G. M., THORSETT, E. D., TUNG, J. S., WU, J., YANG, S., YIN, C. T., SCHENK, D. B., MAY, P. C., ALTSTIEL, L. D., BENDER, M. H., BOGGS, L. N., BRITTON, T. C., CLEMENS, J. C., CZILLI, D. L., DIECKMAN-MCGINTY, D. K., DROSTE, J. J., FUSON, K. S., GITTER, B. D., HYSLOP, P. A., JOHNSTONE, E. M., LI, W. Y., LITTLE, S. P., MABRY, T. E., MILLER, F. D. & AUDIA, J. E. 2001. Functional gamma-secretase inhibitors reduce beta-amyloid peptide levels in brain. *J Neurochem,* 76**,** 173-81.

DRAGUNOW, M. & ROBERTSON, H. A. 1988. Brain injury induces c-fos protein(s) in nerve and glial-like cells in adult mammalian brain. *Brain Res,* 455**,** 295-9.

DU, R., LIU, B., ZHOU, L., WANG, D., HE, X., XU, X., ZHANG, L., NIU, C. & LIU, S. 2018. Downregulation of annexin A3 inhibits tumor metastasis and decreases drug resistance in breast cancer. *Cell Death Dis,* 9**,** 126.

DUFOUR, A., BELLAC, C. L., ECKHARD, U., SOLIS, N., KLEIN, T., KAPPELHOFF, R., FORTELNY, N., JOBIN, P., ROZMUS, J., MARK, J., PAVLIDIS, P., DIVE, V., BARBOUR, S. J. & OVERALL, C. M. 2018. C-terminal truncation of IFN-gamma inhibits proinflammatory macrophage responses and is deficient in autoimmune disease. *Nat Commun,* 9**,** 2416.

DUFOURNY, L., LEVASSEUR, A., MIGAUD, M., CALLEBAUT, I., PONTAROTTI, P., MALPAUX, B. & MONGET, P. 2008. GPR50 is the mammalian ortholog of Mel1c: evidence of rapid evolution in mammals. *BMC Evol Biol,* 8**,** 105.

DUNCAN, J., WANG, N., ZHANG, X., JOHNSON, S., HARRIS, S., ZHENG, B., ZHANG, Q., RAJKOWSKA, G., MIGUEL-HIDALGO, J. J., SITTMAN, D., OU, X. M., STOCKMEIER, C. A. & WANG, J. M. 2015. Chronic Social Stress and Ethanol Increase Expression of KLF11, a Cell Death Mediator, in Rat Brain. *Neurotox Res,* 28**,** 18-31.

DZYUBENKO, E., GOTTSCHLING, C. & FAISSNER, A. 2016. Neuron-Glia Interactions in Neural Plasticity: Contributions of Neural Extracellular Matrix and Perineuronal Nets. *Neural Plast,* 2016**,** 5214961.

EAGLE, A. L., GAJEWSKI, P. A., YANG, M., KECHNER, M. E., AL MASRAF, B. S., KENNEDY, P. J., WANG, H., MAZEI-ROBISON, M. S. & ROBISON, A. J. 2015. Experience-Dependent Induction of Hippocampal DeltaFosB Controls Learning. *J Neurosci,* 35**,** 13773-83.

ECCLES, R. L., CZAJKOWSKI, M. T., BARTH, C., MULLER, P. M., MCSHANE, E., GRUNWALD, S., BEAUDETTE, P., MECKLENBURG, N., VOLKMER, R., ZUHLKE, K., DITTMAR, G., SELBACH, M., HAMMES, A., DAUMKE, O., KLUSSMANN, E., URBE, S. & ROCKS, O. 2016. Bimodal antagonism of PKA signalling by ARHGAP36. *Nat Commun,* 7**,** 12963.

EGAN, M. F., KOJIMA, M., CALLICOTT, J. H., GOLDBERG, T. E., KOLACHANA, B. S., BERTOLINO, A., ZAITSEV, E., GOLD, B., GOLDMAN, D., DEAN, M., LU, B. & WEINBERGER, D. R. 2003. The BDNF val66met polymorphism affects activity-dependent secretion of BDNF and human memory and hippocampal function. *Cell,* 112**,** 257-69.

EGANA, I., KAITO, H., NITZSCHE, A., BECKER, L., BALLESTER-LOPEZ, C., NIAUDET, C., PETKOVA, M., LIU, W., VANLANDEWIJCK, M., VERNALEKEN, A., KLOPSTOCK, T., FUCHS, H., GAILUS-DURNER, V., HRABE DE ANGELIS, M., RASK-ANDERSEN, H., JOHANSSON, H. J., LEHTIO, J., HE, L., YILDIRIM, A. O., HELLSTROM, M. & GERMAN MOUSE CLINIC, C. 2017. Female mice lacking Pald1 exhibit endothelial cell apoptosis and emphysema. *Sci Rep,* 7**,** 15453.

EIGLER, T. & BEN-SHLOMO, A. 2014. Somatostatin system: molecular mechanisms regulating anterior pituitary hormones. *J Mol Endocrinol,* 53**,** R1-19.

EL-GHISSASSI, F., VALSESIA-WITTMANN, S., FALETTE, N., DURIEZ, C., WALDEN, P. D. & PUISIEUX, A. 2002. BTG2(TIS21/PC3) induces neuronal differentiation and prevents apoptosis of terminally differentiated PC12 cells. *Oncogene,* 21**,** 6772-78.

ENDO, M., DOI, R., NISHITA, M. & MINAMI, Y. 2012. Ror family receptor tyrosine kinases regulate the maintenance of neural progenitor cells in the developing neocortex. *J Cell Sci,* 125**,** 2017-29.

ERNFORS, P., HENSCHEN, A., OLSON, L. & PERSSON, H. 1989. Expression of nerve growth factor receptor mRNA is developmentally regulated and increased after axotomy in rat spinal cord motoneurons. *Neuron,* 2**,** 1605-13.

ERNFORS, P., LEE, K. F. & JAENISCH, R. 1994. Mice lacking brain-derived neurotrophic factor develop with sensory deficits. *Nature,* 368**,** 147-50.

ERNFORS, P., WETMORE, C., OLSON, L. & PERSSON, H. 1990. Identification of cells in rat brain and peripheral tissues expressing mRNA for members of the nerve growth factor family. *Neuron,* 5**,** 511-26.

ESPUNY-CAMACHO, I., MICHELSEN, K. A., GALL, D., LINARO, D., HASCHE, A., BONNEFONT, J., BALI, C., ORDUZ, D., BILHEU, A., HERPOEL, A., LAMBERT, N., GASPARD, N., PERON, S., SCHIFFMANN, S. N., GIUGLIANO, M., GAILLARD, A. & VANDERHAEGHEN, P. 2013. Pyramidal neurons derived from human pluripotent stem cells integrate efficiently into mouse brain circuits in vivo. *Neuron,* 77**,** 440-56.

EVANS, M. J., BRADLEY, A., KUEHN, M. R. & ROBERTSON, E. J. 1985. The ability of EK cells to form chimeras after selection of clones in G418 and some observations on the integration of retroviral vector proviral DNA into EK cells. *Cold Spring Harb Symp Quant Biol,* 50**,** 685-9.

EVANS, M. J. & KAUFMAN, M. H. 1981. Establishment in culture of pluripotential cells from mouse embryos. *Nature,* 292**,** 154-6.

FARDILHA, M., ESTEVES, S. L., KORRODI-GREGORIO, L., VINTEM, A. P., DOMINGUES, S. C., REBELO, S., MORRICE, N., COHEN, P. T., DA CRUZ E SILVA, O. A. & DA CRUZ E SILVA, E. F. 2011. Identification of the human testis protein phosphatase 1 interactome. *Biochem Pharmacol,* 82**,** 1403-15.

FARIOLI-VECCHIOLI, S., SARAULLI, D., COSTANZI, M., LEONARDI, L., CINA, I., MICHELI, L., NUTINI, M., LONGONE, P., OH, S. P., CESTARI, V. & TIRONE, F. 2009. Impaired terminal differentiation of hippocampal granule neurons and defective contextual memory in PC3/Tis21 knockout mice. *PLoS One,* 4**,** e8339.

FARLIE, P., REID, C., WILCOX, S., PEETERS, J., REED, G. & NEWGREEN, D. 2001. Ypel1: a novel nuclear protein that induces an epithelial-like morphology in fibroblasts. *Genes Cells,* 6**,** 619-29.

FEI, J. F., HAFFNER, C. & HUTTNER, W. B. 2014. 3' UTR-dependent, miR-92-mediated restriction of Tis21 expression maintains asymmetric neural stem cell division to ensure proper neocortex size. *Cell Rep,* 7**,** 398-411.

FENG, X., GUAN, D., AUEN, T., CHOI, J. W., SALAZAR HERNANDEZ, M. A., LEE, J., CHUN, H., FARUK, F., KAPLUN, E., HERBERT, Z., COPPS, K. D. & OZCAN, U. 2019. IL1R1 is required for celastrol's leptin-sensitization and antiobesity effects. *Nat Med,* 25**,** 575-582.

FERRARI, M. E., BERNIS, M. E., MCLEOD, F., PODPOLNY, M., COULLERY, R. P., CASADEI, I. M., SALINAS, P. C. & ROSSO, S. B. 2018. Wnt7b signalling through Frizzled-7 receptor promotes dendrite development by coactivating CaMKII and JNK. *J Cell Sci,* 131.

FERRER, I., GOUTAN, E., MARIN, C., REY, M. J. & RIBALTA, T. 2000. Brain-derived neurotrophic factor in Huntington disease. *Brain Res,* 866**,** 257-61.

FERRIS, L. T., WILLIAMS, J. S. & SHEN, C. L. 2007. The effect of acute exercise on serum brain-derived neurotrophic factor levels and cognitive function. *Med Sci Sports Exerc,* 39**,** 728-34.

FIGUROV, A., POZZO-MILLER, L. D., OLAFSSON, P., WANG, T. & LU, B. 1996. Regulation of synaptic responses to high-frequency stimulation and LTP by neurotrophins in the hippocampus. *Nature,* 381**,** 706-9.

FINKBEINER, S. 2000. CREB couples neurotrophin signals to survival messages. *Neuron,* 25**,** 11-4.

FINLIN, B. S., SHAO, H., KADONO-OKUDA, K., GUO, N. & ANDRES, D. A. 2000. Rem2, a new member of the Rem/Rad/Gem/Kir family of Ras-related GTPases. *Biochem J,* 347 Pt 1**,** 223-31.

FINN, R. S., DERING, J., CONKLIN, D., KALOUS, O., COHEN, D. J., DESAI, A. J., GINTHER, C., ATEFI, M., CHEN, I., FOWST, C., LOS, G. & SLAMON, D. J. 2009. PD 0332991, a selective cyclin D kinase 4/6 inhibitor, preferentially inhibits proliferation of luminal estrogen receptor-positive human breast cancer cell lines in vitro. *Breast Cancer Res,* 11**,** R77.

FISCHER, E. H. 2010. Phosphorylase and the origin of reversible protein phosphorylation. *Biol Chem,* 391**,** 131-7.

FONTANET, P., IRALA, D., ALSINA, F. C., PARATCHA, G. & LEDDA, F. 2013. Pea3 transcription factor family members Etv4 and Etv5 mediate retrograde signaling and axonal growth of DRG sensory neurons in response to NGF. *J Neurosci,* 33**,** 15940-51.

FONTANET, P. A., RIOS, A. S., ALSINA, F. C., PARATCHA, G. & LEDDA, F. 2018. Pea3 Transcription Factors, Etv4 and Etv5, Are Required for Proper Hippocampal Dendrite Development and Plasticity. *Cereb Cortex,* 28**,** 236-249.

FRANKE, T. F., KAPLAN, D. R., CANTLEY, L. C. & TOKER, A. 1997. Direct regulation of the Akt proto-oncogene product by phosphatidylinositol-3,4-bisphosphate. *Science,* 275**,** 665-8.

GAJEWSKI, P. A., TURECKI, G. & ROBISON, A. J. 2016. Differential Expression of FosB Proteins and Potential Target Genes in Select Brain Regions of Addiction and Depression Patients. *PLoS One,* 11**,** e0160355.

GAJOFATTO, A. & TURATTI, M. 2018. Investigational immunosuppressants in early-stage clinical trials for the treatment of multiple sclerosis. *Expert Opin Investig Drugs,* 27**,** 273-286.

GARCIA-LLORCA, A., ASPELUND, S. G., OGMUNDSDOTTIR, M. H., STEINGRIMSSON, E. & EYSTEINSSON, T. 2019. The microphthalmia-associated transcription factor (Mitf) gene and its role in regulating eye function. *Sci Rep,* 9**,** 15386.

GARDNER, H. P., WERTHEIM, G. B., HA, S. I., COPELAND, N. G., GILBERT, D. J., JENKINS, N. A., MARQUIS, S. T. & CHODOSH, L. A. 2000. Cloning and characterization of Hunk, a novel mammalian SNF1-related protein kinase. *Genomics,* 63**,** 46-59.

GAUTHIER, L. R., CHARRIN, B. C., BORRELL-PAGES, M., DOMPIERRE, J. P., RANGONE, H., CORDELIERES, F. P., DE MEY, J., MACDONALD, M. E., LESSMANN, V., HUMBERT, S. & SAUDOU, F. 2004. Huntingtin controls neurotrophic support and survival of neurons by enhancing BDNF vesicular transport along microtubules. *Cell,* 118**,** 127-38.

GEETHA, T., REGE, S. D., MATHEWS, S. E., MEAKIN, S. O., WHITE, M. F. & BABU, J. R. 2013. Nerve growth factor receptor TrkA, a new receptor in insulin signaling pathway in PC12 cells. *J Biol Chem,* 288**,** 23807-13.

GENTLEMAN, R. C., CAREY, V. J., BATES, D. M., BOLSTAD, B., DETTLING, M., DUDOIT, S., ELLIS, B., GAUTIER, L., GE, Y., GENTRY, J., HORNIK, K., HOTHORN, T., HUBER, W., IACUS, S., IRIZARRY, R., LEISCH, F., LI, C., MAECHLER, M., ROSSINI, A. J., SAWITZKI, G., SMITH, C., SMYTH, G., TIERNEY, L., YANG, J. Y. & ZHANG, J. 2004. Bioconductor: open software development for computational biology and bioinformatics. *Genome Biol,* 5**,** R80.

GEORGALA, P. A., CARR, C. B. & PRICE, D. J. 2011. The role of Pax6 in forebrain development. *Dev Neurobiol,* 71**,** 690-709.

GERKE, V., CREUTZ, C. E. & MOSS, S. E. 2005. Annexins: linking Ca2+ signalling to membrane dynamics. *Nat Rev Mol Cell Biol,* 6**,** 449-61.

GERMAIN, N. D., BANDA, E. C., BECKER, S., NAEGELE, J. R. & GRABEL, L. B. 2013. Derivation and isolation of NKX2.1-positive basal forebrain progenitors from human embryonic stem cells. *Stem Cells Dev,* 22**,** 1477-89.

GERRITSEN, M. E. & WAGNER, G. F. 2005. Stanniocalcin: no longer just a fish tale. *Vitam Horm,* 70**,** 105-35.

GHIRETTI, A. E. & PARADIS, S. 2011. The GTPase Rem2 regulates synapse development and dendritic morphology. *Dev Neurobiol,* 71**,** 374-89.

GIRGENRATH, M., WENG, S., KOSTEK, C. A., BROWNING, B., WANG, M., BROWN, S. A., WINKLES, J. A., MICHAELSON, J. S., ALLAIRE, N., SCHNEIDER, P., SCOTT, M. L., HSU, Y. M., YAGITA, H., FLAVELL, R. A., MILLER, J. B., BURKLY, L. C. & ZHENG, T. S. 2006. TWEAK, via its receptor Fn14, is a novel regulator of mesenchymal progenitor cells and skeletal muscle regeneration. *EMBO J,* 25**,** 5826-39.

GOGTAY, N., ORDONEZ, A., HERMAN, D. H., HAYASHI, K. M., GREENSTEIN, D., VAITUZIS, C., LENANE, M., CLASEN, L., SHARP, W., GIEDD, J. N., JUNG, D., NUGENT, T. F., 3RD, TOGA, A. W., LEIBENLUFT, E., THOMPSON, P. M. & RAPOPORT, J. L. 2007. Dynamic mapping of cortical development before and after the onset of pediatric bipolar illness. *J Child Psychol Psychiatry,* 48**,** 852-62.

GONCALVES, S. A., MACEDO, D., RAQUEL, H., SIMOES, P. D., GIORGINI, F., RAMALHO, J. S., BARRAL, D. C., FERREIRA MOITA, L. & OUTEIRO, T. F. 2016. shRNA-Based Screen Identifies Endocytic Recycling Pathway Components That Act as Genetic Modifiers of Alpha-Synuclein Aggregation, Secretion and Toxicity. *PLoS Genet,* 12**,** e1005995.

GORSKI, J. A., ZEILER, S. R., TAMOWSKI, S. & JONES, K. R. 2003. Brain-derived neurotrophic factor is required for the maintenance of cortical dendrites. *J Neurosci,* 23**,** 6856-65.

GRAY, J., YEO, G., HUNG, C., KEOGH, J., CLAYTON, P., BANERJEE, K., MCAULAY, A., O'RAHILLY, S. & FAROOQI, I. S. 2007. Functional characterization of human NTRK2 mutations identified in patients with severe early-onset obesity. *Int J Obes (Lond),* 31**,** 359-64.

GRILLET, N., SCHWANDER, M., HILDEBRAND, M. S., SCZANIECKA, A., KOLATKAR, A., VELASCO, J., WEBSTER, J. A., KAHRIZI, K., NAJMABADI, H., KIMBERLING, W. J., STEPHAN, D., BAHLO, M., WILTSHIRE, T., TARANTINO, L. M., KUHN, P., SMITH, R. J. & MULLER, U. 2009. Mutations in LOXHD1, an evolutionarily conserved stereociliary protein, disrupt hair cell function in mice and cause progressive hearing loss in humans. *Am J Hum Genet,* 85**,** 328-37.

GROTH, R. D. & MERMELSTEIN, P. G. 2003. Brain-derived neurotrophic factor activation of NFAT (nuclear factor of activated T-cells)-dependent transcription: a role for the transcription factor NFATc4 in neurotrophin-mediated gene expression. *J Neurosci,* 23**,** 8125-34.

GRUNEWALD, E., KINNELL, H. L., PORTEOUS, D. J. & THOMSON, P. A. 2009. GPR50 interacts with neuronal NOGO-A and affects neurite outgrowth. *Mol Cell Neurosci,* 42**,** 363-71.

GUARDAVACCARO, D., CORRENTE, G., COVONE, F., MICHELI, L., D'AGNANO, I., STARACE, G., CARUSO, M. & TIRONE, F. 2000. Arrest of G(1)-S progression by the p53-inducible gene PC3 is Rb dependent and relies on the inhibition of cyclin D1 transcription. *Mol Cell Biol,* 20**,** 1797-815.

GUO, G., VON MEYENN, F., ROSTOVSKAYA, M., CLARKE, J., DIETMANN, S., BAKER, D., SAHAKYAN, A., MYERS, S., BERTONE, P., REIK, W., PLATH, K. & SMITH, A. 2017. Epigenetic resetting of human pluripotency. *Development,* 144**,** 2748-2763.

GUO, G., VON MEYENN, F., SANTOS, F., CHEN, Y., REIK, W., BERTONE, P., SMITH, A. & NICHOLS, J. 2016. Naive Pluripotent Stem Cells Derived Directly from Isolated Cells of the Human Inner Cell Mass. *Stem Cell Reports,* 6**,** 437-446.

GUO, W., PANG, K., CHEN, Y., WANG, S., LI, H., XU, Y., HAN, F., YAO, H., LIU, H., LOPES-RODRIGUES, V., SUN, D., SHAO, J., SHEN, J., DOU, Y., ZHANG, W., YOU, H., WU, W. & LU, B. 2019. TrkB agonistic antibodies superior to BDNF: Utility in treating motoneuron degeneration. *Neurobiol Dis,* 132**,** 104590.

GUPTA, V. K., YOU, Y., GUPTA, V. B., KLISTORNER, A. & GRAHAM, S. L. 2013. TrkB receptor signalling: implications in neurodegenerative, psychiatric and proliferative disorders. *Int J Mol Sci,* 14**,** 10122-42.

HABERT-ORTOLI, E., AMIRANOFF, B., LOQUET, I., LABURTHE, M. & MAYAUX, J. F. 1994. Molecular cloning of a functional human galanin receptor. *Proc Natl Acad Sci U S A,* 91**,** 9780-3.

HAHM, S., MIZUNO, T. M., WU, T. J., WISOR, J. P., PRIEST, C. A., KOZAK, C. A., BOOZER, C. N., PENG, B., MCEVOY, R. C., GOOD, P., KELLEY, K. A., TAKAHASHI, J. S., PINTAR, J. E., ROBERTS, J. L., MOBBS, C. V. & SALTON, S. R. 1999. Targeted deletion of the Vgf gene indicates that the encoded secretory peptide precursor plays a novel role in the regulation of energy balance. *Neuron,* 23**,** 537-48.

HALLBOOK, F., IBANEZ, C. F. & PERSSON, H. 1991. Evolutionary studies of the nerve growth factor family reveal a novel member abundantly expressed in Xenopus ovary. *Neuron,* 6**,** 845-58.

HAMBURGER, V. & LEVI-MONTALCINI, R. 1949. Proliferation, differentiation and degeneration in the spinal ganglia of the chick embryo under normal and experimental conditions. *J Exp Zool,* 111**,** 457-501.

HAN, F., GUAN, X., GUO, W. & LU, B. 2019. Therapeutic potential of a TrkB agonistic antibody for ischemic brain injury. *Neurobiol Dis,* 127**,** 570-581.

HAN, J., LEE, J. D., JIANG, Y., LI, Z., FENG, L. & ULEVITCH, R. J. 1996. Characterization of the structure and function of a novel MAP kinase kinase (MKK6). *J Biol Chem,* 271**,** 2886-91.

HAN, J. C., LIU, Q. R., JONES, M., LEVINN, R. L., MENZIE, C. M., JEFFERSON-GEORGE, K. S., ADLER-WAILES, D. C., SANFORD, E. L., LACBAWAN, F. L., UHL, G. R., RENNERT, O. M. & YANOVSKI, J. A. 2008. Brain-derived neurotrophic factor and obesity in the WAGR syndrome. *N Engl J Med,* 359**,** 918-27.

HAN, J. C., THURM, A., GOLDEN WILLIAMS, C., JOSEPH, L. A., ZEIN, W. M., BROOKS, B. P., BUTMAN, J. A., BRADY, S. M., FUHR, S. R., HICKS, M. D., HUEY, A. E., HANISH, A. E., DANLEY, K. M., RAYGADA, M. J., RENNERT, O. M., MARTINOWICH, K., SHARP, S. J., TSAO, J. W. & SWEDO, S. E. 2013. Association of brain-derived neurotrophic factor (BDNF) haploinsufficiency with lower adaptive behaviour and reduced cognitive functioning in WAGR/11p13 deletion syndrome. *Cortex,* 49**,** 2700-10.

HAQUE, M. E., KIM, I. S., JAKARIA, M., AKTHER, M. & CHOI, D. K. 2018. Importance of GPCR-Mediated Microglial Activation in Alzheimer's Disease. *Front Cell Neurosci,* 12**,** 258.

HARRIS, B. Z. & LIM, W. A. 2001. Mechanism and role of PDZ domains in signaling complex assembly. *J Cell Sci,* 114**,** 3219-31.

HARRIS, S., JOHNSON, S., DUNCAN, J. W., UDEMGBA, C., MEYER, J. H., ALBERT, P. R., LOMBERK, G., URRUTIA, R., OU, X. M., STOCKMEIER, C. A. & WANG, J. M. 2015. Evidence revealing deregulation of the KLF11-MAO A pathway in association with chronic stress and depressive disorders. *Neuropsychopharmacology,* 40**,** 1373-82.

HARRISON, S. & GEPPETTI, P. 2001. Substance p. *Int J Biochem Cell Biol,* 33**,** 555-76.

HARTMANN, M., HEUMANN, R. & LESSMANN, V. 2001. Synaptic secretion of BDNF after high-frequency stimulation of glutamatergic synapses. *EMBO J,* 20**,** 5887-97.

HASBI, A., FAN, T., ALIJANIARAM, M., NGUYEN, T., PERREAULT, M. L., O'DOWD, B. F. & GEORGE, S. R. 2009. Calcium signaling cascade links dopamine D1-D2 receptor heteromer to striatal BDNF production and neuronal growth. *Proc Natl Acad Sci U S A,* 106**,** 21377-82.

HASSON, S. A., KANE, L. A., YAMANO, K., HUANG, C. H., SLITER, D. A., BUEHLER, E., WANG, C., HEMAN-ACKAH, S. M., HESSA, T., GUHA, R., MARTIN, S. E. & YOULE, R. J. 2013. High-content genome-wide RNAi screens identify regulators of parkin upstream of mitophagy. *Nature,* 504**,** 291-5.

HAUSOTT, B., VALLANT, N., SCHLICK, B., AUER, M., NIMMERVOLL, B., OBERMAIR, G. J., SCHWARZER, C., DAI, F., BRAND-SABERI, B. & KLIMASCHEWSKI, L. 2012. Sprouty2 and -4 regulate axon outgrowth by hippocampal neurons. *Hippocampus,* 22**,** 434-41.

HAWES, J. J., BRUNZELL, D. H., WYNICK, D., ZACHARIOU, V. & PICCIOTTO, M. R. 2005. GalR1, but not GalR2 or GalR3, levels are regulated by galanin signaling in the locus coeruleus through a cyclic AMP-dependent mechanism. *J Neurochem,* 93**,** 1168-76.

HAYER, S. N. & BADING, H. 2015. Nuclear calcium signaling induces expression of the synaptic organizers Lrrtm1 and Lrrtm2. *J Biol Chem,* 290**,** 5523-32.

HE, Q., JING, H., LIAW, L., GOWER, L., VARY, C., HUA, S. & YANG, X. 2016. Suppression of Spry1 inhibits triple-negative breast cancer malignancy by decreasing EGF/EGFR mediated mesenchymal phenotype. *Sci Rep,* 6**,** 23216.

HEINZ, L. X., BAUMANN, C. L., KOBERLIN, M. S., SNIJDER, B., GAWISH, R., SHUI, G., SHARIF, O., ASPALTER, I. M., MULLER, A. C., KANDASAMY, R. K., BREITWIESER, F. P., PICHLMAIR, A., BRUCKNER, M., REBSAMEN, M., BLUML, S., KARONITSCH, T., FAUSTER, A., COLINGE, J., BENNETT, K. L., KNAPP, S., WENK, M. R. & SUPERTI-FURGA, G. 2015. The Lipid-Modifying Enzyme SMPDL3B Negatively Regulates Innate Immunity. *Cell Rep,* 11**,** 1919-28.

HEMPSTEAD, B. L., MARTIN-ZANCA, D., KAPLAN, D. R., PARADA, L. F. & CHAO, M. V. 1991. High-affinity NGF binding requires coexpression of the trk proto-oncogene and the low-affinity NGF receptor. *Nature,* 350**,** 678-83.

HIMES, B. E., JIANG, X., HU, R., WU, A. C., LASKY-SU, J. A., KLANDERMAN, B. J., ZINITI, J., SENTER-SYLVIA, J., LIMA, J. J., IRVIN, C. G., PETERS, S. P., MEYERS, D. A., BLEECKER, E. R., KUBO, M., TAMARI, M., NAKAMURA, Y., SZEFLER, S. J., LEMANSKE, R. F., JR., ZEIGER, R. S., STRUNK, R. C., MARTINEZ, F. D., HANRAHAN, J. P., KOPPELMAN, G. H., POSTMA, D. S., NIEUWENHUIS, M. A., VONK, J. M., PANETTIERI, R. A., JR., MARKEZICH, A., ISRAEL, E., CAREY, V. J., TANTISIRA, K. G., LITONJUA, A. A., LU, Q. & WEISS, S. T. 2012. Genome-wide association analysis in asthma subjects identifies SPATS2L as a novel bronchodilator response gene. *PLoS Genet,* 8**,** e1002824.

HOCK, C., HEESE, K., HULETTE, C., ROSENBERG, C. & OTTEN, U. 2000. Region-specific neurotrophin imbalances in Alzheimer disease: decreased levels of brain-derived neurotrophic factor and increased levels of nerve growth factor in hippocampus and cortical areas. *Arch Neurol,* 57**,** 846-51.

HOFER, M., PAGLIUSI, S. R., HOHN, A., LEIBROCK, J. & BARDE, Y. A. 1990. Regional distribution of brain-derived neurotrophic factor mRNA in the adult mouse brain. *EMBO J,* 9**,** 2459-64.

HOFER, M. M. & BARDE, Y. A. 1988. Brain-derived neurotrophic factor prevents neuronal death in vivo. *Nature,* 331**,** 261-2.

HOHN, A., LEIBROCK, J., BAILEY, K. & BARDE, Y. A. 1990. Identification and characterization of a novel member of the nerve growth factor/brain-derived neurotrophic factor family. *Nature,* 344**,** 339-41.

HOLIGHAUS, Y., WEIHE, E. & EIDEN, L. E. 2012. STC1 induction by PACAP is mediated through cAMP and ERK1/2 but not PKA in cultured cortical neurons. *J Mol Neurosci,* 46**,** 75-87.

HOSONO, K., SASAKI, T., MINOSHIMA, S. & SHIMIZU, N. 2004. Identification and characterization of a novel gene family YPEL in a wide spectrum of eukaryotic species. *Gene,* 340**,** 31-43.

HOWARD, J. K., CAVE, B. J., OKSANEN, L. J., TZAMELI, I., BJORBAEK, C. & FLIER, J. S. 2004. Enhanced leptin sensitivity and attenuation of diet-induced obesity in mice with haploinsufficiency of Socs3. *Nat Med,* 10**,** 734-8.

HOWELLS, D. W., PORRITT, M. J., WONG, J. Y., BATCHELOR, P. E., KALNINS, R., HUGHES, A. J. & DONNAN, G. A. 2000. Reduced BDNF mRNA expression in the Parkinson's disease substantia nigra. *Exp Neurol,* 166**,** 127-35.

HSU, C. Y., CHANG, G. C., CHEN, Y. J., HSU, Y. C., HSIAO, Y. J., SU, K. Y., CHEN, H. Y., LIN, C. Y., CHEN, J. S., CHEN, Y. J., HONG, Q. S., KU, W. H., WU, C. Y., HO, B. C., CHIANG, C. C., YANG, P. C. & YU, S. L. 2018. FAM198B Is Associated with Prolonged Survival and Inhibits Metastasis in Lung Adenocarcinoma via Blockage of ERK-Mediated MMP-1 Expression. *Clin Cancer Res,* 24**,** 916-926.

HU, D., ANSARI, D., ZHOU, Q., SASOR, A., SAID HILMERSSON, K. & ANDERSSON, R. 2019. Low P4HA2 and high PRTN3 expression predicts poor survival in patients with pancreatic cancer. *Scand J Gastroenterol,* 54**,** 246-251.

HUANG, E. J. & REICHARDT, L. F. 2003. Trk receptors: roles in neuronal signal transduction. *Annu Rev Biochem,* 72**,** 609-42.

HUANG, E. J., WILKINSON, G. A., FARINAS, I., BACKUS, C., ZANG, K., WONG, S. L. & REICHARDT, L. F. 1999. Expression of Trk receptors in the developing mouse trigeminal ganglion: in vivo evidence for NT-3 activation of TrkA and TrkB in addition to TrkC. *Development,* 126**,** 2191-203.

HUANG, L., WU, K. H., ZHANG, L., WANG, Q., TANG, S., WU, Q., JIANG, P. H., LIN, J. J., GUO, J., WANG, L., LOH, S. H. & CHENG, J. 2018. Critical Roles of Xirp Proteins in Cardiac Conduction and Their Rare Variants Identified in Sudden Unexplained Nocturnal Death Syndrome and Brugada Syndrome in Chinese Han Population. *J Am Heart Assoc,* 7.

HUANG, S. M., HANCOCK, M. K., PITMAN, J. L., ORTH, A. P. & GEKAKIS, N. 2009. Negative regulators of insulin signaling revealed in a genome-wide functional screen. *PLoS One,* 4**,** e6871.

HUBER, W., CAREY, V. J., GENTLEMAN, R., ANDERS, S., CARLSON, M., CARVALHO, B. S., BRAVO, H. C., DAVIS, S., GATTO, L., GIRKE, T., GOTTARDO, R., HAHNE, F., HANSEN, K. D., IRIZARRY, R. A., LAWRENCE, M., LOVE, M. I., MACDONALD, J., OBENCHAIN, V., OLES, A. K., PAGES, H., REYES, A., SHANNON, P., SMYTH, G. K., TENENBAUM, D., WALDRON, L. & MORGAN, M. 2015. Orchestrating high-throughput genomic analysis with Bioconductor. *Nat Methods,* 12**,** 115-21.

HUNT, D., RAIVICH, G. & ANDERSON, P. N. 2012. Activating transcription factor 3 and the nervous system. *Front Mol Neurosci,* 5**,** 7.

HURD, Y. L. 2002. Subjects with major depression or bipolar disorder show reduction of prodynorphin mRNA expression in discrete nuclei of the amygdaloid complex. *Mol Psychiatry,* 7**,** 75-81.

IADAROLA, M. J., SAPIO, M. R., WANG, X., CARRERO, H., VIRATA-THEIMER, M. L., SARNOVSKY, R., MANNES, A. J. & FITZGERALD, D. J. 2017. Analgesia by Deletion of Spinal Neurokinin 1 Receptor Expressing Neurons Using a Bioengineered Substance P-Pseudomonas Exotoxin Conjugate. *Mol Pain,* 13**,** 1744806917727657.

IP, N. Y., IBANEZ, C. F., NYE, S. H., MCCLAIN, J., JONES, P. F., GIES, D. R., BELLUSCIO, L., LE BEAU, M. M., ESPINOSA, R., 3RD, SQUINTO, S. P. & ET AL. 1992. Mammalian neurotrophin-4: structure, chromosomal localization, tissue distribution, and receptor specificity. *Proc Natl Acad Sci U S A,* 89**,** 3060-4.

ISHII, M. & MAEDA, N. 2008. Oversulfated chondroitin sulfate plays critical roles in the neuronal migration in the cerebral cortex. *J Biol Chem,* 283**,** 32610-20.

IWAHARA, N., HISAHARA, S., KAWAMATA, J., MATSUMURA, A., YOKOKAWA, K., SAITO, T., FUJIKURA, M., MANABE, T., SUZUKI, H., MATSUSHITA, T., SUZUKI, S. & SHIMOHAMA, S. 2017. Role of Suppressor of Cytokine Signaling 3 (SOCS3) in Altering Activated Microglia Phenotype in APPswe/PS1dE9 Mice. *J Alzheimers Dis,* 55**,** 1235-1247.

JACOBSEN, L. K., PICCIOTTO, M. R., HEATH, C. J., MENCL, W. E. & GELERNTER, J. 2009. Allelic variation of calsyntenin 2 (CLSTN2) modulates the impact of developmental tobacco smoke exposure on mnemonic processing in adolescents. *Biol Psychiatry,* 65**,** 671-9.

JACOBY, A. S., HORT, Y. J., CONSTANTINESCU, G., SHINE, J. & IISMAA, T. P. 2002. Critical role for GALR1 galanin receptor in galanin regulation of neuroendocrine function and seizure activity. *Brain Res Mol Brain Res,* 107**,** 195-200.

JADEJA, S., SMYTH, I., PITERA, J. E., TAYLOR, M. S., VAN HAELST, M., BENTLEY, E., MCGREGOR, L., HOPKINS, J., CHALEPAKIS, G., PHILIP, N., PEREZ AYTES, A., WATT, F. M., DARLING, S. M., JACKSON, I., WOOLF, A. S. & SCAMBLER, P. J. 2005. Identification of a new gene mutated in Fraser syndrome and mouse myelencephalic blebs. *Nat Genet,* 37**,** 520-5.

JADHAV, K. & ZHANG, Y. 2017. Activating transcription factor 3 in immune response and metabolic regulation. *Liver Res,* 1**,** 96-102.

JALAVA, S. E., URBANUCCI, A., LATONEN, L., WALTERING, K. K., SAHU, B., JANNE, O. A., SEPPALA, J., LAHDESMAKI, H., TAMMELA, T. L. & VISAKORPI, T. 2012. Androgen-regulated miR-32 targets BTG2 and is overexpressed in castration-resistant prostate cancer. *Oncogene,* 31**,** 4460-71.

JANG, S. W., LIU, X., YEPES, M., SHEPHERD, K. R., MILLER, G. W., LIU, Y., WILSON, W. D., XIAO, G., BLANCHI, B., SUN, Y. E. & YE, K. 2010. A selective TrkB agonist with potent neurotrophic activities by 7,8-dihydroxyflavone. *Proc Natl Acad Sci U S A,* 107**,** 2687-92.

JERONIMO-SANTOS, A., VAZ, S. H., PARREIRA, S., RAPAZ-LERIAS, S., CAETANO, A. P., BUEE-SCHERRER, V., CASTREN, E., VALENTE, C. A., BLUM, D., SEBASTIAO, A. M. & DIOGENES, M. J. 2015. Dysregulation of TrkB Receptors and BDNF Function by Amyloid-beta Peptide is Mediated by Calpain. *Cereb Cortex,* 25**,** 3107-21.

JOHNSON, D., LANAHAN, A., BUCK, C. R., SEHGAL, A., MORGAN, C., MERCER, E., BOTHWELL, M. & CHAO, M. 1986. Expression and structure of the human NGF receptor. *Cell,* 47**,** 545-54.

JONES, K. R., FARINAS, I., BACKUS, C. & REICHARDT, L. F. 1994. Targeted disruption of the BDNF gene perturbs brain and sensory neuron development but not motor neuron development. *Cell,* 76**,** 989-99.

JONES, K. R. & REICHARDT, L. F. 1990. Molecular cloning of a human gene that is a member of the nerve growth factor family. *Proc Natl Acad Sci U S A,* 87**,** 8060-4.

JUN, J. I. & LAU, L. F. 2011. Taking aim at the extracellular matrix: CCN proteins as emerging therapeutic targets. *Nat Rev Drug Discov,* 10**,** 945-63.

JUNG, E. H., LEE, H. N., HAN, G. Y., KIM, M. J. & KIM, C. W. 2016. Targeting ROR1 inhibits the self-renewal and invasive ability of glioblastoma stem cells. *Cell Biochem Funct,* 34**,** 149-57.

KADKHODAEI, B., ITO, T., JOODMARDI, E., MATTSSON, B., ROUILLARD, C., CARTA, M., MURAMATSU, S., SUMI-ICHINOSE, C., NOMURA, T., METZGER, D., CHAMBON, P., LINDQVIST, E., LARSSON, N. G., OLSON, L., BJORKLUND, A., ICHINOSE, H. & PERLMANN, T. 2009. Nurr1 is required for maintenance of maturing and adult midbrain dopamine neurons. *J Neurosci,* 29**,** 15923-32.

KANG, H. & SCHUMAN, E. M. 1995. Long-lasting neurotrophin-induced enhancement of synaptic transmission in the adult hippocampus. *Science,* 267**,** 1658-62.

KAPLAN, D. R., HEMPSTEAD, B. L., MARTIN-ZANCA, D., CHAO, M. V. & PARADA, L. F. 1991. The trk proto-oncogene product: a signal transducing receptor for nerve growth factor. *Science,* 252**,** 554-8.

KAPLAN, D. R. & MILLER, F. D. 2000. Neurotrophin signal transduction in the nervous system. *Curr Opin Neurobiol,* 10**,** 381-91.

KAPPOS, L., RADUE, E. W., O'CONNOR, P., POLMAN, C., HOHLFELD, R., CALABRESI, P., SELMAJ, K., AGOROPOULOU, C., LEYK, M., ZHANG-AUBERSON, L., BURTIN, P. & GROUP, F. S. 2010. A placebo-controlled trial of oral fingolimod in relapsing multiple sclerosis. *N Engl J Med,* 362**,** 387-401.

KARACA, G., SWIDERSKA-SYN, M., XIE, G., SYN, W. K., KRUGER, L., MACHADO, M. V., GARMAN, K., CHOI, S. S., MICHELOTTI, G. A., BURKLY, L. C., OCHOA, B. & DIEHL, A. M. 2014. TWEAK/Fn14 signaling is required for liver regeneration after partial hepatectomy in mice. *PLoS One,* 9**,** e83987.

KARANTH, S. & SCHLEGEL, A. 2018. The Monocarboxylate Transporter SLC16A6 Regulates Adult Length in Zebrafish and Is Associated With Height in Humans. *Front Physiol,* 9**,** 1936.

KARNER, C. M., DAS, A., MA, Z., SELF, M., CHEN, C., LUM, L., OLIVER, G. & CARROLL, T. J. 2011. Canonical Wnt9b signaling balances progenitor cell expansion and differentiation during kidney development. *Development,* 138**,** 1247-57.

KATCHE, C., BEKINSCHTEIN, P., SLIPCZUK, L., GOLDIN, A., IZQUIERDO, I. A., CAMMAROTA, M. & MEDINA, J. H. 2010. Delayed wave of c-Fos expression in the dorsal hippocampus involved specifically in persistence of long-term memory storage. *Proc Natl Acad Sci U S A,* 107**,** 349-54.

KATCHE, C. & MEDINA, J. H. 2017. Requirement of an Early Activation of BDNF/c-Fos Cascade in the Retrosplenial Cortex for the Persistence of a Long-Lasting Aversive Memory. *Cereb Cortex,* 27**,** 1060-1067.

KAWAKUBO, H., BRACHTEL, E., HAYASHIDA, T., YEO, G., KISH, J., MUZIKANSKY, A., WALDEN, P. D. & MAHESWARAN, S. 2006. Loss of B-cell translocation gene-2 in estrogen receptor-positive breast carcinoma is associated with tumor grade and overexpression of cyclin d1 protein. *Cancer Res,* 66**,** 7075-82.

KAWAKUBO, H., CAREY, J. L., BRACHTEL, E., GUPTA, V., GREEN, J. E., WALDEN, P. D. & MAHESWARAN, S. 2004. Expression of the NF-kappaB-responsive gene BTG2 is aberrantly regulated in breast cancer. *Oncogene,* 23**,** 8310-9.

KERNIE, S. G., LIEBL, D. J. & PARADA, L. F. 2000. BDNF regulates eating behavior and locomotor activity in mice. *EMBO J,* 19**,** 1290-300.

KIKUCHI, T., MORIZANE, A., DOI, D., MAGOTANI, H., ONOE, H., HAYASHI, T., MIZUMA, H., TAKARA, S., TAKAHASHI, R., INOUE, H., MORITA, S., YAMAMOTO, M., OKITA, K., NAKAGAWA, M., PARMAR, M. & TAKAHASHI, J. 2017. Human iPS cell-derived dopaminergic neurons function in a primate Parkinson's disease model. *Nature,* 548**,** 592-596.

KIM, H., LIM, J., BAO, H., JIAO, B., CANON, S. M., EPSTEIN, M. P., XU, K., JIANG, J., PARAMESWARAN, J., LI, Y., MOBERG, K. H., LANDERS, J. E., FOURNIER, C., ALLEN, E. G., GLASS, J. D., WINGO, T. S. & JIN, P. 2019. Rare variants in MYH15 modify amyotrophic lateral sclerosis risk. *Hum Mol Genet,* 28**,** 2309-2318.

KIM, M. Y., CHOI, T. Y., KIM, J. H., LEE, J. H., KIM, J. G., SOHN, K. C., YOON, K. S., KIM, C. D., LEE, J. H. & YOON, T. J. 2010. MKK6 increases the melanocyte dendricity through the regulation of Rho family GTPases. *J Dermatol Sci,* 60**,** 114-9.

KIM, S. S., CHOI, J. M., KIM, J. W., HAM, D. S., GHIL, S. H., KIM, M. K., KIM-KWON, Y., HONG, S. Y., AHN, S. C., KIM, S. U., LEE, Y. D. & SUH-KIM, H. 2005. cAMP induces neuronal differentiation of mesenchymal stem cells via activation of extracellular signal-regulated kinase/MAPK. *Neuroreport,* 16**,** 1357-61.

KIM, T. G., YAO, R., MONNELL, T., CHO, J. H., VASUDEVAN, A., KOH, A., PEEYUSH, K. T., MOON, M., DATTA, D., BOLSHAKOV, V. Y., KIM, K. S. & CHUNG, S. 2014. Efficient specification of interneurons from human pluripotent stem cells by dorsoventral and rostrocaudal modulation. *Stem Cells,* 32**,** 1789-804.

KLEIN, R., CONWAY, D., PARADA, L. F. & BARBACID, M. 1990. The trkB tyrosine protein kinase gene codes for a second neurogenic receptor that lacks the catalytic kinase domain. *Cell,* 61**,** 647-56.

KLEIN, R., JING, S. Q., NANDURI, V., O'ROURKE, E. & BARBACID, M. 1991a. The trk proto-oncogene encodes a receptor for nerve growth factor. *Cell,* 65**,** 189-97.

KLEIN, R., LAMBALLE, F., BRYANT, S. & BARBACID, M. 1992. The trkB tyrosine protein kinase is a receptor for neurotrophin-4. *Neuron,* 8**,** 947-56.

KLEIN, R., NANDURI, V., JING, S. A., LAMBALLE, F., TAPLEY, P., BRYANT, S., CORDON-CARDO, C., JONES, K. R., REICHARDT, L. F. & BARBACID, M. 1991b. The trkB tyrosine protein kinase is a receptor for brain-derived neurotrophic factor and neurotrophin-3. *Cell,* 66**,** 395-403.

KLEIN, R., SILOS-SANTIAGO, I., SMEYNE, R. J., LIRA, S. A., BRAMBILLA, R., BRYANT, S., ZHANG, L., SNIDER, W. D. & BARBACID, M. 1994. Disruption of the neurotrophin-3 receptor gene trkC eliminates la muscle afferents and results in abnormal movements. *Nature,* 368**,** 249-51.

KLEIN, R., SMEYNE, R. J., WURST, W., LONG, L. K., AUERBACH, B. A., JOYNER, A. L. & BARBACID, M. 1993. Targeted disruption of the trkB neurotrophin receptor gene results in nervous system lesions and neonatal death. *Cell,* 75**,** 113-22.

KLOSTER, E., SAFT, C., AKKAD, D. A., EPPLEN, J. T. & ARNING, L. 2014. Association of age at onset in Huntington disease with functional promoter variations in NPY and NPY2R. *J Mol Med (Berl),* 92**,** 177-84.

KOBAYASHI, M., SUGUMARAN, G., LIU, J., SHWORAK, N. W., SILBERT, J. E. & ROSENBERG, R. D. 1999. Molecular cloning and characterization of a human uronyl 2-sulfotransferase that sulfates iduronyl and glucuronyl residues in dermatan/chondroitin sulfate. *J Biol Chem,* 274**,** 10474-80.

KOOLS, P., VAN IMSCHOOT, G. & VAN ROY, F. 2000. Characterization of three novel human cadherin genes (CDH7, CDH19, and CDH20) clustered on chromosome 18q22-q23 and with high homology to chicken cadherin-7. *Genomics,* 68**,** 283-95.

KOPONEN, E., VOIKAR, V., RIEKKI, R., SAARELAINEN, T., RAURAMAA, T., RAUVALA, H., TAIRA, T. & CASTREN, E. 2004. Transgenic mice overexpressing the full-length neurotrophin receptor trkB exhibit increased activation of the trkB-PLCgamma pathway, reduced anxiety, and facilitated learning. *Mol Cell Neurosci,* 26**,** 166-81.

KORTE, M., CARROLL, P., WOLF, E., BREM, G., THOENEN, H. & BONHOEFFER, T. 1995. Hippocampal long-term potentiation is impaired in mice lacking brain-derived neurotrophic factor. *Proc Natl Acad Sci U S A,* 92**,** 8856-60.

KUCHARSKA, J., DEL RIO, P., ARANGO-GONZALEZ, B., GORZA, M., FEUCHTINGER, A., HAUCK, S. M. & UEFFING, M. 2014. Cyr61 activates retinal cells and prolongs photoreceptor survival in rd1 mouse model of retinitis pigmentosa. *J Neurochem,* 130**,** 227-40.

KUCHIPUDI, S. V., TELLABATI, M., NELLI, R. K., WHITE, G. A., PEREZ, B. B., SEBASTIAN, S., SLOMKA, M. J., BROOKES, S. M., BROWN, I. H., DUNHAM, S. P. & CHANG, K. C. 2012. 18S rRNA is a reliable normalisation gene for real time PCR based on influenza virus infected cells. *Virol J,* 9**,** 230.

KURODA, T. S., FUKUDA, M., ARIGA, H. & MIKOSHIBA, K. 2002. Synaptotagmin-like protein 5: a novel Rab27A effector with C-terminal tandem C2 domains. *Biochem Biophys Res Commun,* 293**,** 899-906.

LABORDA, J. 2000. The role of the epidermal growth factor-like protein dlk in cell differentiation. *Histol Histopathol,* 15**,** 119-29.

LAEREMANS, A., NYS, J., LUYTEN, W., D'HOOGE, R., PAULUSSEN, M. & ARCKENS, L. 2013. AMIGO2 mRNA expression in hippocampal CA2 and CA3a. *Brain Struct Funct,* 218**,** 123-30.

LAM, R. S., TOPFER, F. M., WOOD, P. G., BUSSKAMP, V. & BAMBERG, E. 2017. Functional Maturation of Human Stem Cell-Derived Neurons in Long-Term Cultures. *PLoS One,* 12**,** e0169506.

LAMBALLE, F., KLEIN, R. & BARBACID, M. 1991. trkC, a new member of the trk family of tyrosine protein kinases, is a receptor for neurotrophin-3. *Cell,* 66**,** 967-79.

LAPCHAK, P. A. & HEFTI, F. 1992. BDNF and NGF treatment in lesioned rats: effects on cholinergic function and weight gain. *Neuroreport,* 3**,** 405-8.

LAU, L. F. 2011. CCN1/CYR61: the very model of a modern matricellular protein. *Cell Mol Life Sci,* 68**,** 3149-63.

LAUTENSCHLAGER, N. T., COX, K. L., FLICKER, L., FOSTER, J. K., VAN BOCKXMEER, F. M., XIAO, J., GREENOP, K. R. & ALMEIDA, O. P. 2008. Effect of physical activity on cognitive function in older adults at risk for Alzheimer disease: a randomized trial. *JAMA,* 300**,** 1027-37.

LAW, C. W., ALHAMDOOSH, M., SU, S., DONG, X., TIAN, L., SMYTH, G. K. & RITCHIE, M. E. 2016. RNA-seq analysis is easy as 1-2-3 with limma, Glimma and edgeR. *F1000Res,* 5.

LAW, C. W., CHEN, Y., SHI, W. & SMYTH, G. K. 2014. voom: Precision weights unlock linear model analysis tools for RNA-seq read counts. *Genome Biol,* 15**,** R29.

LE, W. D., XU, P., JANKOVIC, J., JIANG, H., APPEL, S. H., SMITH, R. G. & VASSILATIS, D. K. 2003. Mutations in NR4A2 associated with familial Parkinson disease. *Nat Genet,* 33**,** 85-9.

LEE, H. J. & ZHENG, J. J. 2010. PDZ domains and their binding partners: structure, specificity, and modification. *Cell Commun Signal,* 8**,** 8.

LEE, K. F., DAVIES, A. M. & JAENISCH, R. 1994. p75-deficient embryonic dorsal root sensory and neonatal sympathetic neurons display a decreased sensitivity to NGF. *Development,* 120**,** 1027-33.

LEE, K. F., LI, E., HUBER, L. J., LANDIS, S. C., SHARPE, A. H., CHAO, M. V. & JAENISCH, R. 1992. Targeted mutation of the gene encoding the low affinity NGF receptor p75 leads to deficits in the peripheral sensory nervous system. *Cell,* 69**,** 737-49.

LEE, R., KERMANI, P., TENG, K. K. & HEMPSTEAD, B. L. 2001. Regulation of cell survival by secreted proneurotrophins. *Science,* 294**,** 1945-8.

LEIBROCK, J., LOTTSPEICH, F., HOHN, A., HOFER, M., HENGERER, B., MASIAKOWSKI, P., THOENEN, H. & BARDE, Y. A. 1989. Molecular cloning and expression of brain-derived neurotrophic factor. *Nature,* 341**,** 149-52.

LEVI-MONTALCINI, R. 1952. Effects of mouse tumor transplantation on the nervous system. *Ann N Y Acad Sci,* 55**,** 330-44.

LEVI-MONTALCINI, R. 1987. The nerve growth factor 35 years later. *Science,* 237**,** 1154-62.

LEVI-MONTALCINI, R. & BOOKER, B. 1960. Destruction of the Sympathetic Ganglia in Mammals by an Antiserum to a Nerve-Growth Protein. *Proc Natl Acad Sci U S A,* 46**,** 384-91.

LEVI-MONTALCINI, R. & HAMBURGER, V. 1951. Selective growth stimulating effects of mouse sarcoma on the sensory and sympathetic nervous system of the chick embryo. *J Exp Zool,* 116**,** 321-61.

LEVI-MONTALCINI, R., MEYER, H. & HAMBURGER, V. 1954. In vitro experiments on the effects of mouse sarcomas 180 and 37 on the spinal and sympathetic ganglia of the chick embryo. *Cancer Res,* 14**,** 49-57.

LEVOYE, A., DAM, J., AYOUB, M. A., GUILLAUME, J. L., COUTURIER, C., DELAGRANGE, P. & JOCKERS, R. 2006. The orphan GPR50 receptor specifically inhibits MT1 melatonin receptor function through heterodimerization. *EMBO J,* 25**,** 3012-23.

LI, H., LI, S. H., JOHNSTON, H., SHELBOURNE, P. F. & LI, X. J. 2000. Amino-terminal fragments of mutant huntingtin show selective accumulation in striatal neurons and synaptic toxicity. *Nat Genet,* 25**,** 385-9.

LI, H., WANG, T., SHI, C., YANG, Y., LI, X., WU, Y. & XU, Z. D. 2018. Inhibition of GALR1 in PFC Alleviates Depressive-Like Behaviors in Postpartum Depression Rat Model by Upregulating CREB-BNDF and 5-HT Levels. *Front Psychiatry,* 9**,** 588.

LI, H. S., XU, X. Z. & MONTELL, C. 1999. Activation of a TRPC3-dependent cation current through the neurotrophin BDNF. *Neuron,* 24**,** 261-73.

LI, J., PARKER, B., MARTYN, C., NATARAJAN, C. & GUO, J. 2013. The PMP22 gene and its related diseases. *Mol Neurobiol,* 47**,** 673-98.

LI, Y., GU, J., XU, F., ZHU, Q., GE, D. & LU, C. 2019. Novel methylation-driven genes identified as prognostic indicators for lung squamous cell carcinoma. *Am J Transl Res,* 11**,** 1997-2012.

LIANG, J., ZHAO, H., HU, J., LIU, Y. & LI, Z. 2018. SPOCD1 promotes cell proliferation and inhibits cell apoptosis in human osteosarcoma. *Mol Med Rep,* 17**,** 3218-3225.

LIANG, X. Q., AVRAHAM, H. K., JIANG, S. & AVRAHAM, S. 2004. Genetic alterations of the NRP/B gene are associated with human brain tumors. *Oncogene,* 23**,** 5890-900.

LIAO, Y., SMYTH, G. K. & SHI, W. 2014. featureCounts: an efficient general purpose program for assigning sequence reads to genomic features. *Bioinformatics,* 30**,** 923-30.

LIEBL, D. J., TESSAROLLO, L., PALKO, M. E. & PARADA, L. F. 1997. Absence of sensory neurons before target innervation in brain-derived neurotrophic factor-, neurotrophin 3-, and TrkC-deficient embryonic mice. *J Neurosci,* 17**,** 9113-21.

LIM, M. S., LEE, S. Y. & PARK, C. H. 2015. FGF8 is Essential for Functionality of Induced Neural Precursor Cell-derived Dopaminergic Neurons. *Int J Stem Cells,* 8**,** 228-34.

LIN, S. & TALBOT, P. 2011. Methods for culturing mouse and human embryonic stem cells. *Methods Mol Biol,* 690**,** 31-56.

LIN, Y., BLOODGOOD, B. L., HAUSER, J. L., LAPAN, A. D., KOON, A. C., KIM, T. K., HU, L. S., MALIK, A. N. & GREENBERG, M. E. 2008. Activity-dependent regulation of inhibitory synapse development by Npas4. *Nature,* 455**,** 1198-204.

LINNARSSON, S., BJORKLUND, A. & ERNFORS, P. 1997. Learning deficit in BDNF mutant mice. *Eur J Neurosci,* 9**,** 2581-7.

LIPINA, T. V., PRASAD, T., YOKOMAKU, D., LUO, L., CONNOR, S. A., KAWABE, H., WANG, Y. T., BROSE, N., RODER, J. C. & CRAIG, A. M. 2016. Cognitive Deficits in Calsyntenin-2-deficient Mice Associated with Reduced GABAergic Transmission. *Neuropsychopharmacology,* 41**,** 802-10.

LIU, D., LIU, Z., LIU, H., LI, H., PAN, X. & LI, Z. 2016. Brain-derived neurotrophic factor promotes vesicular glutamate transporter 3 expression and neurite outgrowth of dorsal root ganglion neurons through the activation of the transcription factors Etv4 and Etv5. *Brain Res Bull,* 121**,** 215-26.

LIU, I. Y., LYONS, W. E., MAMOUNAS, L. A. & THOMPSON, R. F. 2004. Brain-derived neurotrophic factor plays a critical role in contextual fear conditioning. *J Neurosci,* 24**,** 7958-63.

LIU, Q., WANG, X. Y., QIN, Y. Y., YAN, X. L., CHEN, H. M., HUANG, Q. D., CHEN, J. K. & ZHENG, J. M. 2018. SPOCD1 promotes the proliferation and metastasis of glioma cells by up-regulating PTX3. *Am J Cancer Res,* 8**,** 624-635.

LIU, X., ERNFORS, P., WU, H. & JAENISCH, R. 1995. Sensory but not motor neuron deficits in mice lacking NT4 and BDNF. *Nature,* 375**,** 238-41.

LLAMBI, F., CAUSERET, F., BLOCH-GALLEGO, E. & MEHLEN, P. 2001. Netrin-1 acts as a survival factor via its receptors UNC5H and DCC. *EMBO J,* 20**,** 2715-22.

LOGRIP, M. L., JANAK, P. H. & RON, D. 2008. Dynorphin is a downstream effector of striatal BDNF regulation of ethanol intake. *FASEB J,* 22**,** 2393-404.

LOUIS SAM TITUS, A. S. C., SHARMA, D., KIM, M. S. & D'MELLO, S. R. 2019. The Bdnf and Npas4 genes are targets of HDAC3-mediated transcriptional repression. *BMC Neurosci,* 20**,** 65.

LOVE, M. I., HUBER, W. & ANDERS, S. 2014. Moderated estimation of fold change and dispersion for RNA-seq data with DESeq2. *Genome Biol,* 15**,** 550.

LU, B., NAGAPPAN, G., GUAN, X., NATHAN, P. J. & WREN, P. 2013. BDNF-based synaptic repair as a disease-modifying strategy for neurodegenerative diseases. *Nat Rev Neurosci,* 14**,** 401-16.

LU, B., NAGAPPAN, G. & LU, Y. 2014. BDNF and synaptic plasticity, cognitive function, and dysfunction. *Handb Exp Pharmacol,* 220**,** 223-50.

LU, Z., JE, H. S., YOUNG, P., GROSS, J., LU, B. & FENG, G. 2007. Regulation of synaptic growth and maturation by a synapse-associated E3 ubiquitin ligase at the neuromuscular junction. *J Cell Biol,* 177**,** 1077-89.

LUBERG, K., WONG, J., WEICKERT, C. S. & TIMMUSK, T. 2010. Human TrkB gene: novel alternative transcripts, protein isoforms and expression pattern in the prefrontal cerebral cortex during postnatal development. *J Neurochem,* 113**,** 952-64.

LUDWIG, A., UVAROV, P., SONI, S., THOMAS-CRUSELLS, J., AIRAKSINEN, M. S. & RIVERA, C. 2011. Early growth response 4 mediates BDNF induction of potassium chloride cotransporter 2 transcription. *J Neurosci,* 31**,** 644-9.

LYONS, W. E., MAMOUNAS, L. A., RICAURTE, G. A., COPPOLA, V., REID, S. W., BORA, S. H., WIHLER, C., KOLIATSOS, V. E. & TESSAROLLO, L. 1999. Brain-derived neurotrophic factor-deficient mice develop aggressiveness and hyperphagia in conjunction with brain serotonergic abnormalities. *Proc Natl Acad Sci U S A,* 96**,** 15239-44.

MA, L., HU, B., LIU, Y., VERMILYEA, S. C., LIU, H., GAO, L., SUN, Y., ZHANG, X. & ZHANG, S. C. 2012. Human embryonic stem cell-derived GABA neurons correct locomotion deficits in quinolinic acid-lesioned mice. *Cell Stem Cell,* 10**,** 455-64.

MA, Y. X., WU, Z. Q., FENG, Y. J., XIAO, Z. C., QIN, X. L. & MA, Q. H. 2015. G protein coupled receptor 50 promotes self-renewal and neuronal differentiation of embryonic neural progenitor cells through regulation of notch and wnt/beta-catenin signalings. *Biochem Biophys Res Commun,* 458**,** 836-42.

MACINTYRE, D. J., MCGHEE, K. A., MACLEAN, A. W., AFZAL, M., BRIFFA, K., HENRY, B., THOMSON, P. A., MUIR, W. J. & BLACKWOOD, D. H. 2010. Association of GPR50, an X-linked orphan G protein-coupled receptor, and affective disorder in an independent sample of the Scottish population. *Neurosci Lett,* 475**,** 169-73.

MAGUIRE, J., SANTORO, T., JENSEN, P., SIEBENLIST, U., YEWDELL, J. & KELLY, K. 1994. Gem: an induced, immediate early protein belonging to the Ras family. *Science,* 265**,** 241-4.

MAISONPIERRE, P. C., BELLUSCIO, L., SQUINTO, S., IP, N. Y., FURTH, M. E., LINDSAY, R. M. & YANCOPOULOS, G. D. 1990. Neurotrophin-3: a neurotrophic factor related to NGF and BDNF. *Science,* 247**,** 1446-51.

MALIK, A. R., URBANSKA, M., GOZDZ, A., SWIECH, L. J., NAGALSKI, A., PERYCZ, M., BLAZEJCZYK, M. & JAWORSKI, J. 2013. Cyr61, a matricellular protein, is needed for dendritic arborization of hippocampal neurons. *J Biol Chem,* 288**,** 8544-59.

MALIK, S. Z., MOTAMEDI, S., ROYO, N. C., LEBOLD, D. & WATSON, D. J. 2011. Identification of potentially neuroprotective genes upregulated by neurotrophin treatment of CA3 neurons in the injured brain. *J Neurotrauma,* 28**,** 415-30.

MANDOLESI, G., GARGANO, S., PENNUTO, M., ILLI, B., MOLFETTA, R., SOUCEK, L., MOSCA, L., LEVI, A., JUCKER, R. & NASI, S. 2002. NGF-dependent and tissue-specific transcription of vgf is regulated by a CREB-p300 and bHLH factor interaction. *FEBS Lett,* 510**,** 50-6.

MARSH, D. J., WEINGARTH, D. T., NOVI, D. E., CHEN, H. Y., TRUMBAUER, M. E., CHEN, A. S., GUAN, X. M., JIANG, M. M., FENG, Y., CAMACHO, R. E., SHEN, Z., FRAZIER, E. G., YU, H., METZGER, J. M., KUCA, S. J., SHEARMAN, L. P., GOPAL-TRUTER, S., MACNEIL, D. J., STRACK, A. M., MACINTYRE, D. E., VAN DER PLOEG, L. H. & QIAN, S. 2002. Melanin-concentrating hormone 1 receptor-deficient mice are lean, hyperactive, and hyperphagic and have altered metabolism. *Proc Natl Acad Sci U S A,* 99**,** 3240-5.

MARTIN-ZANCA, D., HUGHES, S. H. & BARBACID, M. 1986. A human oncogene formed by the fusion of truncated tropomyosin and protein tyrosine kinase sequences. *Nature,* 319**,** 743-8.

MARTIN-ZANCA, D., OSKAM, R., MITRA, G., COPELAND, T. & BARBACID, M. 1989. Molecular and biochemical characterization of the human trk proto-oncogene. *Mol Cell Biol,* 9**,** 24-33.

MASSA, S. M., YANG, T., XIE, Y., SHI, J., BILGEN, M., JOYCE, J. N., NEHAMA, D., RAJADAS, J. & LONGO, F. M. 2010. Small molecule BDNF mimetics activate TrkB signaling and prevent neuronal degeneration in rodents. *J Clin Invest,* 120**,** 1774-85.

MATSUBARA, A., IWAMA, A., YAMAZAKI, S., FURUTA, C., HIRASAWA, R., MORITA, Y., OSAWA, M., MOTOHASHI, T., ETO, K., EMA, H., KITAMURA, T., VESTWEBER, D. & NAKAUCHI, H. 2005. Endomucin, a CD34-like sialomucin, marks hematopoietic stem cells throughout development. *J Exp Med,* 202**,** 1483-92.

MATSUDA, T., NOMI, M., IKEYA, M., KANI, S., OISHI, I., TERASHIMA, T., TAKADA, S. & MINAMI, Y. 2001. Expression of the receptor tyrosine kinase genes, Ror1 and Ror2, during mouse development. *Mech Dev,* 105**,** 153-6.

MAYNARD, K. R., HOBBS, J. W., PHAN, B. N., GUPTA, A., RAJPUROHIT, S., WILLIAMS, C., RAJPUROHIT, A., SHIN, J. H., JAFFE, A. E. & MARTINOWICH, K. 2018. BDNF-TrkB signaling in oxytocin neurons contributes to maternal behavior. *Elife,* 7.

MECHENTHALER, I. 2008. Galanin and the neuroendocrine axes. *Cell Mol Life Sci,* 65**,** 1826-35.

MELA, A. & GOLDMAN, J. E. 2009. The tetraspanin KAI1/CD82 is expressed by late-lineage oligodendrocyte precursors and may function to restrict precursor migration and promote oligodendrocyte differentiation and myelination. *J Neurosci,* 29**,** 11172-81.

MERKOURIS, S., BARDE, Y. A., BINLEY, K. E., ALLEN, N. D., STEPANOV, A. V., WU, N. C., GRANDE, G., LIN, C. W., LI, M., NAN, X., CHACON-FERNANDEZ, P., DISTEFANO, P. S., LINDSAY, R. M., LERNER, R. A. & XIE, J. 2018. Fully human agonist antibodies to TrkB using autocrine cell-based selection from a combinatorial antibody library. *Proc Natl Acad Sci U S A,* 115**,** E7023-E7032.

MILLER, J. A., DING, S. L., SUNKIN, S. M., SMITH, K. A., NG, L., SZAFER, A., EBBERT, A., RILEY, Z. L., ROYALL, J. J., AIONA, K., ARNOLD, J. M., BENNET, C., BERTAGNOLLI, D., BROUNER, K., BUTLER,

S., CALDEJON, S., CAREY, A., CUHACIYAN, C., DALLEY, R. A., DEE, N., DOLBEARE, T. A., FACER, B. A., FENG, D., FLISS, T. P., GEE, G., GOLDY, J., GOURLEY, L., GREGOR, B. W., GU, G., HOWARD, R. E., JOCHIM, J. M., KUAN, C. L., LAU, C., LEE, C. K., LEE, F., LEMON, T. A., LESNAR, P., MCMURRAY, B., MASTAN, N., MOSQUEDA, N., NALUAI-CECCHINI, T., NGO, N. K., NYHUS, J., OLDRE, A., OLSON, E., PARENTE, J., PARKER, P. D., PARRY, S. E., STEVENS, A., PLETIKOS, M., REDING, M., ROLL, K., SANDMAN, D., SARREAL, M., SHAPOURI, S., SHAPOVALOVA, N. V., SHEN, E. H., SJOQUIST, N., SLAUGHTERBECK, C. R., SMITH, M., SODT, A. J., WILLIAMS, D., ZOLLEI, L., FISCHL, B., GERSTEIN, M. B., GESCHWIND, D. H., GLASS, I. A., HAWRYLYCZ, M. J., HEVNER, R. F., HUANG, H., JONES, A. R., KNOWLES, J. A., LEVITT, P., PHILLIPS, J. W., SESTAN, N., WOHNOUTKA, P., DANG, C., BERNARD, A., HOHMANN, J. G. & LEIN, E. S. 2014. Transcriptional landscape of the prenatal human brain. *Nature,* 508**,** 199-206.

MINICHIELLO, L., KORTE, M., WOLFER, D., KUHN, R., UNSICKER, K., CESTARI, V., ROSSI-ARNAUD, C., LIPP, H. P., BONHOEFFER, T. & KLEIN, R. 1999. Essential role for TrkB receptors in hippocampus-mediated learning. *Neuron,* 24**,** 401-14.

MIYASHITA, T., KIKUCHI, E., HORIUCHI, J. & SAITOE, M. 2018. Long-Term Memory Engram Cells Are Established by c-Fos/CREB Transcriptional Cycling. *Cell Rep,* 25**,** 2716-2728 e3.

MIYATA, S., MORI, Y. & TOHYAMA, M. 2008. PRMT1 and Btg2 regulates neurite outgrowth of Neuro2a cells. *Neurosci Lett,* 445**,** 162-5.

MO, H. N. & LIU, P. 2017. Targeting MET in cancer therapy. *Chronic Dis Transl Med,* 3**,** 148-153.

MOCHIZUKI, A. L., KATANAYA, A., HAYASHI, E., HOSOKAWA, M., MORIBE, E., MOTEGI, A., ISHIAI, M., TAKATA, M., KONDOH, G., WATANABE, H., NAKATSUJI, N. & CHUMA, S. 2017. PARI Regulates Stalled Replication Fork Processing To Maintain Genome Stability upon Replication Stress in Mice. *Mol Cell Biol,* 37.

MODARRESI, F., FAGHIHI, M. A., LOPEZ-TOLEDANO, M. A., FATEMI, R. P., MAGISTRI, M., BROTHERS, S. P., VAN DER BRUG, M. P. & WAHLESTEDT, C. 2012. Inhibition of natural antisense transcripts in vivo results in gene-specific transcriptional upregulation. *Nat Biotechnol,* 30**,** 453-9.

MONTAGNOLI, A., GUARDAVACCARO, D., STARACE, G. & TIRONE, F. 1996. Overexpression of the nerve growth factor-inducible PC3 immediate early gene is associated with growth inhibition. *Cell Growth Differ,* 7**,** 1327-36.

MOON, M., JUNG, E. S., JEON, S. G., CHA, M. Y., JANG, Y., KIM, W., LOPES, C., MOOK-JUNG, I. & KIM, K. S. 2019. Nurr1 (NR4A2) regulates Alzheimer's disease-related pathogenesis and cognitive function in the 5XFAD mouse model. *Aging Cell,* 18**,** e12866.

MORI, H., HANADA, R., HANADA, T., AKI, D., MASHIMA, R., NISHINAKAMURA, H., TORISU, T., CHIEN, K. R., YASUKAWA, H. & YOSHIMURA, A. 2004. Socs3 deficiency in the brain elevates leptin sensitivity and confers resistance to diet-induced obesity. *Nat Med,* 10**,** 739-43.

MORIGUCHI, T., KUROYANAGI, N., YAMAGUCHI, K., GOTOH, Y., IRIE, K., KANO, T., SHIRAKABE, K., MURO, Y., SHIBUYA, H., MATSUMOTO, K., NISHIDA, E. & HAGIWARA, M. 1996. A novel kinase cascade mediated by mitogen-activated protein kinase kinase 6 and MKK3. *J Biol Chem,* 271**,** 13675-9.

MOYERS, J. S., BILAN, P. J., ZHU, J. & KAHN, C. R. 1997. Rad and Rad-related GTPases interact with calmodulin and calmodulin-dependent protein kinase II. *J Biol Chem,* 272**,** 11832-9.

MULLER, D., CHERUKURI, P., HENNINGFELD, K., POH, C. H., WITTLER, L., GROTE, P., SCHLUTER, O., SCHMIDT, J., LABORDA, J., BAUER, S. R., BROWNSTONE, R. M. & MARQUARDT, T. 2014. Dlk1 promotes a fast motor neuron biophysical signature required for peak force execution. *Science,* 343**,** 1264-6.

MULLER, L. & LINDBERG, I. 1999. The cell biology of the prohormone convertases PC1 and PC2. *Prog Nucleic Acid Res Mol Biol,* 63**,** 69-108.

MUNDEL, P., HEID, H. W., MUNDEL, T. M., KRUGER, M., REISER, J. & KRIZ, W. 1997. Synaptopodin: an actin-associated protein in telencephalic dendrites and renal podocytes. *J Cell Biol,* 139**,** 193-204.

MUNJI, R. N., CHOE, Y., LI, G., SIEGENTHALER, J. A. & PLEASURE, S. J. 2011. Wnt signaling regulates neuronal differentiation of cortical intermediate progenitors. *J Neurosci,* 31**,** 1676-87.

MUNOZ-SANJUAN, I. & BRIVANLOU, A. H. 2002. Neural induction, the default model and embryonic stem cells. *Nat Rev Neurosci,* 3**,** 271-80.

MURTHY, S. E., LOUD, M. C., DAOU, I., MARSHALL, K. L., SCHWALLER, F., KUHNEMUND, J., FRANCISCO, A. G., KEENAN, W. T., DUBIN, A. E., LEWIN, G. R. & PATAPOUTIAN, A. 2018. The mechanosensitive ion channel Piezo2 mediates sensitivity to mechanical pain in mice. *Sci Transl Med,* 10.

NAGAHARA, A. H. & TUSZYNSKI, M. H. 2011. Potential therapeutic uses of BDNF in neurological and psychiatric disorders. *Nat Rev Drug Discov,* 10**,** 209-19.

NAKANO, T., ANDO, S., TAKATA, N., KAWADA, M., MUGURUMA, K., SEKIGUCHI, K., SAITO, K., YONEMURA, S., EIRAKU, M. & SASAI, Y. 2012. Self-formation of optic cups and storable stratified neural retina from human ESCs. *Cell Stem Cell,* 10**,** 771-85.

NAKAYAMA, M., ISHIDOH, K., KOJIMA, Y., HARADA, N., KOMINAMI, E., OKUMURA, K. & YAGITA, H. 2003. Fibroblast growth factor-inducible 14 mediates multiple pathways of TWEAK-induced cell death. *J Immunol,* 170**,** 341-8.

NEGRAES, P. D., CUGOLA, F. R., HERAI, R. H., TRUJILLO, C. A., CRISTINO, A. S., CHAILANGKARN, T., MUOTRI, A. R. & DUVVURI, V. 2017. Modeling anorexia nervosa: transcriptional insights from human iPSC-derived neurons. *Transl Psychiatry,* 7**,** e1060.

NEHME, R., ZUCCARO, E., GHOSH, S. D., LI, C., SHERWOOD, J. L., PIETILAINEN, O., BARRETT, L. E., LIMONE, F., WORRINGER, K. A., KOMMINENI, S., ZANG, Y., CACCHIARELLI, D., MEISSNER, A., ADOLFSSON, R., HAGGARTY, S., MADISON, J., MULLER, M., ARLOTTA, P., FU, Z., FENG, G. & EGGAN, K. 2018. Combining NGN2 Programming with Developmental Patterning Generates Human Excitatory Neurons with NMDAR-Mediated Synaptic Transmission. *Cell Rep,* 23**,** 2509-2523.

NICHOLS, J. & SMITH, A. 2009. Naive and primed pluripotent states. *Cell Stem Cell,* 4**,** 487-92.

NICHOLSON, S. E., DE SOUZA, D., FABRI, L. J., CORBIN, J., WILLSON, T. A., ZHANG, J. G., SILVA, A., ASIMAKIS, M., FARLEY, A., NASH, A. D., METCALF, D., HILTON, D. J., NICOLA, N. A. & BACA, M. 2000. Suppressor of cytokine signaling-3 preferentially binds to the SHP-2-binding site on the shared cytokine receptor subunit gp130. *Proc Natl Acad Sci U S A,* 97**,** 6493-8.

NIE, F., SU, D., SHI, Y., CHEN, J., WANG, H., QIN, W., CHEN, Y., WANG, S. & LI, L. 2015. A preliminary study on the role of the complement regulatory protein, cluster of differentiation 55, in mice with diabetic neuropathic pain. *Mol Med Rep,* 11**,** 2076-82.

NIKOLETOPOULOU, V., LICKERT, H., FRADE, J. M., RENCUREL, C., GIALLONARDO, P., ZHANG, L., BIBEL, M. & BARDE, Y. A. 2010. Neurotrophin receptors TrkA and TrkC cause neuronal death whereas TrkB does not. *Nature,* 467**,** 59-63.

NIKOLOVSKA, K., SPILLMANN, D., HAIER, J., LADANYI, A., STOCK, C. & SEIDLER, D. G. 2017. Melanoma Cell Adhesion and Migration Is Modulated by the Uronyl 2-O Sulfotransferase. *PLoS One,* 12**,** e0170054.

NILSSON, M. I., NISSAR, A. A., AL-SAJEE, D., TARNOPOLSKY, M. A., PARISE, G., LACH, B., FURST, D. O., VAN DER VEN, P. F. M., KLEY, R. A. & HAWKE, T. J. 2013. Xin is a marker of skeletal muscle damage severity in myopathies. *Am J Pathol,* 183**,** 1703-1709.

NIWA, H., BURDON, T., CHAMBERS, I. & SMITH, A. 1998. Self-renewal of pluripotent embryonic stem cells is mediated via activation of STAT3. *Genes Dev,* 12**,** 2048-60.

OBERMEIER, A., LAMMERS, R., WIESMULLER, K. H., JUNG, G., SCHLESSINGER, J. & ULLRICH, A. 1993. Identification of Trk binding sites for SHC and phosphatidylinositol 3'-kinase and formation of a multimeric signaling complex. *J Biol Chem,* 268**,** 22963-6.

OCHS, G., PENN, R. D., YORK, M., GIESS, R., BECK, M., TONN, J., HAIGH, J., MALTA, E., TRAUB, M., SENDTNER, M. & TOYKA, K. V. 2000. A phase I/II trial of recombinant methionyl human brain derived neurotrophic factor administered by intrathecal infusion to patients with amyotrophic lateral sclerosis. *Amyotroph Lateral Scler Other Motor Neuron Disord,* 1**,** 201-6.

OLIVA, A. A., JR., KANG, Y., FURONES, C., ALONSO, O. F., BRUNO, O., DIETRICH, W. D. & ATKINS, C. M. 2012. Phosphodiesterase isoform-specific expression induced by traumatic brain injury. *J Neurochem,* 123**,** 1019-29.

OOE, N., MOTONAGA, K., KOBAYASHI, K., SAITO, K. & KANEKO, H. 2009. Functional characterization of basic helix-loop-helix-PAS type transcription factor NXF in vivo: putative involvement in an "on demand" neuroprotection system. *J Biol Chem,* 284**,** 1057-63.

ORHAN, E., PREZEAU, L., EL SHAMIEH, S., BUJAKOWSKA, K. M., MICHIELS, C., ZAGAR, Y., VOL, C., BHATTACHARYA, S. S., SAHEL, J. A., SENNLAUB, F., AUDO, I. & ZEITZ, C. 2013. Further insights into GPR179: expression, localization, and associated pathogenic mechanisms leading to complete congenital stationary night blindness. *Invest Ophthalmol Vis Sci,* 54**,** 8041-50.

ORLANDI, C., CAO, Y. & MARTEMYANOV, K. A. 2013. Orphan receptor GPR179 forms macromolecular complexes with components of metabotropic signaling cascade in retina ON-bipolar neurons. *Invest Ophthalmol Vis Sci,* 54**,** 7153-61.

ORLANDI, C., OMORI, Y., WANG, Y., CAO, Y., UENO, A., ROUX, M. J., CONDOMITTI, G., DE WIT, J., KANAGAWA, M., FURUKAWA, T. & MARTEMYANOV, K. A. 2018. Transsynaptic Binding of Orphan Receptor GPR179 to Dystroglycan-Pikachurin Complex Is Essential for the Synaptic Organization of Photoreceptors. *Cell Rep,* 25**,** 130-145 e5.

ORLANDI, C., POSOKHOVA, E., MASUHO, I., RAY, T. A., HASAN, N., GREGG, R. G. & MARTEMYANOV, K. A. 2012. GPR158/179 regulate G protein signaling by controlling localization and activity of the RGS7 complexes. *J Cell Biol,* 197**,** 711-9.

OWUSU, B. Y., GALEMMO, R., JANETKA, J. & KLAMPFER, L. 2017. Hepatocyte Growth Factor, a Key Tumor-Promoting Factor in the Tumor Microenvironment. *Cancers (Basel),* 9.

PAPASSOTIROPOULOS, A., STEPHAN, D. A., HUENTELMAN, M. J., HOERNDLI, F. J., CRAIG, D. W., PEARSON, J. V., HUYNH, K. D., BRUNNER, F., CORNEVEAUX, J., OSBORNE, D., WOLLMER, M. A., AERNI, A., COLUCCIA, D., HANGGI, J., MONDADORI, C. R., BUCHMANN, A., REIMAN, E. M., CASELLI, R. J., HENKE, K. & DE QUERVAIN, D. J. 2006. Common Kibra alleles are associated with human memory performance. *Science,* 314**,** 475-8.

PARDRIDGE, W. M., KANG, Y. S. & BUCIAK, J. L. 1994. Transport of human recombinant brain-derived neurotrophic factor (BDNF) through the rat blood-brain barrier in vivo using vector-mediated peptide drug delivery. *Pharm Res,* 11**,** 738-46.

PATAPOUTIAN, A. & REICHARDT, L. F. 2001. Trk receptors: mediators of neurotrophin action. *Curr Opin Neurobiol,* 11**,** 272-80.

PATTERSON, S. L., ABEL, T., DEUEL, T. A., MARTIN, K. C., ROSE, J. C. & KANDEL, E. R. 1996. Recombinant BDNF rescues deficits in basal synaptic transmission and hippocampal LTP in BDNF knockout mice. *Neuron,* 16**,** 1137-45.

PAUS, S., GRUNEWALD, A., KLEIN, C., KNAPP, M., ZIMPRICH, A., JANETZKY, B., MOLLER, J. C., KLOCKGETHER, T. & WULLNER, U. 2008. The DRD2 TaqIA polymorphism and demand of dopaminergic medication in Parkinson's disease. *Mov Disord,* 23**,** 599-602.

PEACHEY, N. S., RAY, T. A., FLORIJN, R., ROWE, L. B., SJOERDSMA, T., CONTRERAS-ALCANTARA, S., BABA, K., TOSINI, G., POZDEYEV, N., IUVONE, P. M., BOJANG, P., JR., PEARRING, J. N., SIMONSZ, H. J., VAN GENDEREN, M., BIRCH, D. G., TRABOULSI, E. I., DORFMAN, A., LOPEZ, I., REN, H., GOLDBERG, A. F., NISHINA, P. M., LACHAPELLE, P., MCCALL, M. A., KOENEKOOP, R. K., BERGEN, A. A., KAMERMANS, M. & GREGG, R. G. 2012. GPR179 is required for depolarizing bipolar cell function and is mutated in autosomal-recessive complete congenital stationary night blindness. *Am J Hum Genet,* 90**,** 331-9.

PEDERSEN, E. & BRAKEBUSCH, C. 2012. Rho GTPase function in development: how in vivo models change our view. *Exp Cell Res,* 318**,** 1779-87.

PEEL, A. L., SORSCHER, N., KIM, J. Y., GALVAN, V., CHEN, S. & BREDESEN, D. E. 2004. Tau phosphorylation in Alzheimer's disease: potential involvement of an APP-MAP kinase complex. *Neuromolecular Med,* 5**,** 205-18.

PEHKONEN, H., LENTO, M., VON NANDELSTADH, P., FILIPPOU, A., GRENMAN, R., LEHTI, K. & MONNI, O. 2018. Liprin-alpha1 modulates cancer cell signaling by transmembrane protein CD82 in adhesive membrane domains linked to cytoskeleton. *Cell Commun Signal,* 16**,** 41.

PENG, L., YU, Y., LIU, J., LI, S., HE, H., CHENG, N. & YE, R. D. 2015. The chemerin receptor CMKLR1 is a functional receptor for amyloid-beta peptide. *J Alzheimers Dis,* 43**,** 227-42.

PETRYSHEN, T. L., SABETI, P. C., ALDINGER, K. A., FRY, B., FAN, J. B., SCHAFFNER, S. F., WAGGONER, S. G., TAHL, A. R. & SKLAR, P. 2010. Population genetic study of the brain-derived neurotrophic factor (BDNF) gene. *Mol Psychiatry,* 15**,** 810-5.

PHILLIPS, H. S., HAINS, J. M., ARMANINI, M., LARAMEE, G. R., JOHNSON, S. A. & WINSLOW, J. W. 1991. BDNF mRNA is decreased in the hippocampus of individuals with Alzheimer's disease. *Neuron,* 7**,** 695-702.

PIECHA, D., WIBERG, C., MORGELIN, M., REINHARDT, D. P., DEAK, F., MAURER, P. & PAULSSON, M. 2002. Matrilin-2 interacts with itself and with other extracellular matrix proteins. *Biochem J,* 367**,** 715-21.

PILLIDGE, K., HEAL, D. J. & STANFORD, S. C. 2016. The NK1R-/- mouse phenotype suggests that small body size, with a sex- and diet-dependent excess in body mass and fat, are physical biomarkers for a human endophenotype with vulnerability to attention deficit hyperactivity disorder. *J Psychopharmacol,* 30**,** 848-55.

PINTO, F. M., ALMEIDA, T. A., HERNANDEZ, M., DEVILLIER, P., ADVENIER, C. & CANDENAS, M. L. 2004. mRNA expression of tachykinins and tachykinin receptors in different human tissues. *Eur J Pharmacol,* 494**,** 233-9.

PODUSLO, J. F. & CURRAN, G. L. 1996. Permeability at the blood-brain and blood-nerve barriers of the neurotrophic factors: NGF, CNTF, NT-3, BDNF. *Brain Res Mol Brain Res,* 36**,** 280-6.

PORCELLI, S., BALZARRO, B., LEE, S. J., HAN, C., PATKAR, A. A., PAE, C. U. & SERRETTI, A. 2016. PDE7B, NMBR and EPM2A Variants and Schizophrenia: A Case-Control and Pharmacogenetics Study. *Neuropsychobiology,* 73**,** 160-8.

PROENCA, C. C., SONG, M. & LEE, F. S. 2016. Differential effects of BDNF and neurotrophin 4 (NT4) on endocytic sorting of TrkB receptors. *J Neurochem,* 138**,** 397-406.

PRUUNSILD, P., KAZANTSEVA, A., AID, T., PALM, K. & TIMMUSK, T. 2007. Dissecting the human BDNF locus: bidirectional transcription, complex splicing, and multiple promoters. *Genomics,* 90**,** 397-406.

RADEKE, M. J., MISKO, T. P., HSU, C., HERZENBERG, L. A. & SHOOTER, E. M. 1987. Gene transfer and molecular cloning of the rat nerve growth factor receptor. *Nature,* 325**,** 593-7.

RAINGEAUD, J., WHITMARSH, A. J., BARRETT, T., DERIJARD, B. & DAVIS, R. J. 1996. MKK3- and MKK6-regulated gene expression is mediated by the p38 mitogen-activated protein kinase signal transduction pathway. *Mol Cell Biol,* 16**,** 1247-55.

RAUSKOLB, S., ZAGREBELSKY, M., DREZNJAK, A., DEOGRACIAS, R., MATSUMOTO, T., WIESE, S., ERNE, B., SENDTNER, M., SCHAEREN-WIEMERS, N., KORTE, M. & BARDE, Y. A. 2010. Global deprivation of brain-derived neurotrophic factor in the CNS reveals an area-specific requirement for dendritic growth. *J Neurosci,* 30**,** 1739-49.

REICHARDT, L. F. 2006. Neurotrophin-regulated signalling pathways. *Philos Trans R Soc Lond B Biol Sci,* 361**,** 1545-64.

REINHARDT, P., GLATZA, M., HEMMER, K., TSYTSYURA, Y., THIEL, C. S., HOING, S., MORITZ, S., PARGA, J. A., WAGNER, L., BRUDER, J. M., WU, G., SCHMID, B., ROPKE, A., KLINGAUF, J., SCHWAMBORN, J. C., GASSER, T., SCHOLER, H. R. & STERNECKERT, J. 2013. Derivation and expansion using only small molecules of human neural progenitors for neurodegenerative disease modeling. *PLoS One,* 8**,** e59252.

RIAZUDDIN, S. A., PARKER, D. S., MCGLUMPHY, E. J., OH, E. C., ILIFF, B. W., SCHMEDT, T., JURKUNAS, U., SCHLEIF, R., KATSANIS, N. & GOTTSCH, J. D. 2012. Mutations in LOXHD1, a recessive-deafness locus, cause dominant late-onset Fuchs corneal dystrophy. *Am J Hum Genet,* 90**,** 533-9.

RING, D. B., JOHNSON, K. W., HENRIKSEN, E. J., NUSS, J. M., GOFF, D., KINNICK, T. R., MA, S. T., REEDER, J. W., SAMUELS, I., SLABIAK, T., WAGMAN, A. S., HAMMOND, M. E. & HARRISON, S. D. 2003. Selective glycogen synthase kinase 3 inhibitors potentiate insulin activation of glucose transport and utilization in vitro and in vivo. *Diabetes,* 52**,** 588-95.

RIOS, M., FAN, G., FEKETE, C., KELLY, J., BATES, B., KUEHN, R., LECHAN, R. M. & JAENISCH, R. 2001. Conditional deletion of brain-derived neurotrophic factor in the postnatal brain leads to obesity and hyperactivity. *Mol Endocrinol,* 15**,** 1748-57.

RIQUELME, P., AMODIO, G., MACEDO, C., MOREAU, A., OBERMAJER, N., BROCHHAUSEN, C., AHRENS, N., KEKARAINEN, T., FANDRICH, F., CUTURI, C., GREGORI, S., METES, D., SCHLITT, H. J., THOMSON, A. W., GEISSLER, E. K. & HUTCHINSON, J. A. 2017. DHRS9 Is a Stable Marker of Human Regulatory Macrophages. *Transplantation,* 101**,** 2731-2738.

RITCHIE, M. E., PHIPSON, B., WU, D., HU, Y., LAW, C. W., SHI, W. & SMYTH, G. K. 2015. limma powers differential expression analyses for RNA-sequencing and microarray studies. *Nucleic Acids Res,* 43**,** e47.

ROBERTS, D. S., HU, Y., LUND, I. V., BROOKS-KAYAL, A. R. & RUSSEK, S. J. 2006. Brain-derived neurotrophic factor (BDNF)-induced synthesis of early growth response factor 3 (Egr3) controls the levels of type A GABA receptor alpha 4 subunits in hippocampal neurons. *J Biol Chem,* 281**,** 29431-5.

RODRIGUEZ-TEBAR, A., DECHANT, G. & BARDE, Y. A. 1990. Binding of brain-derived neurotrophic factor to the nerve growth factor receptor. *Neuron,* 4**,** 487-92.

ROFFERS-AGARWAL, J., HUTT, K. J. & GAMMILL, L. S. 2012. Paladin is an antiphosphatase that regulates neural crest cell formation and migration. *Dev Biol,* 371**,** 180-90.

ROGALSKI, S. L., APPLEYARD, S. M., PATTILLO, A., TERMAN, G. W. & CHAVKIN, C. 2000. TrkB activation by brain-derived neurotrophic factor inhibits the G protein-gated inward rectifier Kir3 by tyrosine phosphorylation of the channel. *J Biol Chem,* 275**,** 25082-8.

ROSENTHAL, A., GOEDDEL, D. V., NGUYEN, T., LEWIS, M., SHIH, A., LARAMEE, G. R., NIKOLICS, K. & WINSLOW, J. W. 1990. Primary structure and biological activity of a novel human neurotrophic factor. *Neuron,* 4**,** 767-73.

ROSSANT, J. 2015. Mouse and human blastocyst-derived stem cells: vive les differences. *Development,* 142**,** 9-12.

ROSSO, S. B., SUSSMAN, D., WYNSHAW-BORIS, A. & SALINAS, P. C. 2005. Wnt signaling through Dishevelled, Rac and JNK regulates dendritic development. *Nat Neurosci,* 8**,** 34-42.

ROUILLE, Y., WESTERMARK, G., MARTIN, S. K. & STEINER, D. F. 1994. Proglucagon is processed to glucagon by prohormone convertase PC2 in alpha TC1-6 cells. *Proc Natl Acad Sci U S A,* 91**,** 3242-6.

ROUSSELET, E., TRAVER, S., MONNET, Y., PERRIN, A., MANDJEE, N., HILD, A., HIRSCH, E. C., ZHENG, T. S. & HUNOT, S. 2012. Tumor necrosis factor-like weak inducer of apoptosis induces astrocyte proliferation through the activation of transforming-growth factor-alpha/epidermal growth factor receptor signaling pathway. *Mol Pharmacol,* 82**,** 948-57.

RYLSKI, M., AMBORSKA, R., ZYBURA, K., MICHALUK, P., BIELINSKA, B., KONOPACKI, F. A., WILCZYNSKI, G. M. & KACZMAREK, L. 2009. JunB is a repressor of MMP-9 transcription in depolarized rat brain neurons. *Mol Cell Neurosci,* 40**,** 98-110.

SAARELAINEN, T., PUSSINEN, R., KOPONEN, E., ALHONEN, L., WONG, G., SIRVIO, J. & CASTREN, E. 2000. Transgenic mice overexpressing truncated trkB neurotrophin receptors in neurons have impaired long-term spatial memory but normal hippocampal LTP. *Synapse,* 38**,** 102-4.

SAGAR, S. M., SHARP, F. R. & CURRAN, T. 1988. Expression of c-fos protein in brain: metabolic mapping at the cellular level. *Science,* 240**,** 1328-31.

SAITO, T., HANAI, S., TAKASHIMA, S., NAKAGAWA, E., OKAZAKI, S., INOUE, T., MIYATA, R., HOSHINO, K., AKASHI, T., SASAKI, M., GOTO, Y., HAYASHI, M. & ITOH, M. 2011. Neocortical layer formation of human developing brains and lissencephalies: consideration of layer-specific marker expression. *Cereb Cortex,* 21**,** 588-96.

SALAZAR, N., CARLSON, J. C., HUANG, K., ZHENG, Y., ODERUP, C., GROSS, J., JANG, A. D., BURKE, T. M., LEWEN, S., SCHOLZ, A., HUANG, S., NEASE, L., KOSEK, J., MITTELBRONN, M., BUTCHER, E. C., TU, H. & ZABEL, B. A. 2018. A Chimeric Antibody against ACKR3/CXCR7 in Combination with TMZ Activates Immune Responses and Extends Survival in Mouse GBM Models. *Mol Ther,* 26**,** 1354-1365.

SARDI, S. P., MURTIE, J., KOIRALA, S., PATTEN, B. A. & CORFAS, G. 2006. Presenilin-dependent ErbB4 nuclear signaling regulates the timing of astrogenesis in the developing brain. *Cell,* 127**,** 185-97.

SASAI, Y., LU, B., STEINBEISSER, H., GEISSERT, D., GONT, L. K. & DE ROBERTIS, E. M. 1994. Xenopus chordin: a novel dorsalizing factor activated by organizer-specific homeobox genes. *Cell,* 79**,** 779-90.

SCHMID, D. A., YANG, T., OGIER, M., ADAMS, I., MIRAKHUR, Y., WANG, Q., MASSA, S. M., LONGO, F. M. & KATZ, D. M. 2012. A TrkB small molecule partial agonist rescues TrkB phosphorylation deficits and improves respiratory function in a mouse model of Rett syndrome. *J Neurosci,* 32**,** 1803-10.

SCHOLZKE, M. N., ROTTINGER, A., MURIKINATI, S., GEHRIG, N., LEIB, C. & SCHWANINGER, M. 2011. TWEAK regulates proliferation and differentiation of adult neural progenitor cells. *Mol Cell Neurosci,* 46**,** 325-32.

SCHULZ, A., GORODETSKA, I., BEHRENDT, R., FUESSEL, S., ERDMANN, K., FOERSTER, S., DATTA, K., MAYR, T., DUBROVSKA, A. & MUDERS, M. H. 2019. Linking NRP2 With EMT and Chemoradioresistance in Bladder Cancer. *Front Oncol,* 9**,** 1461.

SCOTT, A. M., ALLISON, J. P. & WOLCHOK, J. D. 2012. Monoclonal antibodies in cancer therapy. *Cancer Immun,* 12**,** 14.

SECCO, B., CAMIRE, E., BRIERE, M. A., CARON, A., BILLONG, A., GELINAS, Y., LEMAY, A. M., THARP, K. M., LEE, P. L., GOBEIL, S., GUIMOND, J. V., PATEY, N., GUERTIN, D. A., STAHL, A., HADDAD, E., MARSOLAIS, D., BOSSE, Y., BIRSOY, K. & LAPLANTE, M. 2017. Amplification of Adipogenic Commitment by VSTM2A. *Cell Rep,* 18**,** 93-106.

SEITZ, C., HUANG, J., GEISELHORINGER, A. L., GALBANI-BIANCHI, P., MICHALEK, S., PHAN, T. S., REINHOLD, C., DIETRICH, L., SCHMIDT, C., CORAZZA, N., DELGADO, E., SCHNALZGER, T., SCHOONJANS, K. & BRUNNER, T. 2019. The orphan nuclear receptor LRH-1/NR5a2 critically regulates T cell functions. *Sci Adv,* 5**,** eaav9732.

SENDTNER, M., HOLTMANN, B., KOLBECK, R., THOENEN, H. & BARDE, Y. A. 1992. Brain-derived neurotrophic factor prevents the death of motoneurons in newborn rats after nerve section. *Nature,* 360**,** 757-9.

SEO, S., LOMBERK, G., MATHISON, A., BUTTAR, N., PODRATZ, J., CALVO, E., IOVANNA, J., BRIMIJOIN, S., WINDEBANK, A. & URRUTIA, R. 2012. Kruppel-like factor 11 differentially couples to histone acetyltransferase and histone methyltransferase chromatin remodeling pathways to transcriptionally regulate dopamine D2 receptor in neuronal cells. *J Biol Chem,* 287**,** 12723-35.

SEVIGNY, J., CHIAO, P., BUSSIERE, T., WEINREB, P. H., WILLIAMS, L., MAIER, M., DUNSTAN, R., SALLOWAY, S., CHEN, T., LING, Y., O'GORMAN, J., QIAN, F., ARASTU, M., LI, M., CHOLLATE, S., BRENNAN, M. S., QUINTERO-MONZON, O., SCANNEVIN, R. H., ARNOLD, H. M., ENGBER, T., RHODES, K., FERRERO, J., HANG, Y., MIKULSKIS, A., GRIMM, J., HOCK, C., NITSCH, R. M. & SANDROCK, A. 2016. The antibody aducanumab reduces Abeta plaques in Alzheimer's disease. *Nature,* 537**,** 50-6.

SEWDUTH, R. N., JASPARD-VINASSA, B., PEGHAIRE, C., GUILLABERT, A., FRANZL, N., LARRIEU-LAHARGUE, F., MOREAU, C., FRUTTIGER, M., DUFOURCQ, P., COUFFINHAL, T. & DUPLAA, C. 2014. The ubiquitin ligase PDZRN3 is required for vascular morphogenesis through Wnt/planar cell polarity signalling. *Nat Commun,* 5**,** 4832.

SEWDUTH, R. N., KOVACIC, H., JASPARD-VINASSA, B., JECKO, V., WAVASSEUR, T., FRITSCH, N., PERNOT, M., JEANINGROS, S., ROUX, E., DUFOURCQ, P., COUFFINHAL, T. & DUPLAA, C. 2017. PDZRN3

destabilizes endothelial cell-cell junctions through a PKCzeta-containing polarity complex to increase vascular permeability. *Sci Signal,* 10.

SHAO, D., BAKER, M. D., ABRAHAMSEN, B., RUGIERO, F., MALIK-HALL, M., POON, W. Y., CHEAH, K. S., YAO, K. M., WOOD, J. N. & OKUSE, K. 2009. A multi PDZ-domain protein Pdzd2 contributes to functional expression of sensory neuron-specific sodium channel Na(V)1.8. *Mol Cell Neurosci,* 42**,** 219-25.

SHENG, M. & GREENBERG, M. E. 1990. The regulation and function of c-fos and other immediate early genes in the nervous system. *Neuron,* 4**,** 477-85.

SHEPARD, R., HESLIN, K., HAGERDORN, P. & COUTELLIER, L. 2019. Downregulation of Npas4 in parvalbumin interneurons and cognitive deficits after neonatal NMDA receptor blockade: relevance for schizophrenia. *Transl Psychiatry,* 9**,** 99.

SHI, Y., KIRWAN, P., SMITH, J., ROBINSON, H. P. & LIVESEY, F. J. 2012. Human cerebral cortex development from pluripotent stem cells to functional excitatory synapses. *Nat Neurosci,* 15**,** 477-86, S1.

SHIEH, P. B., HU, S. C., BOBB, K., TIMMUSK, T. & GHOSH, A. 1998. Identification of a signaling pathway involved in calcium regulation of BDNF expression. *Neuron,* 20**,** 727-40.

SIDDIQUI, T. J., PANCAROGLU, R., KANG, Y., ROOYAKKERS, A. & CRAIG, A. M. 2010. LRRTMs and neuroligins bind neurexins with a differential code to cooperate in glutamate synapse development. *J Neurosci,* 30**,** 7495-506.

SIMMONS, D. A., BELICHENKO, N. P., YANG, T., CONDON, C., MONBUREAU, M., SHAMLOO, M., JING, D., MASSA, S. M. & LONGO, F. M. 2013. A small molecule TrkB ligand reduces motor impairment and neuropathology in R6/2 and BACHD mouse models of Huntington's disease. *J Neurosci,* 33**,** 18712-27.

SIMMONS, D. A., REX, C. S., PALMER, L., PANDYARAJAN, V., FEDULOV, V., GALL, C. M. & LYNCH, G. 2009. Up-regulating BDNF with an ampakine rescues synaptic plasticity and memory in Huntington's disease knockin mice. *Proc Natl Acad Sci U S A,* 106**,** 4906-11.

SMEEKENS, S. P., MONTAG, A. G., THOMAS, G., ALBIGES-RIZO, C., CARROLL, R., BENIG, M., PHILLIPS, L. A., MARTIN, S., OHAGI, S., GARDNER, P. & ET AL. 1992. Proinsulin processing by the subtilisin-related proprotein convertases furin, PC2, and PC3. *Proc Natl Acad Sci U S A,* 89**,** 8822-6.

SMEYNE, R. J., KLEIN, R., SCHNAPP, A., LONG, L. K., BRYANT, S., LEWIN, A., LIRA, S. A. & BARBACID, M. 1994. Severe sensory and sympathetic neuropathies in mice carrying a disrupted Trk/NGF receptor gene. *Nature,* 368**,** 246-9.

SMITH, A. 2017. Formative pluripotency: the executive phase in a developmental continuum. *Development,* 144**,** 365-373.

SMITH, P. D., SUN, F., PARK, K. K., CAI, B., WANG, C., KUWAKO, K., MARTINEZ-CARRASCO, I., CONNOLLY, L. & HE, Z. 2009. SOCS3 deletion promotes optic nerve regeneration in vivo. *Neuron,* 64**,** 617-23.

SMITH, W. C. & HARLAND, R. M. 1992. Expression cloning of noggin, a new dorsalizing factor localized to the Spemann organizer in Xenopus embryos. *Cell,* 70**,** 829-40.

SOMMERFELD, M. T., SCHWEIGREITER, R., BARDE, Y. A. & HOPPE, E. 2000. Down-regulation of the neurotrophin receptor TrkB following ligand binding. Evidence for an involvement of the proteasome and differential regulation of TrkA and TrkB. *J Biol Chem,* 275**,** 8982-90.

SONOYAMA, T., STADLER, L. K. J., ZHU, M., KEOGH, J. M., HENNING, E., HISAMA, F., KIRWAN, P., JURA, M., BLASZCZYK, B. K., DEWITT, D. C., BROUWERS, B., HYVONEN, M., BARROSO, I., MERKLE, F. T., APPLEYARD, S. M., WAYMAN, G. A. & FAROOQI, I. S. 2020. Human BDNF/TrkB variants impair hippocampal synaptogenesis and associate with neurobehavioural abnormalities. *Sci Rep,* 10**,** 9028.

SOPPET, D., ESCANDON, E., MARAGOS, J., MIDDLEMAS, D. S., REID, S. W., BLAIR, J., BURTON, L. E., STANTON, B. R., KAPLAN, D. R., HUNTER, T., NIKOLICS, K. & PARADA, L. F. 1991. The neurotrophic factors brain-derived neurotrophic factor and neurotrophin-3 are ligands for the trkB tyrosine kinase receptor. *Cell,* 65**,** 895-903.

SQUINTO, S. P., STITT, T. N., ALDRICH, T. H., DAVIS, S., BIANCO, S. M., RADZIEJEWSKI, C., GLASS, D. J., MASIAKOWSKI, P., FURTH, M. E., VALENZUELA, D. M. & ET AL. 1991. trkB encodes a functional receptor for brain-derived neurotrophic factor and neurotrophin-3 but not nerve growth factor. *Cell,* 65**,** 885-93.

STOILOV, P., CASTREN, E. & STAMM, S. 2002. Analysis of the human TrkB gene genomic organization reveals novel TrkB isoforms, unusual gene length, and splicing mechanism. *Biochem Biophys Res Commun,* 290**,** 1054-65.

STORBECK, C. J., WAGNER, S., O'REILLY, P., MCKAY, M., PARKS, R. J., WESTPHAL, H. & SABOURIN, L. A. 2009. The Ldb1 and Ldb2 transcriptional cofactors interact with the Ste20-like kinase SLK and regulate cell migration. *Mol Biol Cell,* 20**,** 4174-82.

STRAUSBERG, R. L., FEINGOLD, E. A., GROUSE, L. H., DERGE, J. G., KLAUSNER, R. D., COLLINS, F. S., WAGNER, L., SHENMEN, C. M., SCHULER, G. D., ALTSCHUL, S. F., ZEEBERG, B., BUETOW, K. H., SCHAEFER, C. F., BHAT, N. K., HOPKINS, R. F., JORDAN, H., MOORE, T., MAX, S. I., WANG, J., HSIEH, F., DIATCHENKO, L., MARUSINA, K., FARMER, A. A., RUBIN, G. M., HONG, L., STAPLETON, M., SOARES, M. B., BONALDO, M. F., CASAVANT, T. L., SCHEETZ, T. E., BROWNSTEIN, M. J., USDIN, T. B., TOSHIYUKI, S., CARNINCI, P., PRANGE, C., RAHA, S. S., LOQUELLANO, N. A., PETERS, G. J., ABRAMSON, R. D., MULLAHY, S. J., BOSAK, S. A., MCEWAN, P. J., MCKERNAN, K. J., MALEK, J. A., GUNARATNE, P. H., RICHARDS, S., WORLEY, K. C., HALE, S., GARCIA, A. M., GAY, L. J., HULYK, S. W., VILLALON, D. K., MUZNY, D. M., SODERGREN, E. J., LU, X., GIBBS, R. A., FAHEY, J., HELTON, E., KETTEMAN, M., MADAN, A., RODRIGUES, S., SANCHEZ, A., WHITING, M., MADAN, A., YOUNG, A. C., SHEVCHENKO, Y., BOUFFARD, G. G., BLAKESLEY, R. W., TOUCHMAN, J. W., GREEN, E. D., DICKSON, M. C., RODRIGUEZ, A. C., GRIMWOOD, J., SCHMUTZ, J., MYERS, R. M., BUTTERFIELD, Y. S., KRZYWINSKI, M. I., SKALSKA, U., SMAILUS, D. E., SCHNERCH, A., SCHEIN, J. E., JONES, S. J., MARRA, M. A. & MAMMALIAN GENE COLLECTION PROGRAM, T. 2002. Generation and initial analysis of more than 15,000 full-length human and mouse cDNA sequences. *Proc Natl Acad Sci U S A,* 99**,** 16899-903.

STROHMAIER, C., CARTER, B. D., URFER, R., BARDE, Y. A. & DECHANT, G. 1996. A splice variant of the neurotrophin receptor trkB with increased specificity for brain-derived neurotrophic factor. *EMBO J,* 15**,** 3332-7.

SUGIYAMA, Y., SUZUKI, A., KISHIKAWA, M., AKUTSU, R., HIROSE, T., WAYE, M. M., TSUI, S. K., YOSHIDA, S. & OHNO, S. 2000. Muscle develops a specific form of small heat shock protein complex composed of MKBP/HSPB2 and HSPB3 during myogenic differentiation. *J Biol Chem,* 275**,** 1095-104.

SUN, K., LI, X., CHEN, X., BAI, Y., ZHOU, G., KOKIKO-COCHRAN, O. N., LAMB, B., HAMILTON, T. A., LIN, C. Y., LEE, Y. S. & HERJAN, T. 2018a. Neuron-Specific HuR-Deficient Mice Spontaneously Develop Motor Neuron Disease. *J Immunol,* 201**,** 157-166.

SUN, T., DU, S. Y., ARMENIA, J., QU, F., FAN, J., WANG, X., FEI, T., KOMURA, K., LIU, S. X., LEE, G. M. & KANTOFF, P. W. 2018b. Expression of lncRNA MIR222HG co-transcribed from the miR-221/222 gene promoter facilitates the development of castration-resistant prostate cancer. *Oncogenesis,* 7**,** 30.

SURMACZ, B., NOISA, P., RISNER-JANICZEK, J. R., HUI, K., UNGLESS, M., CUI, W. & LI, M. 2012. DLK1 promotes neurogenesis of human and mouse pluripotent stem cell-derived neural progenitors via modulating Notch and BMP signalling. *Stem Cell Rev,* 8**,** 459-71.

SUSEN, K., HEUMANN, R. & BLOCHL, A. 1999. Nerve growth factor stimulates MAPK via the low affinity receptor p75(LNTR). *FEBS Lett,* 463**,** 231-4.

SZKUDLINSKI, M. W., FREMONT, V., RONIN, C. & WEINTRAUB, B. D. 2002. Thyroid-stimulating hormone and thyroid-stimulating hormone receptor structure-function relationships. *Physiol Rev,* 82**,** 473-502.

SZUMSKA, D., CIOROCH, M., KEELING, A., PRAT, A., SEIDAH, N. G. & BHATTACHARYA, S. 2017. Pcsk5 is required in the early cranio-cardiac mesoderm for heart development. *BMC Dev Biol,* 17**,** 6.

TAKADA, H., WAKABAYASHI, N., DOHI, O., YASUI, K., SAKAKURA, C., MITSUFUJI, S., TANIWAKI, M. & YOSHIKAWA, T. 2010. Tissue factor pathway inhibitor 2 (TFPI2) is frequently silenced by aberrant promoter hypermethylation in gastric cancer. *Cancer Genet Cytogenet,* 197**,** 16-24.

TAKAHASHI, F., CHIBA, N., TAJIMA, K., HAYASHIDA, T., SHIMADA, T., TAKAHASHI, M., MORIYAMA, H., BRACHTEL, E., EDELMAN, E. J., RAMASWAMY, S. & MAHESWARAN, S. 2011. Breast tumor progression induced by loss of BTG2 expression is inhibited by targeted therapy with the ErbB/HER inhibitor lapatinib. *Oncogene,* 30**,** 3084-95.

TAKAHASHI, K., LIU, F. C., HIROKAWA, K. & TAKAHASHI, H. 2003. Expression of Foxp2, a gene involved in speech and language, in the developing and adult striatum. *J Neurosci Res,* 73**,** 61-72.

TAKAHASHI, K., TANABE, K., OHNUKI, M., NARITA, M., ICHISAKA, T., TOMODA, K. & YAMANAKA, S. 2007. Induction of pluripotent stem cells from adult human fibroblasts by defined factors. *Cell,* 131**,** 861-72.

TAKAHASHI, K. & YAMANAKA, S. 2006. Induction of pluripotent stem cells from mouse embryonic and adult fibroblast cultures by defined factors. *Cell,* 126**,** 663-76.

TAKAHASHI, M. & OSUMI, N. 2008. Expression study of cadherin7 and cadherin20 in the embryonic and adult rat central nervous system. *BMC Dev Biol,* 8**,** 87.

TAKASHIMA, N., ODAKA, Y. S., SAKOORI, K., AKAGI, T., HASHIKAWA, T., MORIMURA, N., YAMADA, K. & ARUGA, J. 2011. Impaired cognitive function and altered hippocampal synapse morphology in mice lacking Lrrtm1, a gene associated with schizophrenia. *PLoS One,* 6**,** e22716.

TAKEDA, Y., CHOU, K. B., TAKEDA, J., SACHAIS, B. S. & KRAUSE, J. E. 1991. Molecular cloning, structural characterization and functional expression of the human substance P receptor. *Biochem Biophys Res Commun,* 179**,** 1232-40.

TAKEUCHI, M., HARIGAI, M., MOMOHARA, S., BALL, E., ABE, J., FURUICHI, K. & KAMATANI, N. 2007. Cloning and characterization of DPPL1 and DPPL2, representatives of a novel type of mammalian phosphatidate phosphatase. *Gene,* 399**,** 174-80.

TALEB, S., ROMAIN, M., RAMKHELAWON, B., UYTTENHOVE, C., PASTERKAMP, G., HERBIN, O., ESPOSITO, B., PEREZ, N., YASUKAWA, H., VAN SNICK, J., YOSHIMURA, A., TEDGUI, A. & MALLAT, Z. 2009. Loss of SOCS3 expression in T cells reveals a regulatory role for interleukin-17 in atherosclerosis. *J Exp Med,* 206**,** 2067-77.

TAMBURINI, C. & LI, M. 2017. Understanding neurodevelopmental disorders using human pluripotent stem cell-derived neurons. *Brain Pathol,* 27**,** 508-517.

TAMURA, S., MORIKAWA, Y., IWANISHI, H., HISAOKA, T. & SENBA, E. 2004. Foxp1 gene expression in projection neurons of the mouse striatum. *Neuroscience,* 124**,** 261-7.

TAN, T. Y., GORDON, C. T., MILLER, K. A., AMOR, D. J. & FARLIE, P. G. 2015. YPEL1 overexpression in early avian craniofacial mesenchyme causes mandibular dysmorphogenesis by up-regulating apoptosis. *Dev Dyn,* 244**,** 1022-30.

TAN, Y. W., ZHANG, S. J., HOFFMANN, T. & BADING, H. 2012. Increasing levels of wild-type CREB up-regulates several activity-regulated inhibitor of death (AID) genes and promotes neuronal survival. *BMC Neurosci,* 13**,** 48.

TANG, X., JANG, S. W., OKADA, M., CHAN, C. B., FENG, Y., LIU, Y., LUO, S. W., HONG, Y., RAMA, N., XIONG, W. C., MEHLEN, P. & YE, K. 2008. Netrin-1 mediates neuronal survival through PIKE-L interaction with the dependence receptor UNC5B. *Nat Cell Biol,* 10**,** 698-706.

TAUSZIG-DELAMASURE, S., YU, L. Y., CABRERA, J. R., BOUZAS-RODRIGUEZ, J., MERMET-BOUVIER, C., GUIX, C., BORDEAUX, M. C., ARUMAE, U. & MEHLEN, P. 2007. The TrkC receptor induces apoptosis when the dependence receptor notion meets the neurotrophin paradigm. *Proc Natl Acad Sci U S A,* 104**,** 13361-6.

TELEZHKIN, V., SCHNELL, C., YAROVA, P., YUNG, S., COPE, E., HUGHES, A., THOMPSON, B. A., SANDERS, P., GEATER, C., HANCOCK, J. M., JOY, S., BADDER, L., CONNOR-ROBSON, N., COMELLA, A., STRACCIA, M., BOMBAU, G., BROWN, J. T., CANALS, J. M., RANDALL, A. D., ALLEN, N. D. & KEMP, P. J. 2016. Forced cell cycle exit and modulation of GABAA, CREB, and GSK3beta

signaling promote functional maturation of induced pluripotent stem cell-derived neurons. *Am J Physiol Cell Physiol,* 310**,** C520-41.

THOMSON, J. A., ITSKOVITZ-ELDOR, J., SHAPIRO, S. S., WAKNITZ, M. A., SWIERGIEL, J. J., MARSHALL, V. S. & JONES, J. M. 1998. Embryonic stem cell lines derived from human blastocysts. *Science,* 282**,** 1145-7.

THOMSON, P. A., WRAY, N. R., THOMSON, A. M., DUNBAR, D. R., GRASSIE, M. A., CONDIE, A., WALKER, M. T., SMITH, D. J., PULFORD, D. J., MUIR, W., BLACKWOOD, D. H. & PORTEOUS, D. J. 2005. Sex-specific association between bipolar affective disorder in women and GPR50, an X-linked orphan G protein-coupled receptor. *Mol Psychiatry,* 10**,** 470-8.

TRAUB, S., STAHL, H., ROSENBROCK, H., SIMON, E., FLORIN, L., HOSPACH, L., HORER, S. & HEILKER, R. 2017. Pharmaceutical Characterization of Tropomyosin Receptor Kinase B-Agonistic Antibodies on Human Induced Pluripotent Stem (hiPS) Cell-Derived Neurons. *J Pharmacol Exp Ther,* 361**,** 355-365.

TSUCHIDA, A., NONOMURA, T., NAKAGAWA, T., ITAKURA, Y., ONO-KISHINO, M., YAMANAKA, M., SUGARU, E., TAIJI, M. & NOGUCHI, H. 2002. Brain-derived neurotrophic factor ameliorates lipid metabolism in diabetic mice. *Diabetes Obes Metab,* 4**,** 262-9.

TURDO, F., BIANCHI, F., GASPARINI, P., SANDRI, M., SASSO, M., DE CECCO, L., FORTE, L., CASALINI, P., AIELLO, P., SFONDRINI, L., AGRESTI, R., CARCANGIU, M. L., PLANTAMURA, I., SOZZI, G., TAGLIABUE, E. & CAMPIGLIO, M. 2016. CDCP1 is a novel marker of the most aggressive human triple-negative breast cancers. *Oncotarget,* 7**,** 69649-69665.

TUVIKENE, J., PRUUNSILD, P., ORAV, E., ESVALD, E. E. & TIMMUSK, T. 2016. AP-1 Transcription Factors Mediate BDNF-Positive Feedback Loop in Cortical Neurons. *J Neurosci,* 36**,** 1290-305.

UDEMGBA, C., JOHNSON, S., STOCKMEIER, C. A., LUO, J., ALBERT, P. R., WANG, J., MAY, W. L., RAJKOWSKA, G., HARRIS, S., SITTMAN, D. B. & OU, X. M. 2014. The expression of KLF11 (TIEG2), a monoamine oxidase B transcriptional activator in the prefrontal cortex of human alcohol dependence. *Alcohol Clin Exp Res,* 38**,** 144-51.

UEDA, T., YOKOTA, T., OKUZAKI, D., UNO, Y., MASHIMO, T., KUBOTA, Y., SUDO, T., ISHIBASHI, T., SHINGAI, Y., DOI, Y., OZAWA, T., NAKAI, R., TANIMURA, A., ICHII, M., EZOE, S., SHIBAYAMA, H., ORITANI, K. & KANAKURA, Y. 2019. Endothelial Cell-Selective Adhesion Molecule Contributes to the Development of Definitive Hematopoiesis in the Fetal Liver. *Stem Cell Reports,* 13**,** 992-1005.

ULTSCH, M. H., WIESMANN, C., SIMMONS, L. C., HENRICH, J., YANG, M., REILLY, D., BASS, S. H. & DE VOS, A. M. 1999. Crystal structures of the neurotrophin-binding domain of TrkA, TrkB and TrkC. *J Mol Biol,* 290**,** 149-59.

VALENTE, M. M., ALLEN, M., BORTOLOTTO, V., LIM, S. T., CONANT, K. & GRILLI, M. 2015. The MMP-1/PAR-1 Axis Enhances Proliferation and Neuronal Differentiation of Adult Hippocampal Neural Progenitor Cells. *Neural Plast,* 2015**,** 646595.

VAN DEN BERGHE, V., STAPPERS, E., VANDESANDE, B., DIMIDSCHSTEIN, J., KROES, R., FRANCIS, A., CONIDI, A., LESAGE, F., DRIES, R., CAZZOLA, S., BERX, G., KESSARIS, N., VANDERHAEGHEN, P., VAN IJCKEN, W., GROSVELD, F. G., GOOSSENS, S., HAIGH, J. J., FISHELL, G., GOFFINET, A., AERTS, S., HUYLEBROECK, D. & SEUNTJENS, E. 2013. Directed migration of cortical interneurons depends on the cell-autonomous action of Sip1. *Neuron,* 77**,** 70-82.

VANIER, M. T. & MILLAT, G. 2003. Niemann-Pick disease type C. *Clin Genet,* 64**,** 269-81.

VANLANDINGHAM, J. W., CEKIC, M., CUTLER, S., HOFFMAN, S. W. & STEIN, D. G. 2007. Neurosteroids reduce inflammation after TBI through CD55 induction. *Neurosci Lett,* 425**,** 94-8.

VIDARSSON, H., HYLLNER, J. & SARTIPY, P. 2010. Differentiation of human embryonic stem cells to cardiomyocytes for in vitro and in vivo applications. *Stem Cell Rev,* 6**,** 108-20.

VOGT, J., DINGWELL, K. S., HERHAUS, L., GOURLAY, R., MACARTNEY, T., CAMPBELL, D., SMITH, J. C. & SAPKOTA, G. P. 2014. Protein associated with SMAD1 (PAWS1/FAM83G) is a substrate for type I bone morphogenetic protein receptors and modulates bone morphogenetic protein signalling. *Open Biol,* 4**,** 130210.

VOLONTE, C., ANGELASTRO, J. M. & GREENE, L. A. 1993. Association of protein kinases ERK1 and ERK2 with p75 nerve growth factor receptors. *J Biol Chem,* 268**,** 21410-5.

VOLZ, C. & PAULY, D. 2015. Antibody therapies and their challenges in the treatment of age-related macular degeneration. *Eur J Pharm Biopharm,* 95**,** 158-72.

WADDELL, J. N., ZHANG, P., WEN, Y., GUPTA, S. K., YEVTODIYENKO, A., SCHMIDT, J. V., BIDWELL, C. A., KUMAR, A. & KUANG, S. 2010. Dlk1 is necessary for proper skeletal muscle development and regeneration. *PLoS One,* 5**,** e15055.

WALKER, D. G., WHETZEL, A. M. & LUE, L. F. 2015. Expression of suppressor of cytokine signaling genes in human elderly and Alzheimer's disease brains and human microglia. *Neuroscience,* 302**,** 121-37.

WALLGARD, E., NITZSCHE, A., LARSSON, J., GUO, X., DIETERICH, L. C., DIMBERG, A., OLOFSSON, T., PONTEN, F. C., MAKINEN, T., KALEN, M. & HELLSTROM, M. 2012. Paladin (X99384) is expressed in the vasculature and shifts from endothelial to vascular smooth muscle cells during mouse development. *Dev Dyn,* 241**,** 770-86.

WANG, L., ZHANG, Y., CHEN, Y. B., SKALA, S. L., AL-AHMADIE, H. A., WANG, X., CAO, X., VEENEMAN, B. A., CHEN, J., CIESLIK, M., QIAO, Y., SU, F., VATS, P., SIDDIQUI, J., XIAO, H., SADIMIN, E. T., EPSTEIN, J. I., ZHOU, M., SANGOI, A. R., TRPKOV, K., OSUNKOYA, A. O., GIANNICO, G. A., MCKENNEY, J. K., ARGANI, P., TICKOO, S. K., REUTER, V. E., CHINNAIYAN, A. M., DHANASEKARAN, S. M. & MEHRA, R. 2018a. VSTM2A Overexpression Is a Sensitive and Specific Biomarker for Mucinous Tubular and Spindle Cell Carcinoma (MTSCC) of the Kidney. *Am J Surg Pathol,* 42**,** 1571-1584.

WANG, L., ZHOU, W., ZHONG, Y., HUO, Y., FAN, P., ZHAN, S., XIAO, J., JIN, X., GOU, S., YIN, T., WU, H. & LIU, T. 2017. Overexpression of G protein-coupled receptor GPR87 promotes pancreatic cancer aggressiveness and activates NF-kappaB signaling pathway. *Mol Cancer,* 16**,** 61.

WANG, P., LI, H., BARDE, S., ZHANG, M. D., SUN, J., WANG, T., ZHANG, P., LUO, H., WANG, Y., YANG, Y., WANG, C., SVENNINGSSON, P., THEODORSSON, E., HOKFELT, T. G. & XU, Z. Q. 2016. Depression-like behavior in rat: Involvement of galanin receptor subtype 1 in the ventral periaqueductal gray. *Proc Natl Acad Sci U S A,* 113**,** E4726-35.

WANG, R., MA, Z., FENG, L., YANG, Y., TAN, C., SHI, Q., LIAN, M., HE, S., MA, H. & FANG, J. 2018b. LncRNA MIR31HG targets HIF1A and P21 to facilitate head and neck cancer cell proliferation and tumorigenesis by promoting cell-cycle progression. *Mol Cancer,* 17**,** 162.

WANG, S., DONG, Y., ZHANG, Y., WANG, X., XU, L., YANG, S., LI, X., DONG, H., XU, L., SU, L., NG, S. S., CHANG, Z., SUNG, J. J., ZHANG, X. & YU, J. 2015. DACT2 is a functional tumor suppressor through inhibiting Wnt/beta-catenin pathway and associated with poor survival in colon cancer. *Oncogene,* 34**,** 2575-85.

WANG, S., YAO, H., XU, Y., HAO, R., ZHANG, W., LIU, H., HUANG, Y., GUO, W. & LU, B. 2020a. Therapeutic potential of a TrkB agonistic antibody for Alzheimer's disease. *Theranostics,* 10**,** 6854-6874.

WANG, W., YANG, Y., LI, L. & SHI, Y. 2003. Synleurin, a novel leucine-rich repeat protein that increases the intensity of pleiotropic cytokine responses. *Biochem Biophys Res Commun,* 305**,** 981-8.

WANG, X. Q., XU, H., WANG, C. H. & XIE, H. 2020b. Long non-coding RNA GNAS-AS1 promotes cell migration and invasion via regulating Wnt/beta-catenin pathway in nasopharyngeal carcinoma. *Eur Rev Med Pharmacol Sci,* 24**,** 3077-3084.

WANG, Y., HO, G., ZHANG, J. J., NIEUWENHUIJSEN, B., EDRIS, W., CHANDA, P. K. & YOUNG, K. H. 2002. Regulator of G protein signaling Z1 (RGSZ1) interacts with Galpha i subunits and regulates Galpha i-mediated cell signaling. *J Biol Chem,* 277**,** 48325-32.

WANG, Y., LI, Y., DALLE LUCCA, S. L., SIMOVIC, M., TSOKOS, G. C. & DALLE LUCCA, J. J. 2010. Decay accelerating factor (CD55) protects neuronal cells from chemical hypoxia-induced injury. *J Neuroinflammation,* 7**,** 24.

WANG, Y., ZHAO, C., HOU, Z., YANG, Y., BI, Y., WANG, H., ZHANG, Y. & GAO, S. 2018c. Unique molecular events during reprogramming of human somatic cells to induced pluripotent stem cells (iPSCs) at naive state. *Elife,* 7.

WARD, Y., YAP, S. F., RAVICHANDRAN, V., MATSUMURA, F., ITO, M., SPINELLI, B. & KELLY, K. 2002. The GTP binding proteins Gem and Rad are negative regulators of the Rho-Rho kinase pathway. *J Cell Biol,* 157**,** 291-302.

WARYAH, A. M., SHAHZAD, M., SHAIKH, H., SHEIKH, S. A., CHANNA, N. A., HUFNAGEL, R. B., MAKHDOOM, A., RIAZUDDIN, S. & AHMED, Z. M. 2016. A novel CHST3 allele associated with spondyloepiphyseal dysplasia and hearing loss in Pakistani kindred. *Clin Genet,* 90**,** 90-5.

WATANABE, M., MAEMURA, K., KANBARA, K., TAMAYAMA, T. & HAYASAKI, H. 2002. GABA and GABA receptors in the central nervous system and other organs. *Int Rev Cytol,* 213**,** 1-47.

WENG, F. J., GARCIA, R. I., LUTZU, S., ALVINA, K., ZHANG, Y., DUSHKO, M., KU, T., ZEMOURA, K., RICH, D., GARCIA-DOMINGUEZ, D., HUNG, M., YELHEKAR, T. D., SORENSEN, A. T., XU, W., CHUNG, K., CASTILLO, P. E. & LIN, Y. 2018. Npas4 Is a Critical Regulator of Learning-Induced Plasticity at Mossy Fiber-CA3 Synapses during Contextual Memory Formation. *Neuron,* 97**,** 1137-1152 e5.

WERTHEIM, G. B., YANG, T. W., PAN, T. C., RAMNE, A., LIU, Z., GARDNER, H. P., DUGAN, K. D., KRISTEL, P., KREIKE, B., VAN DE VIJVER, M. J., CARDIFF, R. D., REYNOLDS, C. & CHODOSH, L. A. 2009. The Snf1-related kinase, Hunk, is essential for mammary tumor metastasis. *Proc Natl Acad Sci U S A,* 106**,** 15855-60.

WEST, A. E., PRUUNSILD, P. & TIMMUSK, T. 2014. Neurotrophins: transcription and translation. *Handb Exp Pharmacol,* 220**,** 67-100.

WESTRA, D., KURVERS, R. A., VAN DEN HEUVEL, L. P., WURZNER, R., HOPPENREIJS, E. P., VAN DER FLIER, M., VAN DE KAR, N. C. & WARRIS, A. 2014. Compound heterozygous mutations in the C6 gene of a child with recurrent infections. *Mol Immunol,* 58**,** 201-5.

WETHERILL, L., SCHUCKIT, M. A., HESSELBROCK, V., XUEI, X., LIANG, T., DICK, D. M., KRAMER, J., NURNBERGER, J. I., JR., TISCHFIELD, J. A., PORJESZ, B., EDENBERG, H. J. & FOROUD, T. 2008. Neuropeptide Y receptor genes are associated with alcohol dependence, alcohol withdrawal phenotypes, and cocaine dependence. *Alcohol Clin Exp Res,* 32**,** 2031-40.

WETSEL, W. C., RODRIGUIZ, R. M., GUILLEMOT, J., ROUSSELET, E., ESSALMANI, R., KIM, I. H., BRYANT, J. C., MARCINKIEWICZ, J., DESJARDINS, R., DAY, R., CONSTAM, D. B., PRAT, A. & SEIDAH, N. G. 2013. Disruption of the expression of the proprotein convertase PC7 reduces BDNF production and affects learning and memory in mice. *Proc Natl Acad Sci U S A,* 110**,** 17362-7.

WIBRAND, K., MESSAOUDI, E., HAVIK, B., STEENSLID, V., LOVLIE, R., STEEN, V. M. & BRAMHAM, C. R. 2006. Identification of genes co-upregulated with Arc during BDNF-induced long-term potentiation in adult rat dentate gyrus in vivo. *Eur J Neurosci,* 23**,** 1501-11.

WIESMANN, C., ULTSCH, M. H., BASS, S. H. & DE VOS, A. M. 1999. Crystal structure of nerve growth factor in complex with the ligand-binding domain of the TrkA receptor. *Nature,* 401**,** 184-8.

WILKIE, N., WINGROVE, P. B., BILSLAND, J. G., YOUNG, L., HARPER, S. J., HEFTI, F., ELLIS, S. & POLLACK, S. J. 2001. The non-peptidyl fungal metabolite L-783,281 activates TRK neurotrophin receptors. *J Neurochem,* 78**,** 1135-45.

WILLARDSEN, M., HUTCHESON, D. A., MOORE, K. B. & VETTER, M. L. 2014. The ETS transcription factor Etv1 mediates FGF signaling to initiate proneural gene expression during Xenopus laevis retinal development. *Mech Dev,* 131**,** 57-67.

WILLIAMS, J. T., CHRISTIE, M. J. & MANZONI, O. 2001. Cellular and synaptic adaptations mediating opioid dependence. *Physiol Rev,* 81**,** 299-343.

WINTER, C., WEISS, C., MARTIN-VILLALBA, A., ZIMMERMANN, M. & SCHENKEL, J. 2002. JunB and Bcl-2 overexpression results in protection against cell death of nigral neurons following axotomy. *Brain Res Mol Brain Res,* 104**,** 194-202.

WIRTH, T., MARIANI, L. L., BERGANT, G., BAULAC, M., HABERT, M. O., DROUOT, N., OLLIVIER, E., HODZIC, A., RUDOLF, G., NITSCHKE, P., RUDOLF, G., CHELLY, J., TRANCHANT, C., ANHEIM, M.

& ROZE, E. 2020. Loss-of-Function Mutations in NR4A2 Cause Dopa-Responsive Dystonia Parkinsonism. *Mov Disord,* 35**,** 880-885.

WITOELAR, A., RONGVE, A., ALMDAHL, I. S., ULSTEIN, I. D., ENGVIG, A., WHITE, L. R., SELBAEK, G., STORDAL, E., ANDERSEN, F., BRAEKHUS, A., SALTVEDT, I., ENGEDAL, K., HUGHES, T., BERGH, S., BRATHEN, G., BOGDANOVIC, N., BETTELLA, F., WANG, Y., ATHANASIU, L., BAHRAMI, S., LE HELLARD, S., GIDDALURU, S., DALE, A. M., SANDO, S. B., STEINBERG, S., STEFANSSON, H., SNAEDAL, J., DESIKAN, R. S., STEFANSSON, K., AARSLAND, D., DJUROVIC, S., FLADBY, T. & ANDREASSEN, O. A. 2018. Meta-analysis of Alzheimer's disease on 9,751 samples from Norway and IGAP study identifies four risk loci. *Sci Rep,* 8**,** 18088.

WOJCIECH, S., AHMAD, R., BELAID-CHOUCAIR, Z., JOURNE, A. S., GALLET, S., DAM, J., DAULAT, A., NDIAYE-LOBRY, D., LAHUNA, O., KARAMITRI, A., GUILLAUME, J. L., DO CRUZEIRO, M., GUILLONNEAU, F., SAADE, A., CLEMENT, N., COURIVAUD, T., KAABI, N., TADAGAKI, K., DELAGRANGE, P., PREVOT, V., HERMINE, O., PRUNIER, C. & JOCKERS, R. 2018. The orphan GPR50 receptor promotes constitutive TGFbeta receptor signaling and protects against cancer development. *Nat Commun,* 9**,** 1216.

WU, C. Y., WHYE, D., MASON, R. W. & WANG, W. 2012. Efficient differentiation of mouse embryonic stem cells into motor neurons. *J Vis Exp***,** e3813.

XIANG, C., CHEN, J. & FU, P. 2017. HGF/Met Signaling in Cancer Invasion: The Impact on Cytoskeleton Remodeling. *Cancers (Basel),* 9.

XIANG, W., KE, Z., ZHANG, Y., CHENG, G. H., IRWAN, I. D., SULOCHANA, K. N., POTTURI, P., WANG, Z., YANG, H., WANG, J., ZHUO, L., KINI, R. M. & GE, R. 2011. Isthmin is a novel secreted angiogenesis inhibitor that inhibits tumour growth in mice. *J Cell Mol Med,* 15**,** 359-74.

XIE, J., ZHANG, H., YEA, K. & LERNER, R. A. 2013. Autocrine signaling based selection of combinatorial antibodies that transdifferentiate human stem cells. *Proc Natl Acad Sci U S A,* 110**,** 8099-104.

XIE, Y., HAYDEN, M. R. & XU, B. 2010. BDNF overexpression in the forebrain rescues Huntington's disease phenotypes in YAC128 mice. *J Neurosci,* 30**,** 14708-18.

XU, B., GOULDING, E. H., ZANG, K., CEPOI, D., CONE, R. D., JONES, K. R., TECOTT, L. H. & REICHARDT, L. F. 2003. Brain-derived neurotrophic factor regulates energy balance downstream of melanocortin-4 receptor. *Nat Neurosci,* 6**,** 736-42.

YAMAGATA, K., KAUFMANN, W. E., LANAHAN, A., PAPAPAVLOU, M., BARNES, C. A., ANDREASSON, K. I. & WORLEY, P. F. 1994. Egr3/Pilot, a zinc finger transcription factor, is rapidly regulated by activity in brain neurons and colocalizes with Egr1/zif268. *Learn Mem,* 1**,** 140-52.

YAMAMOTO, H. & GURNEY, M. E. 1990. Human platelets contain brain-derived neurotrophic factor. *J Neurosci,* 10**,** 3469-78.

YAN, J., STUDER, L. & MCKAY, R. D. 2001. Ascorbic acid increases the yield of dopaminergic neurons derived from basic fibroblast growth factor expanded mesencephalic precursors. *J Neurochem,* 76**,** 307-11.

YEH, E. S., BELKA, G. K., VERNON, A. E., CHEN, C. C., JUNG, J. J. & CHODOSH, L. A. 2013. Hunk negatively regulates c-myc to promote Akt-mediated cell survival and mammary tumorigenesis induced by loss of Pten. *Proc Natl Acad Sci U S A,* 110**,** 6103-8.

YEO, E. J., CASSETTA, L., QIAN, B. Z., LEWKOWICH, I., LI, J. F., STEFATER, J. A., 3RD, SMITH, A. N., WIECHMANN, L. S., WANG, Y., POLLARD, J. W. & LANG, R. A. 2014. Myeloid WNT7b mediates the angiogenic switch and metastasis in breast cancer. *Cancer Res,* 74**,** 2962-73.

YEO, G. S., CONNIE HUNG, C. C., ROCHFORD, J., KEOGH, J., GRAY, J., SIVARAMAKRISHNAN, S., O'RAHILLY, S. & FAROOQI, I. S. 2004. A de novo mutation affecting human TrkB associated with severe obesity and developmental delay. *Nat Neurosci,* 7**,** 1187-9.

YIN, Y., EDELMAN, G. M. & VANDERKLISH, P. W. 2002. The brain-derived neurotrophic factor enhances synthesis of Arc in synaptoneurosomes. *Proc Natl Acad Sci U S A,* 99**,** 2368-73.

YING, Q. L., WRAY, J., NICHOLS, J., BATLLE-MORERA, L., DOBLE, B., WOODGETT, J., COHEN, P. & SMITH, A. 2008. The ground state of embryonic stem cell self-renewal. *Nature,* 453**,** 519-23.

YU, J., LOH, K., SONG, Z. Y., YANG, H. Q., ZHANG, Y. & LIN, S. 2018. Update on glycerol-3-phosphate acyltransferases: the roles in the development of insulin resistance. *Nutr Diabetes,* 8**,** 34.

YU, M., FU, Y., LIANG, Y., SONG, H., YAO, Y., WU, P., YAO, Y., PAN, Y., WEN, X., MA, L., HEXIGE, S., DING, Y., LUO, S. & LU, B. 2017. Suppression of MAPK11 or HIPK3 reduces mutant Huntingtin levels in Huntington's disease models. *Cell Res,* 27**,** 1441-1465.

YUTSUDO, N., KAMADA, T., KAJITANI, K., NOMARU, H., KATOGI, A., OHNISHI, Y. H., OHNISHI, Y. N., TAKASE, K., SAKUMI, K., SHIGETO, H. & NAKABEPPU, Y. 2013. fosB-null mice display impaired adult hippocampal neurogenesis and spontaneous epilepsy with depressive behavior. *Neuropsychopharmacology,* 38**,** 895-906.

ZHANG, B., SALITURO, G., SZALKOWSKI, D., LI, Z., ZHANG, Y., ROYO, I., VILELLA, D., DIEZ, M. T., PELAEZ, F., RUBY, C., KENDALL, R. L., MAO, X., GRIFFIN, P., CALAYCAY, J., ZIERATH, J. R., HECK, J. V., SMITH, R. G. & MOLLER, D. E. 1999. Discovery of a small molecule insulin mimetic with antidiabetic activity in mice. *Science,* 284**,** 974-7.

ZHANG, K., LINDSBERG, P. J., TATLISUMAK, T., KASTE, M., OLSEN, H. S. & ANDERSSON, L. C. 2000. Stanniocalcin: A molecular guard of neurons during cerebral ischemia. *Proc Natl Acad Sci U S A,* 97**,** 3637-42.

ZHANG, K. Z., WESTBERG, J. A., PAETAU, A., VON BOGUSLAWSKY, K., LINDSBERG, P., ERLANDER, M., GUO, H., SU, J., OLSEN, H. S. & ANDERSSON, L. C. 1998. High expression of stanniocalcin in differentiated brain neurons. *Am J Pathol,* 153**,** 439-45.

ZHANG, L., WANG, Q., LIU, W., LIU, F., JI, A. & LI, Y. 2018. The Orphan Nuclear Receptor 4A1: A Potential New Therapeutic Target for Metabolic Diseases. *J Diabetes Res,* 2018**,** 9363461.

ZHANG, X., ZHANG, L., LIN, B., CHAI, X., LI, R., LIAO, Y., DENG, X., LIU, Q., YANG, W., CAI, Y., ZHOU, W., LIN, Z., HUANG, W., ZHONG, M., LEI, F., WU, J., YU, S., LI, X., LI, S., LI, Y., ZENG, J., LONG, W., REN, D. & HUANG, Y. 2017. Phospholipid Phosphatase 4 promotes proliferation and tumorigenesis, and activates Ca(2+)-permeable Cationic Channel in lung carcinoma cells. *Mol Cancer,* 16**,** 147.

ZHANG, Z., CHEN, C., WANG, G., YANG, Z., SAN, J., ZHENG, J., LI, Q., LUO, X., HU, Q., LI, Z. & WANG, D. 2011. Aberrant expression of the p53-inducible antiproliferative gene BTG2 in hepatocellular carcinoma is associated with overexpression of the cell cycle-related proteins. *Cell Biochem Biophys,* 61**,** 83-91.

ZHENG, D., DECKER, K. F., ZHOU, T., CHEN, J., QI, Z., JACOBS, K., WEILBAECHER, K. N., COREY, E., LONG, F. & JIA, L. 2013. Role of WNT7B-induced noncanonical pathway in advanced prostate cancer. *Mol Cancer Res,* 11**,** 482-93.

ZHENG, F., LUO, Y. & WANG, H. 2009. Regulation of brain-derived neurotrophic factor-mediated transcription of the immediate early gene Arc by intracellular calcium and calmodulin. *J Neurosci Res,* 87**,** 380-92.

ZHU, X., ROTTKAMP, C. A., HARTZLER, A., SUN, Z., TAKEDA, A., BOUX, H., SHIMOHAMA, S., PERRY, G. & SMITH, M. A. 2001. Activation of MKK6, an upstream activator of p38, in Alzheimer's disease. *J Neurochem,* 79**,** 311-8.

ZOBOR, D., WERNER, A., STANZIAL, F., BENEDICENTI, F., RUDOLPH, G., KELLNER, U., HAMEL, C., ANDREASSON, S., ZOBOR, G., STRASSER, T., WISSINGER, B., KOHL, S., ZRENNER, E. & CONSORTIUM, R.-C. 2017. The Clinical Phenotype of CNGA3-Related Achromatopsia: Pretreatment Characterization in Preparation of a Gene Replacement Therapy Trial. *Invest Ophthalmol Vis Sci,* 58**,** 821-832.

ZOLLMAN, S., GODT, D., PRIVE, G. G., COUDERC, J. L. & LASKI, F. A. 1994. The BTB domain, found primarily in zinc finger proteins, defines an evolutionarily conserved family that includes several developmentally regulated genes in Drosophila. *Proc Natl Acad Sci U S A,* 91**,** 10717-21.

ZUCCATO, C. & CATTANEO, E. 2014. Huntington's disease. *Handb Exp Pharmacol,* 220**,** 357-409.

ZUCCATO, C., CIAMMOLA, A., RIGAMONTI, D., LEAVITT, B. R., GOFFREDO, D., CONTI, L., MACDONALD, M. E., FRIEDLANDER, R. M., SILANI, V., HAYDEN, M. R., TIMMUSK, T., SIPIONE, S. & CATTANEO,

E. 2001. Loss of huntingtin-mediated BDNF gene transcription in Huntington's disease. *Science,* 293**,** 493-8.

ZUCCATO, C., LIBER, D., RAMOS, C., TARDITI, A., RIGAMONTI, D., TARTARI, M., VALENZA, M. & CATTANEO, E. 2005. Progressive loss of BDNF in a mouse model of Huntington's disease and rescue by BDNF delivery. *Pharmacol Res,* 52**,** 133-9.